SURFACES, INTERFACES AND COATINGS TECHNOLOGIES

PLASMA PROCESSING AND TECHNOLOGY

SICT 2026

PLASMA TECH 2026

TRIBOLOGY INTERNATIONAL CONFERENCE

Tribology 2026

SICT 2026 / PLASMA TECH 2026 / TRIBOLOGY 2026

JOINT CONFERENCES

06 - 08 May 2026 | Prague - Czech Republic

Book of Abstracts

Organizer

SETCOR
Conferences & Exhibitions

SICT 2026 / PlasmaTech 2026 / Tribology 2026 - Joint Conferences Program

06 - 08 May 2026 | Prague, Czech. Rep

06 May 2026		
08:00 - 12:00	**Participants registration**	
09:30 - 10:30	**Welcoming Coffee**	
SICT 2026 / Plasma Tech 2026 / Tribology 2026 Joint Plenary Session I		
Conference Room Ceremony + Dialog		
Session's Chairs: **Prof. Petr Vasina, Masaryk University, Czech Rep.** **Prof. André Anders,Leibniz Institute of Surface Eng, Germany/Plasma Eng. LLC, USA** **Prof. Tiberiu Minea, Univ. Paris-Saclay- CNRS, France**		
10:00 - 10:30	Lowering the activation temperature of Ti-Zr-V non-evaporable getter films by removing surface carbon contamination **J. Fraxedas**, G. Sauthier, L. Tran and V. Carlino	**Prof. Jordi Fraxedas**, ICN2/ CSIC -Barcelona **Spain**
10:30 - 11:00	A few basic (and Hitoric) remarks on glows arcs and HIPIMS Discharges **H. Kersten**, C. Adam, V. Schneider and T. Trottenberg	**Prof. Holger Kersten**, Univ. Kiel, **Germany**
11:00 - 11:30	Plasma process tool kit for the creation of customizable bio-instructive surfaces and interfaces **M. Bilek**	**Prof. Marcela Bilek**, Univ. of Sydney, **Australia**
11:30 - 12:00	From Collisions to Control: Multiscale Modeling of Process Plasmas **T. Mussenbrock**	**Prof. Thomas Mussenbrock**, Ruhr Univ. Bochum, **Germany**
12:00 - 14:00	**Lunch Break – Grandior Restaurant**	
SICT 2026 Session I. A: **Coating Deposition & Surface Treatment Technologies** **Surface Functionalization & Engineering** **Coating Characterization & Modeling**		
Session's Chairs: **Prof. Jordi Fraxedas, ICN2/ CSIC – Barcelona, Spain** **Prof. Robert Vassen, Ruhr University Bochum, Germany**		
14:00 - 14:15	Sustainable Plasma Enhanced Nanocoatings for Advanced Surface Functionalization P. Vieth, K. Braun, F. Hollmann, I. Ostrovsky and B.Fassbender	**Dr. Pascal Vieth**, Chemetall GmbH, **Germany**
14:15 - 14:30	Deposition of Silazane Precursors by Atmospheric Pressure Plasma for the Development of Ultra-hydrophobic Fluorine-Free coatings **M. Saget,** K. Baba, S. Bulou and R. Quintana	**Dr. Manon Saget**, Luxembourg Institute of Science & Technology, **Luxembourg**
14:30 - 14:45	Hybrid Plasma Spraying for Novel Coatings with Tailored Architectures **T. Tesar**, R. Musalek, F. Lukac and P. Capek	**Dr. Tomas Tesar**, Institute of Plasma Physics, **Czech. Rep**
14:45 - 15:00	Forming novel micro- & nanostructures for advanced coating and bonding applications on copper by environmentally friendly electrochemical etching in seawater like electrolyte **J. Rank**, J. Bahr, J. Carstensen and R. Adelung	**Mr. Jannik Rank**, Christian Albrechts University Kiel, **Germany**
15:00 - 15:15	A Systematic Approach to Parameter Selection for Laser-Textured Grooves in Cemented Carbide Cutting Inserts **A. Moreno Arenas**, F. J. Trujillo Vilches, S. Martín-Béjar and L. Sevilla Hurtado	**Mr. Adrian Moreno Arenas**, Univ. Málaga, **Spain**
15:15 - 15:30	Al-Doped ZnO Transparent Conductors Deposited from a Two-Component Target: Properties and Flexibility Assessment **S. Kiełczawa**, A. Wiatrowski, M. Mazur, W. Posadowski and J. Domaradzki	**Mr. Szymon Kielczawa**, Wroclaw University of Science and Technology, **Poland**

15:30 - 15:45	Combinatorial deposition of gallium oxynitride thin films **M. Gajdics**, I. Cora, T. Kolonits, Gy. Safran and B. Pecz	**Dr. Marcell Gajdics**, HUN-REN Centre for Energy Research, **Hungary**
15:45 - 16:00	Optimization for the composition gradient of Al-O-N thin film deposited by reactive RF sputtering technology **M. Serenyi**, M. Gajdics, D. Olasz and G. Safran	**Dr. Miklos Serenyi**, HUN-REN Centre for Energy Research, **Hungary**
16:00 - 16:30	**Coffee Break / Posters Session**	
Session's Chairs: **Dr.Tomas Tesar, Institute of Plasma Physics, Czech. Rep** **Dr. Vassilis Constantoudis, Nanometrisis P.C, Greece** **Dr. Marcell Gajdics, HUN-REN Centre for Energy Research, Hungary** **Dr. Miklos Serenyi, HUN-REN Centre for Energy Research, Hungary**		
16:30 - 16:45	Hierarchical surfaces: theory, computational analysis and experimental characterization G. Papavieros, **V. Constantoudis**, A. Zeniou, S. Stavromitros and E.Gogolides	**Dr. Vassilis Constantoudis**, Nanometrisis P.C, **Greece**
16;45 - 17:00	High-Throughput Combinatorial Characterization of thin Binary and Ternary Layers **G. Safran**, M. Gajdics, D. Olasz, N. Szász, N. Quang Chinh and M. Serényi	**Dr. Gyorgy Safran**, HUN-REN Centre for Energy Research, **Hungary**
17:00 - 17:15	Piezo-Assisted RF Magnetron Sputtering of Ni Nanoparticles on TiO_2 Powder Supports for Electrocatalytic Applications **C.R. Chandraiahgari**, G. Gottardi, G.. Speranza, D. Dalessandro, M. Bordin, V. Micheli, R. Bartali and M. Testi	**Dr. Chandrakanth R. Chandraiahgari**,Fondazione Bruno Kessler (FBK), **Italy**
17:15 - 17:30	Safe and sustainable by design approach for omniphobic PFAS free ceramic like coatings for glass packaging **E. Khousakoun**, M. Poelman, S. Desprez, A. L. Dechief, B. Belloncle, A. Mezy, J. Alcodori, P. Lledo, A. Rashid and A. Nelson	**Dr. Eric Khousakoun**, Materia Nova, **Belgium**
17:30 - 17:45	From Lignin Depolymerization to BPA-Free Epoxy Coatings: A Scalable Biobased Route for Construction Materials **M. Comí**	**Dr. Marc Comi**, VITO, **Belgium**
17:45 - 18:00	Non-destructive automated mechanical characterization for coatings and surfaces using surface acoustic wave spectroscopy **S. Makowski,** M. Zawischa, R. Knieß, A. Arshad and F. Härtwig	**Dr. Stefan Makowski**, Fraunhofer Institute for Material and Beam Technology, **Germany**
18:00 - 18:15	Microstructured impregations of Carbon Yarns for Graded Interphases in Concrete **L. Flechsig**, G. K. Auernhammer and C. Scheffler	**Ms. Lissy Flechsig**, Leibniz Institute of Polymer Research, **Germany**
18:15 - 18:30	From Challenge to Insight: Exploring Analytical Methods at the Fiber-Matrix Interphase **R. Reichenbächer** and C. Scheffler	**Mr. Rudi Reichenbächer**, Leibniz-Institute for Polymer Research, **Germany**
18:30 - 18:45	Mechanical Properties of minature samples of Spark Plasma Sintered NiTi Alloy **S. Samal,** J. Kopeček, E. Iaparova and P. Sittner	**Dr. Sneha Samal**, Institute of Physics of Czech Acad. of Science, **Czech Rep**
18:45 - 19:00	Investigation of Mechanical Interlocking Using Sculptured Aluminum Foils for Joining Two Dissimilar Polymers **P. Hakimi**, F. Hahnewald, J. Carstensen, C. Balzer, C. Laugwitz and R. Adelung	**Ms. Parisa Hakimi**, Christian-Albrechts University Kiel, **Germany**

06 May 2026		
Plasma Tech Session I. B: **Plasma fundamentals / Modelling / Atomic and Molecular Processes** **Plasma Source Design and Diagnostics**		
Conference Room Forum		
Session's Chairs: **Prof. Petr Vasina, Masaryk University, Czech. Rep** **Prof. Holger Kersten, Univ. Kiel, Germany**		
14:00 - 14:30	High-power electron beams for technological applications **T. Minea**	**Prof. Tiberiu Minea**, Univ. Paris-Saclay- CNRS, **France**
14:30 - 14:45	Anode erosion and gas flow symmetry in plasma spray torch **R. Zhukovskii**, R. Molz, R. Enzl, M. Messina and M. Giglmaier	**Dr. Rodion Zhukovskii**, Oerlikon Metco AG, **Switzerland**
14:45 - 15:00	Study of ion beam sources by self consistent simulation approach **M. Queck**, K.M. Rettig and T. Dunger	**Dr. Martina Queck**, Scia Systems GmnH, **Germany**
15:00 - 15:15	Simulation of the electron density time evolution in the ignition process of an Ar RF-CCP plasma discharge **P. Mandracci**	**Prof. Pietro Mandracci**, Politecnico di Torino, **Italy**
15:15 - 15:30	Chemistry Data Generation for Plasma Simulations **S. Mohr**, G.S.J. Armstrong, R. Brook and J. Tennyson	**Dr. Sebastian Mohr**, Quantemol Ltd., **UK**
15:30 - 15:45	Superposition of HiPIMS with RF on a single magnetron: Generation of high ion energies **C. Adam**, L. Hansen, T.A. Hahn, J. Niemann, D. Zuhayra, G. Mark, J. Löffler, J. Benedikt and H. Kersten	**Ms. Caroline Adam**, Kiel University, **Germany**
15:45 - 16:00	Establishing an Atomic Oxygen Test Facility for Space Hardware Based on an Inductively Coupled Plasma Source **S. Zoehrer**, W. Engel, L. Bettiol, B. Seifert	**Dr. Siegfried Zoehrer**, FOTEC GmbH, **Austria**
16:00 - 16:30	**Coffee Break / Posters Session**	
Session's Chairs: **Dr. Dirk Hegemann, Empa, Switzerland** **Prof. Pietro Mandracci, Politecnico di Torino, Italy**		
16:30 - 17:00	Generation and Manipulation of Pulsed-Driven Dielectric Barrier Discharges using Tailored High-Voltage Waveforms **H. Höft**, J. J. van Oorschot, R. Brandenburg, T. Huiskamp and M. M. Becker	**Dr. Hans Höftq**, Leibniz Institute for Plasma Science and Technology, **Germany**
17:00 - 17:15	Numerical and Experimental Investigation of Collector Geometry Ef-fects in Gridded Electrohydrodynamic Thrusters **G. Mongaretto**, F. Ragazzi, D. Usuelli, S. Trovato, R. Terenzi, A. Popoli, A. Cristofolini and M. Belan	**Mr. Giorgio Mongaretto**, University of Bologna, **Italy**
17:15 - 17:30	MHD multiphase modelling of electrical explosions confined in air and dense media **F. Tholin**, A. Jarnac, B. Khiar, F. Pechereau, C. Zaepffel, V. Gaudineau and K. Thomas	**Dr. Fabien Tholin**, ONERA-Univ. Paris-Saclay, **France**
17:30 - 17:45	Phase-Resolved Optical Diagnostics of Scaled Plasma Jets Operated with Ar/Ar-Mixtures at Ambient Conditions **T. Satish Babu**, P S N S R Srikar, S; M. Maliyekkal and R. Kumar Gangwar	**Mr. Thota Satish Babu,** IIT Tirupati, **India**

06 May 2026		
SICT 2026 / Tribology 2026 Joint Session I. C: Fundamentals of Tribology & Advanced Surfaces Coatings and Surfaces Corrosion / Tribological Properties Testing, Measurement & Methodologies		
Conference Room Gracie		
Session's Chairs: Prof. Maria Clelia Righi, Univ. of Bologna, Italy Prof. Jerzy Szpunar, Univ. of Saskatchewan, Canada Prof. Rafal Reizer, University of Rzeszow, Poland		
14:00 - 14:30	The Effects of Build Parameters on the Reciprocating Wear Response of Al2O3 Ceramics Produced Using DLP Additive Manufacturing A.M.S. David, G. Boubnova, S. Clemens and **K.P. Plucknett**	**Prof. Kevin P. Plucknett**, Dalhousie Univ., **Canada**
14:30 - 15:00	Dry friction behavior of Ceramic Matrix Composites (CMC) obtained by duplex treatment combining cold spray aluminum layers with alumina, zirconia and rutile particles followed by plasma electrolytic oxidation (PEO) treatments **T. Czerwiec,** A. Maizeray, G. Marcos, A. Cappella, M.-P. Planche, H. Liao, G. Henrion, S. Philippon and J. Martin	**Prof. Thierry Czerwiec**, Univ. de Lorraine, **France**
15:00 - 15:15	Design and generation of sealing shaft counter-surfaces by two-stage turning for the reduction of friction in sealing contacts **T. Junge**, L. M. de C. Silva, A. Nestler, A. Schubert and O. Koch	**Mr. Thomas Junge**, Chemnitz Univ. of Technology, **Germany**
15:15 - 15:30	Effects of DLC and CrN thin coatings on the wear behaviour of L-PBF AlSi10Mg alloy M. Merlin, C. Morales, S. Urbinati, C. Mopty and **C. Soffritti**	**Mrs. Chiara Soffritti**, University of Ferrara, **Italy**
15:30 - 15:45	Influence of O2 flow rate on scratch and wear behavior of silver oxide thin films fabricated via RF magnetron sputtering deposition **K. Win**, K. Kulikowski and M. Koba	**Dr. Khunnay Win**, Warsaw University of Technology, **Poland**
15:45 - 16:00	Improved wear protection of tribological boundary layers **N. Gregarek**, G. Jacobs and S. Zhang	**Mr. Nico Gregarek**, RWTH Aachen University, **Germany**
16:00 - 16:30	**Coffee Break / Posters Session**	
Session's Chairs: Prof. Kevin P. Plucknett, Dalhousie Univ., Canada Prof. Czerwiec Thierry, Univ. de Lorraine, France		
16:30 - 16:45	The self-healing corrosion resistant coatings for AZ-31 magnesium alloy **J. Szpunar**	**Prof. Jerzy Szpunar**, Univ. of Saskatchewan, **Canada**
16:45 - 17:00	Friction mode and humidity effects on tribological behavior of DC magnetron sputtered (NbMoTaW)100-z-(CN)z coatings **F. Lofaj**, P. Hviščová, D. Kondrakhova and J. Dobrovodský	**Dr. Frantisek Lofaj**, Institute of Materials Research of the Slovak Acad. of Sciences, **Slovakia**
17:00 - 17:15	Friction of GO/MoSe2 films in ambient air and vacuum conditions **A. Kozak**, M. Precner, M. Precnerová, M. Ilčíková, N. Konios, M. Mičušík, J. Osička, V. Vretenár, J. Mosnáček and M. Ťapajna	**Dr. Andrii Kozak**, Institute of Electrical Engineering, Slovak Acad. of Sciences, **Slovakia**
17:15 - 17:30	Replacing PTFE with Self-Organizing HDPE Particle containing Composites for low Friction Applications **N. Kubat**, J. Rank, J. Bahr, J. Carstensen and R. Adelung	**Mr. Niklas Kubat**, Christian-Albrecht's Univ. Kiel, **Germany**
17:30 - 17:45	Friction in Polymer Systems under Low-Temperature Conditions **A. Ptak**, M.Kiełb and W.Wieleba	**Dr. Anita Ptak**, Wroclaw University of Science and Technology, **Poland**
17:45 - 18:00	Effect of Microstructure on the Wear Behavior of Eutectic and Non-Eutectic BCC High-Entropy Alloys **L. Chen**, W. Ma and O. Tisov	**Mr. Liming Chen**, Xi'an Jiaotong University, **China**
18:00 - 18:15	Tribological behaviour of Soybean oil-based biolubricants **P.Mostaza**, M.D. Avilés, T. Caparrós, M.D. Bermúdez and F.J. Carrion-Vilches	**Ms. Paloma Mostaza Ucedo**, University Politécnica de Cartagena, **Spain**

07 May 2026		
Conference Room Ceremony + Dialog		
SICT 2026 / Plasma Tech 2026 / Tribology 2026 Joint Plenary Session II		
Session's Chairs: **Prof. Jordi Fraxedas, ICN2/ CSIC -Barcelona Spain** **Prof. Holger Kersten, Univ. Kiel, Germany**		
09:00 - 09:30	Plasma Fluxes and Their Atomic-Scale Heating Effects on Thin Film Growth **A. Anders**, D. Kalanov and Y. Unutulmazsoy	**Prof. André Anders,** Leibniz Institute of Surface Eng, **Germany**/Plasma Eng. LLC, **USA**
09:30 - 10:00	Methane pyrolysis in a constant-current DC gliding arc discharge: impact of discharge regime on the process performances and soot formation P. Mathieu, Y. Tian, A. Abdirakhmanov, A. Chatterjee and **R. Snyders**	**Prof. Rony Snyders**, Univ. of Mons, **Belgium**
10:00 - 10:30	Green Plasma Processing – from Deposition to Gas Conversion **D. Hegemann**, P. Navascués and R. Snoeckx	**Dr. Dirk Hegemann**, Empa, **Switzerland**
10:30 - 11:00	**Coffee Break / Posters Session**	
SICT 2026 Session II. A: **Advanced Materials & Emerging Coating Systems** **Performance-Oriented Coating Applications**		
Session's Chairs: **Prof. Jordi Fraxedas, ICN2/ CSIC -Barcelona Spain** **Dr. Vassilis Constantoudis, Nanometrisis P.C, Greece**		
11:00 - 11:30	The use of thermal spray technologies in energy conversion systems **R. Vassen**	**Prof. Robert Vassen,** Ruhr University Bochum, **Germany**
11:30 - 12:00	Study of Thermal and Environmental Barrier Coatings for Aero-engine Applications **P. Xiao**	**Prof. Ping Xiao**, Univ. of Manchester, **UK**
12:00 - 14:00	**Lunch Break – Grandior Restaurant**	
Group Photo at 13:45		
Session's Chairs: **Prof. Robert Vassen, Ruhr University Bochum, Germany** **Prof. Ping Xiao, Univ. of Manchester, UK**		
14:00 - 14:15	The influence of the thickness of the buried ITO thin film on charge dissipation and optical properties in functional multilayer oxide coatings **A. Obstarczyk**	**Dr. Agata Obstarczyk**, Wroclaw Univ. of Science and Technology, **Poland**
14:15 - 14:30	The impact of the thickness on the properties of CuO **E. Mańkowska**	**Dr. Ewa Mańkowska**, Wroclaw Univ. of Science and Technology, **Poland**
14:30 - 14:45	Gas sensing properties of copper and titanium oxides thin films deposited by magnetron sputtering **P. Pokora** and E. Mańkowska	**Dr. Patrycja Pokora**, Wroclaw Univ. of Science and Technology, **Poland**
14:45 - 15:00	Fluorescent Nanocomposites of Polydiacetylene-ZnO Quantum Dots-Zn(II) ion with Temperature/Acid-Responsive Properties **N.Traiphol**, S. Boonmak, K. Phetnam and R.Traiphol	**Prof. Nisanart Traiphol**, Chulalongkorn University, **Thailand**
15:00 - 15:15	High-Temperature Reversible Thermochromic and Acid-responsive Polydiacetylene/Li+ Assemblies for Smart Coatings **R.Traiphol**, K. Phetnam, S. Boonmak and N.Traiphol	**Prof. Rakchart Traiphol**, Mahidol University, **Thailand**
15:15 - 15:30	Development of a Specialized Coating for Moisture and Aggressive Environment Resistance **O. Ghorab**, L. Chetibi, I. Calliari, M. Pigato, M. Dabalà, D. Hamana, F,Ahani, S.Achour and Lorenzo Dambrosi	**Ms. Ouissal Ghorab**, Univ. of Padua, **Italy**

15:30 - 15:45	High-temperature failure mechanism of TiAlSiN coating deposited on pristine and plasma nitride tool steel **V. Terek**, L. Kovačević, A. Drnovšek, M. Čekada, M. Zagoričnik, Z. Bobić and P. Terek	**Mr. Vladimir Terek**, University of Novi Sad, **Serbia**
15:45 - 16:00	Stable Polydopamine–Gallic Acid Suspension as a Functional Surface Treatment for Improved Adhesion in Bamboo/PP Composites **C. N. Schnell**, A. Laachachi, D. Ruch and C.A. Fuentes	**Dr. Carla Natali Schnell**, Luxembourg Institute of Science and Technology, **Luxembourg**
16:00 - 16:30	**Coffee Break / Posters Session**	
SICT 2026 / Plasma Tech 2026 Joint Session II. B: Bio-interfaces, Biomedical / Bioactive surfaces and coatings Plasma applications for biology, medicine, and agriculture		
Session's Chairs: Prof. Marcela Bilek, Univ. of Sydney, Australia Dr. Adina Coroaba, Petru Poni Institute of Macromolecular Chemistry, Romania		
16:30 - 17:00	Self-Templated Highly Porous Gold as Antibiofouling strategy in Electrochemical Biosensing: application in a microneedles-based bio-sensor for β-hydroxybutyrate (β-HB) detection A. Degjoni, C. Tortolini, D. Passeri, A. Lenzi and **R. Antiochia**	**Prof. Riccarda Antiochia**, Sapienza Univ. of Rome, **Italy**
17:00 - 17:15	Low-Remanence Iron-Oxide Thin Films and Microdiscs for Cell-Interactive Biointerfaces and Biomedical Actuators **I. Lasa**, C. Redondo, D. Salazar and R. Morales	**Ms. Irati Lasa Uriarte**, Univ. of the Basque Country, **Spain**
17:15 - 17:30	Surface Functionalization of Inner Microchannel Surfaces in a Power-Free Microfluidic Chip for Extracellular Vesicle Detection **R. Ishihara**, M. Hosono, M. Ogawa, H. Yazawa, T. Nakajima, E. Shimura, T. Baba and H. Shibata	**Dr. Ryo Ishihara**, Juntendo University, **Japan**
17:30 - 17:45	Challenges in Detecting Biotoxins and Biomolecules by using Surface-enhanced Raman Scattering Spectroscopy on Nanopatterned Substrates **N. E. Dina**, A. Colniță, D. Marconi, I. A. Brezeștean and A. S. Tătar	**Dr. Nicoleta Dina**, INCDTIM Cluj-Napoca, **Romania**
17:45 - 18:00	Innovative SiO_2/PEG/Caffeic Acid Sol-Gel Coatings on Stainless Steel: Toward Bioactive and Biocompatible Prosthetic Surfaces **F. Barrino**, F. Giuliano, H. de la Rosa-Ramírez and M.D. Samper	**Dr. Federico Barrino**, University of Palermo, **Italy**
18:00 - 18:15	Effects of growth defects on corrosion performance of PVD coatings and hybrid PVD/ALD layers for implant applications **P. Terek**, Z. Bobić, L. Kovačević, V. Terek, A. Csík, M. Čekada and A. Drnovšek	**Dr. Pal Terek**, University of Novi Sad, **Serbia**
18:15 - 18:30	Surface functionalization of micro-textured surfaces for antibiofouling applications of ocean sensors **B. Nanda Sahoo**, P. James Thomas and M. Møller Greve	**Dr. Bichitra Nanda Sahoo**, University of Bergen, **Norway**
18:30 - 18:45	Microwave Cold Plasma Jets for Microbial Inactivation: From RONS Chemistry to Cell Morphology **K. Trebulová**, V. Loupová, B. Chobotská, L. Kletzander, P. Kulich, Z. Kozáková and F. Krčma	**Ms. Kristína Trebulová**, Brno University of Technology, **Czech Rep.**

Conference Dinner
07 May 2026, from 19:30

07 May 2026		
Conference Room Forum		
SICT 2026 / Plasma Tech 2026 Joint Session II. C: Plasma fundamentals / Modelling / Atomic and Molecular Processes Plasma Processing / Materials Interactions / Coatings		
Session's Chairs: Prof. Tiberiu Minea, University Paris-Saclay - CNRS, France Prof. Holger Kersten, University Kiel, Germany		
11:00 - 11:30	Comparative Study of Metal Atom, Metal Ion, and Argon Ion Fluxes in Laboratory and Industrial Sputtering Using Metallic and Alloy Targets **P. Vesina**	**Prof. Petr Vasina,** Masaryk University, **Czech. Rep**
11:30 - 12:00	Technological Change for future Speciality Glass Production **S. Wolf**, M. Hauf, B. Bochtler, T. Golubeva, W. Schmidbauer, J. Hessenkemper, K. Jochem, S. Knoche, S. Knoche, J. Costard and M. Hahn	**Dr. Sebastian Wolf**, SCHOTT AG, **Germany**
12:00 -12:15	Plasma Tailoring of Celluloses for Advanced Applications V. Shvalya, A. Oberlintner, N. M. Santhosh and U. Cvelbar	**Dr. Vasyl Shvalya**, Jožef Stefan Institute, **Slovenia**
12:00 - 14:00	**Lunch Break – Grandior Restaurant**	
Group Photo at 13:45		
Session's Chairs: Prof. André Anders, Leibniz Institute of Surface Eng, Germany / Plasma Eng. LLC, USA Prof. Pietro Mandracci, Politecnico di Torino, Italy Prof. Tiberiu Minea, Univ. Paris-Saclay- CNRS, France		
14:00 - 14:15	Complex plasma with active Janus particles in patterned confinement **V. Nosenko**	**Dr. Volodymyr Nosenko**, German Aerospace Center, **Germany**
14:15 - 14:30	Investigation of the chemical behaviour of an electrolytic discharge used to synthesize low-density mesoporous metals **C. Boudat**, R. Botrel, F. Durut, C. Noël and T. Belmonte	**Ms. Claire Boudat,** CEA, **France**
14:30 - 14:45	Plasma-Catalytic Pyrolysis Via Water-Stabilized Plasma Torch for Single-Walled Carbon Nanotubes Synthesis **J. Fathi**, A. Mašláni and O. Jankovský	**Mr. Jafar Fathi**, Institute of Plasma Physics Prague, **Czech Rep.**
14:45 - 15:00	Synthesis of higher order organic compounds from hydrocarbons, alcohols and amines using a microsecond-pulsed dielectric barrier discharge **P-L. Girard-Lauriault**, A. Banerjee, S. Marji, O Armstrong and G. Baez-Zaldivar	**Prof. Pierre-Luc Girard-Lauriault** McGill University, **Canada**
15:00 - 15:15	Production of nitrogen oxides as fertilizers precursors via an atmospheric microwave air plasma torch **M. Troia**, K. Wiegers, A. Schulz and M. Walker	**Dr. Mariagrazia Troia**, University of Stuttgart, **Germany**
15:15 - 15:30	Scalable nanopulsed plasma seed disinfection using a long wire-plate DBD module **L.F.A. Wymenga** and J. van Turnhout	**Mr. Luutzen Wymenga**, Delft University of Technology, **The Netherlands**
15:30 - 15:45	Cold Plasma-Assisted Drying: A Promising Strategy for Enhancing Drying Characteristics and Quality Retention in Cannabis Processing P.C. Das, L.G. Tabil and **O.D. Baik**	**Prof. Oon-Doo Baik**, University of Saskatchewan, **Canada**
15:45 - 16:00	Electrochemical Reduction of Metal Oxalates and Tartrates Using Non-Equilibrium Hydrogen/Argon Plasma A. Guillemin, F. Rousseau and C. Guyon	**Mr. Antonin Guillemin**, ENSCP -Chimie ParisTech, **France**
16:00 - 16:30	**Coffee Break / Posters Session**	
SICT 2026 / Plasma Tech 2026 Session II D: Plasma Processing / Materials Interactions / Coatings Plasma application in Energy and environment		

Session's Chairs: Prof. Rony Snyders, Univ. of Mons, Belgium Dr. Dirk Hegemann, Empa, Switzerland Dr. Marcia Oliveira, University of Leon, Spain		
16:30 - 16:45	Selective single-step microwave plasma conversion of hazardous aromatic hydrocarbons into few-layer graphene **O. Jašek**	**Dr. Ondrej Jasek**, Masaryk University, **Czech Rep.**
16:45 - 17:00	Conversion of plastic waste into high-quality soot by microwave-based plasma pyrolysis **D. Schüpfer**, L. Beran, I. Kinski, G. Homm and T. Kraus	**Dr. Dominique Schüpfer,** Fraunhofer IWKS, **Germany**
17:00 - 17:15	Experimental and simulation-based investigations into sustainable metal-catalytic plasma etching of silicon using hydrogen **L. Böhm**, N. Reghunath, G. Umlauf, X. Hu, M. Haas and J. Schuster	**Ms. Lenia Böhm**, Fraunhofer ENAS, **Germany**
17:15 - 17:30	Degradation of Methylene Orange in Aqueous Solution Using Non-Thermal Plasma **T. Nguyen**, H. Gerard, L. Sonhafouo Mbantio, G. Thomas and N. Cedric	**Dr. Truong Son Nguyen**, Univ. Lorraine, **France**
17:30 - 17:45	Nanosecond-pulsed plasma bubbles for pollutant and pathogen elimination in water **C.A. Aggelopoulos**, K. Papalexopoulou and M. Kariofillis	**Dr. Christos Aggelopoulos**, FORTH/ ICE-HT, **Greece**
17:45 - 18:00	Air atmospheric pressure plasma, a green approach for the sanitation of leafy greens vegetables **Zh. Aliyeva**, T. Maho, Ph. Guillot and C. Muja	**Mrs. Zhanel Aliyeva**, INUC- Univ Toulouse, **France**
18:00 - 18:15	Cold plasma for Food Safety: Process Optimization and Quantification of Reactive Chemical Species for Effective Fungal Inactivation **T. Pushparaj Gandhia**, R. Kumar Gangwarb and S.M. Maliyekkala	**Mr. Pushparaj Gandhi Tadavarthi**, IIT Tirupati, **India**

Conference Dinner
07 May 2026, from 19:30 **The Grand Mark Prague (The Pavillon Space)** **Hybernská 1008/12** **110 00 Nové Město (Prague 1)** **Prague**

07 May 2026		
Tribology 2026 Session II. E: **Physics or Chemistry of Tribo-Surfaces / Nanotribology** **Sustainable & Green Tribology**		
Conference Room Gracie		
Session's Chairs: **Prof. Kevin P. Plucknett, Dalhousie Univ., Canada** **Prof. Juliette Cayer-Barrioz, Ecole centrale de Lyon - CNRS, France**		
11:00 - 11:30	Fracture and adhesion of viscoelastic materials **G. Carbone**	**Prof. Giuseppe Carbone**, Nanjing Univ. of Science & Tech, **China/** Polytechnic Univ. of Bari, **Italy**
11:30 - 12:00	Advancing Lubricant Design with Machine Learning Molecular Dynamics **M. Clelia Righi**	**Prof. Maria Clelia Righi,** Univ. of Bologna, **Italy**
12:00 - 12:30	Tribological Behavior of 2D MXene-reinforced Polymer and Metal Matrix Composites **M. Marian**	**Prof. Max Marian,** Leibniz Univ. Hannover, **Germany**
12:00 - 14:00	**Lunch Break – Grandior Restaurant**	
Group Photo at 13:45		
Session's Chairs: **Prof. Czerwiec Thierry, Univ. de Lorraine, France** **Prof. Giuseppe Carbone, Nanjing Univ. of Science & Tech, China/ Polytechnic Univ. of Bari, Italy**		
14:00 - 14:30	Ice-Rubber Friction Mechanisms across Scales **J. Cayer Barrioz**	**Prof. Juliette Cayer-Barrioz**, Ecole centrale de Lyon – CNRS, **France**
14:30 - 14:45	Molecular dynamic characterization of surface active additives – sorption, solubility and diffusion **K. Falk**, L. Kruse, S. Peeters, G.Moras and M. Moseler	**Dr. Kerstin Falk**, Fraunhofer IWM, **Germany**
14:45 - 15:00	Energy Fingerprints of Wear: Decoupling Friction Instability from Thermal Dissipation in Reciprocating Tribotests **J. Qin**, S. Zhao and D. Lindell	**Dr. Jian Qin**, ABB Corporate Research Center, **Sweden**
15:00 - 15:15	Tribological Performance of Contaminated Grease: Three-Body Contact and Wear–Pitting Characterization **J.H. Horng**, T.N. Ta, S.J. Liao and C.C. Wei	**Prof. Jeng-Haur Horng**, Cheng Kung University, **Taiwan**
15:15 - 15:30	Enhancement of Wear Resistance and Cooling Efficiency of Additively Manufactured Nylon Gears C. He, **W. Li**, A. Daman, Z. Peng	**Mr. Wenhan Li**, UNSW Sydney, **Australia**
15:30 - 15:45	Solid particle erosion behavior of cold-rolled austenitic stainless steels under Martian regolith simulant **M. Gragnanini**, A. Fortini, N. Zanini, A. Suman and M. Pierret	**Mr. Michele Gragnanini**, University of Ferrara, **Italy**
15:45 - 16:00	Study on In Situ Damage Evaluation in Rolling Friction using Acoustic Emission Sensing **Y. Hirai** and A. Hase	**Mr. Yuto Hirai**, Saitama Institute of Technology, **Japan**
16:00 - 16:30	**Coffee Break / Posters Session**	
Session's Chairs: **Prof. Max Marian, Leibniz Univ. Hannover, Germany** **Prof. Zhongxiao Peng, University of New South Wales, Australia**		
16:30 - 16:45	Estimations of wear scar volumes based on profile measurements **P. Pawlus**, S. Woś and R. Reizer	**Prof. Pawel Pawlus**, Rzeszow University of Technology, **Poland**
16:45 - 17:00	From damaging to protective oxidation: high-temperature friction and wear regimes in binder-modified cemented carbides and cermets	**Dr. Sandra Tarancón**, Univ. Politec Madrid, **Spain**

	S. Tarancón, E. Tejado, J.Y. Pastor, B. Ferrari, A.J. Sanchez-Herencia and T. Polcar	
17:00 - 17:15	A novel approach based on Greenwood-Williamson theory for the estimation of tribocorrosive wear **M. De Stefano** and A. Ruggiero	**Dr. Marco De Stefano**, University of Salerno, **Italy**
17:15 - 17:30	Modulating the Boundary Lubrication of Orthokeratology Lenses via Polysaccharide-Protein Interfacial Interactions **H. W. Fang** and Y. C. Chang	**Dr. Hsu-Wei Fang**, National Taipei University of Technology, **Taiwan**
17:30 - 17:45	Development of an Artificial Ageing Procedure for Polyalphaolefin (PAO) Base Oil Contaminated with Alternative Fuel **M. Kovacs** and D. Pintér	**Mr. Marko Kovacs**, Szechenyi Istvan Univ., **Hungary**
17:45 - 18:00	Superlubricity with ta-C Coatings: From Model Tests to Journal Bearing Application **F. Härtwig**, S. Makowski, S. Kattookaren and V. Weihnacht	**Mr. Fabian Härtwig**, Fraunhofer IWS Dresden, **Germany**
18:00 - 18:15	Circular Valorization of End-of-Life Tires into High-Performance Rubber-Carbon Composites: Mechanical and Tribological Performance **A. Hussain** and D. Bajare	**Dr. Abrar Hussain**, Riga Technical University, **Latvia**

Conference Dinner
07 May 2026, from 19:30 **The Grand Mark Prague (The Pavillon Space)** **Hybernská 1008/12** **110 00 Nové Město (Prague 1)** **Prague**

07 May 2026		
EU projects Workshop: **Antimicrobial Nanocoatings: Aligning Innovation, Regulatory Compliance and Market Uptake**		
Conference Room Harmony		
11:00 - 11:05	Welcome & Opening Remarks - Framing the Ambition	**Mrs. Ana Hristova**, Europroject, **Bulgaria (*RELIANCE Project*)**
Workshop Session 1 - Smart Material Design & Antimicrobial Functionality		
Session Chair: Miren Blanco, RELIANCE		
11:05 - 11:20	Controlled-release of carvacrol oil from stimuli-responsive copper doped mesoporous silica particles **M. Argaiz**, L. Fiore, A. M Goitandia, F. Arduini, M. Blanco and B. Coto	**Dr. Maialen Argaiz,** Tekniker, **Spain *(RELIANCE Project)***
11:20 - 11:35	Antibacterial Performance of Nanoparticle-Based Coatings on Textile **B. Erol**, S. Akkermans, E. Merli, D. Spinelli, I. Canesi, A. Karagianni, A. Zourou, I. Kitsou, E. Roussi, A. Tsetsekou, K.V. Kordatos, D. Katerinopoulou, A. Stoumpidi, G. Kiriakidis, D. Kozak, M. Polanska and J.F.M. Van Impe	**Mrs. Büşra Erol**, KU Leuven, Ghent, **Belgium (*SUPREME Project)***
11:35 - 11:50	Photoactive Nanoparticles for Antimicrobial Inactivation **V. Liska** and J. Mosinger	**Mr. Vojtech Liska,** Charles University, **Czech Rep. *(MIRIA Project)***
11:50 - 12:05	Encapsulation of Essential Oils in Silica Nanopores: A Molecular Dynamics simulation study **I. Papageorgiou**, K.S. Karadima, L. Peristeras and V.G. Mavrantzas	**Mrs. Ioanna Papageorgiou**, University of Patras, **Greece (*RELIANCE Project*)**
12:05 - 12:20	Q&A	
12:00 - 14:00	**Lunch Break – Grandior Restaurant**	
Workshop Session 2: Validation and Performance on Real Surfaces		
Session Chair: Angelica Luceri, NANOBLOC		
14:00 - 14:15	A Safety-By-Design Approach for Hazard Evaluation of Bio-Based Self-Disinfecting Nano-Coatings **T. Loret**	**Dr. Thomas Loret**, Ineris, **France *(RELIANCE Project)***
14:15 - 14:30	Particle Release from Light-Activated Antimicrobial Coatings under Simulated Dermal Contact and Cleaning **N. Mutlua**, P. Kockb, S. Fischerb, S. Schulteb and B. Nowacka	**Dr. Nurshen Mutlu,** Empa**, Switzerland (NOVA Project)**
14:30 - 14:45	A decorative and antibacterial coating for high-traffic objects: effectiveness and durability after testing in a real-life-like scenario. **R. Ortiz**, I. Ciarsolo, O. Areitioaurtena, S. Alves, B. Coto and E, Gutiérrez	**Dr. Rocío Ortiz,** Tekniker**, Spain *(NANOBLOC Project)***
14:45 - 15:00	Q&A	
Workshop Session 3: From Lab to Scale & Compliance		
Session Chair:Dr. Jan Vam Impe, SUPREME		
15:00 - 15:15	NanoBloc: From Laboratory Development to Industrial Upscaling of Sputtered Antimicrobial Coatings **A. Luceri**, O. Benzine, M. Donalisio, D. Lembo and C. Balagna	**Dr. Angelica Luceri**, Politecnico di Torino, **Italy *(NANOBLOC Project)***
15:15 - 15:30	A novel 3D-printed stamping device to assess antibacterial performance of coatings under simulated realistic touch transfer **A.J Cunliffe**, P. Askew, G. Iredale, A. Marchant, A. Awan and J. Redfern	**Dr. Alexander J Cunliffe**, Manchester Metropolitan Univ., **UK (NOVA Project)**

15:30 - 15:45	Atmospheric Plasma-assisted Deposition of Antimicrobial Coatings on Complex 3D Automotive Interior Surfaces **M. Nilkar** and M. Milani	**Dr. Maryam Nilkar**, Molecular Plasma Group, **Belgium** (***RELIANCE Project***)
15:45 - 16:00	Q&A	
16:00 - 16:30	**Coffee Break / Posters Session**	
Workshop Session 4: **The Future: Aligning Research, Regulation and Sustainability Real Surfaces** **Moderated Interactive Roundtable**		
Session Chair: Sara Espinoza, NOVA		
16:20 - 16:35	**Predictive & Digital Design** • How far are we from modelling-driven material approval? • What research gaps remain?	**Plenary**
16:35 - 16:50	**Safety, SSbD & Environmental Impact** • How do we operationalise Safe and Sustainable by Design? • What test methods need harmonisation?	**Plenary**
16:50 - 17:05	**Industrial Deployment & Standardisation** • What standards are missing? • What demonstration cases are still needed? • What should FP10 fund?	**Plenary**
17:10 - 17:30	**Synthesis of findings:** • Repeated bottlenecks • Common regulatory issues • Shared funding needs • Standardisation gaps **Joint Workshop Outcome:** Prague Position Paper on Safe and Sustainable Antimicrobial Nanocoatings (policy-oriented)	**Dr. Sara Espinoza,** DECHEMA e.V., **Germany** (***NOVA Project)***

Conference Dinner
07 May 2026, from 19:30 **The Grand Mark Prague (The Pavillon Space)** **Hybernská 1008/12** **110 00 Nové Město (Prague 1)** **Prague**

08 May 2026		
SICT 2026 / Plasma Tech 2026 Session III. A: Coatings for Energy and Environmental Applications		
Conference Room Ceremony		
Session's Chairs: Prof. Pierre-Luc Girard-Lauriault McGill University, Canada Dr. Sneha Samal, Institute of Physics of Czech Acad. of Science, Czech Rep		
09:00 - 09:30	Metal oxide cathode coating of NASICON cathode materials to enhance cathode performance in Na-ion batteries S. Lavela, C. Pérez Vicente, P. Lavela and **J. L. Tirado**	**Prof. José L. Tirado**, Univ. Cordoba, **Spain**
09:30 - 09:45	Optimizing Slot-Die Coating of High-Viscous Slurries for Energy and Green Technology Applications K.V. Graae, J. Hansen and **V. Popok**	**Dr. Vladimir Popok**, FOM Technologies, **Denmark**
09:45 - 10:00	Sequential Surface Treatment and Insulation Testing of Additively Manufactured Litz Conductors **A.P Sankowski**, D. North and N. Simpson	**Dr. Andrzej P. Sankowski**, University of Bristol, **UK**
10:00 - 10:30	**Coffee Break**	
Session's Chairs: Prof. José L. Tirado, Univ. Cordoba, Spain Dr. Sneha Samal, Institute of Physics of Czech Acad. of Science, Czech Rep		
10:30 - 10:45	Surface Engineering of 3D-Printed PVA Structures for the Integration of Functionalized UCNPs into Stable Hydrogel Systems. **D.A. P. Guachalla**, M. Maturi, A. Sanz de León and M. Herrera	**Ms. Damaris. A.P. Guachalla**, Univ. de Cadiz, **Spain**
10:45 - 11:00	Characterization and Optimization of a Plasma Source for the Biological Decontamination of Wastewater in Volume **M. Saba**, C. Muja, Ph. Guillot and Th. Maho	**Mrs. Maria Saba**, INUC- Univ Toulouse, **France**
11:00 - 11:15	How Silicone–Acrylic Coatings Deliver Durable Ice Repellency for Wind Turbine Blades under Harsh Environmental Conditions **F. Eslampanah**, G. Momen and R. Jafari	**Mrs. Fateme Eslampanah**, Univ. Québec Chicoutimi **Canada**
11:15 - 11:30	Enhancing the Photocatalytic Activity of BiOBr Supported by Graphene Oxide for Antibiotic Degradation in Wastewater **S. Promrit**, C. Sronsri and S. Kaowphong	**Mr. Stanon Promrit**, Chiang Mai University, **Thailand**
11:30 - 11:45	Atmospheric-Pressure Plasma for the Degradation of Bisphenols as Emerging Contaminants in Aqueous Systems **C. Ruzafa Silvestre**, V.M. Serrano Martínez, L. Peinado Medrano, M.I. Maestre López, H. Pérez Aguilar and M.D. Romero Sánchez	**Dr. Carlos Ruzafa Silvestre**, INESCOP, **Spain**

08 May 2026		
Tribology 2026 Session III. B: Health, Safety & Industrial Impact / Biotribology		
Conference Room Dialog		
Session's Chairs: **Prof. Giuseppe Carbone, Nanjing University of Science & Tech, China / Polytechnic Univ. of Bari, Italy** **Prof. Jerzy Szpunar, University of Saskatchewan, Canada**		
09:00 - 09:30	Recent insights and persectives in silico modelling of synovil luvricated total Hip replacements **A.Ruggiero**	**Prof. Alessandro Ruggiero,** Univ. of Salerno, **Italy**
09:30 - 10:00	Tribological Investigation of Gear Ratio Effect on Wear Behaviour in Standard Spur Gears Y. Li, H. K Nguyen and **Z. Peng**	**Prof. Zhongxiao Peng**, University of New South Wales, **Australia**
10:00 - 10:30	**Coffee Break / Posters Session**	
10:30 - 10:45	Tribological Evaluation of Oral Lubrication and Soft Tissue Interactions **Y.C. Chang** and H.-W. Fang	**Dr. You-Cheng Chang**, National Taipei University of Technology, **Taiwan**
10:45 - 11:00	Simulating Tire Wear in the Laboratory: Linking Wear Behaviour of NR/BR Rubber Compounds with Fracture Energy **D. Rebenda** and R. Stocek	**Dr. David Rebenda**,, Tomas Bata University, **Czech Rep.**
11:00 - 11:15	Development of Process Optimization for FNC Brake Disc using DOE method **SM. Lee**	**Dr. Sangmok Lee**, Hyundai Motor Company, **Rep. of Korea**
11:15 - 11:30	Adhesive Performance of Mushroom-Shaped Microstructure in Wet Condition: the Role of Deformation **L. Nasca**, M. Santeramo, C. Putignano, E. Pierro and G. Carbone	**Dr. Luciana Nasca**, Polytechnic University of Bari, **Italy**

SICT 2026 / PlasmaTech 2026 / Tribology 2026 Joint Conferences Posters

06 and 07 May 2026 Sessions (No Posters session on 08 May 2026)

N.	Poster Title	Author, Affiliation, Country
1.	Influence of Diffusion-Modified Sublayers on the Performance of PVD Coatings on Austenitic Stainless Steel **K. Korsos** and D. Kovacs	**Mr. Krisztian Korsos**, Budapest University of Technology and Economics, **Hungary**
2.	Patterned Nafion–Enabled Selective-Area Doping and Stable Low-Resistance Contacts in 2D WSe_2 **S. Oh** and S. Im	**Mr. Sewoong Oh**, Yonsei University, Seoul, **Rep. of Korea**
3.	Functionalization of silica by nitrogen-containing silanes **K. Simanová** and I. Melnyk	**Mrs. Klaudia Simanova**, Institute of Geotechnics of SAS, **Slovak Rep.**
4.	Voltex-Assisted Scale-Up of Intense Pulsed Light Surface Treatment of Low-Grade Carbon Fibers for Epoxy Composite Applications Y.-J. Park, T.-Y. Kim and **K.-S. Kim**	**Dr. Kwang-Seok Kim**, Korea Institute of Industrial Tech. Jeonju, **Rep. of Korea**
5.	Bouncing characteristics of multi-component droplets with viscosity contrast for a control of the hydrodynamics **S. Yun**	**Prof. Sungchan Yun**, Korea National University of Transportation, **Rep. of Korea**
6.	Effect of Post-Heat Treatment on the Structural and Mechanical Properties of CrAlN/Al2O3 Functionally Graded Coatings for Tool Applications **W. R. Kim**, B. M. Lee, I. W. Park and S. B. Heo	**Dr. Wangryeol Kim**, Korea Institute of Industrial Technology- Busan, **Rep. of Korea**
7.	Thermo-mechanical analysis of the cutting interface during dry machining of UNS A97075 aluminium with uncoated tools **S. Martín-Béjar,** A. Moreno Arenas, F. Bañón García, L. Sevilla Hurtado and F. J. Trujillo Vilches	**Dr. Sergio Martín Béjar**, Univ. of Malaga, **Spain**
8.	Functional exterior and interior coatings involving surface treated nano-dispersions **S. Yilmaz Turan** , W. Zhao and P. Kasaplar	**Dr. Secil Yilmaz Turan** RISE Research Institutes of Sweden, **Sweden**
9.	Preparation and characterisation of YIG thin films deposited via DC Magnetron Sputtering for magnonic research applications **V. Faldu**, T. Reimann, O. Surzhenko, T. Friedrich, A. Gopakumar, O. Beier and A. Pfuch	**Mr. Vivek Bharatbhai Faldu**, INNOVENT, **Germany**
10.	Influence of Gas Admixtures and Target Materials on Plasma Gun Emission Characteristics **M. Moravčík**, K. Trebulová, E. Robert, A. Stancampiano and F. Krčma	**Mr. Marek Moravčík**, Brno University of Technology, **Czech Rep.**
11.	Challenges in determining the surface loss coefficient of hydrogen atoms on stainless steel in low-temperature plasmas A. Remigy, **M. Kassayova**, S.-J. Klose, A. Vahl, F. Hempel, N. Lang and J. H. van Helden	**Dr. Miroslava Kassayova**, Leibniz Institute for Plasma Science & Tech, **Germany**
12.	Cold Plasma–Liquid Synthesis and Optical Tuning of Surfactant-Free Au and Ag Nanoparticles for SERS Trace Explosives Detection **J. Olenik**, J. Štrbac, U. Cvelbar, J. L. Walsh and V.Shvalya	**Dr. Jaka Olenik**, Jozef Stefan Institute, **Slovenia**
13.	Laser irradiation for removal of a metallized coating on polymeric substrate S. Monteiro, G. Marques, P. Santos, R. Santos, L. Rodriges, F.M. Costa, A. Lopes da Silva, A. Barros and **N.M. Ferreira**	**Dr. Nuno Ferreira**, University of Aveiro, **Portugal**
14.	Optimization of laser parameters for the injection moulds residues cleaning P. Silva, F. Batista, R. Santos, T. Ferreira, **M.Ferro**, J. Figueiredo, F. Oliveira, L. Pereira, F.M. Costa and N. M. Ferreira	**Mrs. Marta Ferro**, University of Aveiro, **Portugal**
15.	New hybrid technology for deposition of transparent conductive oxide films for solar cell applications **A. Lacoste**, Z. Ennaji, A. Bès, P. Carroy and S. Béchu	**Prof. Ana Lacoste**, Univ. Grenoble Alpes, **France**
16.	Atomistic Insight into Sustainable Etching: Unraveling Halogen-Free Hydrogen and Fluorine Reaction Kinetics on the Si Surface **B. Bamdad**, X. Hu and J. Schuster	**Dr. Bahareh Bamdad**, Chemnitz Univ. of Technology, **Germany**
17.	Influence of the plasma discharge regime on the structure of metallic foams synthesized by plasma electrolytic **R. Botrel**, C. Boudat, F. Durut, A. Zentz, C. Noël and T. Belmonte	**Mr. Ronan Botrel**, CEA, **France**

18.	Plasma-Induced Polymerization of an Allyl Ether-Substituted Six-Membered Cyclic Carbonate with High Functional Group Retention E.M. Niemczyk, A. Gomez-Lopez, J.R.N. Haler, G. Frache, H. Sardon and **R.Quintana**	**Dr. Roberto Quintana**, Luxembourg Institute of Science and Technology, **Luxembourg**
19.	Quantitative measurement of hydrogen peroxide from plasma jet on soft materials **W. Zhang** and D. Caruana	**Ms. Wanqi Zhang**, UCL, **UK**
20.	Comparison of DECR and ASPN Plasma Contamination Inspection Using the Temporal Evolution of NO-γ and OH UV Emission Bands L. Bortoletto, C. Noël, R. Hugon, T. Czerwiec, A. Vidal and **G. Marcos**	**Mr. Gregory Marcos**, Institut Jean Lamour, Univ. Lorraine, **France**
21.	Improvement of the surface tribological properties of 42CrMo4 steel through the slide burnishing process **A. Dzierwa**	**Prof. Andrzej Dzierwa**, Rzeszow University of Technology, **Poland**
22.	Testing of friction connections of the spherical cap type **M. Wozniak**, A. Ryslki, S. Zakrzewski, D. Batory and K. Siczek	**Dr. Marek Wozniak**, Lodz University of Technology, **Poland**
23.	Anodic Aluminum Oxide Coating as a Dielectric Platform for Electrically Tunable Lubrication **M. García-Pérez**, S. D. Fernández-Silva, C. Roman, L. Lazar, J. D. Mozo, M. A. Delgado and M. García-Morales	**Ms. Maria Garcia Perez,** University of Huelva, **Spain**
24.	Modelling of the wear process in a two-surface system separated by a granular medium using DEM and reconstruction of the contact fields **K. Ligier**, M. Lemecha and O. Vrublevskyj	**Dr. Krzysztof Ligier**, University of Warmia and Mazury in Olsztyn, **Poland**
25.	Geometric modeling of granular bed particles in DEM simulations using image analysis methods **M. Lemecha**, K. Ligier and O. Vrublevskyi	**Dr. Magdalena Lemecha**, University of Warmia and Mazury in Olsztyn, **Poland**
26.	Tribo-induced microstructural evolutions and wear mechanisms of CoCrFeMnNi high-entropy alloy composite enhanced by Al/Ti doping and hBN/TiC dual ceramic reinforcement at elevated temperatures **W. Ma** and O. Tisov	**Mr. Wenbo Ma,** Xi'an Jiaotong University, **China**
27.	Investigation of contact-separation induced phenomena at the Silica-Gold interface **N. Ranjan**, T. Acartürk and U. Starke	**Dr. Nisha Ranjan,** Max-Planck Institute For Solid State Research, **Germany**
28.	Rapid Detection of Indoor Microbial Toxins on Various Surfaces with Direct Analysis in Real Time - Mass Spectrometry **R. Mikkola** and S. Heidi	**Dr. Raimo Mikkola**, Aalto University, **Finland**
29.	In Situ Gold Functionalization of Gallium Nitride Nanoparticles Mediated by Polyethyleneimine for Enhanced Electrochemical Sensing of Erythromycin **O-E. Carp**, D-L. Bostiog, E.L. Ursu, R. Mocanu, N-L. Marangoci, I. Tighineanu and A. Rotaru	**Dr. Oana-Elena Carp**, Petru Poni Institute of Macromolecular Chemistry, **Romania**
30.	Functionalized Carbon Dots as Multifunctional Biointerface Nano-materials for MRI and Fluorescence Imaging **A. Coroaba**, B-F. Craciun, A. Fifere and N-L. Marangoci	**Dr. Adina Coroaba**, Petru Poni Institute of Macromolecular Chemistry, **Romania**
31.	Practical Applications of Electron Microscopy for the Structural and Functional Characterization of Organic Nanoparticles **F. Doroftei**, R. Ghiarasim, N. Marangoci and M. Pinteala	**Dr. Florica Doroftei**, Petru Poni Institute of Macromolecular Chemistry, **Romania**
32.	Antibacterial Textile Surfaces Enabled by the Fungal Pigment Xylindein Produced by Chlorociboria aeruginascens **T. Onggar**, E. Sommer, M. Zschätzsch, A. Werner, L. Kliem, A. Pfriem, Th. Walther and Ch. Cherif	**Dr. Toty Onggar**, Technische Universität Dresden, **Germany**
33.	Characterization of a plasma discharge for the treatment of chronic wounds **S.N. Deguenon**, C. Muja, F. Sainct, T. Maho and P. Guillot	**Mr. Sessi Narcisse Deguenon**, INUC- Univ Toulouse, **France**
34.	Non-Thermal Plasma for Sustainable Seed Technologies **P. Lickova**, D. Kostolani, S. Mosovská, M. Khalaf, R. Švubová, V. Medvecká, D. Kováčik and A. Zahoranová	**Dr. Petra Lickova**, Comenius University Bratislava, **Slovakia**
35.	Non-Thermal Atmospheric Plasma-Induced Transformation of Agro-Industrial By-Products into Soil Improvers V. Crespo-Torbado, A. Álvarez-Ordóñez, R. Bodelón, Y. Chourak , PF. Rizzo, E. Garcia-Muchart, M. González-Raurich, M. Prieto, M. López and **M. Oliveira**	**Dr. Marcia Oliveira**, University of Leon, **Spain**
36.	Influence of Plasma and Plasma Treated Water on Plant Vitality in Short and Long-Term Applications	**Dr. Zdenka Kozáková**, Brno University of Technology, **Czech Rep.**

	Z. Kozáková, L. Krejsová, K. Šindelková, E. Neroda and K. Šťastná	
37.	Growth, Hydrogen Permeation, and Crystal field induced Stark shifts of Er2O3 thin film on SS316L and Si (001) H. Choi and **Y. Kim**	**Prof. Yongmin Kim**, Dankook University, **Rep. of Korea**
38.	Development of Pd and Pd-Ag Thin Films by Magnetron Sputtering for High-Performance Hydrogen Separation Membranes **A. D'Angelo**, S. Esposito, G. Rossi, C. Diletto, R. Volpe and M. Lanchi	**Mr. Antonio D'Angelo**, ENEA, **Italy**
39.	Surface Modification Approaches on Porous Hastelloy for Long-Lasting Hydrogen Separation Membranes **G. Rossi**, A. D'Angelo, C. Diletto, S. Esposito, A. Gugliemo and G. Rametta	**Dr. Gabriella Rossi**, ENEA, **Italy**
40.	Radiative cooling coating solution: principle and applications **H. Lee**, H. K. Im and J. I. Park	**Prof. Heon Lee**, Korea Univ. Seoul, **Rep. of Korea**
41.	Bismuth-Rich Oxyiodides as Highly Efficient Photocatalysts for the Visible-Light Photooxidation of As(III) **S. Kittiwachana**, S. Kaowphong, T. Charoensuk and C. Sronsri	**Dr. Sila Kittiwachana**, Chiang Mai University, **Thailand**
42.	Hydrothermal synthesis of BiOBr/Bi24O31Br10 Heterojunction Under pH-Controlled Conditions for Enhanced Dye Degradation, Antibiotic Removal, and Arsenite Oxidation **S. Kaowphong**, P. Wisedkoon and C. Sronsri	**Dr. Sulawan Kaowphong**, Chiang Mai University, **Thailand**
43.	Titanium Nitride Protective Coatings for High-Performance Proton Exchange Membrane Water Electrolysis **B. Chavan**, R. Kortlever and J. Ruud van Ommen	**Mr. Bhavesh Chavan**, Delft University of Technology, **The Netherlands**
44.	Equivalent-circuit based electrical characterization of an immersed DBD plasma source for liquid decontamination M. Saba, C. Muja, Ph. Guillot and **T. Maho**	**Dr. Thomas Maho**, INUC Univ. Toulouse, **France**
45.	Sustainable removal of carbamazepine from aqueous solutions using dielectric barrier discharge plasma: Efficiency, toxicity assessment, and environmental impact **Q.U. Din**, G. Iervolino and V. Vaiano	**Mr. Qayam U. Din**, University of Salerno, **Italy**
46.	Revealing the role of temperature in Non-Thermal Atmospheric Plasma-based water disinfection Á. Francés, M. Oliveira, R. Cordero-García, M. González-Raurich, A. Alvarez-Ordóñez and **M. López**	**Prof. Mercedes López**, University of Leon, **Spain**
47.	COLD PLASMA as novel technological strategy on fungal growth and metabolic inhibition: algal fungal isolates as case of study M; Gazquez-Coronado, M. Beyrer, C. Esteve, E; Mateo and M.C. Pina-Pérez	**Mrs. Maria Gazquez Coronado**, Univ. Valencia, **Spain**

SICT 2026 / Plasma Tech 2026 / Tribology 2026 Joint Plenary Session

Lowering the activation temperature of Ti-Zr-V non-evaporable getter films by removing surface carbon contamination

J. Fraxedas[1*], G. Sauthier [1], L. Tran[2] and V. Carlino[2]
[1] Catalan Institute of Nanoscience and Nanotechnology (ICN2), CSIC and BIST, Campus UAB, Bellaterra, Barcelona, 08193, Spain
[2] IBSS Group Inc., Burlingame, CA 94010, USA.

Abstract:
Distributed pumping on the inner walls of UHV chambers using thin films of non-evaporable getters (NEG) provides large pumping speeds and low ultimate pressures, outgassing/degassing rates and secondary electron yields, which is crucial for particle accelerators. Thin films of the successful quasi-stoichiometric combination of titanium, vanadium and zirconium exhibit activation temperatures of 180 degrees C after 24 h bakeout [1]. However, for several UHV systems this temperature is too high for sensitive instrumentation such as optics in beamlines of synchrotron radiation and free-electron lasers facilities, electron and gas analysers, detectors, motors, electronics such as preamplifiers, cables, special coatings, etc. Thus, the quest for lower activation temperatures continues to be an important goal, in particular in the particle accelerators and storage rings communities [2]. Here, we show that the removal of surface carbon contamination in Ti-Zr-V NEG films grown on stainless steel can decrease the activation temperature down to 150 degrees C after 20 h annealing, hence approaching the temperatures that the delicate instrumentation can tolerate. Carbon removal is achieved in situ by using a low-pressure inductively-coupled GV10x DS (downstream) Asher RF plasma source (http://ibssgroup.com/products/gv10x/) and the evidence of surface activation is assessed by means of in situ X-ray photoemission spectroscopy (XPS), as shown in Fig. 1. The films become fully activated after exposure to a 60 W plasma for 2 h using a mixture of argon (80%) and oxygen (20%) at 5×10^{-3} mbar and a subsequent annealing at 150 degrees C. For specific applications, the saturation of the NEG films after several activation cycles should be carefully considered and the systems designed accordingly.

Keywords: Ti-Zr-V non-evaporable getter coatings, surface activation, inductively-coupled RF plasma, carbon removal, X-ray photoemission spectroscopy.

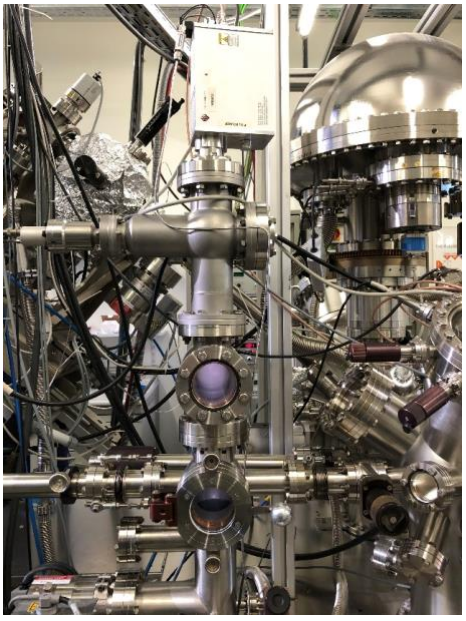

Figure 1: XPS system showing the GV10x DS Asher plasma source (top) attached to the fast-entry lock system (bottom) and the SPECS PHOIBOS150 hemispherical analyser (right).

References:

1. Benvenuti, C., Cazeneuve, J. M., Chiggiato, P., Cicoira, F., Santana, A. E., Johanek, V., Ruzinov, V., Fraxedas, J. (1999), A novel route to extreme vacua: the non-evaporable getter thin film coatings, *Vacuum* 53, 219.
2. Fraxedas, J., Schütte, M., Sauthier, G., Tallarida, M., Ferrer, S., Carlino, V., Pellegrin, E. (2021), In-situ XPS analysis of the electronic structure of silicon and titanium thin films exposed to low-pressure inductively-coupled RF plasma, *Appl. Surf. Sci.* 542 148684.
3. Fraxedas, J., Sauthier, G., Tran, L., Carlino, V. (2025), Lowering the Activation Temperature of Ti-Zr-V Non-Evaporable Getter Films by Removing Surface Carbon Contamination: An in Situ XPS Study. *Vacuum* 234, 114063.

A few basic (and historic) remarks on glows, arcs and hipims discharges

H. Kersten[1,2], C. Adam[1], V. Schneider[1], T. Trottenberg[1]
[1]Institute of Experimental and Applied Physics IEAP, Kiel University, 24098 Kiel, Germany
[2]Kiel Nano, Surface and Interface Science KiNSIS, Kiel University, 24118 Kiel, Germany

Abstract:
Gas discharges involving electrode and sheath phenomena have been studied for more than 250 years [1-3]. Already in the 19th century, papers were published regarding the use of optical emission to investigate the transition between a continuous glow discharge and an arc, the electrical structure and configuration of dc glow discharges, and the nature of metal atoms ejected from the cathode by sputtering [3].
Classification of discharge modes was initially based on their visual appearance and later by their current-voltage characteristics [2]. Oscillating or pulsing of power supplied, involvement of magnetic fields, gas flow pattern effects or of electrode geometry make the situation more complicated. Familiar terms such as “glow,” “arc,” “spark,” “corona” discharges hav evolved [4] and later further refinements such as “normal glow” vs “anomalous glow” and “thermionic arc” vs “cathodic arc” gave more structure to classifications and indicated growing insights into the various processes and conditions leading to specific discharges and their technological applications. Effects like secondary electron emission, thermionic emission, drifts in magnetic fields, gas heating and flow etc. affect the discharge mechanism as well and may influence complex electrode erosion used in magnetron sputtering and HiPIMS [5,6].
Some of the related plasma phenomena will be illustrated and a few historic remarks will be given in respect to basics, diagnostics and applications.

References

1. J. Cipo, H. Kersten, Vakuum in Forschung und Praxis **30**(2018), 34.
2. A. Anders, Appl. Phys. Rev. **11**(2024), 031310.
3. J.E. Greene, J. Vac. Sci. Technol. A **35**(2017), 05C204.
4. M. Faraday, Philosoph. Trans. Roy. Soc. London **128**(1838), 125.
5. A.P. Ehiasarian, R. New, W.-D. Münz, L. Hultman, U. Helmersson, V. Kouznetsov, Vacuum **65**(2002), 147.
6. C. Adam, L. Hansen, T. Hahn, J. Niemann, D. Zuhayra, G. Mark, J. Löffler, J. Benedikt, H. Kersten, Surf. Coat. Technol. **520**(2026), 133060.

Plasma process tool kit for the creation of customizable bio-instructive surfaces and interfaces

M. Bilek [1,2,3,4*]
[1] School of Physics, A28, University of Sydney, NSW 2006, Australia
[2] School of Biomedical Engineering, University of Sydney, NSW 2008, Australia
[3] Charles Perkins Centre, University of Sydney, NSW 2006, Australia
[4] Sydney Nano Institute, University of Sydney, NSW 2006, Australia

Abstract:
The growth and study of living cells outside their native organisms forms the foundation of modern biology and underpins medicine. It has led to the identification of stem cells and the development of methods that can reprogram mature cells into pluripotent states, creating enormous potential for new therapies that can cure previously untreatable conditions and enable the repair of patient-specific tissues and organs. Accessing these advances, however, will require the development of sophisticated new cell culture materials and technologies.
As cell behavior is directed by biochemical signals and local stiffness, our strategy is to enable reagent-free covalent immobilization of biomolecules and hydrogels onto cell-contacting surfaces. Energetic ion implantation into carbon-based surfaces or surface coatings creates buried radicals whose unpaired electrons migrate to the surface and form covalent bonds with proximate molecules. We have developed plasma processes that create these reactive surfaces on any material or structure. For structures created by 3D bioprinting, which is not compatible with low pressures, we developed a localized atmospheric pressure plasma treatment.
Functional molecules that can be immobilized include, but are not limited to, oligonucleotides, enzymes, peptides, aptamers, cytokines, antibodies, cell-adhesion extracellular matrix molecules, histological dyes, and hydrogels. Controlled application of the functional molecules in solution via droplet dispensing or contact printing enables the immobilization of biomolecular and hydrogel patterns onto the plasma-activated surfaces.
This talk will present our plasma processing tool kit and explain how it enables the creation of bio-instructive and biomimetic surfaces for wide-ranging applications in biomedicine, showing how the processes are adapted and engineered to be deployed on virtually any material and structure, including complex 3D or microporous structures as well as those formed by 3D bioprinting. Our processes are scalable and are currently being translated to industry for the production tunable bespoke biomimetic cell culture microwell plates.
Powered by renewable electricity, such plasma processing technologies, which require minimal amounts of gaseous reactants and generate virtually no waste, can provide sustainable solutions to a wide range of existing and emerging needs in biomedicine and biotechnology.

Keywords: plasma surface engineering, ion implantation, free-radical reactions, surface functionalisation within 3D bioprinting, surface surface modification for complex and internal structures, micropatterning, biomedical applications.

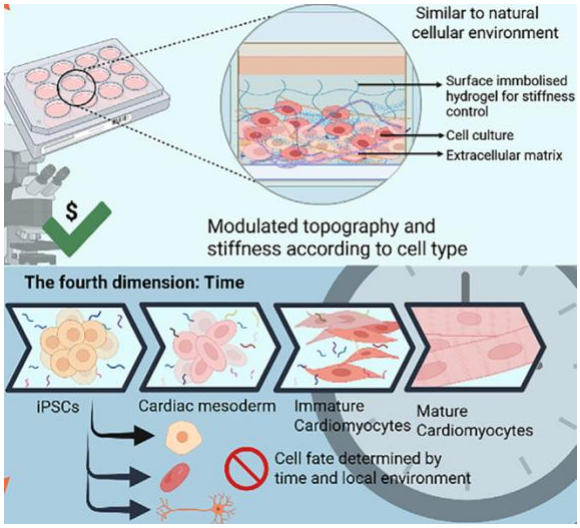

Figure 1: Diagram illustrating the complexity required for a truly biomemtic cell culture system that can accurately direct cell behaviours. Plasma processes that enable on contact tethering of functional biomolecules and hydrogels provide the capability to construct such cell culture systems for applications in drug discovery, cell therapy, diagnostics and personalized medicine. Adapted from [1].

References:

1. Gilmour et al, (2026) Appl. Phys. Lett. 128, 050501; doi: 10.1063/5.0301610

From Collisions to Control: Multiscale Modeling of Process Plasmas

Thomas Mussenbrock
Applied Electrodynamics and Plasma Technology (AEPT), Ruhr University Bochum, Germany

Abstract:
Low-temperature process plasmas are inherently nonequilibrium systems in which microscopic collision processes govern macroscopic behavior. Energetic electrons transfer electrical energy into internal degrees of freedom of atoms and molecules, thereby initiating excitation, ionization, and chemical transformation pathways that are inaccessible under thermal equilibrium conditions. As a consequence, macroscopic process characteristics such as conversion, selectivity, and efficiency are not imposed externally but emerge from the underlying microscopic kinetics.

This keynote presents a unified view on process plasma modeling that bridges scales from particle-level collisions to reactor-scale transport. Starting from the central role of electron kinetics and the electron energy distribution function as key control parameters, it is shown how different modeling approaches, including kinetic, fluid, and hybrid descriptions, arise naturally from the multiscale nature of the system. Particular emphasis is placed on the interplay between fast, localized energy deposition and slower transport processes, which together determine the overall process outcome.

Using selected examples from plasma-supported conversion and abatement processes, it is demonstrated that seemingly different applications share a common physical foundation: the control of reaction pathways through tailored electron energy distributions. The central message is that predictive modeling and rational design of process plasmas require a consistent description of this micro-to-macro coupling.

Controlling collisions means controlling plasma processes.

SICT 2026 Session I. A: Coating Deposition & Surface Treatment Technologies Surface Functionalization & Engineering Coating Characterization & Modeling

Sustainable Plasma -Enhanced Nanocoatings for Advanced Surface Functionalization

Pascal Vieth[a,*], Kevin Braun[b,*], Frank Hollmann[a], Ilya Ostrovsky[a], Birgit Fassbender[a]
[a] Chemetall GmbH, Frankfurt a. M., Germany
[b] Molecular Plasma Group BV, Leuven, Belgium

Abstract:
MPG's innovative coating technology uses cold, atmospheric plasma to activate and covalently bond organic precursors onto any substrate material. The ultra-thin films created by the single-step, dry and solvent-free process gives the surface a clearly defined functionality. The key distinction of the technology is its ability to process a wide range of chemical precursors, which extends across the entire spectrum of organic chemistry.
Combining MPG's technology now with Chemetall's extensive chemical solutions and expertise in surface treatment allows the development of specialized solutions for many different applications and industries. The joint development focuses on sustainable, application-specific solutions that enhance key surface functionalities including corrosion protection, adhesion promotion, hydrophobicity/hydrophilicity control and barrier performance.
Within the broader scope of the investigation, corrosion resistance was assessed through electrochemical methods such as impedance spectroscopy and neutral salt spray tests. The results demonstrated that the ultra-thin films were highly uniform and crosslinked, leading to superior corrosion resistance. These findings prove that applied organic nanolayers can significantly reduce process complexity while improving sustainability through solvent-free, energy efficient operation. By merging complementary strengths, MPG's scalable plasma technology and Chemetall's comprehensive chemical surface treatment solutions, the partnership aims to establish a new class of high-performance, customizable surface solutions that meet current and future industrial requirements.

Keywords: Atmospheric plasma, Ultra-thin films, corrosion protection, sustainable processing, surface functionalization

Deposition of Silazane Precursors by Atmospheric Pressure Plasma for the Development of Ultra-hydrophobic Fluorine-Free coatings

M. Saget*, K. Baba, S. Bulou, R. Quintana
Luxembourg Institute of Science and Technology, Advanced Plasma and Vapor Deposition Processes Engineering, L-4362 Esch-sur-Alzette, Luxembourg

Abstract:
Superhydrophobic surfaces are necessary in many application fields for repelling water-based solutions and providing non-adhesive properties. Since the 1950s, these coatings have been made of PFAS (per- and polyfluoroalkyl substances). However, fluorine-based coatings are persistent and accumulate in the environment and in human body raising health risks. Several strategies have been reported to replace PFAS in non-adhesive/repellent coatings. Nevertheless, these alternatives involve multiple processes, making them expensive and time-consuming to fabricate. In this study, an atmospheric pressure plasma jet (APPJ) was used, enabling a rapid and easily scalable deposition approach for large-scale production. Recently, we reported on the deposition of a cyclic silazane precursor exhibiting ultra-hydrophobic properties (i.e. water rolled off the surface). Based on this previous result, a series of silazane-based precursors were selected for this further study. Specifically, linear disilazanes (Si-N-Si), tetramethyldisilazane (TMDSN) and hexamethyldisilazane (HMDSN), and cyclic trisilazanes ($(Si\text{-}N)_3$), 1,1,3,3,5,5-hexamethylcyclotrisilazane (1,1,3,3,5,5-HMCTSN) and 1,2,3,4,5,6-hexamethylcyclotrisilazane (1,2,3,4,5,6-HMCTSN), were deposited onto silicon wafer surfaces. However only the later cyclic isomer demonstrated ultra-hydrophobic properties, even with lower deposition times. This result will be discussed based on the fully and partially methylated-Si, the location of the reactive bonds (N-H or Si-H), and their role in the formation of the resulting cauliflower-like morphology that developed on the wafer surface, where aggregates and smaller particles generate dual-scale roughness (Figure 1). Surface topography was calculated at two different scales using two techniques: confocal microscopy and atomic force microscopy (AFM), and surface chemistry was assessed using Fourier-transform infrared spectroscopy (FTIR) and X-ray photoelectron spectroscopy (XPS). Wettability behaviour was evaluated static and dynamic through droplet bouncing.

Keywords: atmospheric pressure plasma, remote discharge, superhydrophobic, fluorine-free, silazane, dual roughness

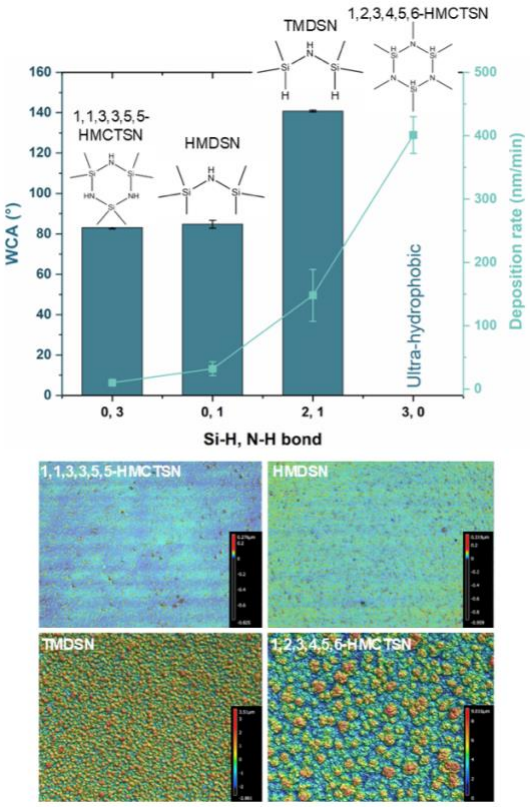

Figure 1: Top: Wettability and Deposition rate as the function of Si-H and N-H bonds, Bottom: 3D images showing cauliflower morphology.

References:

1. Meegoda, J. N., Kewalramani, J. A., Li, B., Marsh, R. W. (2020) A review of the applications, environmental release, and remediation technologies of per-and polyfluoroalkyl substances, *Int. J. Environ. Res. Public Health*, 17, 21, 8117
2. Rendon Piedrahita, C., Baba, K., Quintana, R., Choquet, P. (2024), Superhydrophobic surface development via atmospheric pressure plasma deposition of cyclic silazane, *Plasma Process. Polym.* 21:e2400097
3. Ward, L.J., Schofield, W.C.E., Badyal, J. P.S. (2003) Atmospheric Pressure Glow Discharge Deposition of Polysiloxane and SiOx Films, *Langmuir*, 19, 2110-2114
4. Pai, C.S., Miner, J. F., Foo. P. D. (1993) Electron cyclotron resonance microwave discharge for oxide deposition using tetramethylcyclotetrasiloxane, *J. Appl. Phys.*, 73, 7, 3531-3538

Hybrid Plasma Spraying for Novel Coatings with Tailored Architectures

T. Tesar [1,*], R. Musalek [1], F. Lukac [1], P. Capek [1]
[1] The Czech Academy of Sciences, Institute of Plasma Physics, Prague, Czechia

Abstract:
Hybrid plasma spraying is an innovative process combining powder and liquid feedstocks to deposit coatings with bimodal structure. Using this process, both feedstocks are injected simultaneously into the plasma jet and the primary particles are melted and deposited onto the workpiece as splats with vastly different dimensions. This approach enables the incorporation of a very fine secondary phase from the liquid feedstock into a relatively conventional coating formed from coarse splats (Figure 1). This process, however, requires specific conditions in order to successfully deposit both types of feedstocks as the powders generally require longer stand-off distances (SD), while SD required for liquid feedstocks are generally shorter due to the low inertia of the fine particles. In this study, we demonstrated the variability of this process using a high-enthalpy WSP-H plasma torch for ceramic feedstocks. Alumina (Al_2O_3) powder-based coatings were doped with several oxidic materials (chromia – Cr_2O_3, titania – TiO_2, yttria-stabilized zirconia – YSZ, zirconia – ZrO_2) as well as with high-temperature-sensitive sulfides (MoS_2, WS_2) using a modified external hybrid feeding setup to prevent decomposition of these materials. We showed how the deposition conditions, namely the stand-off distance, liquid injection geometry, and thermal loading influence the content and composition of the secondary phase, and in turn the functional properties of the coatings, such as wear resistance and adhesion strength.

Keywords: hybrid plasma spraying, ceramic coatings, alumina-based coatings, mechanical properties, wear resistance, tribology

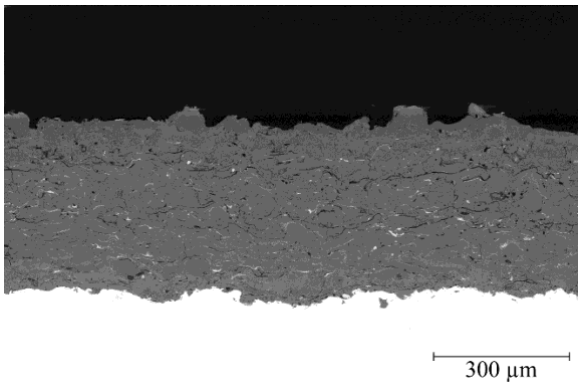

Figure 1: Cross-section of a hybrid plasma-sprayed coating from coarse alumina powder (Al_2O_3) and fine chromia suspension (Cr_2O_3). Alumina splats are displayed as darker gray matrix forming majority of the coating, chromia splats are visible as bright particles homogeneously distributed in the matrix. Pores and cracks are visible as dark spots and lines within the coating.

References:

1. Tejero-Martin, D., Rezvani Rad, M., McDonald, A., Hussain, T. (2019) Beyond Traditional Coatings: A Review on Thermal-Sprayed Functional and Smart Coatings, *J. Thermal. Spray. Technol.,* 4, 598-644.
2. Björklund, S., Goel, S., Joshi, S. (2018) Function-dependent coating architectures by hybrid powder-suspension plasma spraying: Injector design, processing and concept validation. *Materials and Design* 142, 56–65.

Forming novel micro- & nanostructures for advanced coating and bonding applications on copper by environmentally friendly electrochemical etching in seawater like electrolyte

J. Rank[1]*, J. Bahr[1], J. Carstensen[1] & R. Adelung[1]
[1] Department of Material Science,Christian-Albrechts-University Kiel, Germany

Abstract:
High-performance polymer coatings on metal substrates often require the use of chemical adhesion promoters. Several of these are known to be harmful to people or the environment and will therefore be banned in the European Union under the REACH regulation. This work presents a novel and promising approach to nanostructuring copper to enable advanced metal-polymer bonds and new coating possibilities.

This work introduces an environmentally friendly electrochemical sculpting process that uses a seawater-like electrolyte to create micro- and nanostructured surfaces on copper feature sub-micrometer undercuts that promote mechanical interlocking and wettability with polymers. Unlike conventional polymer coatings, whose performance relies on chemical surface interactions, these hierarchical structures eliminate the need for chemical bonding, thereby drastically increasing the range of compatible materials for strong, durable coatings. Furthermore, it could significantly reduce the need for harmful adhesion promoters in future applications.

While these structures are currently known for a variety of metals, such as stainless steel, aluminum and nickel titanium, they could not easily be reproduced on copper due to the lack of a chemically stable oxide. This talk will provide an overview of the newly established electrochemical etching process, as well as the requirements and possible pretreatments for the copper parts used.

Keywords: nanoscale sculpturing, microscale sculpturing, mechanical interlocking, REACH regulation, hierarchical structures, environmentally friendly, copper, polymeric coatings, electrochemical structuring,

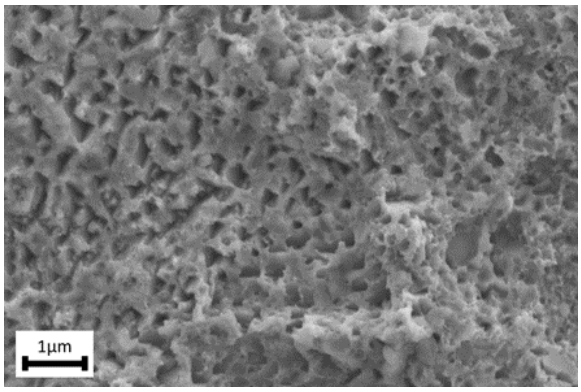

Figure 1: Copper Micro and Nanostructure showing a variety of possible interlocking features.

References:

1. Patent: DE102024111115A1, GEPULSTES ANODISCHES ÄTZ-HERSTELLUNGSVERFAHREN VON VERZAHNUNGSSTRUKTUREN AUF OBERFLÄCHEN VON KUPFER UND/ODER KUPFERLEGIERUNGEN, KUPFER UND/ODER KUPFERLEGIERUNGEN.

A Systematic Approach to Parameter Selection for Laser-Textured Grooves in Cemented Carbide Cutting Inserts

A. Moreno Arenas[1], F. J. Trujillo Vilches[1] , S. Martín-Béjar[1] , L. Sevilla Hurtado[1]
[1] Department of Civil, Materials and Manufacturing Engineering, Universidad de Málaga, Spain

Abstract:
The optimization of machining processes is critical for manufacturing efficiency, particularly in the aeronautical sector where the UNS A97075 (Al-Zn) alloy is widely used. This alloy presents significant challenges during machining, including poor chip fragmentation and the formation of Built-Up Edge (BUE) and Built-Up Layer (BUL), which compromise tool life and surface quality [1].
Laser Surface Texturing (LST) has emerged as a sustainable and precise method to modify tool topography, reducing friction and improving lubricant retention, which can lead to better chip morphology control and tool wear reduction [2,3]. However, achieving precise micro-geometries on cemented carbide requires a rigorous selection of laser parameters, especially when nanosecond equipment is used. Therefore, establishing a reliable methodology for parameter selection is essential before these tools can be implemented in high-performance machining processes.
In this work, a systematic methodology has been established to evaluate the influence of laser parameters on the geometry of micro-grooves, manufactured by LST techniques on cemented carbide inserts. The methodology relied on different Designs of Experiments (DoE). The study examines the influence of four basic laser parameters: laser speed (V), power (P), frequency (F), and pulse width (W) on groove morphology (depth, width, and burr height). Two initial exploratory studies have been performed. The first one testing a range of high-frequency parameters. While this stage resulted in almost no measurable groove depth, due to the material's resistance at those specific settings, it provided the critical feedback necessary to redirect the research. Hence, the preliminary trials carried out seem to indicate that laser frequency is one of the most influential parameters regarding material removal efficiency.
Initial observations suggest that lower frequency ranges are essential for achieving well-defined grooves and sufficient depth in the cemented carbide. This input was used to calibrate a second, more effective DoE, which shifted the focus toward lower frequencies. Furthermore, the results point toward laser speed as a critical factor for process stability, where reduced speeds appear to allow for more reproducible and controlled geometries. These findings establish a first fundamental understanding of the parameter-response landscape for texturing hard metal tools by nanosecond laser equipment, which may provide a low-cost means of implementing this technology at an industrial level, compared to the much more expensive use of femtosecond lasers.

Keywords: Laser Surface Texturing, Machining, Light Alloys, UNS A97075, Optimization.

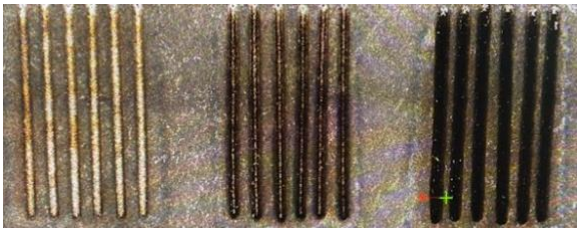

Figure 1: Textured micro-grooves on WC inserts using different laser parameters.

References:

1. Trujillo, F. J., Sevilla, L., Martín, F., & Bermudo, C. (2017). "Analysis of the Chip Geometry in Dry Machining of Aeronautical Aluminum Alloys." Applied Sciences, 7(2), 132.
2. Wan, Q., Zhong, W., Hu, X., & Yang, S. (2024). Review on the effect of surface textured tool in the field of machining. International Journal of Precision Engineering and Manufacturing, 25(1), 1–20.
3. García-Fernandez, J., Salguero, J., Batista, M., Vázquez-Martínez, J. M., & del Sol, I. (2024). Laser Surface Texturing of Cutting Tools for Improving the Machining of Ti6Al4V: A Review. Metals.

Acknowledgements: This work has received funding from the Ministerio de Ciencia e Innovación (Gobierno de España), through the research project "Sustainable Machining Artificial Intelligence- Optimized Textured Tools" (SMART-T) with reference PID2024-157116OB-I00

Al-Doped ZnO Transparent Conductors Deposited from a Two-Component Target: Properties and Flexibility Assessment

S. Kiełczawa [1], A. Wiatrowski [1], M. Mazur [1], W. Posadowski [1], J. Domaradzki [1]
[1]Department of Electronic and Photonic Metrology, Wroclaw University of Science and Technology, Wroclaw, Poland

Abstract:
Al-doped ZnO (AZO) thin films were deposited by reactive medium-frequency magnetron sputtering using a custom two-component Zn–Al metallic target, enabling stable aluminium incorporation without relying on expensive ceramic AZO sputtering targets. Three technological points (T1–T3) were fabricated on Corning glass by varying the Ar/O_2 ratio (80/20, 82/18, 84/16). Optical and electrical characterization revealed a clear trade-off between conductivity and transparency: layers produced closer to the dielectric mode exhibited the highest transmittance (≈84%) but elevated resistivity, whereas those deposited nearer to the metallic mode achieved significantly lower resistivity at the expense of reduced optical transmission. The T2 condition (Ar/O_2 = 82/18) provided the optimal balance, yielding ≈83% visible transmittance and a resistivity of $1.4 \cdot 10^{-3}$ Ω·cm. SEM imaging confirmed a dense, fine-grained morphology typical for AZO layers grown under well-stabilized reactive conditions, while EDS analysis revealed a uniform elemental distribution and an Al/Zn atomic ratio consistent with values commonly reported in the literature for high-quality AZO thin films [1, 2]. These results validate the effectiveness of the two-component metallic target concept in achieving controlled Al incorporation and reproducible material properties.
Using the optimized T2 parameters, AZO films were subsequently deposited on flexible polymer substrates, including Mylar®, Melinex® and standard industry-grade PET foil. Mechanical durability was assessed through repeated tensile and compressive bending across radii representative of flexible electronics testing. While all films maintained electrical continuity throughout cycling, clear differences between substrates were observed. AZO layers on Mylar and Melinex exhibited the highest mechanical stability, with only minor resistance evolution under repeated deformation, indicating strong adhesion and favourable strain distribution within the oxide layer. In contrast, films deposited on standard PET showed noticeably lower tolerance to mechanical stress, with an earlier onset of resistance drift and increased sensitivity to both bending radius and deformation mode.
Overall, the results demonstrate that AZO films obtained from a two-component Zn–Al target combine high transparency, low resistivity and robust mechanical performance. Their favourable behaviour on Mylar and Melinex substrates highlights their strong potential for next-generation flexible and transparent electronic devices, including sensors, displays and lightweight photovoltaic components.

Keywords: AZO, thin-films, magnetron sputtering, properties, two-element target

References:

1. Kim,K.H., Park, K.C., Ma, D.Y. (1997) Electrical and Optical Properties of Aluminum Doped Zinc Oxide Films Prepared by Radio Frequency Magnetron Sputtering,
J. Appl. Phys. 81, 7764–7772.
2. Minami, T. (2005) Transparent Conducting Oxide Semiconductors for Transparent Electrodes. *Semicond. Sci. Technol., 20, 35–44.*

Combinatorial deposition of gallium oxynitride thin films

M. Gajdics [1,2,*], I. Cora [1], T. Kolonits [1], Gy. Sáfrán [1], B. Pécz [1]
[1]Institute for Technical Physics and Materials Science, HUN-REN Centre for Energy Research, H-1121 Budapest, Hungary
[2]Department of Materials Physics, Eötvös Loránd University, ELTE, Pázmány Péter sétány 1/A, Budapest H-1117, Hungary

Abstract:
Recently, Ga-based wide bandgap semiconductor materials received an increasing interest. The investigations mainly focused on GaN-based power devices, such as high electron mobility transistors [1] and Ga_2O_3-based electronic and optoelectronic applications [2]. The ternary compound, gallium oxynitride can also have interesting properties for such applications, for example, optical properties may be tuned by changing the composition of the layer [3,4]. However, there are only limited amount of research dedicated to the sputter deposition of gallium oxynitride thin films.

In this work, our aim was to deposit gallium oxynitride films by reactive sputtering using a combinatorial method that enables to characterize the properties of the material with high troughput over a wide composition range. For the deposition, a liquid Ga target was used and the flow rate of the oxygen reactive gas was varied. In the combinatorial deposition, the elemental composition of the film has a gradient along the sample length, thus a whole composition range can be studied in one sample. The optical properties were investigated by spectroscopic ellipsometry, while the structure of the film was characterized by X-ray diffraction and transmission electron microscopy. The refractive index, optical bandgap and the crystal structure were determined and their variation was correlated with the change of elemental compostion. It was also shown that these properties can be tuned by carefully controlling the deposition conditions.

Keywords: gallium oxynitride, reactive sputtering, combinatorial deposition, optical properties

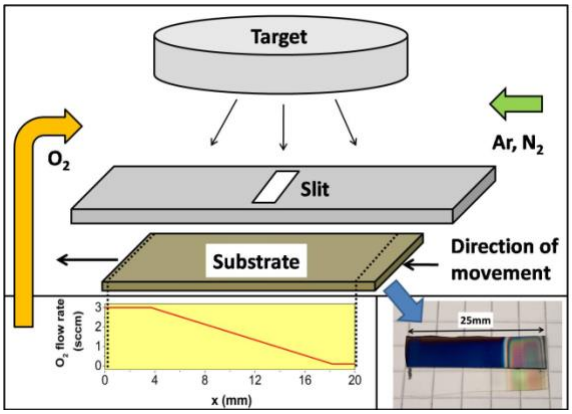

Figure 1: Schematic illustration of the combinatorial deposition setup with a moving substrate and changing oxygen flow rate.

References:

1. He, J., Cheng, W.-C., Wang, Q., Cheng, K., Yu, H., Chai, Y. (2021) Recent Advances in GaN-Based Power HEMT Devices, *Adv. Electron. Mater*. 7, 2001045.
2. Pearton, S.J., Yang, J., Cary, P.H., Ren, F., Kim, J., Tadjer, M.J., Mastro, M.A., (2018) A review of Ga_2O_3 materials, processing, and devices, *Appl. Phys. Rev*., 5, 011301.
3. He, H., Wu, C., Hu, H., Wang, S., Zhang, F., Guo, D., Wu, F., (2023) Bandgap Engineering and Oxygen Vacancy Defect Electroactivity Inhibition in Highly Crystalline N-Alloyed Ga_2O_3 Films through Plasma-Enhanced Technology, *J. Phys. Chem. Lett.,* 14, 6444-6450.
4. Ma, H-P., Li, X-X., Jang, J-H., Cheng, P., Huang, W., Zhu, J., Jen, T-C., Guo, Q., Lu, H-L., Zhang, D.W., (2019) Composition and Properties Control Growth of High-Quality GaO_xN_y Film by One-Step Plasma-Enhanced Atomic Layer Deposition, *Chem. Mater*., 31, 7405-7416.

Optimization for the composition gradient of Al-O-N thin film deposited by reactive RF sputtering technology

M. Serényi[1*], M. Gajdics[1,2], D. Olasz[1,2] and G. Sáfrán[1]
[1]Institute for Technical Physics and Materials Science, HUN-REN Centre for Energy Research, 1121 Budapest Konkoly-Thege 29-33, Hungary
[2]Department of Materials Physics, Eötvös Loránd University, 1117 Budapest, Pázmány Péter sétány 1/A, Hungary

Abstract:
In samples produced by combinatorial deposition with varying compositions [1], the concentration gradient of the different components should ideally be constant, or at least not extremely steep. This facilitates the interpretation of characterization results, such as EDS, ellipsometry, or TEM measurements. In this work, a combinatorial approach was used to achieve efficient synthesis and characterization of the entire aluminium-oxynitride (AlON) layer system ranging from Al-oxide to Al-nitride. The layers were deposited from an Al target on Si wafers by reactive RF sputtering. In our preliminary experiments, we found that due to so-called target poisoning, the O/(O+N) concentration gradient became unmanageably steep. In order to produce a combinatorial sample with the appropriate gradient features the equations of the Berg model describing the process were studied. A simple graph of the processing parameters (pumping speed, partial pressure) was created with the aim of avoiding the hysteresis, typically, characteristic of the reactive sputtering process. Based on the results of the model calculation, we selected the sputtering technological parameters: while the partial pressures of argon and nitrogen were kept constant in the vacuum chamber, oxygen was introduced by gas pulse control technique. This technique prevented target poisoning and enabled a smooth transition between aluminium oxide and aluminium nitride components in the combinatorial sample. The present approach has facilitated the efficient exploration of the relationship between sputtering parameters, structure and material properties of the Al-O-N layer system. SEM, TEM, EDS revealed amorphous to wurtzite type crystalline structure along with the compositional change from Al-oxide to Al nitride, respectively [3]. Spectroscopic ellipsometry showed that the refractive index of the sample varied between 1.63 and 2.08.

Keywords: RF sputtering, Alumina, Aluminium nitride, Oxynitrides, Berg model, hysteresis

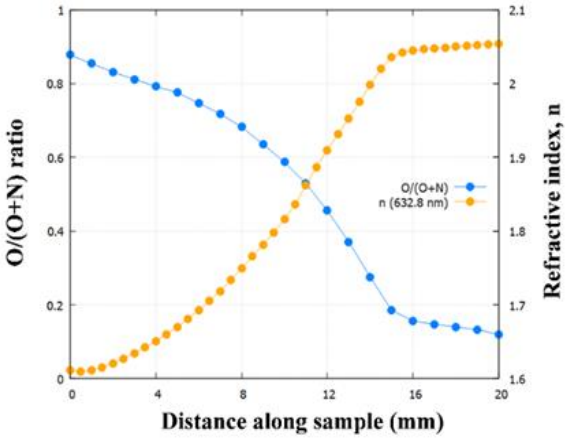

Figure 1: Variation of O/(O + N) ratio along the combinatorial Al-O-N layer and the corresponding refractive index (n) revealed by EDS and spectroscopic ellipsometry at 632.8 nm wavelength. Both composition and refractive index show a smooth transition from Al-oxide to Al-nitride**.**

References:

1. Sáfrán, G. (2008) "One-sample concept" micro-combinatory for high throughput TEM of binary films, *Ultramicroscopy*, 187, 50-55.
2. Gajdics, M., Hegedüs, N., Olasz, D., Serényi, M. (2025) Assistance to Determine the Stability State of a Reactive Sputtering Process Based on the Analytical Solution of the Classical Berg Model, *Coatings*, 15, 499.
3. Frick, S.et al. (2025) Accelerating the development of oxynitride thin films: A combinatorial investigation of the Al-Si-O-N system, *Phys. Rev. Mat.,* 9, 103803.

Hierarchical surfaces: theory, computational analysis and experimental characterization

G. Papavieros[1,2], V. Constantoudis[1,2], Aggelos Zeniou[1], Stavros Stavromitros[2], E.Gogolides[1,2]
[1]Institute of Nanoscience and Nanotechnology NCSR Demokritos, Agia Paraskevi, 15341, Greece
[2]Nanometrisis P.C, Agia Paraskevi, 15341, Greece

Abstract:
Despite the wide usage of hierarchical surfaces today in many research areas and applications, a systematic theoretical framework and computational methodology for their quantitative characterization and deeper understanding is missing. To fill this gap, first we elaborate a) a theoretical framework with the proper definitions and clarifications, b) a classification scheme to highlight the multiple types of hierarchical surfaces and c) a mathematical and computational methodology mainly based on Correlation, Fourier and multifractal analysis for their quantitative characterization. The latter aims at the identification of their hierarchy type, the calculation of their critical parameters and the quantification of the interactions between their hierarchy levels [1].
In order to validate the developed methodology, we apply it in synthesized surfaces consisting of periodic, mound and self-affine hierarchy levels to highlight the meaning of the output metrics (see Fig.1).
Then we proceed to applications in real experimental surfaces, as the proposed methodology can provide the necessary information to assess the quality and features of the produced surfaces and structures and consequently tune their process parameters and predict their performance. The first case includes polymer surfaces etched in a newly developed plasma reactor, where the gradual formation of hierarchy on surface topography can be witnessed and controlled [2]. The second case focuses on the sidewall roughness of lithographic line/space patterns (i.e. Line Edge Roughess) used in the manufacturing of modern integrated circuits. Both synthesized and real Scanning Electron Microscopy images will be employed to detect and quantify the different hierarchical levels in LER while special emphasis will be paid on the impact of etch-induced pattern transfer process on LER hierarchy levels. In both experimental cases, the analysis focuses on distinguishing the different types and levels of hierarchy, quantify them with the proper set of parameters and elaborate the role of level interaction analyzing the multifractal spectra of surface morphology.

Keywords: hierarchy, multiscale surfaces, Fourier analysis, multifractals, spatial correlations

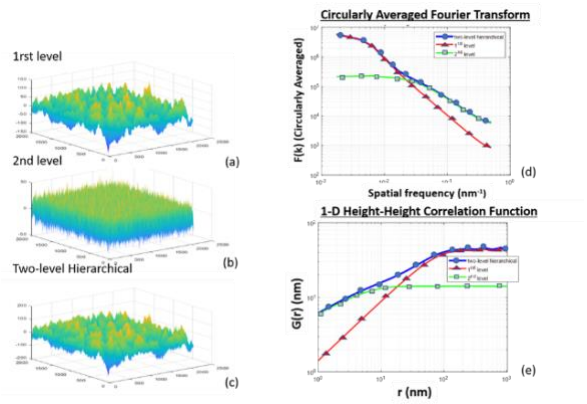

Figure 1: Formation of a synthetic hierarchical surface (c) by the addition of two self-affine surfaces with high (a) and small (b) correlation length respectively. Their Fourier spectra are also shown (d) along with their correlation functions (e) indicating the characteristic presence of a knee in the metrics of hierarchy.

References:

1. G Papavieros *et al* 2023 *Nanotechnology* **34** 405702
2. A Zeniou *et al* 2021 *Nanotechnology* 32 235305

Acknowledgment

This work is supported by the project "Enhancing plasma etching efficiency, repeatability, and
environmental footprint via AI-based modeling and optimization (plasmAI)" of the program "AIAware Pathways to Sustainable Semiconductor Process and Manufacturing Technologies", Intel Corporation & Merck KGaA.

High-Throughput Combinatorial Characterization of thin Binary and Ternary Layers

G. Sáfrán[1], M. Gajdics[1,2], D. Olasz[1,2] N. Szász[1], Nguyen Quang Chinh[2] and M. Serényi[1]
[1]Institute for Technical Physics and Materials Science, HUN-REN Centre for Energy Research, 1121 Budapest Konkoly-Thege 29-33, Hungary
[2]Department of Materials Physics, Eötvös Loránd University, 1117 Budapest, Pázmány Péter sétány 1/A, Hungary

Abstract:
The novel, single-sample concept combinatorial method developed for direct sputter deposition and TEM investigation of whole 2- and 3 component layer systems has been shown to be suitable for the high-throughput comprehensive characterization of multicomponent thin films over an entire composition range. This paper, after a short description of the method, focuses on recent results regarding the characteristics of different binary and ternary films prepared by direct current (DC) and radiofrequency (RF) sputtering using the micro-combinatorial technique. In addition to the 3 mm diameter grid used for TEM microstructural and EDS analysis, scaling up the substrate size to 10 x 25 mm^2, this novel approach has allowed for a comprehensive study of the properties of the materials as a function of their composition, which has been determined via transmission electron microscopy (TEM), scanning electron microscopy (SEM), Rutherford backscattering spectrometry(RBS), X-ray diffraction analysis (XRD), atomic force microscopy (AFM), spectroscopic ellipsometry, and nanoindentation studies. Thanks to the micro-combinatory technique, the characterization of multicomponent layers can be studied in greater detail and efficiency than before, which is beneficial for both research and practical applications. In addition to new scientific advances, we will briefly explore the potential for innovation with respect to this new high-throughput concept, including the creation of databases for two- and three-component thin films. The structural and mechanicalproperties i.e., the hardness and deformation mechanisms of AlMg and AlCu layer systems were revealed at up to 30%Mg and in the full concentration range, respectively. By using micro-combinatory methods, the optical properties (n and k) of the complete binary system of amorphous H:SiGe were revealed as a whole material database. The variations in the refractive index (n) of the ternary systems of Me-oxinitrides (Me=Hf, Si, Ge, Al) were revealed in the whole composition range from Me-oxide through Me-oxynitride to Me-nitride. Figure 1 shows, for the first time, an entire thin film phase map (database) of a reactively DC magnetron sputtered YxTi1-xOy layer system over the entire Y/Ti composition range, from room temperature up to 800 °C

Keywords: micro-combinatorial approach, efficient characterization, two- and three-component films; entire range of composition

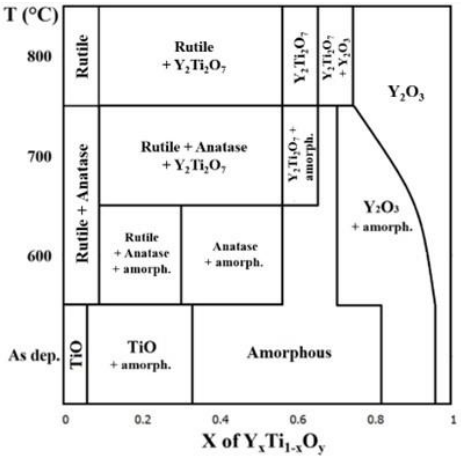

Figure 1: Compiled phase map (database) of the reactive DC magnetron sputtered YxTi1-xOy thin film system over the entire Y/Ti composition range, up to 800 °C.

References:

1. Sáfrán, G. (2018) "One-sample concept" micro-combinatory for high throughput TEM of binary films, *Ultramicroscopy*, 187, 50-55.
2. Olasz, D.; Kis, V.; Cora, I.; Németh, M.; Sáfrán, G. (2024) High-Throughput Micro-Combinatorial TEM Phase Mapping of the DC Magnetron Sputtered $Y_xTi_{1-x}O_y$ Thin Layer System NANOMATERIALS 14 : 11, Paper 925.

Piezo-Assisted RF Magnetron Sputtering of Ni Nanoparticles on TiO_2 Powder Supports for Electrocatalytic Applications

Chandrakanth Reddy Chandraiahgari[1], Gloria Gottardi[1], Giorgio. Speranza[2], Domenico Dalessandro[1], Matteo Bordin[1], Victor Micheli[1], Ruben Bartali[1], Matteo Testi[1].
[1]Center for Sustainable Energy, Fondazione Bruno Kessler (FBK), Trento, 38123, Italy
[2]Center for Sensors and Devices, Fondazione Bruno Kessler (FBK), Trento, 38123, Italy

Abstract:
Water electrolysis is a strategic technology for renewable hydrogen production, but its commercialization is limited by the cost and availability of efficient electrocatalysts.[1] Nickel (Ni) has emerged as a promising non-precious metal catalyst due to its high activity, stability, and durability.[2] This study presents a green, dry, and scalable approach for the preparation of Ni-coated TiO_2 nanopowders via plasma-assisted radio frequency (RF) magnetron sputtering.[3] The process introduces a unique piezo-assited vibrating sample holder, which promotes tumbling of the nanopowder during deposition, improving nanoparticle dispersion, and surface coverage on commercial TiO_2 powder supports. Morphological analysis using FE-SEM and STEM revealed spherical TiO_2 NPs (10–90 nm) uniformly coated with Ni, while XRD confirmed the preservation of anatase/rutile phases and the presence of Ni (111) planes with crystallite sizes of ~18 nm. EDX and XPS surface chemical analysis demonstrated chemical purity and homogeneous Ni distribution. Electrochemical testing in 0.5 M KOH showed enhanced hydrogen evolution reaction (HER) performance for the vibrating-mode samples, with an onset potential of 0.6 V, a Tafel slope of 33 mV/dec, and stable operation at 10 mA/cm² over 2 hours.[4] These findings demonstrate that mechanical vibration during RF sputtering significantly improves structural uniformity and electrocatalytic performance. The approach represents a versatile, single-step, and environmentally friendly method to prepare high-purity Ni/TiO_2 nanohybrids. Ongoing work focuses on extending this method to NiFe/TiO_2 nanohyrbids to further enhance catalytic activity and durability for green hydrogen production.

Keywords: RF Magnetron Sputtering, Nanohybrids, Ni coated TiO_2, Piezo-assited sputtering, Sputtering on powders, Hydrogen Evolution Reaction (HER).

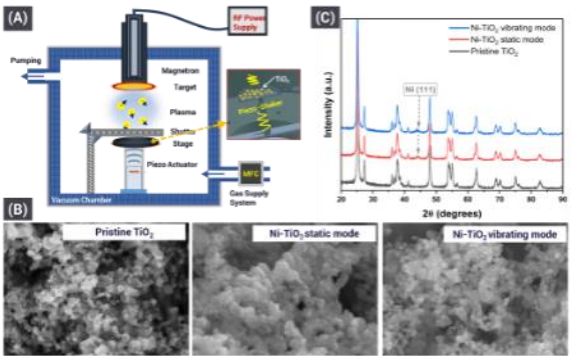

Figure 1: (A) Shematic Illustration of Piezo-assited RF sputtering, (B) FE-SEM images, and (C) XRD spectra, of pristine Ni coated powders.

References:

(1) Al-Douri, A.; Groth, K. M. Hydrogen Production via Electrolysis: State-of-the-Art and Research Needs in Risk and Reliability Analysis. *Int. J. Hydrog. Energy* **2024**, *63*, 775–785.
(2) Dilshara, P.; Abeysinghe, B.; Premasiri, R.; Dushyantha, N.; Ratnayake, N.; Senarath, S.; Sandaruwan Ratnayake, A.; Batapola, N. The Role of Nickel (Ni) as a Critical Metal in Clean Energy Transition: Applications, Global Distribution and Occurrences, Production-Demand and Phytomining. *J. Asian Earth Sci.* **2024**, *259*, 105912.
(3) Chandraiahgari, C.; Gottardi, G.; Speranza, G.; Pedrielli, A.; Micheli, V.; Bartali, R.; Laidani, N.; Testi, M. Role of Oxygen Plasma for Improved Preparation of Cu/CNT Nanohybrids by RF Sputtering. *Surf. Coat. Technol.* **2025**, *513*, 132469.
(4) Chattopadhyay, J.; Srivastava, R.; Srivastava, P. K. Ni-Doped TiO2 Hollow Spheres as Electrocatalysts in Water Electrolysis for Hydrogen and Oxygen Production. *J. Appl. Electrochem.* **2013**, *43* (3), 279–287.

Safe and sustainable by design approach for omniphobic PFAS-free ceramic-like coatings for glass packaging

E. Khousakoun[1], M. Poelman[1], S. Desprez[1] , A.-L. Dechief[1], B. Belloncle[1], A. Mezy[2] , J. Alcodori, P. Lledo[3], A. Rashid[4], A. Nelson[4]

[1.] MATERIA NOVA, Avenue Copernic 3 7000 Mons Belgium

[2.] SIKEMIA Cap Gamma, 1682 rue de la Valsière 34790 GRABELS, France

[3.] ITENE Calle Albert Einstein 1, Parque Tecnológico de Valencia, 46980 Paterna (Valencia), Spain

[4.] School of Chemistry and Faculty of Engineering and Physical Sciences, University of Leeds, Leeds LS2 9JT, United Kingdom

Abstract:

BIO-SUSHY, a Horizon Europe initiative, aims to develop innovative, PFAS-free coating technologies aligned with the EU Chemical Strategy for Sustainability and its objective of achieving a toxic-free environment. The project focuses on bio-based, durable water- and oil-repellent coatings designed through an integrated approach combining research and innovation in coating development, performance-driven computational modelling, toxicity assessment, and the Safe and Sustainable by Design (SSbD) framework.

Glass packaging domain for cosmetic applications is one of the case studies. Hybrid organic–inorganic coatings based on sol-gel technologies are being developed for application on the inner surfaces of cosmetic glass containers to ensure product quality, protect the formulation, and enable complete product recovery. These coatings comply with restrictions on hazardous substances in cosmetic products while providing additional functionalities, including reduced product waste (up to 20–25%), improved cleanability of the containers to support reuse, and preservation of surface aesthetics. Hybrid sol-gel technology offers a particularly suitable platform for achieving these combined performance objectives.

By enabling complete product recovery and facilitating packaging reuse, BIO-SUSHY coatings contribute to waste reduction and enhanced circularity in cosmetic packaging. The systematic implementation of the SSbD framework throughout development ensures minimal reagent toxicity, limits the environmental impact of emitted chemical species, and prevents their release into the packaging content.

Acknowledgment

The BIO-SUSHY project is funded by the European Union under the Grant Agreement Number 101091464. Views and opinions expressed are however those of the author(s) only and do not necessarily reflect those of the European Union or the European Health and Digital Executive Agency (HaDEA). Neither the European Union nor the granting authority can be held responsible for them.

From Lignin Depolymerization to BPA-Free Epoxy Coatings: A Scalable Biobased Route for Construction Materials

M. Comí [1]
[1] Safe & Sustaniable Polymer Technologies (SPOT) Research Group,
Materials & Chemistry (MatCh) Unit, VITO N.V. Mol, Belgium.

Abstract:
The LEGACY project demonstrates the availability of biobased alternatives to bisphenol-A (BPA) for the epoxy resin sector, addressing the environmental and health concerns associated with this endocrine disruptor by eliminating BPA from epoxy resin formulations used as high-performance coatings, particularly for heavy-duty construction applications. The project has investigated the viability, efficiency, and reproducibility of producing biobased bio-epoxy precursors, while continuously monitoring their environmental safety and sustainability. Based on these intermediates, novel BPA-free epoxy resin formulations have been designed with the objective of achieving high material performance and reduced surface degradation.

The approach reduces fossil resource dependency by valorizing lignin, the most abundant natural aromatic biopolymer, largely generated as a byproduct of the Kraft pulping process and predominantly incinerated. The complex lignin structure was fractionated using dissolution and reductive catalytic depolymerization to reduce molecular weight, increase functional group accessibility, and improve solubility. Pilot-scale production was enabled through VITO's Pillar II and LignoValue infrastructures, generating reliable scale-up data. The resulting lignin monomers were functionalized via glycidylation, The new biobased intermediates were evaluated for eco-toxicological impact under a Safe and Sustainable by Design (SSbD).
Fully biobased epoxy resin formulations with high lignin content were subsequently developed, overcoming limitations observed in existing bio-epoxy systems. Structural, thermal, mechanical, and morphological characterizations confirmed performance comparable to conventional BPA-based resins. Coating formulations were applied to different substrates, and large-scale demonstrations on concrete flooring enabled assessment of real-use performance and degradation behavior. Environmental release during surface treatment and degradation was analyzed and benchmarked against commercial BPA-based coatings. The results demonstrate that BPA-free biobased epoxy coatings can achieve high performance with reduced environmental impact, supporting their viability for industrial and construction applications.

Figure 1: Scheme of LEGACY project step, from bio-based lignin precursors to BPA-free coating for construction applications.

Keywords: Biobased epoxy resins, lignin valorization, bisphenol-A replacement, glycidylation, Safe and Sustainable by Design (SSbD), construction coatings, pilot-scale production, environmental performance.

References:

1. Comí, M., Apellaniz, E., Jusner, P., Sridharan, B., Servaes, K., Vendamme, R. (2025), Monitoring pilot-scale lignin depolymerization via nanoparticle size in water: A sustainable qualitative method, Materials Today Sustainability, 32, 101245.
2. Celada, I., Apellaniz, E., Pérez, A., Jusner, P., Vendamme, R., Comí, M. (2026), Impact of the biobased transition on the properties of depolymerized lignin-derived epoxy resin for metal coating applications, Progress in Organic Coatings, 213, 109931.

Non-destructive automated mechanical characterization for coatings and surfaces using surface acoustic wave spectroscopy

S. Makowski [1,*], M. Zawischa [1], R. Knieß [1], Arshad Arshad [1], Fabian Härtwig [1]
[1] Department of Thin Film Technology, Fraunhofer Institute for Material and Beam Technology IWS, Dresden, Germany

Abstract:
In recent years, non-destructive surface acoustic wave spectroscopy has emerged as a powerful method for studying the mechanical properties of surfaces and coatings, including the influence of defects such as pores, cracks, and delamination. The method has already been applied in several scenarios, including HVOF-sprayed cemented carbide coatings, laser-cladded brake disks, nitride and case-hardened surfaces, PVD coatings in the range of few micro meters, as well as ALD coatings in the nano meter range. The ability to complete a measurement in less than a minute enables data collection from many measurement points with minimal effort. Automating the measurement process allows mapping of samples to study how factors like plasma distribution, coating gun trajectories, and heat distribution affect mechanical properties without destroying the part or sample[1].
Historically, the evaluation of surface acoustic waves was a manual process, typically involving fitting a substrate-coating material model to the dispersion curve of the measured data. While this step can be automated for some applications, this approach is limited when deviations from the ideal material cannot be modeled as a homogeneous coating.
In this work, a new strategy is employed in which a modified LAwave measurement system is used for automated measurements to obtain large-volume data for training a neural network. It is demonstrated that different coating characteristics such as defects can be distinguished fully automatically and with high precision. Investigated surfaces include thermally sprayed cemented carbide coatings, laser-cladded brake disks, and superhard tetrahedral amorphous carbon coatings.

Keywords: non-destructive testing, surface acoustic wave spectroscopy, brake disk coating, HVOF coatings, mapping, ta-C, DLC, quality control

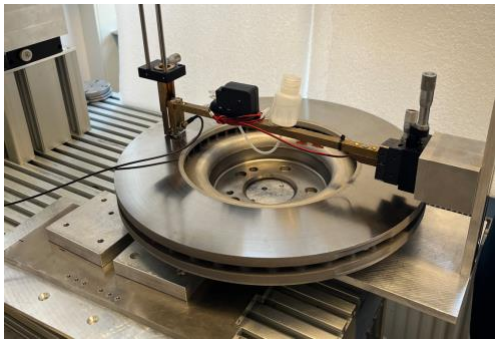

Figure 1: Experimental setup for mechanical characterization of full scale mapping of brake disk with lasser-cladded coatings

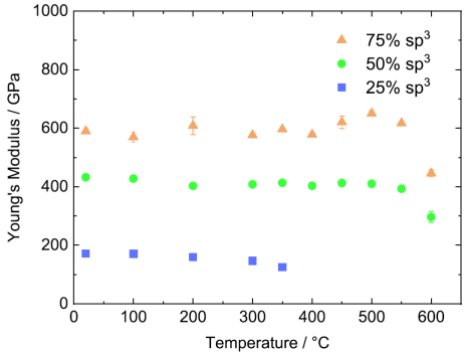

Figure 2: Mechanical characterization of (tetrahedral) amorphous carbon coatings with in-situ high-temperature measurement shows temperature stability with strong dependence of sp^3-carbon content[2].

References:

1. Zawischa, M., Makowski, S., Toma, F.-L., (2024) Fast and Nondestructive Mechanical Characterization of Thermally Sprayed and Laser Cladded Coatings: Automated Surface Acoustic Wave Spectroscopy as a New Tool for Quality, *J Therm Spray Tech,* 34, 928-938
2. Makowski, S., Zawischa, M., Schneider, D., et al., (2024) Surface acoustic wave spectroscopy for non-destructive coating and bulk characterization at temperatures up to 600°C enabled by piezoelectric aluminum nitride coated sensor, *Surf Interface Anal.* 2024; 1-14

Microstructured impregations of Carbon Yarns for Graded Interphases in Concrete

L. Flechsig [1*], G. K. Auernhammer[1],C. Scheffler[1,2]
[1] Department Fiber-Engineering, Leibniz Institute of Polymer Research, Dresden, Germany
[2] Institute of Construction Materials, Dresden University of Technology, Dresden, Germany

Abstract:
Carbon concrete uses textile fabrics made up of numerous individual filaments instead of steel reinforcement. The corrosion resistance of the material allows for reduced concrete cover, enabling thinner, more resource-efficient, and climate-friendly constructions.[1] For optimal force transmission within the textile, the filaments are typically impregnated with a polymer that bonds the individual filaments and stabilizes the geometry.[2] However, this impregnation creates a smooth, closed surface that reduces the bond with the concrete and can lead to premature, brittle failure mechanisms. [3]

The aim of this work is to improve the bond by specifically structuring the impregnation layer: open pores in the outer surface of the carbon yarns are intended to allow the concrete matrix to penetrate, thus creating a gradual material transition and forming mechanical interlocking. The microstructured interphase is produced by the particulate leaching technique: Carbon yarns are impregnated with epoxy resin, then water-soluble sacrificial particles are applied. After the resin has cured, the particles are washed out, leaving behind an open-pored system (Fig. 1). Significant optimization tasks relate to the particle surface energy in order to avoid thin resin coatings on the particles, which lead to closed pores. The successful formation of the open pore structure is verified using SEM and µ-CT.

Additionally the wetting properties of the porous surface was optimised to ensure optimal penetration of the concrete matrix. To quantify wetting, contact angle measurements are performed on non-porous layers using a model solution of the concrete matrix. Penetration into porous layers is analyzed using camera-based imaging.

Keywords: epoxy resin, impregnation, sacrificial template, microstructured surface, contact angle.

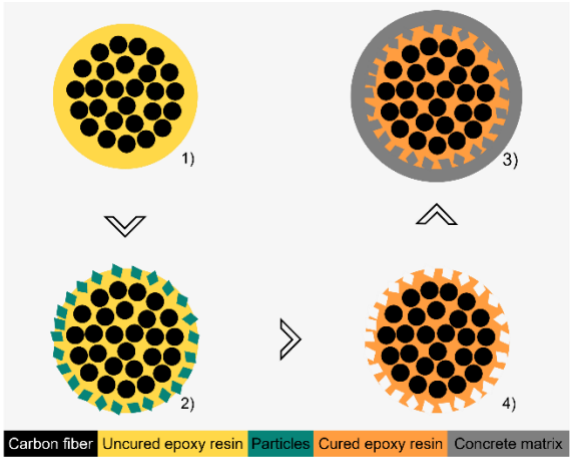

Figure 1: Schematic representation of the procedure to achieve a open-pore structured surface of an impregnated carbon yarn: 1) Impregnation with epoxy resin 2) Application of sacrificial particles 3) Leaching of the particles after curing 4) Optimized penetration of concrete matrix into pores for mechanical interlocking.

References:

1. Curbach M, Hegger J, Bielak J, Schmidt C, Bosbach S, Scheerer S, et al. (2024) New perspectives on carbon reinforced concrete structures—Why new composites need new design strategies, *Civil Engineering Design.*, 5(5–6), 67–94.
2. Friese, D., Scheurer, M., Hahn, L., Gries, T., & Cherif, C. (2022). Textile reinforcement structures for concrete construction applications—a review. *Journal of Composite Materials*, 56(26), 4041–4064.
3. Preinstorfer, P., Yanik, S., Kirnbauer, J., Lees, J. M., & Robisson, A. (2023). Cracking behaviour of textile-reinforced concrete with varying concrete cover and textile surface finish. *Composite Structures*, 312, 116859.

From Challenge to Insight: Exploring Analytical Methods at the Fiber-Matrix Interphase

R. Reichenbächer,[1,*], C. Scheffler[1,2]
[1] Department Fiber Engineering, Leibniz-Institute for Polymer Research, Dresden, Germany
[2] Institute of Construction Materials, Dresden University of Technology, Dresden, Germany

Abstract:
Fiber reinforced composite materials play a central role in modern engineering applications, ranging from renewable energy systems to transportation, automotive components, high-performance structures, and medical devices. Their key advantage lies in combining the distinct properties of the matrix and the reinforcing phase; most commonly, glass fibers are employed. A prerequisite for realizing this synergistic effect is a sufficiently strong and tailored interaction between these two constituents. To enable this, sizings are applied as thin coatings during fiber production. These sizings are typically water-based and primarily consist of a polymeric film former and, in the case of glass fibers, a silane coupling agent and lubricants. The sizing does not only promote fiber–matrix adhesion, but also the processability of the fibrous material is improved by protecting the fibers from mechanical damage and chemical attack during handling and processing [1]. Furthermore, the fiber surface treatment strongly determines the tensile strength. Despite their pivotal influence on composite performance, sizings remain an often overlooked research topic. Fibers are commonly delivered pre-sized by manufacturers, and the exact composition of the sizing is often a black box.
A central challenge in sizing research lies in its characterization. Because the sizing content is typically only 0.4–2.5 wt-%, the application of direct analytical methods is limited. Direct observation of the sizing layer is possible via Scanning Electron Microscopy (SEM) and Atomic Force Microscopy (AFM), complemented by compositional analysis using Energy Dispersive X-ray spectroscopy (EDX). Additional information on the molecular structure of the sizing can be obtained via Infrared Spectroscopy, X-ray Photoelectron Spectroscopy (XPS), Time of Flight Secondary Ion Mass Spectrometry (TOF-SIMS), and Nuclear Magnetic Resonance Spectroscopy (NMR) [2,3]. Indirect access to the fiber surface and the fiber–matrix interphase is given by micro- and micromechanical testing methods, such as single-fiber tensile tests, roving tensile tests, unidirectional composite laminate tests, single-fiber pull-out tests, and wetting investigations. In this work, we present an overview of the role of sizings in fiber-reinforced composite materials and explore the potential of various analytical techniques to characterize the difficult-to-access interphase between fiber and matrix.

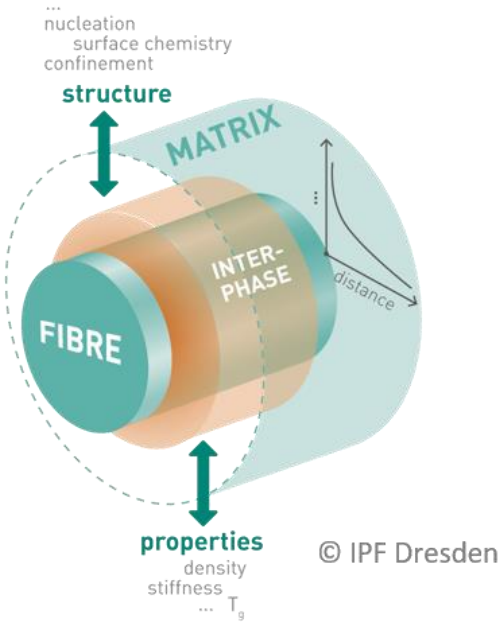

Figure 1: Interphase formation between reinforcing fiber and polymer matrix leading to a zone of chemical, physical and mechanical properties that differ from the bulk polymer matrix.

Keywords: composites, glass fibers, fiber sizing, surface investigation, mechanical analysis, XPS, TOF-SIMS, SEM-EDX, micromechanical testing

References:

1. Petersen, H. N. (2017) Investigation of sizing - from glass fibre surface to composite interface, *DTU Nanotech*.
2. Wang, D., Jones, F. R., Denison, P. (1992), TOF SIMS and XPS study of the interaction of hydrolysed γ-aminopropyltriethoxysilan with E-glass surfaces, *Journal of Adhesion Science and Technology*, 6:1, 79-98.
3. Huang, S., Fu, Q., Yan, L., Kasal, B. (2021), Characterization of interfacial properties between fibre and polymer matrix in composite materials - A critical review, *Journal of Materials Research and Technology,* 13, 1441-1484

Mechanical Properties of minature samples of Spark Plasma Sintered NiTi Alloy

Sneha Samal, Jaromír Kopeček, Elizaveta Iaparova and Petr Sittner
Institute of Physics of Czech Academy of Science, Na Slovance 2
182 00 Prague, Czech Republic

Abstract

The mechanical properties of miniatured spark plasma sintered (SPS) NiTi alloy was investigated in tensile mode in dynamical mechanical analyzer using stress control operation. Two SPS samples were fabricated at load of 50 MPa at two different temperature of 1100 and 1150 °C. The temperature has significance influence in compactness of the alloy with limited porosity. Thermal analysis were carried out to investigate phase transofrmation temperature. The minature tensile samples were prepared by laser cutting from the bulk samples in both transverse and radial direction. Both directions samples were tested to observe the shape memory effect at various testing temeparature ranges from -100 to +150 °C. The grain size evolution was examined using elctron back scattered diffraction method with misorientation direction. These mechanical and grain orientation findings are correlate with compactness of the sample structutre.

Keywords:

Spark plasma sintered; Miniature; Mechanical; Transverse direction; Shape memory; Grain size

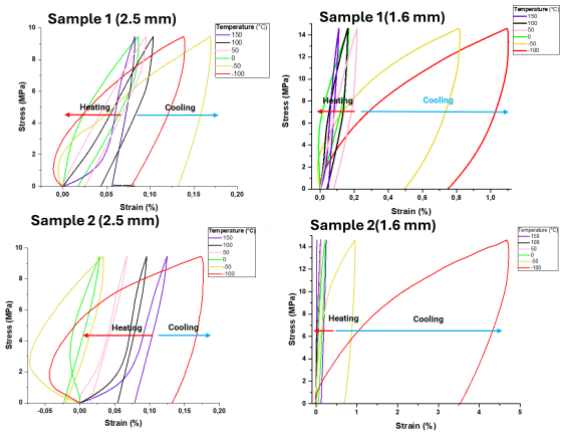

Figure 1: Figure illustrating the mechanical properties of the sps sample at transverse direction for two different dimension of 2.5 and 1.6 mm for both samples 1 and 2.

References:

1. Sneha Samal, Mohit Chandra, Wei Li, Stanislav Habr, Jaromír Kopeček, Ivo Stachiv, Petr Šittner, Effect of sintering temperature on microstructure, phase evolution, thermo-mechanical properties of spark plasma sintering of NiTi alloy, Surface and Coatings Technology, Volume 507, 2025, 132152, 10.1016/j.surfcot.2025.132152.
2. S. Samal, O. Molnárová, F. Průša, J. Kopeček, L. Heller, P. Šittner, M. kodová, L. Abate, I. Blanco, Net-shape NiTi shape memory alloy by spark plasma sintering method, Appl. Sci., 2021 (1802), p. 11, 10.3390/app11041802

Acknowledgement

High school students as interns participated in the work during their internship and contributed part of this work by Tadeas Tehan, Esme Erika Kalovcova.

Funding

This research was funded by the EU structural fund project FerrMion (CZ.02.01.01/00/22_008/0004591) and CzechNanoLab Research Infrastructure supported by MEYS CR (LM2023051).

Investigation of Mechanical Interlocking Using Sculptured Aluminum Foils for Joining Two Dissimilar Polymers

P. Hakimi [1], F. Hahnewald [1], J. Carstensen [1], C. Balzer [2], C. Laugwitz [2], R. Adelung [1]
[1] Material science, Christian-Albrechts-University, Kiel, Germany
[2] SKZ – Das Kunststoff – Zentrum, Würzburg, Germany

Abstract:
The joining of dissimilar polymers is a challenge in many industrial applications such as automotive, electronics, and medical technology. Many polymer combinations cannot be joined using conventional thermal welding techniques because of incompatible material properties. Another solution is the use of adhesives, however they have several drawbacks, such as toxicity and limited chemical resistance. One possible application to overcome these limitations is the use of sculptured metallic interlayers. Aluminum can be electrochemically etched to form hooking structures on its surface (i.e. sculptured, see e.g. [1]) and applied as an interlayer between dissimilar polymers. Reaction conditions and aluminum geometry are adjusted to produce surface features that enable mechanical interlocking. the structured aluminum linkers are integrated into established polymer welding processes to enable the joining of dissimilar polymers without the use of adhesives.

In this work, 30 µm thin aluminum foils are electrochemically etched to generate hooking surface structures on both sides. The structured aluminum foils are then placed between two dissimilar polymers and used as interlayers. This approach allows the investigation of mechanical interlocking between the aluminum foil and the surrounding polymers, as well as the evaluation of the resulting joint performance. (Figure 1). The effect of the fraction of hooking structures and smooth surface areas on joint performance and how crack propagation leads to delamination and adhesive failure is investigated.

Keywords: electrochemically sculptured aluminum foil, surface structuring, hooking structures, mechanical interlocking, dissimilar polymer joining.

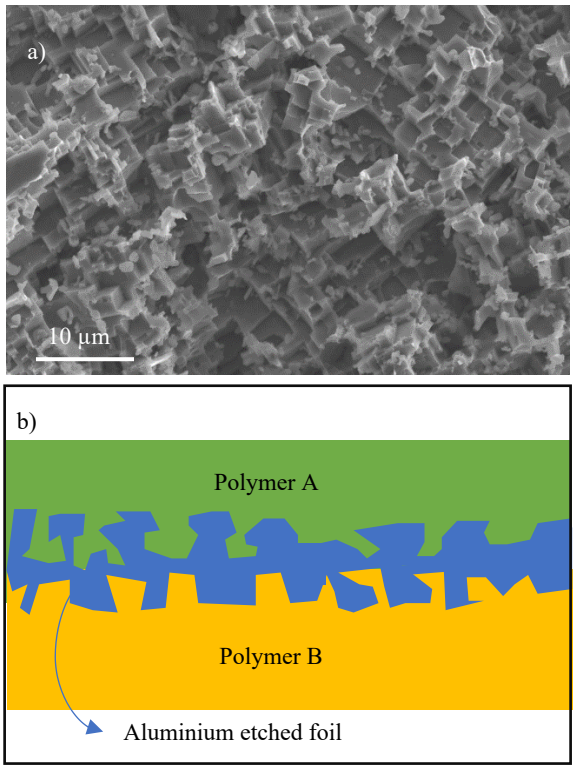

Figure 1: Figure 1a) Surface of the aluminum foil after the formation of hooking structures on both sides. 1b) Schematic illustration of mechanical interlocking between dissimilar polymers by a hooked aluminum foil on both sides.

References:

1. Qiu, H., Schmidt, C., Carstensen, J., Kaps, S., Adelung, R. (2021), Nanoscale-sculptured Al microparticles as universal hierarchical adhesion promoters , *J. Phys. Status Solidi*., 15,1-5.

Plasma Tech Session I. B:
Plasma fundamentals / Modelling / Atomic and Molecular Processes Plasma Source Design and Diagnostics

High-power electron beams for technological applications

Tiberiu MINEA[1*]
[1] Laboratoire de Physique des Gaz et des Plasmas – LPGP
Université Paris-Saclay, CNRS, F-91405 Orsay, FRANCE
tiberiu.minea@universite-paris-saclay.fr

Abstract:
Electron beams (e-beams) are widely used in a large panel of applications. Among these, electron microscopy and surface analysis are the most common. Besides, the generation of synchrotron radiation, vacuum microwave tube amplifiers, and free-electron lasers requires dense, synchronized e-beams.
The last decade has seen renewed interest in very high power DC (direct current) e-beams for metallurgical applications, such as 3D metal (ceramic) printing and space assembly by welding in a vacuum.
This communication focuses on novel devices specifically designed for high-power e-beam generation, modeling, and characterization, and provides a few examples.

Figure 1: ECR plasma-source for e-beam generation.

First, a high-density low-pressure plasma generated by electron cyclotron resonance (ECR) will be introduced together with the main beam features (**Fig. 1**).

After, the device for high-power e-beam diagnostic is introduced and discussed with respect to the beam profile. An alternative method using optical emission spectroscopy gives similar results [1].

Further, a homemade 3D e-beam simulation software, SASAM, is presented [2]. It is a flexible parallel software that uses the MPI protocol, exploits the Particle-In-Cell algorithm, accounts for beam space charge, and includes collisions via a Monte Carlo treatment (**Fig. 2**). The space-charge effects are critical for currents exceeding 10 mA (about 10^4 times larger than in scanning electron microscopes) and for which the smallest focusing spot possible is required (< 100 µm radius). Electron production has also been extensively studied [3].

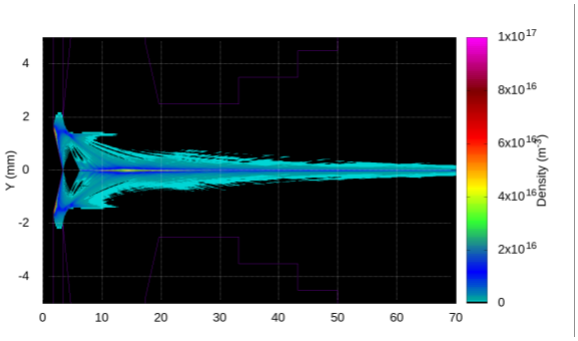

Figure 2: Simulation of a high-current (100 mA) high-voltage (80 kV) e-beam using SESAM [2].

Finally, the detailed analysis of secondary electrons produced by these energetic beams using electrostatic probes can be used to characterize the energy deposited in a metal, even when molten [4]. An example of highly efficient e-beam welding in a vacuum using a novel-designed e-gun for space applications will be shown.

Keywords: e-beams, low pressure, vacuum, PIC, 3D metal printing, space welding.

References:

1 M. Ugoletti, C. Ballage, T. Minea, G. Serianni, O. Vasilovici, M. Agostini Rev. Sci. Instrum 96 (2025) 023705;
2 A. Revel & T. Minea - SESAM « Saclay Electron Solution for BeAm Modelling » software: Owners CNRS/Univ. Paris-Saclay, 2023/01/9, N° DL 16346-01
3 B. Seznec, Tiberiu Minea, Ph. Testé, Ph. Dessainte, G. Maynard – Theoretical Treatment of Electron Emission and Related Phenomena, Springer, 2022
4 V.G. Antunes, A. El Farsy, B. Seznec, T. Minea, Additive Manufacturing 80 (2024) 103957

Anode erosion and gas flow symmetry in plasma spray torch

R. Zhukovskii [1,*], R. Molz [2], R. Enzl [1], M. Messina [1], M. Giglmaier [3]
[1] Oerlikon Metco AG, Wohlen, Switzerland
[2] Oerlikon Metco (US) Inc., Westbury, NY, USA
[3] Oerlikon AM Europe GmbH, Garching, Germany

Abstract:
Plasma spray torch is a device that uses an electric arc to produce a plasma jet that is used to heat up and accelerate powder particles to form a coating onto a substrate. Plasma torch design presents challenges in achieving not only the required performance during operation but also in service lifetime of consumable parts, more specifically the electrodes. An electric arc inside a plasma torch does not only transform the gas flow into a plasma jet, but also transfers a significant amount of heat to the anode surface via electric current, thermal diffusion and radiation. The anode operation in plasma torch is accompanied by a multitude of processes, e.g. thermal deformation, recrystallization, cracking, melting, and spitting, that are collectively called erosion. Utilizing diatomic plasma gases provides high energy operating regimes of the plasma gun which is beneficial for many applications in the industry. Meanwhile, it results in a more constricted arc and significantly increased heat flux and consequently anode erosion. Diatomic gases are valuable in plasma spray process due to their higher specific enthalpy compared to argon, the most common monoatomic gas in the industry. However, the conventional plasma torch MHD simulation dealing with electromagnetic and thermodynamic aspects of the plasma jet formation process (Figure 1) is not capable of predicting the sophisticated anode erosion. Thus, alternative solutions are necessary to investigate the reasons of accelerated anode erosion in preliminary plasma torch design stages and reduce it eventually. Here, a model of swirling cold gas flow in the gas feeding line and plasma cavity is used to improve axial symmetry of the gas flow (Figure 2). Hence, a Reynolds Stress Model was applied to take the anisotropic turbulent flow characteristics into account. It was found that the plasma forming gas was fed with ±40% asymmetry with the initial configuration of the gas feeding line and resulted in anode failure after a few hours of operation. After adjustment of the gas feeding line, the gas feeding axial asymmetry reduced to ±5% which allowed to extend the anode erosion spot and extend the anode service lifetime multiple times. This indicates how even a seemingly more primitive approach than plasma simulation still can be instrumental in designing a plasma device when applied correctly.

Keywords: plasma torch, electric arc, simulation, gas flow, anode erosion.

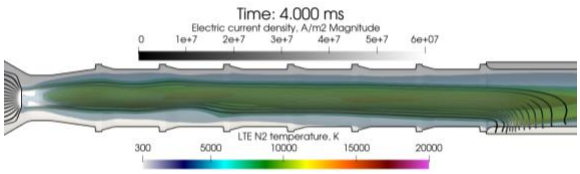

Figure 1: Isosurfaces of LTE temperature in nitrogen plasma and streamlines of electric current density of electric arc inside plasma channel of plasma torch

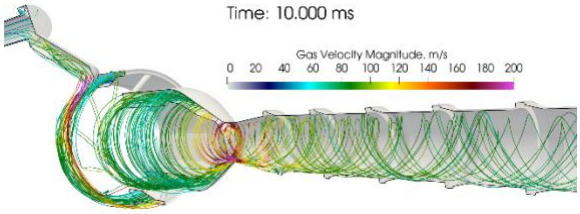

Figure 2: Cold gas velocity streamlines in gas feeding line and plasma cavity

References:

1. Belashchenko, V. et al. (2015), High Stability, High Enthalpy APS Process Based on Combined Wall and Gas Stabilizations of Plasma, In: Thermal Spray: Proceedings from the ITSC, May 11-14, 2015 (Long Beach, CA, USA), ASM International, pp. 437-444.
2. Jeon, B., Kwon, H., Yoo, Y. W., Kim, D. H., Park, Y., Kang, Y.-j., Murphy, A. B., Park, H. (2025). Computational Modeling of the Effect of Nitrogen on the Plasma Spray Process with Ar–H_2–N_2 Mixtures, *Processes*, *13*(4), 1155.
3. Zhukovskii, R., Chazelas, C., Rat, V., Vardelle, A., Molz, R. (2022), Predicted Anode Arc Attachment by LTE and 2-T Arc Models in a Cascaded-Anode DC Plasma Spray Torch, *J. Therm. Spray Tech.,* 31, 28–45.
4. Escue, A., Cui, J. (2010), Comparison of turbulence models in simulating swirling pipe flows, *Appl. Math. Model.,* 34 (10) (2010), pp. 2840-2849

Study of ion beam sources by self consistent simulation approach

M. Queck[1*] , K.M. Rettig [2], T. Dunger [1]
[1] Scia Systems GmnH, Chemnitz, Germany
[2] Simulation of Semiconductor Technologies, Fraunhofer ENAS, Chemnitz, Germany

Abstract:
Ion beam etching is a widely used technique for high-precision surface treatment and modification. Such applications require a well-defined and predictable ion beam, which can be optimized with respect to its shape, ion current density, angular distribution, and ion energy, depending on the specific process requirements. Since this involves the description of charged particles, their mutual interactions, and their interaction with external fields in a high-dimensional parameter space, a simulation-based approach is used to predict ion beam properties for various source configurations and process parameters.

We developed a combined model that enables the simultaneous simulation of both the plasma source and ion beam extraction, including their mutual interaction. The main advantage of this approach is that particle trajectories are derived self-consistently, without requiring additional assumptions such as look-up tables or else. An inductively coupled plasma (ICP) source is used in the model, with geometry, gas flow rates, and applied RF power serving as input parameters. The geometry of the extraction grid system is varied with respect to hole size and spatial distribution, and the resulting influence on ion beam shape and ion current density distribution is systematically investigated.

To validate the model and the simulation results, the predicted plasma and ion beam properties are compared with corresponding experimental measurements.

Keywords:inductively coupled plasma, plasma simulation, self-consistent global model, kinetic particle simulation, PIC-DSMC, plasma processing, ion beam processing, plasma sheath, ion extraction, Langmuir

probe.

References:

1. Rettig et al., *Plasma Sources Sci. Technol.*, in prep.

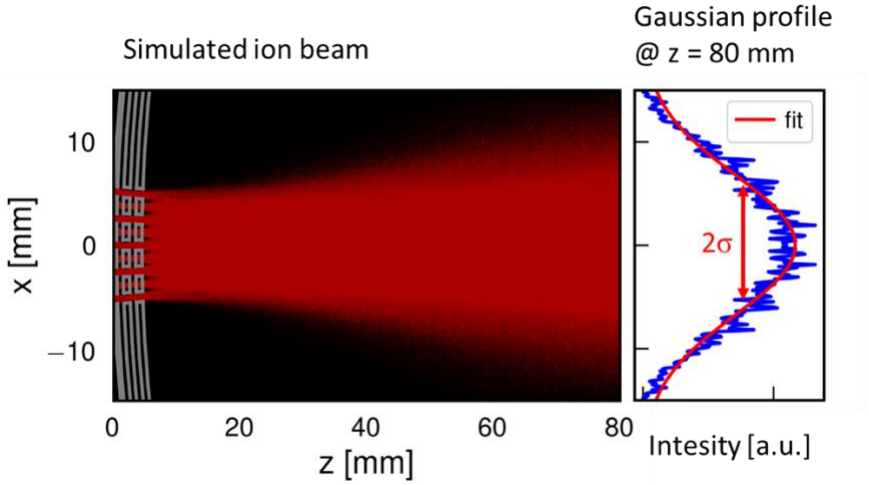

Figure 1: Figure illustrating principle results of simulation of ion beam, consisting of various beamlets. Properties depending on extractions geometry. Comparison to example measurement of respective system.

Simulation of the electron density time evolution in the ignition process of an Ar RF-CCP plasma discharge

P. Mandracci [1]
[1] Department of Applied Science and Technology, Politecnico di Torino, Turin, Italy

Abstract:
The time evolution of cold plasma discharges during their ignition process is by far less studied in literature, compared to their steady state. However, the first few discharge microseconds are of great importance for the understanding of the discharge time evolution. In this work, the ignition of an Ar RF-CCP discharge was simulated in the first few microseconds by the 1d3v PIC-MCC method, considering pressures in the range 400-600 mTorr, RF bias amplitudes in the range 100-400 V, and RF frequencies in the range 10-30 MHz. The time evolution of the electron and ion density, as well as other plasma parameters, was simulated (see Figure 1). The simulated data showed a transition between two regimes, the first one being characterized by an exponential increase of electron and ion densities, strongly modulated by the bias voltage oscillations, while the second showed a linear increase of these quantities, with much smaller oscillations. Two analytical models were fitted to the simulated electron density in the two observed regimes, and were used to obtain an analytical definition of the time required for the transition between them, which ranged from about 10 to more than 100 RF cycles. The effect on the transition time of pressure, bias voltage and RF frequency was investigated, showing that these parameters have a strong influence on the time required for the discharge activation.

Keywords: CCP, time evolution, plasma ignition, Ar plasma, electron density, ion density.

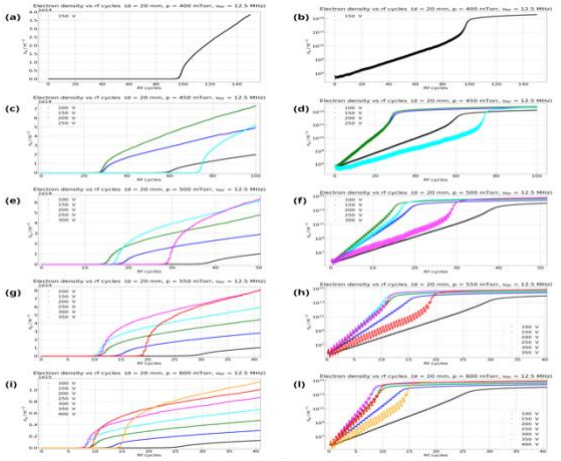

Figure 1: Electron density as a function of RF cycles for a simulated Ar CCP discharge excited at 12.5 MHz and a electrode distance of 20 mm, at pressures of 400 mTorr (a, b), 450 mTorr (c, d), 500 mTorr (e, f), 550 mTorr (g, h), and 600 mTorr (i, l). The results are show in linear (a, c, e, g, l) and semi-logarithmic (b, d, f, h, l) scales. For each pressure, results are shown for the interval of bias voltages for which an activation of the discharge was obtained. For voltages lower or greater than the ones shown in the plots, the electron density dropped to zero after a few RF cycles.

References:

1. Mandracci, P. (2022), Simulation of the First Two Microseconds of an Ar CCP Cold Plasma Discharge by the PIC-MCC Method, *Plasma*, 5, 366-383.
2. Mandracci, P. (2024), A Review of Experimental Investigations into the Time Evolution of Low-Pressure Capacitively Coupled Plasmas in Their Early Stages of Development, *Plasma*, 7, 531–565.

Chemistry Data Generation for Plasma Simulations

S. Mohr [1], G.S.J. Armstrong[1], R. Brook[1], J. Tennyson[2]
[1] Quantemol Ltd., London, United Kingdom
[2] Department of Physics, University College London, London, United Kingdom

Abstract:
Plasma simulations are commonly used in both academic and industrial settings to gain further understanding of fundamental plasma phenomena and optimize processes. Apart from robust physical simulations these need chemical data such as electron collision cross-sections, reaction rate coefficients, surface reaction coefficients, or species properties.
While these data are typically available for commonly used gases such as argon or oxygen, they are sparse for newly synthesized gases and especially radicals formed in the plasma by dissociative reactions or reactions between neutrals. Furthermore, they are typically scattered between several papers, so collecting data for a specific gas mixture can be an arduous process. We aim to develop methods and tools which can provide yet unknown data and ease the process of combining them into comprehensive chemistry sets optimised for specific process conditions. Here, we present our latest development with regards to, for example:

- Automatic chemistry set generation and optimization [1]
- Machine learning techniques to quickly estimate missing data [2]
- Prediction of neutral dissociation breakup patterns via molecular dynamics simulations [3]
- Cross-section calculations for molecules containing heavy atoms such as W via use of effective core potentials [4]

Effective core potentials, for example, are necessary to overcome two obstacles when calculating cross-sections for molecules containing heavy atoms; relativistic effects and the large number of electrons in their shells. While taking these explicitly into account is possible in theory, the necessary computational expense makes them impractical. Effective core potentials replace the explicit treatment of the inner electrons with a static potential, reducing the number of electrons which need to be taken into account explicitly.

Keywords: plasma simulation, chemistry data, electron impact cross-sections, rate coefficients, machine learning, neutral dissociation

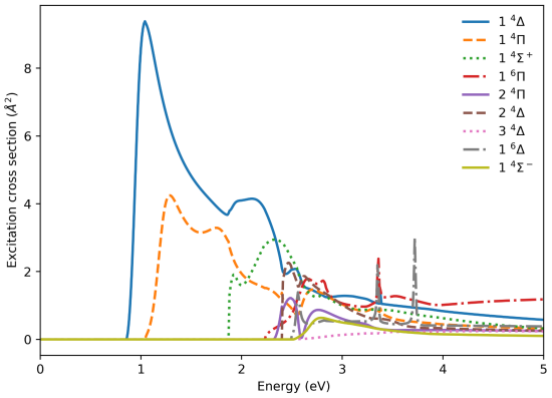

Figure 1: Electron-impact electronic excitation cross sections for the lowest excited states of WH, calculated using an effective core potential for W [4].

References:

1. M. Hanicinec *et al* (2020) *Plasma Sources Sci. Technol.*, 29, 125024
2. K.M. Lemishko et al (2025) *J. Phys. D: Appl. Phys.*, 58, 105208
3. R. Brook et al (2025) *J. Vac. Sci. Technol. A*, 43, 043003
4. Z. Masin et al (2025) *J. Chem. Theory Comput*, submitted

Superposition of HiPIMS with RF on a single magnetron: Generation of high ion energies

Caroline Adam [1,*], Luka Hansen [1,2], Tobias A. Hahn [1], Jessica Niemann [1], Daniel Zuhayra [1], Günter Mark [3], Jonathan Löffler [3], Jan Benedikt [1,2], Holger Kersten [1,2]
[1] Institute of Experimental and Applied Physics, Kiel University, Kiel, Germany
[2] Kiel Nano, Surface and Interface Science KiNSIS, Kiel University, Kiel, Germany
[3]MELEC GmbH, Baden-Baden, Germany

Abstract:
High power impulse magnetron sputtering (HiPIMS) has shown significant potential for thin film deposition by providing high ionized flux fractions [1] and ion energies [2]. To optimize the deposition process, HiPIMS can be operated in superposition with an additional discharge on the same magnetron, such as DC [3] or MF (mid-frequency pulses) [4]. This leads to an increase of the deposition rate and facilitates low-pressure operation by utilizing the pre-ionization of the continuously running discharge during the off-time between HiPIMS pulses.
In this study, a novel combination of HiPIMS and RF (radio-frequency, 13.56 MHz) is investigated in continuous superposition on the same magnetron, using a planar copper target in argon atmosphere [5]. The discharge is characterized at varied power ratios of HiPIMS and RF with plasma diagnostics employed to analyze the system. This includes measuring the combined HiPIMS/RF voltage signal and conducting optical emission spectroscopy (OES) to gain insights into the plasma composition. Two key factors influencing the microstructure of deposited films are the kinetic energy of particles bombarding the growing film and the substrate temperature [6]. Substrate heating from the plasma is evaluated using a passive thermal probe (PTP) [7], a "non-conventional" calorimetric diagnostic that measures the total energy flux to the substrate surface. The kinetic energy is assessed through energy-selective mass spectrometry [8], including time-resolved operation. The results regarding the plasma parameters are compared with the morphology of the deposited copper films, analyzed using scanning electron microscopy (SEM).

The addition of an RF plasma provides pre-ionization for the HiPIMS pulses, which allows to reduce the process pressure. Time-resolved OES reveals the transition from the copper-dominated emission during the HiPIMS pulse to an argon plasma in in the HiPIMS off-time. The RF plasma exhibits a pronounced influence on the ion energy distribution, increasing the ion energy by more than 50 eV depending on the applied RF power. This effect is attributed to an increased plasma potential caused by the RF sheath, which accelerates ions in the sheath region toward the substrate, resulting in elevated ion energies. The potential of this process is demonstrated by the deposition of copper thin films, showing significant influence of the deposition mode for their properties [5].

Keywords: HiPIMS, magnetron sputtering, ion energy distribution, energy flux, plasma diagnostic

References:

1. T. Kubart *et al.* (2014) Investigation of ionized metal flux fraction in HiPIMS discharges with Ti and Ni targets, *Surf. Coat. Technol.*, 238, 152–157.
2. A. Hecimovic and A. P. Ehiasarian (2009) Time evolution of ion energies in HIPIMS of chromium plasma discharge, *J. Phys. D: Appl. Phys.*, 42, 13520.
3. Samuelsson, M. *et al.* (2012) Influence of ionization degree on film properties when using high power impulse magnetron sputtering, *J. Vac. Sci. Technol. A*, 30, 031507.
4. Diyatmika, W. *et al.* (2018) Superimposed high power impulse and middle frequency magnetron sputtering: Role of pulse duration and average power of middle frequency, *Surf. Coat. Technol.*, 352, 680–689.
5. Adam, C. *et al.* (2026) Superposition of HiPIMS with RF on a single magnetron: Generation of high ion energies, *Surf. Coat. Technol.*, 520, 133060.
6. Anders, A. (2010) A structure zone diagram including plasma-based deposition and ion etching, *Thin Solid Films*, 518, 4087–4090.
7. Kersten, H. *et al.* (2000) Investigations on the energy influx at plasma processes by means of a simple thermal probe, *Thin Solid Films*, 377–378, 585–591.
8. Benedikt, J. *et al.* (2012) Quadrupole mass spectrometry of reactive plasmas, *J. Phys. D: Appl. Phys.*, 45, 403001.

Establishing an Atomic Oxygen Test Facility for Space Hardware Based on an Inductively Coupled Plasma Source

S. Zoehrer [1*], W. Engel [1], L. Bettiol [1], B. Seifert [1]
[1] FOTEC Forschungs- und Technologietransfer GmbH, Wiener Neustadt, Austria

Abstract: Radiation, thermal extremes, low pressure, and Atomic Oxygen (ATOX) are inevitable factors limiting lifetime and functionality of spacecraft in Earth orbits. Particularly ATOX is considered as one of the most serious hazards to spacecraft materials at altitudes of 200 to 700 km [1]. Due to its reactivity and relative orbital speed of about 8 km/s, it leads to spacecraft material erosion, and degradation, performance issues, and potential system failure.

Ground testing is crucial for qualifying space hardware to reduce operational risks. ATOX test facilities are becoming an important factor due to increased popularity of Very Low Earth Orbits (VLEO). These facilities try to mimic the projected atmospheric conditions like particle flux, velocity distribution, elemental composition, ion fraction, and ambient pressure. However, it is experimentally challenging and complex to measure such parameters reliably. Most facilities only report very limited data, if at all.

By applying diagnostics in form of a Retarding Potential Analyzer (RPA), a Faraday cup, an internal plasma electrode, a residual gas analyzer, and Kapton witness samples, we try to characterize the extracted ion beam of our oxygen plasma source to assess similarity with the targeted atmospheric conditions. Using a cylindrical quartz glass plasma chamber (10 cm length, 4 cm diameter) wrapped by a copper coil (3-4 windings) we generate an inductively coupled oxygen plasma with a radio frequency generator and matching network at 13.56 MHz. A mass flow controller supplies O_2 to the plasma chamber, which is differentially pumped by the vacuum chambers turbomolecular pump(s) through three grid electrodes. These electrodes are used to extract a positive oxygen ion beam from the plasma (see Fig. 1) similar to a gridded ion thruster.

Results show that oxygen flowrates (0.1 to 0.3 mg/s), Radio Frequency (RF) power (100 to 300 W), applied potentials (<1 kV) and size/shape of electrodes cause very different (inductively coupled) plasma regimes to emerge. These show significantly different balances of atomic and molecular oxygen species, quite different plasma and floating potentials, and generally a strong influence of surrounding (wall) materials. Effects of RF radiation and the electronegativity of the oxygen plasma have to be considered in addition. Based on RPA measurements, strategies applied to control the ion velocity distribution while sustaining sufficient flux are presented. Furthermore, ideas on how to neutralize extracted oxygen ions and assess elemental/neutral/ion fractions are discussed.

The overall goal is to better physically understand and advance the ion source to a state where a controllable and tunable ATOX particle stream with known parameters can be provided for environmental testing of space hardware as a service for internal use and third parties.

Keywords: Atomic oxygen, inductively coupled plasma, oxygen plasma, environmental testing, satellites, very low earth orbit, oxygen ion beam, ion energy distribution

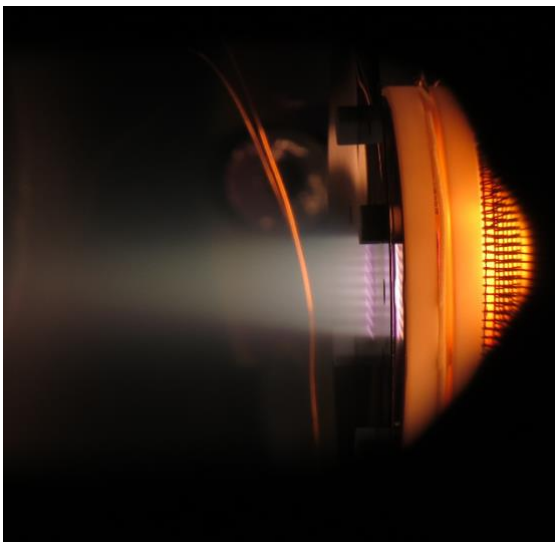

Figure 1: Oxygen ion beam extracted from the ICP with most likely kinetic ion energies of about 150 eV.

References:

1. A. de Rooij, (2010) Corrosion in Space, Encyclopedia of Aerospace Engineering, John Wiley & Sons Ltd.

Generation and Manipulation of Pulsed-Driven Dielectric Barrier Discharges using Tailored High-Voltage Waveforms

H. Höft[1,*], J. J. van Oorschot[2], R. Brandenburg[1,3], T. Huiskamp[2], M. M. Becker[1]
[1] Leibniz Institute for Plasma Science and Technology (INP), Greifswald, Germany
[2] Dept. of Electrical Engineering, Eindhoven University of Technology, Eindhoven, The Netherlands
[3] Institute of Physics, University of Rostock, Rostock, Germany

Abstract:
Dielectric barrier discharges (DBDs) are a common tool in atmospheric-pressure plasma technology, enabling applications from pollution control and ozone generation to surface modification [1]. One effective method to control the characteristics of DBDs is the shape of the applied high-voltage (HV) waveform, which is determined by properties like the amplitude, rise time or specific slope shapes. DBDs are often AC-powered, however, pulsed operation offers more possibilities to tweak the HV shape. Therefore, this contribution aims to investigate how precisely shaped HV pulses modulate the ignition dynamics and spatio-temporal structure of a single-filament DBD operated in a binary N_2–O_2 mixture. A custom-built, impedance-matched solid-state Marx generator delivers unipolar positive square pulses (10 kV, 5 kHz) with adjustable rise times (≈ 50 ns) [2] and pulse widths (a different HV pulse source was used for pulse width variation [3]). Two pin electrodes, each covered by a hemispherical dielectric, are separated by a 1 mm gas gap and operated in O_2 concentrations ranging from 0.1 vol% to 20 vol% in N_2 at atmospheric pressure. The discharge is monitored by synchronised fast electrical probes and by streak and iCCD cameras, providing insight into streamer propagation and emission with sub-nanosecond and sub-millimetre resolutions. Time-dependent, one-dimensional fluid simulations provide a complementary insight into how tailored waveform parameters affect the Townsend pre-phase and subsequent discharge dynamics. By varying the O_2/N_2 ratio at constant pulse width, or by extending the pulse width at constant O_2 concentration [3], it was demonstrated that the pre-breakdown phase can be selectively controlled by the pre-ionisation, offering a route to tailor plasma properties for specific applications. The roadmap to control discharge inception and propagation properties as well as electrical characteristics is given in Figure 1.

These results underscore the critical role of HV waveform shaping and gas composition in governing the physics of atmospheric-pressure DBDs. They open pathways toward highly controllable, application-optimised plasma sources (not restricted to single-filament DBDs only [4,5]), from efficient ozone generation to precise surface treatment and beyond.

Keywords: Pulsed discharges, dielectric barrier discharges, HV pulse parameters, electrical diagnostics, optical diagnostics, air-like gas mixtures, atmospheric pressure, plasma modelling

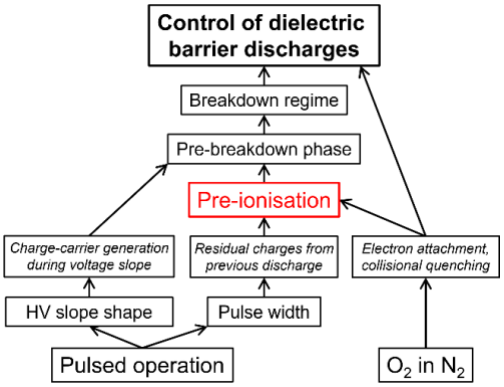

Figure 1: Impact of HV pulse parameters and the O_2 concentration in N_2 on the pre-ionisation and consequently on the breakdown of pulsed-driven DBDs in air-like gas mixtures at atmospheric pressure.

Acknowlegments:
This work is supported by the German Research Foundation (DFG) - project number 535827833 and by the Dutch growth fund “Nxtgen hightech plasma4agrifood”.

References:

1. R. Brandenburg *et al.*, *Plasma Chem. Plasma Process.* **43**, 1303–1334 (2023)
2. J. J. van Oorschot, T. Huiskamp, IEEE Trans. Plasma Sci. **51**, 560-571 (2023)
3. H. Höft *et al.*, *J. Phys. D: Appl. Phys.* **47**, 465206 (2014)
4. T. Huiskamp *et al.*, *J. Phys. D: Appl. Phys.* **55**, 024001 (2022)
5. H. Höft *et al.*, *J. Phys. D: Appl. Phys.* **55**, 424003 (2022)

Numerical and Experimental Investigation of Collector Geometry Effects in Gridded Electrohydrodynamic Thrusters

G. Mongaretto [1*], F. Ragazzi [1], D. Usuelli [2], S. Trovato [2], R. Terenzi [2], A. Popoli [1], A. Cristofolini [1], M. Belan [2].

[1] Department of Electrical, Electronic and Information Engineering "Guglielmo Marconi", University of Bologna, Bologna, Italy

[2] Department of Aerospace Science and Technology (DAER), Politecnico di Milano, Milano, Italy

Abstract:

In recent years, electrohydrodynamic (EHD) thrusters, initially developed for aerospace applications, have gained interest for atmospheric propulsion due to their simple design, absence of moving parts, and low noise emissions. These devices use ambient air to generate thrust through momentum transfer between ions from a corona discharge and neutral molecules, following the ionic wind principle. Characterizing corona discharges is therefore essential to understand and improve EHD thruster performance and guide propulsion optimization. Gridded configurations have emerged as the most promising in terms of thrust efficiency [1], prompting research on optimizing collector number and geometry. In this work, we present a combined numerical and experimental study to identify optimal electrode arrangements for electrical performance. Three collector geometries are considered: (i) a single-level array of cylindrical collectors (1–10 cylinders, 50 µm radius); (ii) blade-shaped collectors (1–10 blades, 0.1 mm height, lengths 2, 4, 6 mm); and (iii) double-level cylindrical arrays (2–6 cylinders, same radius, inter-level spacings 2, 4, 6 mm). The discharge behavior is simulated using Merlino2D, a MATLAB-based time-dependent drift–diffusion solver supporting detailed kinetic schemes. In this study, a six-species, thirteen-reaction model (e, N_2, O_2, N_2^+, O_2^+, O_2^-) from [2] is used. The numerical results reproduce the experimentally observed current trends across all geometries, confirming the model's capability to capture the underlying discharge physics. In addition, the model predicts the onset of back-discharge phenomena caused by strong electric fields at the collector grid, resulting in local ionization and the formation of a negative space-charge region through electron attachment and recombination processes (Figure 1). The presence of negative space charge modifies the electrohydrodynamic force density distribution, partially opposing the ion-driven acceleration of neutrals and thus limiting the achievable thrust.

Keywords: Electrohydrodynamic propulsion, Corona discharge, ionic wind, gridded EHD, thrusters, plasma fluid modeling, atmospheric pressure plasmas, back discharge.

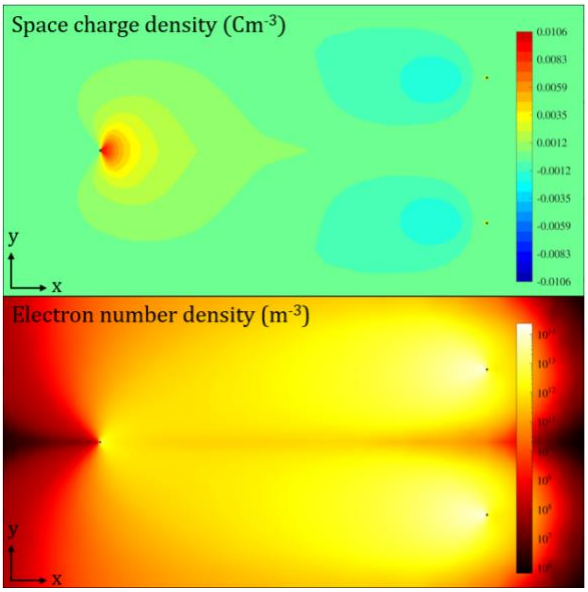

Figure 1: Space charge and electron number density distribution for a single-level array collector configuration composed of 2 cylindrical collectors and a cylindrical emitter. Each electrode has a radius of 50 µm, the emitter-collector spacing is 20 mm, and the applied voltage is 20 kV.

References:

1. Terenzi R. *et al.*, Atmospheric electroaerodynamic thrusters with grid collectors. *Scientific Reports* 15.1 (2025), 41513.
2. Parent B. *et al.*, Electron and ion transport equations in computational weakly-ionized plasma dynamics. Journal of Computational Physics 259, 51–69 (2014).

MHD multiphase modelling of electrical explosions confined in air and dense media

F. Tholin [1], A. Jarnac [1], B. Khiar [1], F. Pechereau [1], C. Zaepffel[1], V. Gaudineau [1], K. Thomas [1]

[1] DPHY, ONERA, Université Paris-Saclay, 91120, Palaiseau, France

Abstract:
The electrical explosion of metals subject to intense Joule heating is of crucial importance for many applications. From a modelling point of view, this phenomenon is challenging since it requires to model matter in a very wide range of density-temperature conditions, taking into account the many phase transitions from solid state to plasma state. A modelling strategy based on a multiphase resistive MHD solver is described in this work, that intend to model electrical explosions confined in air or in dense media.

The MHD multiphase model relies on different kind of equation of states (EOS) to describe the different materials. The conducting materials subject to intense Joule heating and phase transitions are described by the QEOS approach [1]. The confinment media are described by simpler EOS, such as SGE (Stiffened Gas Equation) or Mie-Grüneisen EOS. To deal with the different species and EOS, the MHD solver uses an Eulerian diffuse interface model with solid mechanics inspired by [2]. The Joule heating and the magnetic forces are computed by solving the induction equation on the magnetic field.

To validate this model, experiments of exploding wires in air have been conducted at ESRF (European Synchrotron Radiation Facility), as part of the ShockBag access group, on the beamline ID19. This access group, dedicated to material under extreme loading pools together MHz X-ray imaging and a generator able to produce current waves reaching 150 kA in 500 ns.

Different wire radii, ranging from 100 µm to 600 µm have been considered, as well as different materials, such as aluminum, titanium and tungsten. 2D current constrictions have also been considered to study the dynamics of punctual electrical explosions confined by solid epoxy resin. **Figure 1** shows an example of such a constriction during electrical explosion.

Numerical simulations have been conducted in 1D and 2D to demonstrate the ability of the MHD multiphase solver to model such explosions. As an example, **Figure 2** shows numerical results of the the electrical explosion of an aluminum wire confined between a solid Al skin and a solid epoxy layer with pseudo-Schlieren. The pressure build-up can reach several GPa in the wire, leading to the mechanical breakup of the confinement. The goal of this work is to model the experiments performed at ESRF both on exploding wires and current constrictions.

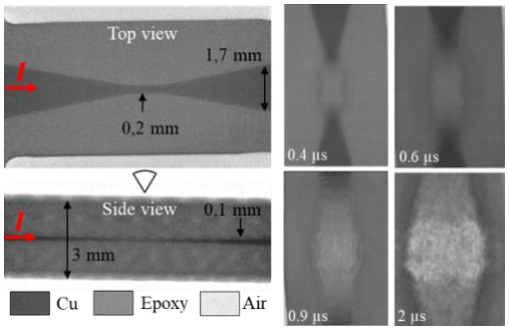

Figure 1: X-ray imaging of a PCB current constriction during electrical explosion.

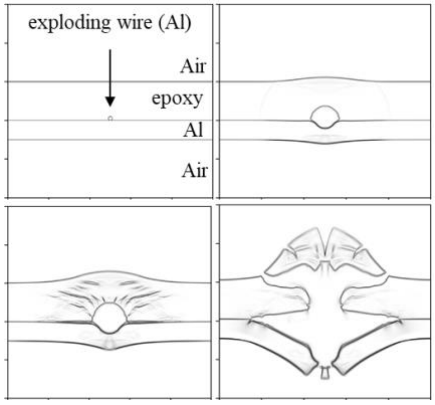

Figure 2: Simulation of an exloding wire confined between an Al skin and an epoxy layer.

Keywords: MHD, electrical explosion, phase transition, numerical simulation, X-ray.

References:

1. More, R. *et al* (1988), A New Quotidian Equation of State (QEOS) for Hot Dense Matter, *Physics of Fluids*, 31, 10, 3059.
2. Ndanou, S., Favrie, N., and Gavrilyuk, S. (2015) Multi-Solid and Multi-Fluid Diffuse Interface Model: Applications to Dynamic Fracture and Fragmentation, *Journal of Computational Physics*, 295, 523–555.

Phase-Resolved Optical Diagnostics of Scaled Plasma Jets Operated with Ar/Ar-Mixtures at Ambient Conditions

Thota Satish Babu[1,#], P S N S R Srikar[1], Shihabudheen M. Maliyekkal[2], Reetesh Kumar Gangwar[1,*]
[1] Department of Physics & CAMOST, IIT Tirupati, India
[2] Department of Civil and Environmental Engineering, IIT Tirupati, India
[#]Presenting author: ph22d505@iittp.ac.in
*Corresponding authors: shihab@iittp.ac.in, reetesh@iittp.ac.in

Abstract:
Atmospheric-pressure nonthermal plasmas are widely utilized in various applications, including materials processing, food, agriculture, and environmental remediation. In these applications, it is preferred to process in ambient conditions, which often limits the range of operating conditions. These restrictions could pose challenges in achieving efficient processing while maintaining the nonthermal nature of the plasma throughout the processing. Therefore, to develop efficient plasma reactors, it is essential to carry out reliable diagnostics of these plasma systems.

In this work, we have developed a scaled plasma jet reactor comprising an array of 8 plasma jets. To understand the generation of reactive chemical species in these scaled systems, we employed time- and phase-resolved optical emission spectroscopy (OES). The measurements were carried out under various operating conditions, including electrode gap, jet arrangement, and operating frequency.

The optical measurements were performed using synchronized ICCD imaging and time-resolved optical-emission spectroscopy. We recorded the emission features of OH (A-X), N_2 (C-B), Ar I, and O I, enabling us to track the evolution of plasma chemistry during each waveform cycle.

Our initial analysis revealed that the square waveform generates strong and short-lived bursts of reactive species across the jets, whereas the waveform shapes can significantly affect the production of reactive species. Additionally, we are currently estimating the profiles of electron temperature and electron density by coupling the OES measurements with the collision radiative model. To accelerate the predictions, we plan to implement and train a machine learning model so that information can be extracted in real-time.

I-V measurements and power estimation were also performed to understand the discharge characteristics. The detailed results, along with analysis, will be presented during the conference.

Keywords: Atmospheric-pressure plasma jet; multi-jet system; waveform modulation; reactive species; energy efficiency; optical emission spectroscopy; ICCD imaging.

References:

1. P S N S R Srikar, S M Allabakshi, S Gomosta, S M Maliyekkal, and R K Gangwar, Development of efficient nonthermal atmospheric-pressure Ar-plasma jet through simultaneous spectroscopic characterization and radical quantification, J. Phys. D: Appl. Phys. 57, 395204 (2024). https://doi.org/10.1088/1361-6463/ad5c76

SICT 2026 / Tribology 2026 Joint Session I. C: Fundamentals of Tribology & Advanced Surfaces Coatings and Surfaces Corrosion / Tribological Properties Testing, Measurement & Methodologies

The Effects of Build Parameters on the Reciprocating Wear Response of Al_2O_3 Ceramics Produced Using DLP Additive Manufacturing

A.M.S. David[1], G. Boubnova[1], S. Clemens[1], and K.P. Plucknett[1*]
[1] Department of Mechanical Engineering, Dalhousie University, 1360 Barrington Street, Halifax, NS, B3H 4R2, Canada

Abstract:
In the current work, digital light processing (DLP) has been used in order to manufacture alumina (Al_2O_3) based ceramics to investigate their reciprocating wear behaviour. DLP is a 'layer-by-layer' vat photo polymerization, additive manufacturing (AM) technique, which allows highly complex-shaped components to be produced, with a build resolution potentially as fine as 10 µm. The influence of fundamental DLP processing parameters, specifically the build inclination angle and layer thickness, on the reciprocating wear behaviour will be discussed. In this instance, the build inclinations angle was varied from 0° to 90° in 15° increments, while layer thicknesses were varied between 10 and 75 µm. After DLP printing of parts pre-conditioning and burnout stages were applied, before the Al_2O_3 samples were sintered in air. Wear rates were measured under reciprocating sliding, with a counter face material of β-Si_3N_4 spheres. The wear tests were conducted at a frequency of 5 Hz, for a duration of 60 minutes, and with applied normal loads of up to 60 N; loads above 60 N were determined to be in the ultra-severe wear zone and were not assessed. It is shown that both build inclination angle and layer thickness have a strong impact on the surface roughness and consequently the wear behaviour. In particular, it is important to minimize or eliminate secondary periodicity in surface steps to reduce wear degradation. This study highlights the influence of the DLP printing parameters on the coefficients of friction, specific wear rates, and observed tribological damage. These studies also highlight the important design criteria that need to be considered when utilising AM techniques for the production of high performance ceramics for use in tribological applications.

Keywords: alumina, silicon nitride, vat photo polymerization, reciprocating wear, coefficient of friction, abrasive wear, adhesive wear, tribolayer.

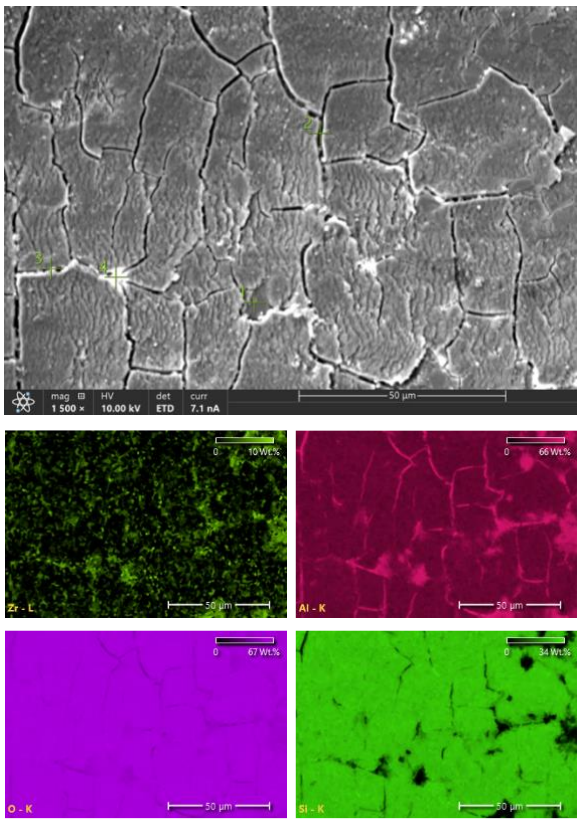

Figure 1: SEM image of tribolayer formation and damage. The sample is prepared with a 45° inclination angle, 25µm layer thickness, and is tested under an applied load of 40 N for 60 minutes. The tribolayer contains Si, Al, and O, highlighting material transfer from the β-Si_3N_4 counter face.

Dry friction behavior of Ceramic Matrix Composites (CMC) obtained by duplex treatment combining cold spray aluminum layers with alumina, zirconia and rutile particles followed by plasma electrolytic oxidation (PEO) treatments

T. Czerwiec[1], A. Maizeray[1], G. Marcos[1], A. Cappella[2], M.-P. Planche[3], H. Liao[3], G. Henrion[1], S. Philippon[2], J. Martin[1]

[1] Université de Lorraine, CNRS, IJL, F-54000 Nancy, France

2 Université de Lorraine, CNRS, LEM3, Arts et Métiers ParisTech, F-57000 Metz, France

3 Université de Technologie de Belfort Montbéliard, ICB, F-90400 Sevenans, France

Abstract:

In the field of advanced materials, Metal Matrix Composites (MMC) and Ceramic Matrix Composites (CMC) occupy a prominent place. They are composed of a metallic or ceramic matrix reinforced by other materials, generally ceramic, metallic or polymer particles. MMCs and CMCs have improved mechanical, thermal and physical properties, making them useful in many potential applications. It is particularly advantageous to produce MMC and CMC coatings with varying compositional gradients. For example, combining a CMC surface layer with an MMC sublayer would provide a combination that offers both good wear resistance from the CMC surface layer and good deformation resistance from the MMC sublayer.

The present study focused on the tribological properties of a duplex surface treatment combining cold-spray deposition and plasma electrolytic oxidation (PEO) to produce Ceramic Matrix Composite (CMC) on Metal Matrix Composite (MMC) with aluminium coatings, including dispersed α-Al_2O_3, t-ZrO_2 and r-TiO_2 particles with improved tribological properties. Al/α-Al_2O_3, Al/t-ZrO_2 and Al/r-TiO_2 composite MMC coatings were first deposited by cold-spray, in various thickness and particles contents. First, the feasibility of cold-spraying thick, compact and adherent aluminium coatings containing well-dispersed α-Al_2O_3, t-ZrO_2 and r-TiO_2 particles (up to 14 vol%) will be demonstrated in this work. In a second step, a partial oxidation of these MMC layers allow the bulding of CMC layers using the PEO process under various processing durations and sparking regimes (arcs or soft regime).

Sliding wear tests were performed at room temperature under dry condition using the ball-on-disc test in the linearly reciprocating configuration (Anton-Paar TRN tribometer). The counterpart is a corundum ball with 6 mm diameter. The normal load and the sliding distance were adjusted depending on the nature of the coating (AMC or CMC).

The results obtained on the tribological properties of MMC aluminium coatings, including dispersed α-Al_2O_3 treated and untreated by PEO were published in reference 1. It was shown that the PEO oxide coatings exhibit strongly improved tribological properties compared with the as-sprayed coatings. The objective of this communication is to present the results obtained on MMC aluminium coatings t-ZrO_2 and r-TiO_2 treated and untreated by PEO.

Keywords: Tribology of Metral Matrix Composite (MMC); Tribology of Ceramic Matrix Composite (CMC); Cold-spray deposition; Plasma electrolytic oxidation (PEO); friction and Wear resistance

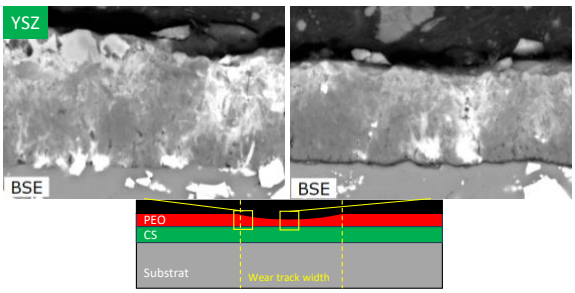

***Figure 1**: Cross-section under the CMC layer (PEO-treated) and the AMC sub-layer (untreated cold spray coating) after a friction test observed by Scanning Electron microscope. The transformed t-ZrO_2 particles in the PEO layer and the untransformed t-ZrO_2 particles in the cold spray sub-layer are visible, as is the good mechanical behavior of the CMC+AMC composite.*

References:

1. Maizeray, A., Marcos, G., Cappella, A., Planche, M. P., Liao, H., Henrion, G., ... & Martin, J. (2024), Surface and Coatings Technology, 482, 130713..

Design and generation of sealing shaft counter-surfaces by two-stage turning for the reduction of friction in sealing contacts

T. Junge [1*], L. M. de C. Silva [2], A. Nestler [1], A. Schubert [1], O. Koch [2]
[1] Professorship Micromanufacturing Technology, Chemnitz University of Technology, Chemnitz, Germany
[2] Chair for Machine Elements, Gears and Tribology (MEGT), University of Kaiserslautern-Landau, Kaiserslautern, Germany

Abstract:
For the sealing of shaft feedthroughs in pressure-free areas or sections with minor pressure difference typically radial shaft seals (RSS) are applied. However, their frictional torque is very high, compared to other machine elements such as roller bearings, resulting in corresponding wear of the machine element. Therefore, the objective of the investigations is to reduce the friction and wear of RSS by a function-oriented modification of the turning process for the production of the sealing shaft counter-surfaces (SCS). In this context, the influence of deterministic microstructures generated by hard turning on the tribological properties of the RSS in sealing contact is investigated.
In a first process step, the tool kinematics during external longitudinal turning is superimposed with a high-frequency oscillation in the ultrasonic range perpendicular to the specimen surface. The vibration of the tool creates a micro-structured surface which exhibits a sinusoidal profile in the cutting direction. In the second process step, machining is carried out without the superimposition of an ultrasonic vibration, whereby the depth of cut is selected to be smaller than the microstructure depth generated in the first process step. The resulting calottes can be varied in terms of their areal size (width, length), spacing and depth. These geometric parameters depend on the corner radius and cutting edge angles of the tool, the amplitude and frequency of the ultrasonic oscillation as well as the cutting parameters depth of cut, feed and cutting speed.
After the machining process the friction torque of the manufactured SCS in the sealing system is determined on a multi-shaft test bench. Each specimen with an diameter of 40 mm is tested on 8 different speed stages ranging from 500 to 4000 rpm. The results show that a larger width and depth of the calottes appear to reduce the friction torque in sealing contacts in comparison to ground SCS showing the high potential of microstructures machined by two-stage turning.

Keywords: radial shaft seal, friction, hard machining, two-stage turning.

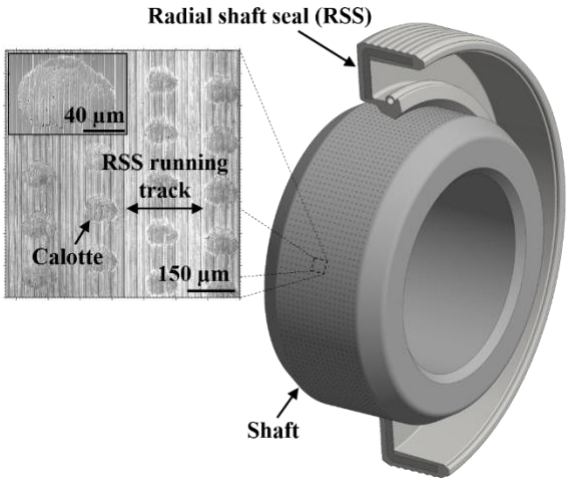

Figure 1: Depiction of the surface microstructure on the sealing shaft counter-surface resulting from the two-stage turning process (marking of the running track of the RSS after the frictional torque tests)

Effects of DLC and CrN thin coatings on the wear behaviour of L-PBF AlSi10Mg alloy

M. Merlin [1,*], C. Morales [1], S. Urbinati [1], C. Mopty [2], C. Soffritti [1]
[1] Department of Engineering (DE), University of Ferrara, Ferrara, Italy
[2] ISAE-Supméca, Higher Institute of Mechanics of Paris, Saint-Ouen, France

Abstract:
In the literature, many works have been published on improving the mechanical response of the laser-powder bed fusion (L-PBF) AlSi10Mg alloy through optimized heat treatments and/or the deposition of thin film coatings, but fewer publications report the achievement of satisfactory tribological properties [1,2]. In [3] the evolution of hardness and impact toughness after thermal exposure at high temperatures of the AlSi10Mg alloy produced by L-PBF was investigated in order to assess the possibility of combining the aging step of heat treatments and physical vapor deposition treatments.
In this work, a nanostructured doped CrN coating with a broad spectrum of applications, deposited using the environmentally friendly physical vapor deposition (PVD) sputtering technology, was applied to an L-PBF AlSi10Mg alloy substrate after the application of a NiP binder layer with medium phosphorus content. The coating was deposited to the as-built material, but also to the substrate after undergoing hot isostatic pressing (HIP) or HIP plus T6 heat treatment, the latter performed directly inside the HIP vessel. The influence of the different microstructural and mechanical characteristics of the substrate on the tribological performance of the innovative doped CrN coating was investigated. The tribological tests were conducted by a ball-on-disk device, in reciprocating condition, using 6 mm diameter Al_2O_3 balls as counterpart material, and with a normal load of 10 N. A deep microstructural characterization was conducted using optical and scanning electron microscopy to highlight the role of the substrate properties on the performnce of the coating. A DLC coating applied to the same substrate and in the same treated conditions was used as benchmark.
The research activities were conducted within the ALERT project with the financial support of the PR-FESR EMILIA ROMAGNA 2021-2027.

Keywords: L-PBF AlSi10Mg alloy, HIP and heat treatment conditions, CrN and DLC coatings, wear properties, microstructure.

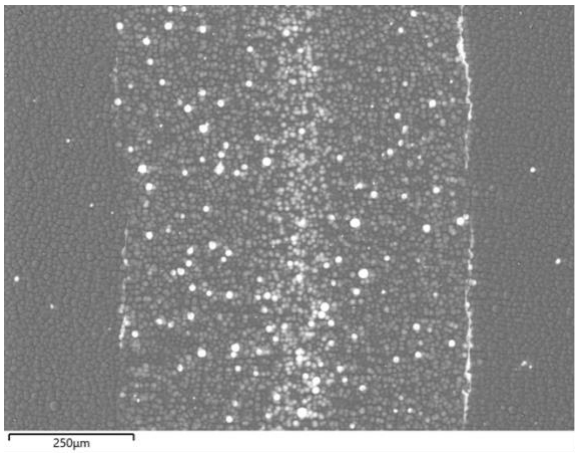

Figure 1: Example of worn surface of a L-PBF AlSi10Mg disc in the HIP condition against the Al_2O_3 counterpart material.

References:

1. Di Egidio, G., Martini, C., Ghassemali, E., Morri, A. (2025) Electroless Ni-P + diamond-like carbon multilayer: Influence on tribological bahaviour of AlSi10Mg produced by powder bed fusion – Laser beam, *Wear,* 205803, 566-567.
2. Kan, W. H., Huang, S., Man, Z., Yang, L., Huang, A., Chang, L., Nadot, Y., Cairney, J. M., Proust, G. (2021), Effect of T6 treatment on additively-manufactured AlSi10Mg sliding against ceramic and steel, *Wear*, 203961, 482-483.
3. Lattanzi, L., Merlin, M., Fortini, A., Morri, A., Garagnani, G. L. (2021) Effect of thermal exposure simulating vapor deposition on the impact behavior of additively manufactured AlSi10Mg alloy, *JMEPEG,* 31, 2859-2869.

Influence of O_2 flow rate on scratch and wear behavior of silver oxide thin films fabricated via RF magnetron sputtering deposition

Khunnay Win[1], Krzysztof Kulikowski[2], Marcin Koba[1]
[1]Warsaw University of Technology, Institute of Microelectronics and Optoelectronics, Koszykowa 75, 00-662 Warsaw, Poland.
[2]Warsaw University of Technology, Faculty of Materials Science and Engineering, ul. Woloska 141, 02-507 Warsaw, Poland.

Abstract:
Silver oxide (AgO) thin films are widely used in electronic and optical applications; however, their scratch and wear behavior remains insufficiently understood. In this work, AgO thin films were deposited on silicon and glass substrates by radio-frequency (RF) magnetron sputtering, with the oxygen (O_2) flow rate varied from 5 to 40 sccm. The influence of O_2 flow rate on the mechanical and tribological properties of the films was systematically investigated. Nanohardness was evaluated by nanoindentation, while scratch resistance was assessed using a micro-scratch tester. Friction and wear behavior were examined against Si_3N_4 counter balls using ball-on-disc micro-tribological tests. The results demonstrate that the O_2 flow rate significantly affects the mechanical response and tribological performance of AgO thin films. Compared with bare substrates, AgO-coated samples exhibited reduced friction coefficients and improved wear resistance, indicating a protective and potentially self-lubricating role of the AgO layer. These findings provide insight into the optimization of deposition conditions for AgO thin films intended for applications involving mechanical contact.

Keywords: AgO; thin films; RF magnetron sputtering; nanohardness; scratch resistance; wear

Improved wear protection of tribological boundary layers

N. Gregarek [1*], G. Jacobs [1], S. Zhang [1]
[1] Institute for Machine Elements and Systems Engineering, RWTH Aachen University, Aachen, Germany

Abstract:
Sliding-rolling contacts, as found in rolling bearings, are prone to wear when operating under mixed lubrication regimes. To reduce the wear damage, Zinc-dithiophosphates (ZDDP) additive is used in lubricants to form wear-protective tribological boundary layers (TBL). However, ZDDP is ecotoxicologically questionable. Therefore, alternative approaches which can form the boundary layer with less ZDDP are essential.
TBLs are formed during the running in process. As shown in Figure 1, a distinction is made between inner and outer boundary layer [1]. While the inner TBL is formed by plastic deformation of the base material, the outer TBL is formed by adsorption of ZDDP molecules and by chemical reaction of the ZDDP and surface material [2]. These adsorption layers improve wear protection in mixed friction by separating the contacting surfaces [3].
In addition to the running in process, TBL can be pre-formed during the manufacturing process. In rolling bearings, surfaces are finished by external cylindrical grinding. During grinding, the thermo-mechanical loads influence the inner boundary layer, whereas chemical reactions with the cooling lubricants contribute to the formation of an outer boundary layer. TBLs pre-formed during bearing manufacturing potentially help to reduce ZDDP usage during operation.
However, wear protection capacity of TBL formed by the combined processes of grinding and running in remines unknown. A deeper understanding of the cause-effect relationships connecting grinding, running in, TBL formation and wear protection is necessary.
To address this question, this study investigated the cause-effect chain from the initial grinding process, over the running in process, to the wear protection of the formed TBL. A grinding machine is used to manufacture the surface of the tested bearing inner rings. Afterwards, the rings are mounted on a two-disc tribometer, shown in Figure 2, to test TBL formation during running-in and wear protection. TBL composition was investigated with EPMA and EDX. Wear protection capacity was evaluated by wear loss, surface profiles and optical microscopy.
It is found that the grinding parameters have a noteworthy influence on TBLs formed during run-in. Optimal grinding parameters for TBL formation and wear protection are reported.

Keywords: Tribological boundary layer, tribofilm, grinding, wear, ZDDP, rolling bearing, tribology, sliding-rolling contact.

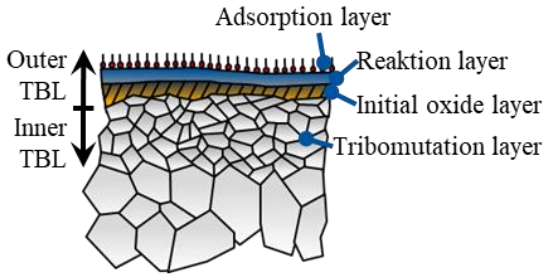

Figure 1: Schematic structure of TBLs (based on [1]).

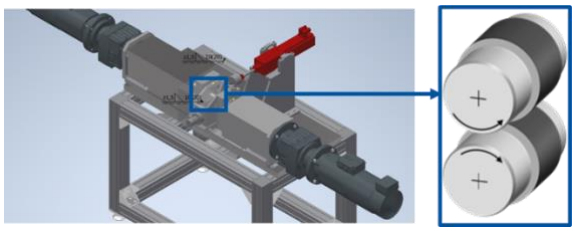

Figure 2: A schematic view of two-disc tribometer and tested rings

References:

1. Burghardt, Gero. *Wirkung tribologischer Grenzschichten in Wälzlagern unter Mischreibung: Mechanism of tribological boundary layers in rolling bearings under mixed friction*. Verlagsgruppe Mainz GmbH, 2018.
2. Evans, Ryan D., et al. "Transmission electron microscopy of boundary-lubricated bearing surfaces. Part II: mineral oil lubricant with sulfur-and phosphorus-containing gear oil additives." *Tribology transactions* 48.3 (2005): 299-307.
3. Hsu, Stephen M., and Richard S. Gates. "Boundary lubricating films: formation and lubrication mechanism." *Tribology international* 38.3 (2005): 305-312.

The self-healing corrosion resistant coatings for AZ-31 magnesium alloy

Abstract:
The self-healing materials attract a lot of attention as self-healing ability considerably improves the reliability of service and elongates the life time of materials. However, the present self-healing materials lack the mechanical strength and thus cannot be used in practical applications. The industrial elastomer (VHB 4910) is a strong polymer which has been used as a dielectric actuator. Surprisingly, we observed that VHB 4910 has autonomic self-healing ability. As it is considered to be an acrylic polymer, we analyzed the hydrogen bonding between carbonyl and hydroxyl groups and consider that this bonding and the molecular chain entanglement contributes to its self-healing ability. The tensile test, X-ray diffraction (XRD), Raman and Fourier transform infrared (FTIR) spectroscopy were employed to analyze the self-healing processes. The tensile test demonstrates the self-healing process based on recovery of strength of VHB 4910. The XRD result shows that VHB 4910 is amorphous. The random associated molecular chains have a widely distributed hydrogen bonding. The Raman and FTIR spectra demonstrate that the strong hydrogen bonding initiates the self-healing process and the molecular chain diffusion contributes to the self-healing ability. This study provides an insight into the mechanism of self-healing behavior and ability of VHB 4910 to recover its strength.

Friction mode and humidity effects on tribological behavior of DC magnetron sputtered $(NbMoTaW)_{100-z}$-$(CN)_z$ coatings

F. Lofaj[1*], P. Hviščová[1], D. Kondrakhova[1], Jozef Dobrovodský[2]
[1] Institute of Materials Research of the Slovak Academy of Sciences, Košice, Slovakia,
[2]Advanced Technologies Research Institute, Slovak University of Technology in Bratislava, Trnava, Slovakia

Abstract:
The work describes the influence of the friction mode and humidity on friction behavior of $NbMoTaW_{100-z}(CN)_z$ coatings with variable stoichiometry [1]. Two series of coatings weredeposited using reactive DC magnetron co-sputtering from a composite NbMoTaW and carbon targets. Two levels of power (300 W and 600 W) were applied to the carbon target in each series, respectively, while nitrogen flow varied from 0 sccm upp to 10 sccm. Time-of-flight elastic recoil analysis (ToF ERDA) showed that the carbon concentrations in the corresponding series were around 18 at% at 300 W and ~40 at% at 600 W on the carbon target, whereas nitrogen concentrations increased proportionally to nitrogen flow. The summary concentrations of carbon and nitrogen, *z*, exceeded 50 at%, stoichiometric limit in the coatings with the highest additions of nitrogen due to the presence of free carbon phase. The friction tests were performed in the linear reciprocal mode against alumina ball under the loads of 0.3 N and 1.0 N for 10^4 cycles (~70 m) in the ambient air atmosphere. The coefficients of friction (COF) depended on the coating stoichiometry, applied load and air humidity. The coatings with low carbon and nitrogen concentrations (low *z*) tested under 1 N load at 51-56 % relative humidity exhibited COF just below 0.3 and they decreased to 0.16 at 7 sccm N_2 corresponding to z = 52 at%. The differences in COFs were related to the differences in wear track morphologies. The tracks with high COFs in low *z* coatings contained relatively large areas covered by thin transfer films (Fig. 1). Their SEM/EDS observations indicated high oxygen concentrations. The Raman spectra from these transfer films contained strong double peak in the region 720 - 960 cm^{-1} attributed to the oxides. The spectra from the debris around the track, besides the oxide peaks, exhibited two peaks centered around 1350 cm^{-1} and 1570 cm^{-1} related to the disordered graphitic carbon. In contrary, the formation of transfer films coatings with high *z* exhibiting the lowest COF values were strongly suppressed - wear tracks were mostly clean, with smooth grooves and with the same composition as the as-deposited coating. The counterpart – alumina ball – exhibited only grooves witout any transfer layer. Thus, the formation of transfer film in the wear track was concluded to control COFs. Its formation reguires oxidation of the ME-CN compound. The proposed model assumes that the asperities in the carbonitride coating are subjected to highly localized tribo-oxidation. It means that C and N were partially or fully replaced by oxygen from the ambient atmosphere. Released nitrogen is volatile whereas two possibilities can be considered for "free" carbon behavior. If the primary oxide particle released from the asperity is pushed aside of the track as a debris, residual carbon may still be present. In the opposite case, particle would be subjected to cyclic shear forces during reciprocal movement and free carbon can be fully "burned" producing the oxide transfer film. COF in more metallic-like coatings (low *z*) would be controlled by the friction between alumina ball and oxide transfer film, whereas in (near-)stoichiometric carbonitride (high z) coatings, which are more resistant to oxidation than metals, COFs would be determined by adhesion mechanisms between alumina and carbonitride surface.
Tribochemical reactions involved in transfer film formation would be strongly affected by the humidity which could be a source of -OH groups facilitating nitrogen and carbon release. The additional tests on low *z* coatings at lower (31-42 %) relative humidities revealed enhanced transfer film formation accompanied by strong COF variations (Fig. 2).
Another important factor involved in the above transfer film model is the stability of a transfer film. Reciprocating movement involves cyclic generation and destruction of transfer film with permanent changes in its area covering the wear track. Altough the rotational (ball-on-disc) mode is also cyclic, formation of a continuous transfer film would be enhanced and its destruction suppressed due to only one direction of the mutual movement. The results comparing the

behavior in the linear reciprocating and rotation modes will be presented.

ACKNOWLEDGMENT

This work was supported by the EU NextGenerationEU through the Recovery and Resilience Plan for Slovakia under project No. 09I03-03-V04-00281 and by the Slovak Research and Development Agency (project APVV-24-0038).

Keywords: high entropy carbonitride coatings, substoichiometric compounds, friction, transfer film, tribochemical reactions, humidity effect.

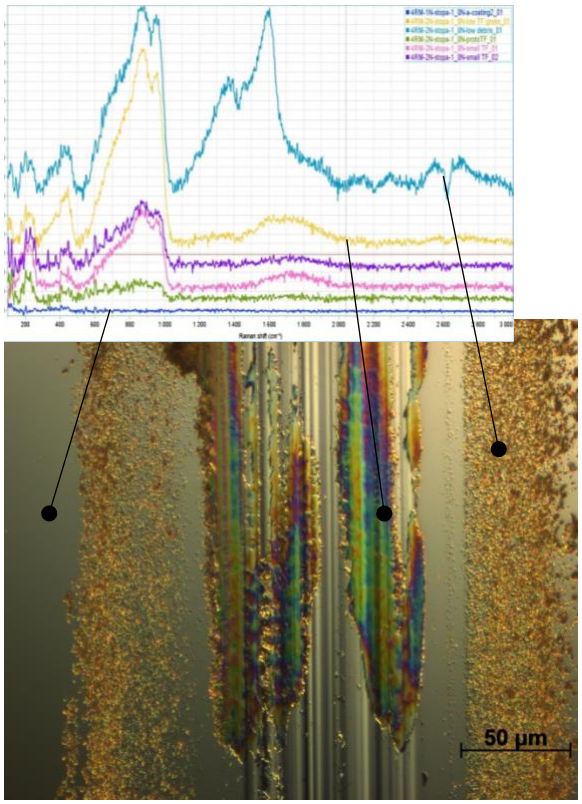

Figure 1: Transfer film in the wear track of DCMS $(NbMoTaW)_{100-z}$-$(CN)_z$ coatings (z = 39.8 at% = 14.7 at% C + 25.1 at% N) formed after 10^4 cycles of reciprocal friction under the load of 1.0 N in air with the relative humidity of 51%. The insert show Raman spectra in the coating, transfer film and wear debris, respectively.

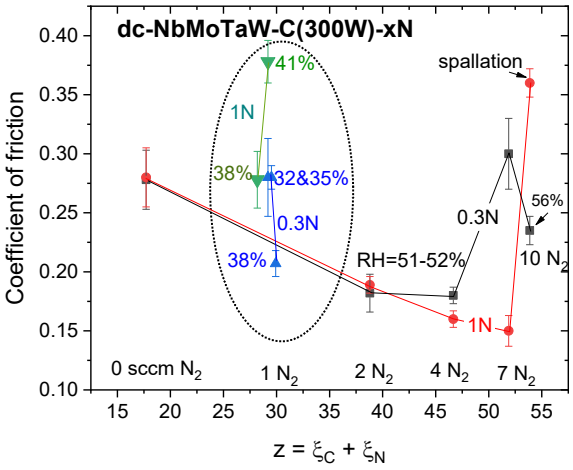

Figure 2: The dependences of the coefficient of friction (COF) on the summary concentration of carbon and nitrogen (*z*, respectively coating stoichiometry) in $(NbMoTaW)_{100-z}(CN)_z$ coatings at two loads (0.3 N and 1.0 N) and different relative humidities.

References:

1. Lofaj, F., Hviščová, P., Pristáš, G., Dobrovodský, J., Albov, D., Lisnichuk, M., Gabáni, S., Flachbart, K. (2025), The effects of carbon and nitrogen incorporation on the structure, mechanical properties and superconducting transition temperature of $(NbMoTaW)_{100-z}(CN)_z$ coatings, *Thin Solid Films*, 823, 140704. Doi:10.1016/j.tsf.2025.140704

Friction of GO/$MoSe_2$ films in ambient air and vacuum conditions

A. Kozak [1*], M. Precner[1], M. Precnerová [2], M. Ilčíková [3,4,5], N. Konios [3], M. Mičušík [3], J. Osička [4], V. Vretenár [6] J. Mosnáček [3], M. Ťapajna [1],

[1] Institute of Electrical Engineering, Slovak Academy of Sciences, Bratislava, Slovakia
[2] Centre for Advanced Materials Application, Slovak Academy of Sciences, Bratislava, Slovakia
[3] Polymer Institute SAS, Dúbravská cesta 9, Bratislava 845 41, Slovakia
[4] Centre of Polymer Systems, Tomas Bata University, Trida Tomase Bati 5678, Zlin 76001, Czechia
[5] Faculty of Technology, Tomas Bata University, Vavreckova 5669, Zlín 76601, Czechia
[6] Centre for Nanodiagnostics of Materials, Faculty of Materials Science and Technology, Slovak University of Technology, Vazovova 5, 812 43 Bratislava, Slovakia

Abstract:

Owing to their layered structure and ability to reduce friction and wear through ultra-low shear strength, two-dimensional (2D) van der Waals materials are emerging as key candidates for lubrication in MEMS and high-precision devices [1]. Furthermore, the solid nature of 2D materials makes them essential for effective lubrication under high temperatures or low pressures where classical liquid lubricants fail [2]. However, current research primarily focuses on their use as additives in liquid lubrication systems.

Molybdenum diselenide ($MoSe_2$) is a layered crystal known for its promising tribological properties, such as high humidity stability and lower friction coefficients (COF) than MoS_2 at high temperatures [3]. Additionally, $MoSe_2$ is considered as an additive to carbon allotropes for reducing COF at low humidity and in a vacuum. In this work, we investigate the COF of $MoSe_2$/graphene oxide (GO) films in different environments for the first time. Our analysis focuses on CVD-synthesized $MoSe_2$ layers consisting of isolated flakes (up to 500 nm thick), spin-coated isolated GO flakes (up to 3 μm thick), and $MoSe_2$/GO bilayer formed by spin-coating GO onto CVD $MoSe_2$.

Friction measurements were conducted using a SiN ball (0.5 N load) in both ambient air and vacuum (1×10^{-5} mbar) enviroments. In ambient air, pure $MoSe_2$ demonstrated the lowest COF 0.09. The bilayer samples showed COF 0.17, while GO exhibited the highest COF 0.23. This trend was reversed in a vacuum. While $MoSe_2$ remained stable due to its low humidity dependence, the GO-containing samples showed significantly reduced COF. COF of GO dropped to 0.02, and bilayers dropped to 0.06 (Fig.1).

After the friction test, the wear tracks were analyzed by optical profilometry, Raman, AFM, SEM, XPS, and TEM. The transfer layers were investigated by Raman and optical profilometry. These investigations show that the low COF of pure GO is attributed to substrate modification, while $MoSe_2$ and bilayer samples rely on the formation of a transfer layer on the ball. Lowering of the COF of bilayer samples is accompanied by the penetration of GO flakes into the sliding interface. This trend is observed in bilayers under both ambient air and vacuum conditions. In contrast, the pure GO samples suffer from relatively quick coating exhaustion and subsequent substrate wear in ambient air. Finally, formation of the tribolayer and transfer layer pair in pristine $MoSe_2$ samples is responsible for COF stability in both ambient and vacuum environments.

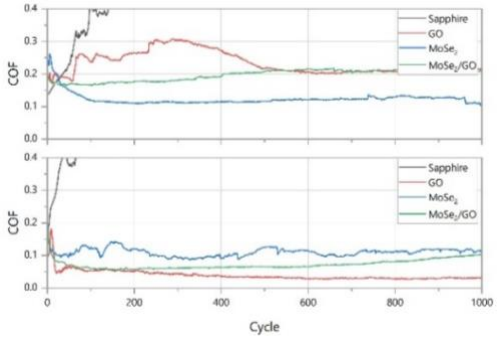

Figure 1: COF of samples of $MoSe_2$/GO system.

This work was funded by the EU NextGenerationEU through the Recovery and Resilience Plan for Slovakia under the project No. 09I03-03-V04-00709.

Keywords: 2D materials, friction in vacuum , ultrathin layers, Graphene oxide, $MoSe_2$

References:

1. Lee C., Li Q., et. all,. (2010) Frictional characteristics of atomically thin sheets, Science (80). 328 76–80.
2. Song H., Chen J., et. all,. (2020) Low friction and wear properties of carbon nanomaterials in high vacuum environment, Tribol. Int. 143, 106058.
3. Kubart T., Polcar T., et. all,. (2005) Temperature dependence of tribological properties of MoS_2 and $MoSe_2$ coatings, Surf. Coat. Techn. 193 230-233.

Replacing PTFE with Self-Organizing HDPE Particle containing Composites for low Friction Applications

N. Kubat[1*], J. Rank[1], J. Bahr[1], J. Carstensen[1], R. Adelung[1]
[1] Functional Nanomaterials Chair, Christian-Albrecht's-University, Kiel, Germany

Abstract:
The increasing regulatory and societal pressure to eliminate PFAS from devices in various fields poses a significant challenge, particularly for coatings used in low friction applications. PFAS are environmentally persistent, bio accumulative substances associated with long-term ecological contamination and potential adverse health effects.
Due to the exceptional low surface energy of PFAS Materials, conventional coatings on metals are typically done as a Multilayer system, for example with PAI as a base layer. As global efforts intensify to restrict persistent fluorochemicals, the development of high-performance, PFAS-free alternatives has become increasingly urgent. One of the few polymers that offer comparable friction properties is HDPE. However, the coating possibilities are rather limited, especially for thin coatings in the range of 10-50µm.
This paper presents a PFAS-free coating concept for metal substrates based on a self-organizing HDPE/PAI composite, where HDPE particles are dispersed in a commercially established PAI coating. The HDPE-PAI coating is produced through a temperature optimized curing process that preserves particle integrity and ensures uniform distribution within the matrix, yielding a functional surface texture with particles breaching the surface. Thereby the HDPE particles can act as sliding elements which dominates the friction behavior of the coating, while maintaining the general properties of the already established PAI coating. A comparison of these composites with the conventional PAI–PTFE system will be discussed and thereby highlight a viable pathway toward a sustainable, fluorine-free coating systems for low friction applications.

Keywords: PFAS-free, low friction composites, HDPE, PAI, Dispersion, environmentally friendly, Low Friction coatings, self-organizing.

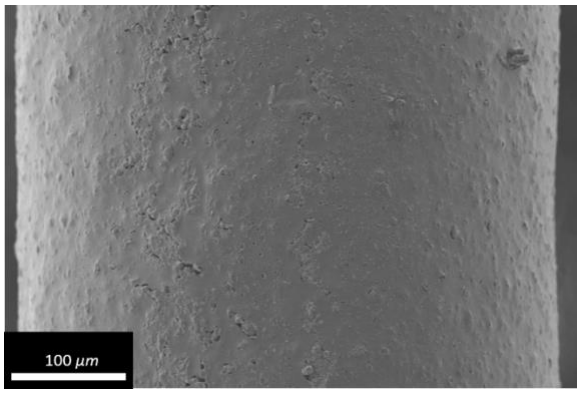

Figure 1: HDPE-particle embedded PAI coatings for low friction applications.

Friction in Polymer Systems under Low-Temperature Conditions

A. Ptak [1,*], M.Kiełb[1], W.Wieleba[1]
[1] Department of Fundamentals of Machine Design and Mechatronic Systems, Wroclaw University of Science and Technology, Faculty of Mechanical Engineering, Wrocław, Poland

Abstract:
This study investigates the effect of reduced temperature and contact pressure on the tribological behavior of self-mated polymer – polymer pairs under technically dry friction conditions. Three widely used engineering polymers – polyoxymethylene (POM), polyamide 6 (PA6), and polyethylene terephthalate (PET) – were examined over a temperature range from 21 °C to −50 °C.
The coefficient of static friction was determined using a custom-built pin-on-plate test rig based on the inclined plane principle, enabling evaluation under different nominal contact pressures. Complementary analyses included scanning electron microscopy (SEM), surface roughness measurements using 3D optical profilometry, and microhardness testing.
The results demonstrated a clear increase in the coefficient of static friction with decreasing temperature for all investigated materials, which is attributed to reduced polymer chain mobility and increased stiffness of the surface layer. Increasing contact pressure led to a reduction in friction values, particularly at higher temperatures. Surface analyses revealed a transition in wear mechanisms from deformation – dominated behavior to brittle–abrasive processes at lower temperatures, accompanied by increased surface roughness and the presence of wear debris. Microhardness measurements confirmed temperature-induced stiffening for POM and PET, while PA6 exhibited non-monotonic behavior at the lowest temperatures, likely related to changes in hydrogen bonding.
Overall, the findings highlight the dominant role of temperature in governing the tribological performance of polymer – polymer sliding pairs, emphasizing the importance of combined mechanical, topographical, and microstructural analysis for understanding friction mechanisms under low-temperature conditions..

Keywords: polymer tribology, low-temperature behavior, static friction, polymer – polymer contact, surface roughness, microhardness, SEM analysis, dry friction.

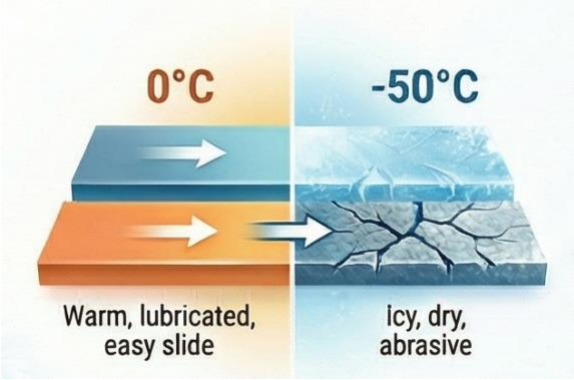

Figure 1: Schematic illustration of the influence of temperature on the tribological behavior of polymer surfaces: at higher temperatures (0 °C), sliding is characterized by smoother motion and lower resistance, whereas at low temperatures (-50 °C), increased stiffness leads to brittle surface behavior, crack formation, and more abrasive friction conditions.

References:

1. Nikonovich M, Ramalho AL, Emami N. (2024) Effect of cryogenic aging and test environment on the tribological and mechanical properties of PEEK composites. *Tribol International*; 194:109554.
2. Ramesh V, van Kuilenburg J, Wits WW. (2019) Experimental Analysis and Wear Prediction Model for Unfilled Polymer–Polymer Sliding Contacts. *Tribology Transactions*; 62(1):1-13.
3. Bashandeh K, Tsigkis V, Lan P, Polycarpou AA. (2021) Extreme environment tribological study of advanced bearing polymers for space applications. *Tribology International*;153:106634.
4. Kim Y, Kim MS, Jeon HJ, Kim JH, Chun KW. (2022) Mechanical performance of polymer materials for low-temperature applications. *Appl Sci*.;12(23):12251.

Effect of Microstructure on the Wear Behavior of Eutectic and Non-Eutectic BCC High-Entropy Alloys

Liming Chen [1*], Wenbo Ma [1], Oleksandr Tisov [1]
[1] School of Aerospace Engineering, Xi'an Jiaotong University, Xi'an, China

Abstract:
The increasing demand for wear-resistant materials in aerospace, energy, and advanced manufacturing industries has stimulated extensive research on novel alloys with superior tribological performance. In particular, high-entropy alloys (HEAs) have attracted significant attention due to their unique compositional design and promising mechanical and tribological properties. This study investigates the room-temperature dry wear behavior of five body-centered cubic (BCC) high-entropy alloys (HEAs), namely $Al_{0.75}$CrFeNi, AlCrFeNi, AlCrFeNiMn, AlCoCrFeNi, and AlCoCrFeNiMn, under reciprocating sliding conditions. Among them, $Al_{0.75}$CrFeNi, AlCrFeNi, and AlCrFeNiMn exhibit eutectic BCC+B2 microstructures, whereas AlCoCrFeNi and AlCoCrFeNiMn present non-eutectic BCC structures. Hardness measurements show relatively small differences among these five HEAs. However, the eutectic BCC HEAs exhibit significantly narrower and shallower wear tracks than the non-eutectic BCC HEAs, following the order: AlCrFeNi < $Al_{0.75}$CrFeNi < AlCrFeNiMn < AlCoCrFeNi < AlCoCrFeNiMn (Figure 1). The enhanced wear resistance is likely associated with the characteristic BCC+B2 microstructure and the formation of oxide debris during sliding. The results indicate that the room-temperature wear resistance is not solely governed by hardness but is also influenced by microstructure and tribo-oxidation. Furthermore, the addition of Mn is found to reduce the room-temperature wear resistance of BCC HEAs in both eutectic and non-eutectic systems. These findings provide new insights into the relationship between microstructure and tribological performance in BCC HEAs and offer useful guidance for the design of wear-resistant high-entropy alloys.

Keywords: high-entropy alloys, body-centered cubic, eutectic structure, room temperature, friction and wear, tribo-oxidation.

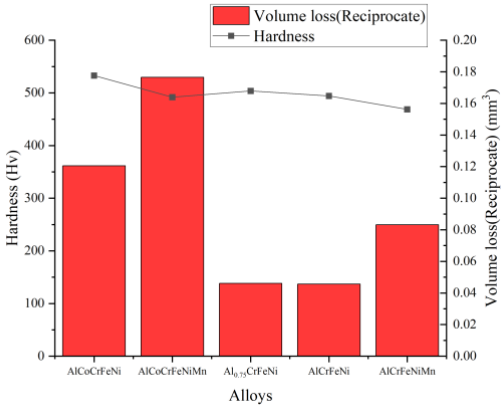

Figure 1: Figure illustrating the hardness and volume loss of five HEAs after reciprocating wear test.

References:

1. Lu, Y., et al. (2020), Promising properties and future trend of eutectic high entropy alloys. *Scripta Materialia*, 187: p. 202–209.
2. Sasi, R., Gallo, S. C., Attar, H., Taherishargh, M., Barnett, M. R., & Fabijanic, D. M. (2024). The effect of phase constituents on the low and high stress abrasive wear behaviour of high entropy alloys. *Wear*, 556, 205531.

Tribological behaviour of Soybean oil-based biolubricants

P.Mostaza[1*], M.D. Avilés[1], T. Caparrós[1] , M.D. Bermúdez[1] and F.J. Carrion-Vilches[1]

[1]Grupo de Ciencia de Materiales e Ingeniería Metalúrgica. Universidad Politécnica de Cartagena
C/ Doctor Fleming sn, 30201 Cartagena (SPAIN)

Abstract:
The growing demand for environmentally friendly solutions in industrial lubrication has led to increased interest in biodegradable and bio-based lubricants. Vegetable oils are considered promising alternatives to mineral-based lubricants due to their excellent lubricity, renewability, additive compatibility, and non-toxic nature.

Nevertheless, their limited thermal stability and poor oxidation resistance restrict their use under high-performance conditions. To overcome these drawbacks, chemical modifications such as epoxidation have been employed to improve oxidative stability and viscosity behavior [1]. Additionally, the incorporation of graphene-based [2] nanomaterials has shown great potential in enhancing the tribological performance, due to its exceptional thermal conductivity, mechanical strength, and anti-wear properties.

These strategies, along with the use of protic ionic liquids (PILs) as functional additives, contribute to the development of advanced eco-lubricants with superior tribological characteristics and minimal environmental impact [3].

This work presents the tribological performance of neat and epoxidized soybean oils, as well as formulations enhanced with IL and graphene. The study aims to evaluate the effect of chemical modification and nanoparticle addition on friction and wear behavior.

Tribological tests were conducted using a pin-on-disc tribometer with a sapphire/stainless steel tribopair, applying a Hertz contact pressure of 1.4 GPa. Wear rate was determined by means of profilometry. Optical and electron microscopy, along with various spectroscopic and characterization techniques, were used to establish the wear mechanisms and the stability of the oils under tribological conditions.

The results show (Figure 1) that epoxidized soybean oil (ESy) combined with the different additives improves its tribological behaviour. These improvements are attributed to the effect of ionic liquid enhancing tribological behaviour and graphene providing superior load-carrying capacity and anti-wear properties.

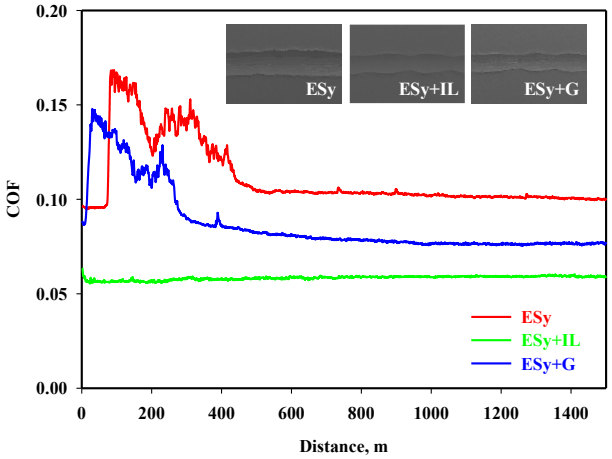

Figure 1: Friction coefficient and wear track for the tribopair sapphire/stainless steel using an epoxidized soybean oil modified with ionic liquid or graphene.

Keywords: vegetable oil, epoxidized oil, ecolubricant, ionic liquids, tribology, graphene

References:

1. Avilés, M.D., Caparrós, T., Mostaza, P., Bermúdez, M.D., Carrion, F.J. (2025) Novel vegetable biolubricants containing ionic liquid, *Tribology International*, 202, 110255.
2. Berman, D., Erdemir, A., Sumant, A.V. (2014) Graphene: a new emerging lubricant, *Materials Today*, 17, 31-42.
3. Bermúdez, M.D., Jiménez, A.E., Sanes, J., Carrion, F.J. (2009) Ionic liquids as advanced lubricant fluids, *Molecules*, 14, 2888-2908.

SICT 2026 / Plasma Tech 2026 / Tribology 2026 Joint Plenary Session II

Plasma Fluxes and Their Atomic-Scale Heating Effects on Thin Film Growth

A. Anders[1,2,*], D. Kalanov[1], Y. Unutulmazsoy[1]
[1] Plasma Engineering LLC, El Cerrito, California, USA
[2] Leibniz Institute of Surface Engineering, Leipzig, Germany
* andre.anders@plasmaengineering.com

Abstract:
Plasma deposition and plasma-assisted deposition bring energetic particles (especially ions) to the surface that contribute to heating of the growing film. In contrast to conventional substrate heating, which is accomplished by radiative or ohmic heaters, particle fluxes provide what could be called non-equilibrium heating because the initial effects are transient and highly localized [1]. Over the course of film growth, each surface atom is subject to several non-equilibrium heating events, which do not overlap due to their short duration (ps) and small spatial extent (nm²). These events are very efficient because the energy is brought directly to the surface where growth occurs, as opposed to heating the entire film and substrate. After impact events, the particle energy is distributed by heat conduction throughout the film and into the heat sink (substrate).
Plasma particles in this context are primarily ions, often accelerated in the sheath adjacent to the surface, but also include electrons, atoms, and photons [3-5]. Besides kinetic energy effects, the role of potential energy is discussed, in particular the effects of multiply charged ions, which are present in some plasmas such as cathodic arc plasmas and, to a lesser degree, in HiPIMS plasmas. In this talk, the various contributions are parsed, and the concept, advantages, and limitations of non-equilibrium heating are highlighted.

Keywords: arc plasma, HiPIMS plasma, non-equilibrium heating, plasma deposition, sheath, ion acceleration, ion charge state, transparent conducting oxide, transition metal nitrides

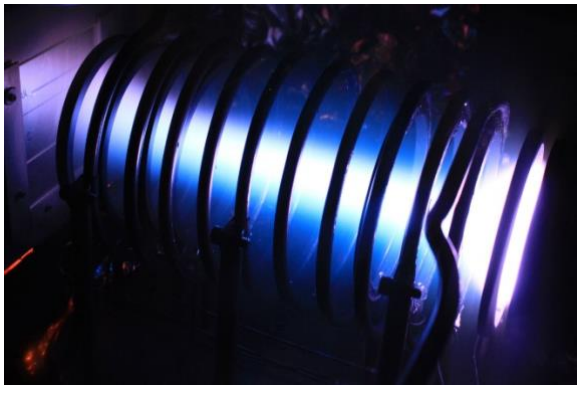

Figure 1: Example of a plasma that is "engineered" to maximize non-equilibrium heating, here a HiPIMS plasma of zinc in an argon–oxygen mixture that is transported through an axial magnetic field to enhance positive ion flux while reducing damaging negative oxygen ions [2].

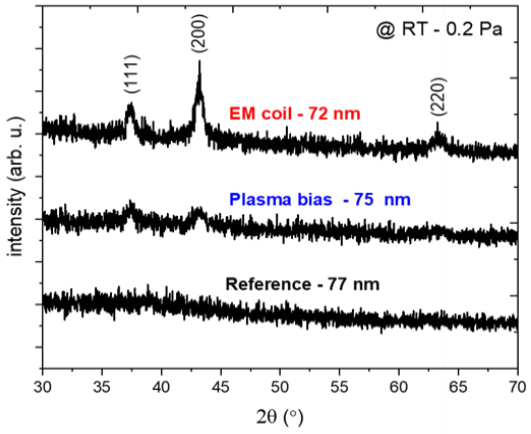

Figure 2: Example of the effects of non-equilibrium heating on AlVN thin films deposited at room temperature, where films with enhanced ion charge states (labeled here as "EM coil") show nanocrystalline features without conventional substrate heating [3].

References:

1. A. Anders, Surf. Coat. Technol. 520, 132946 (2026).
2. A. Anders and J. Brown, IEEE Trans. Plasma Sci. 39, 2528 (2011).
3. Y. Unutulmazsoy et al., J. Vac. Sci. Technol. A 41, 063106 (2023).
4. S. Karimi Aghda et al., Acta Mater. 250, 118864 (2023).
5. D. Kalanov et al., Surf. Coat. Technol. 497, 131720 (2025).

Methane pyrolysis in a constant-current DC gliding arc discharge: impact of discharge regime on the process performances and soot formation

Pierre Mathieu[1], Yuan Tian[1,2], Assan Abdirakhmanov[1], Abhyuday Chatterjee[1], Rony Snyders[1,3]
[1]Research group ChIPS, University of Mons, Mons, Belgium
[2]Research Unit Plasma Technology (RUPT), Ghent University, Ghent, Belgium
[3]Materia Nova research centre, Mons, Belgium

Abstract:
An atmospheric Ar-based 2D gliding arc discharge was tested for the clean reforming of CH_4 into H_2 and valuable by-products, primarily C_2H_2 and carbon-based powders. The effect of feed gas flow, CH_4 admixture in Ar and fixed current on the performance of the process was investigated. The discharge achieved a maximum CH_4 conversion of about 30% for a specific energy input of 60 kJ mol^{-1}. The arc's gas temperature and electron density are in the order of 6000 K and 10^{14} to 10^{16} cm^{-3}, as respectively determined by rotational and Stark spectroscopy. Planck's radiation law was fitted to the spectrum's background and suggests the solid phase reaches temperatures as high as 4000 K.

Green Plasma Processing – from Deposition to Gas Conversion

D. Hegemann [1*], P. Navascués [1*], R. Snoeckx [1]
[1] Plasma & Coating Group, Empa, St.Gallen, Switzerland

Abstract:
Electrically excited plasmas contribute to "green processing" by supplying energy to molecules, allowing chemistry at dry and low-temperature conditions since the plasma is in a non-equilibrium state with high electron temperatures. In a low-pressure plasma, electron impact excitation is the predominant way to transfer energy to molecules, whereby several inelastic collisions during the residence time of a molecule in the plasma result in an average energy uptake per molecule, the specific energy input [1]. In this case, thermodynamic principles can still be applied governing plasma chemistry in the gas phase, emphasizing the role of entropy changes in an open system driving by the external electric field as illustrated in Figure 1 [2,3].
Different examples are presented considering plasma polymer film growth with organosilicons to potentially replace per- and polyfluorinated substances (PFAS) in repellent coatings, following safe and sustainable by design (SSbD) principles [4]. Requirements to enhance functionality and durability, to enable up-scaling as well as safe applications including end-of-life are discussed. Furthermore, the conversion of hydrocarbons into valuable products using elevated pressure and temperature is investigated, focusing on plasma activation by electron impact and gas heating [3].
Plasma technology thus offers huge potential to contribute to environmentally friendly processes.

Keywords: plasma chemistry, plasma deposition, plasma gas conversion, PFAS alternatives, environmental aspects.

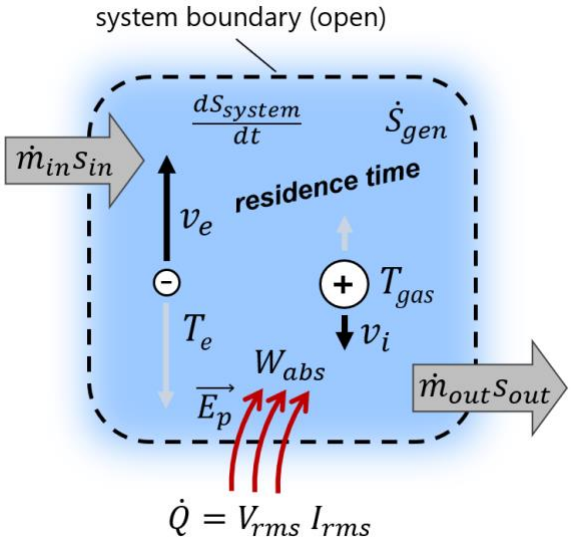

Figure 1: Energy transfer and entropy export in an electrically excited plasma (open system) via electron impact reactions (temperature T_e and drift velocity v_e) and Joule heating through ionic motion (temperature T_{gas} and drift velocity v_i).

References:

1. Hegemann, D. (2023) Plasma Activation Mechanisms Governed by the Specific Energy Input: Potential and Perspectives, *Plasma Process. Polym.*, 20, e2300010.
2. Hegemann, D., Navascués, P., Snoeckx, R. (2025) Plasma gas conversion in nonequilibrium conditions, *Int. J. Hydrogen Energy*, 100, 548.
3. Hegemann, D., Snoeckx, R. (2026) Entropy Export and Chemical Reactions in Plasmas, *Plasma Process. Polym.*, 23, e70134.
4. Hegemann, D., Southam, A., Heuberger, M., Navascués, P. (2026) Potential and Challenges to Replace PFAS Coatings Considering Safe and Sustainable by Design Aspects: Review and Perspectives, *Plasma Process. Polym.*, 23, e70125.

SICT 2026 Session II. A: Advanced Materials & Emerging Coating Systems Performance-Oriented Coating Applications

The use of thermal spray technologies in energy conversion systems

Robert Vaßen[1,2]
[1] Forschungszentrum Jülich GmbH, IMD-2, Jülich, Germany
[2] Ruhr-Universität Bochum, Institut für Werkstoffe, Bochum, Germany

Abstract:
Thermal spraying is a versatile technology which is used frequently in different mechanical engineering applications. The presentation will give examples of the use of this technology specifically in energy conversion systems.
A major application of thermal spray is found in gas turbines. So, the components of the high-pressure turbine are often protected with thermally sprayed thermal barrier coating systems (TBCs), which consist of both a metallic corrosion resistant layer and a thermally insulating, porous ceramic top coat. In recent years, ceramic fiber composite materials have also been increasingly used as structural material in gas turbines. These also require a protective layer system, whereby a dense, oxidation-resistant silicon layer is often applied first followed by a dense, corrosion-resistant rare earth silicate layer. An additional application in gas turbines is the spray of abradable seals which will also be discussed briefly. New developments of these coatings for gas turbines will be presented.
The use of thermal spray techniques in energy conversion systems is not restricted to gas turbines. As the technology can produce thick, dense and porous metallic and ceramic layers there are frequent applications. Examples in the field of fusion reactor technology and concentrated power will be given. In addition, dense ceramic coatings applied for solid oxide fuel cell applications and also for membrane technologies will be presented.
Thermal spray coatings were also successfully used in electrolysis cells. So, with cold gas spraying (CGS) the amount of expensive Titanium could be reduced in PEM electrolysis cells. In alkaline electrolysis cells, both electrodes and diaphragm were applied by the atmospheric plasma spraying (APS) processes.

Characterisation Study of Thermal and Environmental Barrier Coatings for Aero-engine Applications

Ping Xiao, University of Manchester, UK

Abstract:
Thermal barrier coatings (TBCs) are applied to metallic components used in aero-engines to protect from high temperature environments. Environmental barrier coatings (EBCs) are used to protect underline SiC composites from steam environments in aero-engines. The failure of thermal barrier coatings and environmental barrier coatings is influenced by a complex interdependence of microstructure, residual stress, and thermomechanical properties. This talk will cover characterisation studies of TBCs and EBCs carried out at University of Manchester for over 2 decades particularly focusing on mechanistic understanding of microstructure, residual stresses and micromechanical properties that contribute to failure of TBCs and EBCs. Examples of characterization studies at University of Manchester will be given to present on 1) how electron microscopy combined with an imaging tool can be used to examine degradation of TBCs and EBCs; 2) micro-mechanical study have been used to measure mechanical properties of TBCs; 3) X-ray Tomography has been used to examine TBC degradation at high temperature, 4) Raman spectroscopy, XRD and synchron X-ray diffraction have been explored to examine residual stresses in TBCs and EBCs. Targeted coating development that is both effective and efficient depends on these characterisation studies to obtain superior coatings with improved performance and lifetime.

The influence of the thickness of the buried ITO thin film on charge dissipation and optical properties in functional multilayer oxide coatings

A. Obstarczyk
Faculty of Electronics, Photonics and Microsystem, Wroclaw University of Science and Technology, Janiszewskiego 11/17, 50-372 Wroclaw, Poland

Abstract:
Electrostatic charges are widespread and can lead to injury or serious consequences for human health and safety or cause irreparable damage to electronic devices and industrial production [1]. In addition, electrostatic discharges may occur at seemingly harmless points on electronic devices such as USB ports, output terminals, motherboard connectors, or any location physically connected to internal circuits, damaging sensitive components. Static electric charge causes a potential hazard, ranging from increased attraction of dust particles to damage of electronic components (due to sudden, spontaneous discharge) [1]. These problems particularly affect surfaces such as eyeglass lenses, displays and monitors, where dust and dirt particles reduce the quality of vision [2]. Since classic multilayer AR (antireflective) coatings [3, 4] are based on dielectrics (e.g., TiO_2, HfO_2, TiO_2/SiO_2), there is a risk of charge accumulation on their surface and associated ESD discharges or deterioration of performance parameters. One of the proposed solutions is to introduce a thin, buried ITO layer inside the multilayer stack (Figure 1).
We report a new approach to anti-reflective and antistatic multilayer coatings based on dielectric oxides (TiO_2, HfO_2, and mixed Hf–Ti oxides) combined with a buried ITO layer of varying thickness (Figure 2). The coatings were prepared by magnetron sputtering, incorporating embedded ITO layers with thicknesses of 10 nm, 30 nm, 90 nm, and 270 nm to provide antistatic properties.

Keywords: bilayer, ESD, ITO buried coating, optical properties, functional multilayer, magnetron sputtering

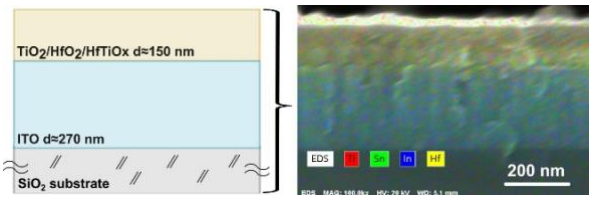

Figure 2: Schematic and cross-sectional SEM/EDS of the $TiO_2/HfO_2/HfTiOx/ITO$ multilayer.

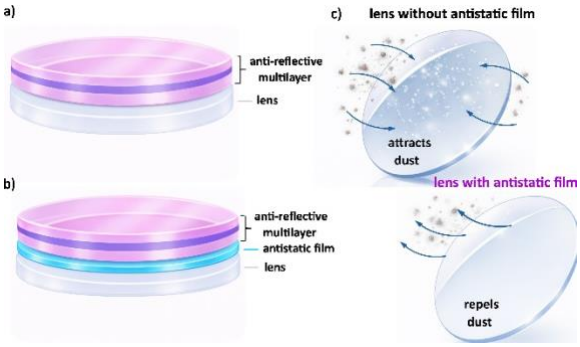

Figure 1: Schematic view of: a) simple anti-reflective multilayer, b) anti-reflective with antistatic coating, and c) a possible result of its application.

References:

1. Li, Z., Xie, X., Zhou, M., Zhu, L., Fu, C., Chen, S. (2023), High water-stable, hard and strong-adhesive antistatic films from waterborne PEDOT:PSS composites, *Synth. Met*., 293, 117290.
2. Deschamps, C., Simpson, N., Dornbusch, M. (2020), Antistatic properties of clearcoats by the use of special additives, *Coat. Technol. Res*., 17, 693-710.
3. Song, J., Kumar, P., Raouf, I., Kim, H.S. (2025), Advancements and challenges in anti-reflective coatings: A comprehensive review, *J. Mater. Res. Technol*., 39, 2926-2938.
4. Mazur, M., Wojcieszak, D., Kaczmarek, D., Domaradzki, J., Song, S., Gibson, D., Placido, F., Mazur, P., Kalisz, M., Poniedzialek, A. (2016), Functional photocatalytically active and scratch resistant antireflective coating based on TiO_2 and SiO_2, *Appl. Surf. Sci*., 380, 165-171.

Acknowledgement:
This work was funded within the project DEC-2024/55/D/ST7/00326 from the Polish National Science Centre in the years 2025-2028.

The impact of the thickness on the properties of CuO

Ewa Mańkowska
Faculty of Electronics, Photonics and Microsystems, Wroclaw University of Science and Technology, Janiszewskiego 11/17, 50-372 Wrocław, Poland

Abstract:
Copper oxides (Cu_xO) gain an increas-ing interest due to their numerous potential applications, nontoxic character, low cost, abundance in nature [1]. In addition, they exhibit p-type semiconducting properties, which make them attractive for various sensing applications. Among them, copper(II) oxide is one of the p-type metal oxides most intensively studied as a resistive gas sensor for gases such as NO_x, CO, CO_2, N_2, H_2, and ethanol [2]. The growing demand for efficient and reliable gas sensors for environmental monitoring and industrial safety further increases the importance of research on copper oxide-based sensing materials [3]. Copper oxide (Cu_xO) thin films can be prepared by various deposition methods; however, post-process annealing is often applied in order to improve the structural and sensing properties of the material [1].
In this study, copper oxides of various thicknesses ranging from 50 nm to 2100 nm were tested to evaluate their hydrogen-sensing performance. Copper oxides were deposited using magnetron sputtering, followed by annealing at 300°C.
Obtained samples were characterized using scanning electron microscopy to investigate their surface morphology, optical transmission coefficient measurements, and X-ray diffraction analysis to verify the crystalline structure of the films. The gas sensing measurements were performed at an operating temperature of 300°C in a wide hydrogen concentration range from several ppm to 1000 ppm.
The thickness of the thin films significantly influenced the crystalline structure: the thinnest films were amorphous, while thicker films exhibited a polycrystalline CuO structure. Additionally, the films were composed of fibrous grains with sharp edges at the surface, resembling nanosheet-like structures.
For gas sensing measurements, ceramic substrates with interdigitated electrodes were used. The measurements were performed on CuO films and CuO with an additional Pd catalytic adlayer. Based on the observed results, an optimal CuO film thickness was identified, and it will be used for further gas sensing measurements of more advanced structures based on copper oxides or hybrid systems combined with other metal oxides.

Keywords: copper oxides, gas sensing, hydrogen, thickness, magnetron sputtering, annealing.

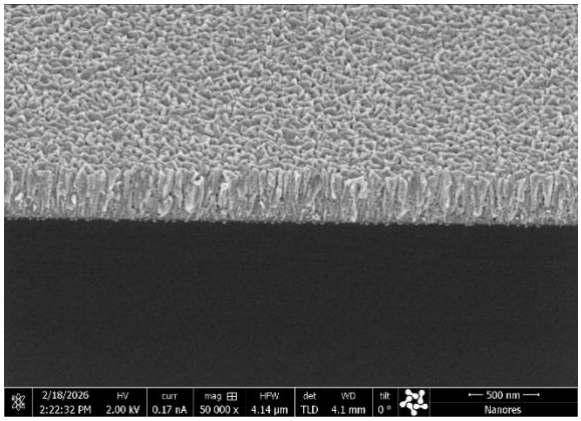

Figure 1: Scaning electron microscopy image of cross-section of CuO film showing the fibrous grains ended with sharp edges.

References:

1. Wojcieszak, D., Obstarczyk, A., Mańkowska, E.; Mazur, M., Kaczmarek, D., Zakrzewska, K., Mazur, P., Domaradzki, J. (2022) Thermal Oxidation Impact on the Optoelectronic and Hydrogen Sensing Properties of P-Type Copper Oxide Thin Films. *Mater. Res. Bull.*147, 111646
2. Nunes, D., Pimentel, A., Goncalves, A., Pereira, S., Branquinho, R., Barquinha, P., Fortunato, E., Martins, R. (2019) Metal Oxide
Nanostructures for Sensor Applications. *Semicond. Sci. Technol.* 34, 043001.
3. Lupan O., Postica V., Ababii N., Hoppe M., Cretu V., Tiginyanu I., Sontea V., Pauport´e T., Viana B., Adelung R. (2016) Influence of CuO nanostructures morphology on hydrogen gas sensing performances. *Microelectron Eng* 164, 63–70.

Acknowledgements
This work was financed from the sources provided by the Polish National Science Centre as a project number 2024/53/N/ST7/01699.

Gas sensing properties of copper and titanium oxides thin films deposited by magnetron sputtering

P. Pokora [1], E. Mańkowska [1]
[1] Faculty of Electronics, Photonics and Microsystems, Wroclaw University of Science and Technology, Janiszewskiego 11/17, 50-372 Wrocław, Poland

Abstract:
The TiO_2/CuO thin films with varying TiO_2 layer thicknesses were deposited using the custom-developed magnetron sputtering workstation, that was designed for simultaneous sputtering from three magnetrons. Fused silica, silicon, and ceramic substrates designed for electrical measurements with interdigitated electrodes were used for deposition. The hydrogen gas sensing properties of TiO_2/CuO bilayers were investigated, and the influence of the TiO_2 top layer thickness on the heterojunction properties was analyzed. The structure and morphology of the bilayers were characterized using X-ray diffraction (XRD), scanning electron microscopy (SEM) (fig. 1), energy-dispersive X-ray spectroscopy (EDS) (fig. 1), and atomic force microscopy (AFM), while the optical band gap was determined from Tauc plots based on transmission measurements (fig. 2). Hydrogen sensing measurements were performed at two operating temperatures: 250°C and 300°C, over a hydrogen concentration range from 25 to 1000 ppm (fig. 3). Upon exposure to hydrogen, the resistance of the TiO_2/CuO bilayer increased, indicating typical p-type sensing behavior. The best sensing performance (highest response, the shortest response and recovery times) was achieved with TiO_2/CuO bilayer of the thinnest top layer. Characterization of the layer revealed uniformly distributed, small grains with an amorphous structure of TiO_2 and its bandgap energy of 3.3 eV. In-situ X-ray diffraction (XRD) performed under hydrogen exposure indicated that the TiO_2/CuO structure undergoes strong reduction, suggesting significant structural and electronic modifications during sensing.

Keywords: hydrogen, gas sensing, bilayers, p-n heterojunction, copper oxide, titanium oxide, magnetron sputtering

Funding: This work was co-financed from the sources given by the Polish National Science Centre (NCN) as a research project number 2024/53/N/ST7/01699.

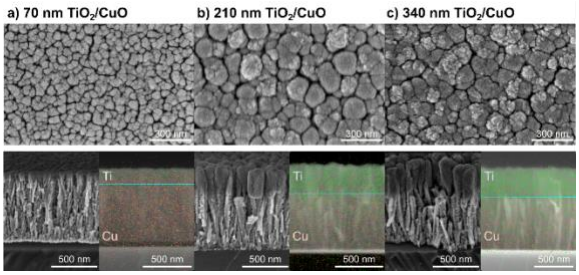

Figure 1: The topography and cross-section scanning electron microscopy images of bilayers combined with Cu and Ti EDS maps

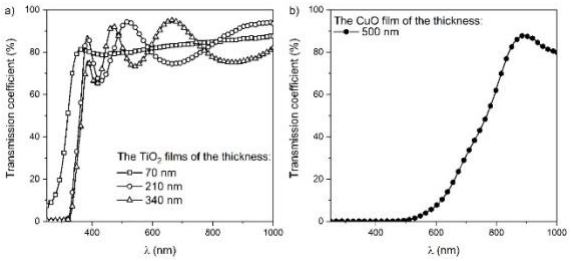

Figure 2: Transmission characteristics of a) TiO_2 with different thickness and b) CuO thin film

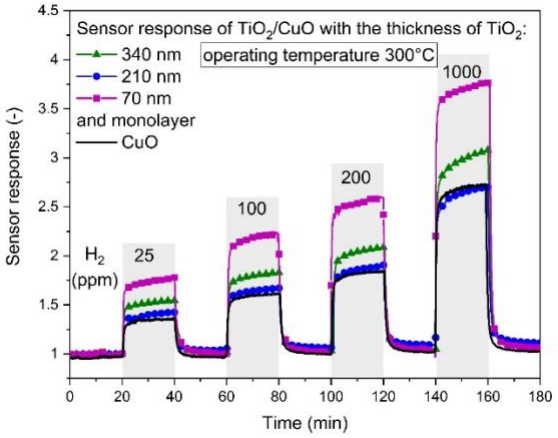

Figure 3: The sensor response of TiO_2/CuO bilayers and CuO to 25-1000 ppm of hydrogen

Fluorescent Nanocomposites of Polydiacetylene-ZnO Quantum Dots-Zn(II) ion with Temperature/Acid-Responsive Properties

N.Traiphol [1,3]*, S. Boonmak [1], K. Phetnam [2], R.Traiphol [2]
[1] Laboratory of Advanced Chromic Materials, Department of Materials Science, Faculty of Science, Chulalongkorn University, Bangkok 10300, Thailand
[2] Laboratory of Advanced Polymer and Nanomaterials, School of Materials Science and Innovation, Faculty of Science, Mahidol University at Salaya, Phuttamonthon 4 Rd, Nakorn Pathom 73170, Thailand
[3] Center of Excellence on Petrochemical and Materials Technology, Chulalongkorn University, Bangkok 10300, Thailand
*Corresponding author's e-mail address: Nisanart.T@chula.ac.th

Abstract:
Polydiacetylene (PDA) materials have been applied in many technologies derived from their colorimetric response upon exposure to different types of stimuli. Our group has developed a new class of nancomposites where Zn^{2+} ions and ZnO nanoparticles strongly interact with PDA structures. The obtained PDA/Zn^{2+}/ZnO nanocomposites have shown many interesting repsonsive properites. The nanocomposites exhibit reversible thermochromism and show colorimetric response to acid and base. These properties allow the utilzation as stimuli-responsive coatings as illustrated in Figure 1a. This study introduces a new approach to increase the fluorescent properties of nanocomposites, which in turn broaden their applications. ZnO quantum dots (QDs) synthesized in ethanol are incoporated into PDA structures via co-assembly method. The resultant nanocomposites show a blue color under room-light conditions (Figure 1b). When exposed to UVA light (368 nm), interestingly, the nanocomposites exhibit strong fluorescent light emission (Figure 1c). By varying the concentrations of ZnO QDs, the fluorescent intensity can be tuned. Furthermore, the PDA/Zn^{2+}/ZnO QDs nanocomposites respond to temperature and acid. The preparation method of nanocomposites is simple and low-cost, desirable for industrial applications. This class of materials show potential for stimuli-repsonsive coatings.

Keywords: Smart coatings, polydiacetylene, ZnO quantum dots, color-transition, thermochromism, acid-responsive

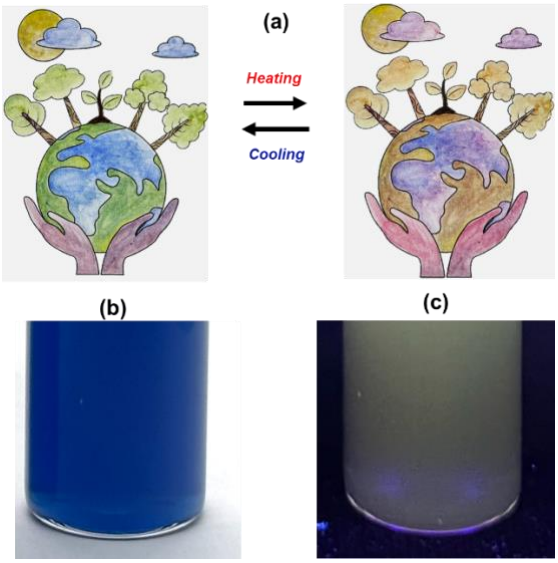

Figure 1: (a) Painted picture showing reversible color transition during heating/cooling cycles. The paints with different colors were prepared by mixing PDA/Zn^{2+}/ZnO nanocomposites with acrylic paints. Photographs of PDA/Zn^{2+}/ZnO QDs nanocomposites taken under (b) room light and (c) exposure to UVA light (368).

References:

1. Siriboon, J., Traiphol, N., Traiphol, R. (2023) ZnO quantum dots-diacetylenes-zinc(II) nanocomposites for colorimetric detection of ultraviolet-B light: The size effects, *Mater. Today Chem.*, 32, 101664.
2. Kaewnukulkit, N., Boonmak, S., Traiphol, N., Traiphol R. (2025) Synthesis of polydiacetylene/Zn^{2+}/ZnO nanocomposites in alcohols for colorimetric detection of temperature and fatty acids, *Mater. Today Comm.*, 49, 113797.

High-Temperature Reversible Thermochromic and Acid-responsive Polydiacetylene/Li^+ Assemblies for Smart Coatings

R.Traiphol[1]*, K. Phetnam[1], S. Boonmak[2], N.Traiphol[2,3]
[1] Laboratory of Advanced Polymer and Nanomaterials, School of Materials Science and Innovation, Faculty of Science, Mahidol University at Salaya, Phuttamonthon 4 Rd, Nakorn Pathom 73170, Thailand
[2] Laboratory of Advanced Chromic Materials, Department of Materials Science, Faculty of Science, Chulalongkorn University, Bangkok 10300, Thailand
[3] Center of Excellence on Petrochemical and Materials Technology, Chulalongkorn University, Bangkok 10300, Thailand
*Corresponding author's e-mail address: Rakchart.tra@mahidol.ac.th

Abstract:
Polydiacetylenes (PDAs) are smart materials that exhibit color transition when exposed to various stimuli such as temperature, acids, bases, solvents, and surfactants. This unique property can be utilzed for smart coatings that illustrate different colors depending on their local environments. Generally, commercial PDAs with carboxylic headgroup exhibit an irreversible blue-to-red color transition upon increasing temperature. To expand their applications, tremendous efforts have been dedicated for achieving reversible thermochromism. In this study, PDAs are induced to assembly in an aqeoues solution under the presence of LiOH. Depending on the LiOH concentration, the strong interaction of PDA carboxylate headgroup with Li^+ ion results in the formation of PDA/Li^+ assemblies with new properties. In solution state, this material exhibits reversible blue-to-purple thermochromism at 80 ºC (Figure 1a). When the PDA/Li^+ assemblies are coated on a glass slide, the color-transiton temperature shifts to 120 ºC (Figure 2b). Furthermore, the nature of reversible thermochromism persists upto 270 ºC, which is much higher than those of the previous reports. These properties are important for the development of temperature-sensitive smart coatings. This class of materials also exhibit colorimetric response to acid in solution and gas phases. The synthesis of PDA/Li^+ assemblies is simple, making it suitable for large-scale production.

Keywords: Stimuli-responsive coatings, polydiacetylene, color-transition, reversible thermochromism, acid-responsive

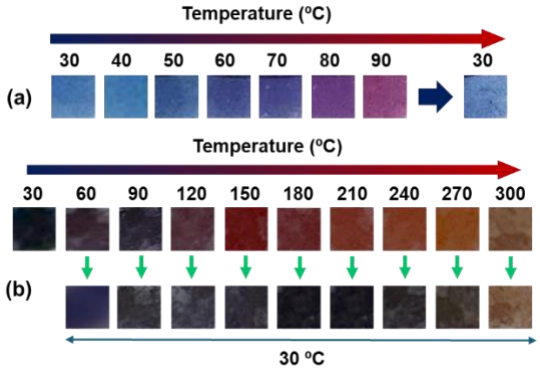

Figure 1: (a) Photographs of PDA/Li^+ assemblies in aqeoues solution taken upon increasing temperature from 30 to 90 °C followed by cooling back to 30 °C. (b) Photographs of PDA/Li^+ assemblies coated on glass slide taken upon increasing temperature from 30 to 300 °C. The sample was cooled to 30 °C at each heating temperature to check the color reversibility.

References:

1. Kingchok, S., Siriboon, J., Sun, L., Seery, T.A.P., Traiphol, N., Traiphol, R. (2022) Polydiacetylene-Na^+ nanoribbons for naked eye detection of hydrogen chloride gas, *ACS Appl. Nano Mater.*, 5, 4146-4156.
2. Saymung, R., Potai, R., Papadakis, C.M., Traiphol, N., Traiphol, R. (2024) Acid-responsive polydiacetylene-Na^+ assemblies with unique red-to-blue color transition, *Heliyon*, 10, e27574.

Development of a Specialized Coating for Moisture and Aggressive Environment Resistance

O. Ghorab[1,2], L. Chetibi[1], I. Calliari[2], M. Pigato[2], M. Dabalà[2], D. Hamana[1], F,Ahani[2], S.Achour[1],Lorenzo Dambrosi[2].
[1]Department of Materials Engineering, National Polytechnic School, Constantine, Algeria
[2]Department of Industrial Engineering (DII), University of Padua, Via Marzolo 9, Padua, Italy

Abstract:
Corrosion under insulation (CUI) of pipelines represents a growing challenge in Algerian regions due to the humid and chemically aggressive environment. This study aims to identify an effective, low-cost, and environmentally friendly coating system that can be easily applied by painting, using local materials, in order to enhance the corrosion resistance of steel pipelines. Zinc phosphate coatings modified with selected inorganic additives were investigated. The structural and morphological characteristics of the coated steel were analyzed using X-ray diffraction (XRD), scanning electron microscopy (SEM), and energy-dispersive spectroscopy (EDS). The corrosion performance of uncoated and coated steel samples was evaluated by electrochemical impedance spectroscopy (EIS) and potentiodynamic polarization measurements.

The results demonstrate that the incorporation of sodium metasilicate promotes pore sealing and reduces coating permeability. Calcium nitrate and zinc nitrate were added to refine the phosphate crystal structure, while polymeric stabilizing additives were used to control drying stresses and minimize coating cracking. Together, these additives significantly improve the corrosion resistance of zinc phosphate coatings. Under optimized pH, temperature, solution viscosity, and concentration conditions, the impedance of the coated steel under industrial conditions (different temperatures), measured by EIS, showed that the coating resistance increased by approximately 4.5 times compared to uncoated steel, indicating enhanced barrier and protective properties, Additionally, controlling the drying process was found to reduce coating cracking, which directly affects corrosion resistance

Overall, this study confirms the effectiveness of a simple painting-based coating strategy for mitigating corrosion under insulation. However, further optimization of coating parameters is required to reduce porosity and improve long-term resistance to moisture penetration.

Keywords:CUI; Zinc phosphate coating; Electrochemical impedance spectroscopy; Potentiodynamic polarization; Pipeline steel; Corrosion protection.

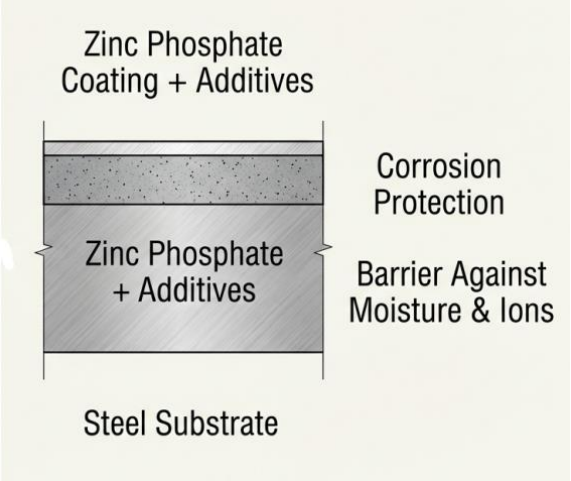

Figure 1: Schematic Representation of the Corrosion Protection Mechanism.

References:

1. Tamilselvi, M., Kamaraj, P., Arthanareeswari, M., Devikala, S., &Selvi, J. A. (2015). Development of nano SiO2 incorporated nano zinc phosphate coatings on mild steel. Applied Surface Science, 332, 12-21.
2. Zhao, X., Liu, R., Qi, W., & Yang, Y. (2020). Corrosion resistance of concrete reinforced by zinc phosphate pretreated steel fiber in the presence of chloride ions. Materials, 13(16), 3636.
3. Cao, Q., Pojtanabuntoeng, T., Esmaily, M., Thomas, S., Brameld, M., Amer, A., & Birbilis, N. (2022). A review of corrosion under insulation: a critical issue in the oil and gas industry. *Metals*, *12*(4), 561.

High-temperature failure mechanism of TiAlSiN coating deposited on pristine and plasma nitride tool steel

V. Terek [1,*], L. Kovačević [1], A. Drnovšek [2], M. Čekada [2], M. Zagoričnik [1], Z. Bobić [1], P. Terek [1]
[1] Faculty of technical sciences, University of Novi Sad, Novi Sad, Serbia
[2] Jožef Stefan Institute, Ljubljana, Slovenia

Abstract:
Physical vapor deposition (PVD) hard coatings are regularly used to improve tool life of tools used for high temperature processing of materials (hot forging, hot extrusion, high-pressure die casting) [1]. Ti-based coatings, such as TiAlSiN, are extensively used for such purposes. Nonetheless, the failure of this coated system is often induced by the degradation of the underlying substrate material. Therefore, a good understanding of the mechanisms of substrate material failure is crucial. An effective approach to assess and prevent (or at least hinder) system failure is by simulating the actual use of the coated tools using laboratory equipment. This is commonly performed using pin-on-disk high temperature tribometer. This investigation aims to provide additional information on the failure mechanisms and degradation of coated tool steel during high temperature sliding conditions. Tribological tests were conducted at room temperature and at high temperatures (up to 700 °C). Al_2O_3 counterbody was used to simulate tool contact with oxidized Al (Al extrusion, die casting). Pristine and plasma nitrided hot-work tool steel were used as a substrate for the deposition of TiAlSiN coating. After the tribological tests, the samples were analyzed using profilometry, optical microscopy, SEM and FIB to determine wear rate and failure mechanisms of the coated system. Loss of tool steel substrate's hardness at high temperatures and thermo-mechanical load during tribological testing resulted in formation of inter- and trans-columnar cracks inside the coating. These cracks allowed iron oxide to penetrate inside the wear track, which affected wear rate and coefficient of friction and led to coating failure.

Keywords: PVD coatings, TiAlSiN, hot-work tool steel, high temperature tribology, diffusion treatment, wear rate

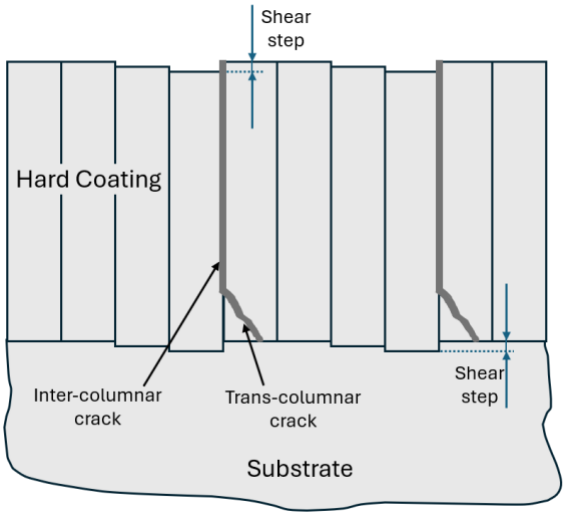

Figure 1: Schematic representation of the TiAlSiN coating fracture. Adapted from [2].

References:

1. B.S. Johny, M. Alphonse, Friction and wear behaviour of AlCrN and TiN coated H13 tool steel, Tribol. Mater. 3 (2024) 131–140. https://doi.org/10.46793/tribomat.2024.015.
2. P. Panjan, A. Miletić, A. Drnovšek, P. Terek, M. Čekada, L. Kovačević, M. Panjan, Cracking Resistance of Selected PVD Hard Coatings, Coatings 14 (2024). https://doi.org/10.3390/coatings14111452.

Stable Polydopamine–Gallic Acid Suspension as a Functional Surface Treatment for Improved Adhesion in Bamboo/PP Composites

C. N. Schnell [1*], A. Laachachi[1], D. Ruch[1], C.A. Fuentes [1,2]
[1] Structural Composite Unit, Luxembourg Institute of Science and Technology (LIST), 5 rue Bommel, L-4940 Hautcharage, Luxembourg
[2] Department of Materials Engineering, KU Leuven, Leuven, Belgium

Abstract:
Efforts to reduce the environmental impact of composite materials have increased the use of natural fibres as alternatives to glass and carbon reinforcements. Among the various lignocellulosic options, bamboo is particularly attractive because of its fast renewability (3–5 year growth cycle), low density and specific mechanical properties comparable to glass fibres[1]. Despite these advantages, bamboo fibres still face significant limitations when combined with non-polar thermoplastic matrices, primarily due to poor fibre–matrix interfacial adhesion. Engineering the fibre–matrix interface is therefore crucial: tailoring the fibre surface chemistry can improve compatibility, promote efficient stress transfer, and enhance the overall mechanical performance of the composite. Wet-chemical functionalization offers a practical and scalable approach to achieve this, enabling controlled surface modification under mild conditions and strengthening the fibre–matrix interface.
In this context, bio-inspired surface functionalization strategies based on catechols and phenolic antioxidants provide versatile routes to tailor fibre surface chemistry under aqueous, mild conditions. Previous work has shown that dopamine-based treatments enhance fibre–matrix adhesion through the formation of polydopamine (PDA) coatings rich in catechol and amine groups. However, conventional PDA protocols often require long in-situ polymerization steps (12–24 h) and may produce non-uniform coatings on natural fibres due to uncontrolled particle growth. Polyethyleneimine (PEI) has been used to control PDA nanoparticle size and accelerate deposition[2], but as a synthetic, non-bio-based additive, it motivates the search for more sustainable alternatives based on naturally derived phenolic compounds such as gallic acid.
This work presents a stable polydopamine–gallic acid (PDA–GA) suspension developed as a functional surface treatment to enhance interfacial adhesion in bamboo/PP composites. The PDA–GA formulation was optimized by controlling pH, concentration, and reaction time to tune nanoparticle formation. UV–Vis spectroscopy, dynamic light scattering, and TEM analyses confirmed that gallic acid enables control of particle size during polymerization, promoting the formation of a stable PDA–GA suspension. Bamboo longfibres (15 cm length and 200 µm diameter) were functionalized using a fast dipping process with the optimized suspension. Preliminary single-fibre pull-out and composite tests showed improved interfacial shear strength in PP systems, demonstrating the potential of the PDA–GA suspension as a scalable, bio-based surface treatment to enhance flexural strength and flexural modulus by 13% and 21%, respectively.

Keywords: Bamboo Fiber, Biocomposite, Polydopamine, Gallic Acid, Fiber-matrix adhesion, Stable Suspension, Wet Surface Treatment.

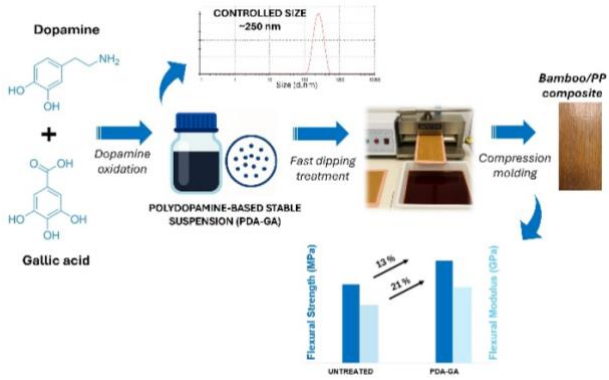

Figure 1: Overview of the PDA–GA surface functionalization process: formation of a stable PDA–GA suspension with controlled nanoparticle size, deposition on long bamboo fibers via padding/dipping, and resulting improvements in interfacial and mechanical performance in bamboo/PP composites.

References:

1. Tran, L. Q. N., Fuentes, C., Verpoest, I., & Van Vuure, A. W. (2019). Tensile behavior of unidirectional bamboo/coir fiber hybrid composites. Fibers, 7(7), 62.
2. Schnell, C. N., Mertz, G., Hao, J., Van Vuure, A. W., Laachachi, A., & Fuentes, C. A. (2025). Stable polydopamine-based suspension for scalable surface modification of bamboo fibre–reinforced composites. Composites Part A: Applied Science and Manufacturing, 109206.

SICT 2026 / Plasma Tech 2026 Joint Session II. B: Bio-interfaces, Biomedical / Bioactive surfaces and coatings Plasma applications for biology, medicine, and agriculture

Self-Templated Highly Porous Gold as Antibiofouling strategy in Electrochemical Biosensing: application in a microneedles-based biosensor for β-hydroxybutyrate (β-HB) detection

A. Degjoni[1], C. Tortolini[1], D. Passeri[2,3], A. Lenzi[1], R. Antiochia[1,*]
[1]Department of Experimental Medicine, Sapienza University of Rome, Rome, Italy
[2] Department of Basic and Applied Sciences for Engineering, Sapienza University of Rome, Rome, Italy
[3] Research Center for Nanotechnology Applied to Engineering of Sapienza University of Rome (CNIS), P.le A. Moro 5, 00185 Rome, Italy

Abstract:
Electrochemical biosensors represent a fundamental class of analytical devices demonstrating immense utility in clinical diagnostics, environmental monitoring, and continuous health surveillance. The performance and long-term stability of electrochemical biosensors are fundamentally compromised by a ubiquitous phenomenon known as biofouling [1]. Biofouling refers to the non-specific accumulation of different organic molecules, including proteins, lipids, polysaccharides, and nucleotides, onto the electrode surface. This process is particularly pronounced in biological environments, where a vast array of species competes for adsorption sites [2]. The consequences of biofouling are as follows: (i) a notable decrease in sensitivity; (ii) obstruction of mass transfer pathways; (iii) inhibition of electron transfer (ET) between the electrode and the target analyte; iv) necessity of frequent biosensor recalibration; and (v) eventual complete loss of functionality. In response to the pervasive problem of biofouling, researchers have historically developed several strategies aimed at either attenuating or outright inhibiting the non-specific adsorption of interfering species, particularly large proteins, such as the use of poly (ethylene glycol), reduced graphene oxide with glutaraldehyde (GA) cross-linked bovine serum albumin (BSA), nanoporous gold fabricated according to the classical dealloying treatment [2].
In this work, the antibiofouling properties of a self-templated electrodeposited highly nanoporous gold (h-nPG) modified screen-printed gold electrode were investigated in physiological concentrations of albumin and in human serum and plasma. To the best of our knowledge, this is the very first time that an electrochemically generated h-PG film was investigated for its antifouling properties [2].

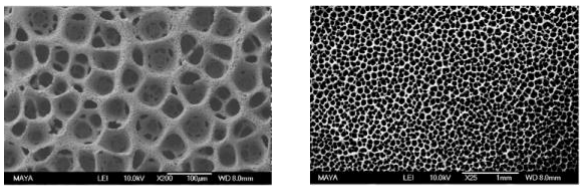

Figure 1: Figure illustrating the SEM images of the self-termplated h-nPG modified electrode at two different magnifications.

The promising results obtained allowed the use of the self-templated h-nPG for the modification of a gold microneedles-array electrode for the development of a minimally-invasive continuous monitoring biosensor for β-HB in artificial interstitial fluid (ISF) and in a simulated skin model [3,4].
The obtained results are encouraging for the use of the proposed antibiofouling h-nPG film for surface modification of gold microneedles-based biosensors for the development of wearable devices to be used in medicine for the continuous monitoring of several bioanalytes.

References:

1. Szunerits, S.; Pagneux, Q.; M'Barek, Y.B.; Vassal, S.; Boukherrou, R. (2023) Do not let electrode fouling be the enemy of bioanalysis. *Bioelectrochem.* 153, 108479.
2. Degjoni, A.; Tortolini, C.; Passeri, D.; Lenzi, A.; Antiochia, R. (2026) Self-Templated Highly Porous Gold as Antibiofouling strategy in Electrochemical Sensing, *Nanomaterials*, 16, 87
3. Tortolini, C.; Caprio, M.; Gianfrilli, D.; Lenzi, A.; Antiochia, R. (2025) Towards precision nutrition: a novel smartphone connected biosensor for POC detection of β-HB in human blood and saliva, *Sensors*, 25, 4336
4. Bollella P.; Sharma S.; Cass, A.; Tasca, F; Antiochia, R., *Catalysis*, (2019), 9, 580.

Low-Remanence Iron-Oxide Thin Films and Microdiscs for Cell-Interactive Biointerfaces and Biomedical Actuators

I. Lasa[1], C. Redondo[1], D. Salazar[2], R. Morales[3,4*]
[1] Department of Chemical-Physics, University of the Basque Country - EHU, Leioa, Spain
[2] BCMaterials, Basque Center for Materials, Applications and Nanostructures, Leioa, Spain
[3] Department of Chemical-Physics, University of the Basque Country – EHU and BCMaterials, Leioa, Spain
[4] IKERBASQUE, Basque Foundation for Science, Bilbao, Spain

Abstract:
Controlling the magnetic phase and properties of iron oxides is essential for the design of micro and nanostructures intended for biomedical applications.[1] In this work we investigate how oxidation and reduction treatments of Fe allow us to transform metallic layers into iron oxide thin films and microdisks with low magnetic remanence.

Fe layers of 20–100 nm were deposited by electron-beam evaporation and subjected to thermal treatments in air and reducing Ar/H_2 atmospheres. Structural analyses revealed that the oxidation of Fe strongly depends on the initial thickness: after 2 h at 400 ºC thin layers (<50 nm) fully convert into γ-Fe_2O_3, while 100 nm films retain a metallic layer. Atomic force microscopy confirmed the expected volume expansion associated with oxide formation, with thickness increases of up to a factor of two. Magnetization measurements showed a reduction above 90% in saturation magnetization after oxidation, along with a significant decrease in remanence, consistent with the formation of ferrimagnetic iron oxide phases. Partial reduction of γ-Fe_2O_3 in Ar/H_2 atmosphere recovers ~50 % of the lost magnetization.

Microdiscs fabricated by direct laser writing and lift-off also show their low-remanence featured after oxidation and exhibited slight lateral expansion due to volumetric changes during phase transformation (Figure 1).[2] When aluminium underlayers were used as sacrificial layers, X-ray diffraction measurements revealed interfacial diffusion during annealing and the appearance of additional oxide phases. Pre-oxidation of the Al layer partially suppressed this diffusion, improving the magnetic stability of the resulting Fe-oxide microstructures.

These results demonstrate that the interplay between geometry, oxidation kinetics and interfacial chemistry is central to achieving iron-oxide systems with minimal remanence and controlled magnetic response. These insights support the development of biocompatible magnetic coatings and microactuators for sensors, therapeutic tools and medical device interfaces.

The materials developed here are well suited for low-frequency magneto-mechanical stimulation, targeted cellular disruption and emerging micro-actuation strategies in biomedicine.

Keywords: iron oxides; thin films; microdiscs; thermal oxidation; maghemite; magnetite; low remanence; magneto-mechanical actuation; biomedical applications.

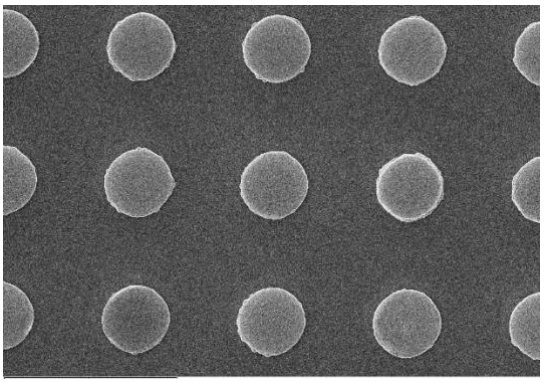

Figure 1: Scanning electron microscopy (SEM) image of patterned iron-oxide microdiscs (4 µm diameter) obtained after oxidizing a single Fe layer at 400 °C.

References:

1. Peixoto, L., Magalhães, R., Navas, D., Moraes, S., Redondo, C., Morales, R., Araújo, J. P., & Sousa, C. T. (2020). Magnetic nanostructures for emerging biomedical applications. *Applied Physics Reviews,* 7, 011310. https://doi.org/10.1063/1.5121702
2. Pinheiro, T., Morais, M., Silvestre, S., Carlos, E., Coelho, J., Almeida, H. V., Barquinha, P., Fortunato, E., & Martins, R. (2024). Direct laser writing: From materials synthesis and conversion to electronic device processing. *Advanced Materials*, 36, 2402014. https://doi.org/10.1002/adma.202402014

Surface Functionalization of Inner Microchannel Surfaces in a Power-Free Microfluidic Chip for Extracellular Vesicle Detection

R. Ishihara[1,*], M. Hosono[2], M. Ogawa[2], H. Yazawa[2], T. Nakajima[3], E. Shimura[1], T. Baba[1], and H. Shibata[2]
[1] Faculty of Medicine, Juntendo University, Chiba, Japan
[2] Department of Applied Chemistry, Chiba Institute of Technology, Chiba, Japan
[3] Department of Science, Yokohama City University, Kanazawa, Japan

Abstract:
In this study, a surface-functionalized power-free microchip (SF-PF microchip) was developed to enable sensitive and selective detection of extracellular vesicles (EVs) secreted by metastatic cancer cells toward point-of-care testing[1]. The core concept of this platform lies in the chemical modification of the microchannel inner surfaces of the power-free microchip, which allows specific EV capture without the need for external pumping systems. As a disease-relevant target, integrin β1 (ITG-β1) was identified as a characteristic antigen highly expressed on EVs derived from metastatic breast cancer cells (MDA-MB-231).
To maximize detection performance, the surface modification conditions were systematically optimized to achieve high-density immobilization of anti-ITG-β1 antibodies on the microchannel walls. This optimized surface functionalization enabled specific antigen–antibody interactions within the confined microfluidic space. Using the SF-PF microchip, EV detection experiments demonstrated a statistically significant increase in fluorescence signal in the presence of cancer cell–derived EVs compared with EV-free controls. Control experiments employing normal mouse IgG instead of anti-ITG-β1 confirmed that the observed signals originated from specific interactions between ITG-β1 on EV surfaces and the immobilized antibodies.
Furthermore, comparative analysis revealed a statistically significant difference in the signal-to-blank ratio between EVs derived from metastatic cancer cells and those from healthy cells, highlighting the high specificity achieved through surface engineering. The limit of detection, calculated using the 3σ method, was 5.0×10^{10} particles/mL, corresponding to approximately one-tenth of the total EV concentration[2] typically present in blood. Notably, the assay required only 2.0 µL of sample and a detection time of 20 min, underscoring the efficiency of the surface-functionalized microchannel design.
For practical applications, EV detection in serum was also investigated (**Figure 1**). Stable fluid flow and successful EV detection were achieved using 50% diluted serum, demonstrating the robustness of the SF-PF microchip. Future efforts will focus on further optimizing surface properties to enable EV detection in undiluted serum and on validating the platform using clinical samples. Overall, this study emphasizes the critical role of microchannel surface functionalization in advancing simple, rapid, and clinically relevant EV-based cancer diagnostics.

Keywords: surface-functionalized power-free microchip, extracellular vesicles, breast cancer, point-of-care testing.

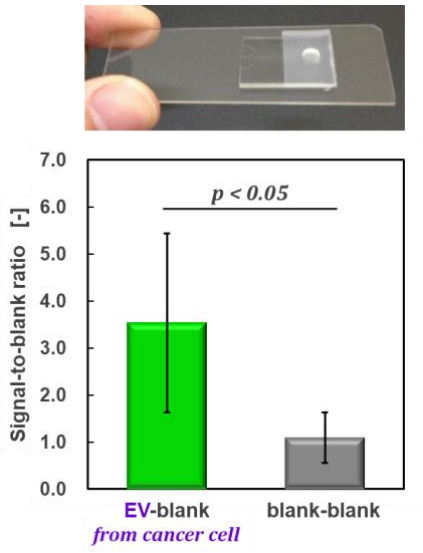

Figure 1: Detection of extracellular vesicles secreted from cancer cells on a SF–PF microchip.

References:

1. Ishihara, R. *et al*. (2026) Development of surface-functionalized power-free microchip for breast cancer cell-derived extracellular vesicle detection, *Anal. Sci*., 42, 37-47.
2. Eitan, E. *et al*. (2017) Age-Related Changes in Plasma Extracellular Vesicle Characteristics and Internalization by Leukocytes, *Sci. Rep.,* 7, 1342.

Challenges in Detecting Biotoxins and Biomolecules by using Surface-enhanced Raman Scattering Spectroscopy on Nanopatterned Substrates

N. E. Dina [1*], A. Colniță [1], D. Marconi [1], I. A. Brezeștean [1], A. S. Tătar [1]
[1] Department of Isotopic and Molecular Technologies, National Institute for Research and Development of Isotopic and Molecular Technologies, Cluj-Napoca, Romania

Abstract:
The incorporation of nanopatterned substrates with plasmonic properties into surface-enhaced Raman spectroscopic (SERS) sensing platforms is a crucial part of the development of new miniaturized detection devices with on-site applications. We employed nanoimprint lithography (NIL) and magnetron sputtering to fabricate plasmonic nanostructures able to detect environmental contaminants and toxins. Thus, networks of tunable nanopillars were imprinted in thermoplastic polymers and metallized with Ag/Au thin films using magnetron sputtering technique. The structural and topographical properties were assesed by SEM and AFM techniques. The nanostructured sensing platforms were very suitable for SERS detection of crystal violet for example, reaching a limit of detection of 10 pM for Ag nanotrenches and of 1 μM in case of the Au nanopillars. After assessing these figures of merit for the fabricated SERS-active substrates, relevant biotoxins from natural acquifers or biomolecules present as biomarkers in chronic non-communicative diseases were considered as analytes for testing their performance in practice.

Keywords: nanopatterning, biomedical applications, biotoxins, SERS, nanoimprint lithography, sensing.

Acknowledgements:

This work was supported by a grant of the Ministry of Research, Innovation and Digitization, CCCDI - UEFISCDI, project number PN-IV-P7-7.1-PED-2024-0052, within PNCDI IV.

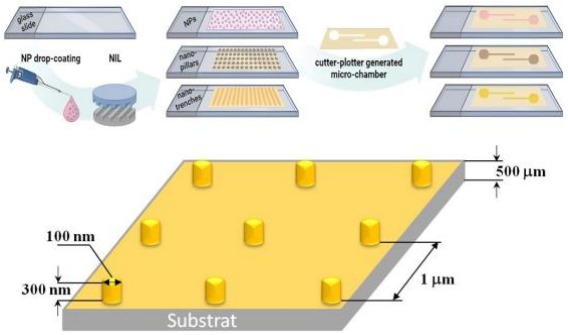

Figure 1: *Flexible substrates:* a network of periodical pillars (width: 100 nm, pitch: 1 μm, height: 300 nm) fabricated by thermal nanoimprint lithography (NIL) and their envisioned integration in a miniaturized device.

References:

1. A. Colniță, D. Marconi, N. E. Dina, I.A. Brezeștean, *et al. Spectrochim. Acta A,* 276, 121232, 2022.
2. I. A. Brezeștean, A.M.R. Gherman , ..., N.E. Dina, *Int J Mol Sci,* 23, 15741, 2022.
3. N.E. Dina *et al. Biosens. Bioelectron,* 219, 114843, 2023.
4. A. Colniță, D. Marconi, Vlad Al. Toma, I. Brezeștean, .., N.E. Dina, *Microchemical. J.,* 206, 111589, 2024.

Innovative SiO_2/PEG/Caffeic Acid Sol-Gel Coatings on Stainless Steel: Toward Bioactive and Biocompatible Prosthetic Surfaces

F. Barrino[1,*], F. Giuliano [1], H. de la Rosa-Ramírez[2] and M.D. Samper[2]
[1] Department of Engineering, University of Palermo, Viale delle Scienze, 90128 Palermo, Italy
[2] Institute of Materials Technology (IUTM), Universitat Politècnica de València (UPV), 46022 Alicante, Spain

Abstract:
The development of advanced multifunctional coatings for biomedical applications is a growing area of research, driven by the need to improve the performance, durability, and biological integration of metallic implants. In this context, sol-gel technology offers significant advantages due to its versatility, low processing temperatures, and ability to produce homogeneous hybrid organic–inorganic networks[1]. In the present study, innovative sol-gel formulations based on silica (SiO_2) and polyethylene glycol (PEG, 24 wt %) were successfully developed and functionalized with different concentrations of caffeic acid (CafA 5, 10, and 15 wt %), a bioactive molecule known for its antioxidant and potential biological properties[2]. The resulting sols were deposited onto AISI 304 and 316 stainless steel substrates via dip-coating, without any prior surface pre-treatment, with the aim of simplifying the coating process while maintaining high film quality (Figure 1).
The obtained coatings were visually uniform, crack-free, and well-adherent, demonstrating the effectiveness of the sol-gel approach in achieving controlled film formation even on untreated metallic substrates. Thermal analysis was carried out to investigate the stability and structural evolution of the hybrid materials, providing insight into the interactions between the inorganic silica network and the organic components (PEG and caffeic acid). These analyses confirmed the formation of stable hybrid systems and highlighted the influence of caffeic acid content on the thermal behavior of the coatings.
Furthermore, the bioactivity of the coated substrates was evaluated through in vitro tests in simulated body fluid (SBF), focusing on the ability to induce apatite formation on the surface[3]. The results revealed that all functionalized coatings promoted the nucleation and growth of apatite layers, with enhanced performance observed as a function of caffeic acid concentration. This behavior suggests that the incorporation of caffeic acid plays a key role not only in modulating the physicochemical properties of the coatings but also in enhancing their interaction with biological environments.

Overall, this study demonstrates that SiO_2–PEG-based sol-gel coatings enriched with caffeic acid represent a promising strategy for the development of next-generation bioactive and biocompatible surfaces for prosthetic and implantable devices. The combination of process simplicity, absence of substrate pre-treatment, and improved biological response makes these materials particularly attractive for future biomedical applications.

Keywords: sol–gel coatings, stainless steel implants, bioactive materials, apatite formation..

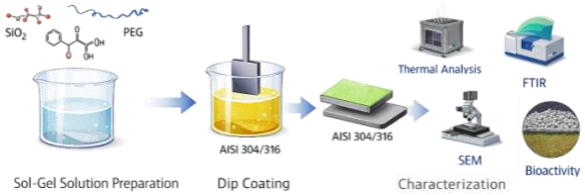

Figure 1: Graphical abstract

References:

1. Barrino, F. (2024). Hybrid organic–inorganic materials prepared by sol–gel and sol–gel-coating method for biomedical use: Study and synthetic review of synthesis and properties. Coatings, 14(4), 425.
2. Catauro, M., Barrino, F., Dal Poggetto, G., Crescente, G., Piccolella, S., & Pacifico, S. (2020). New SiO2/caffeic acid hybrid materials: Synthesis, spectroscopic characterization, and bioactivity. Materials, 13(2), 394.
3. Barrino, F., Giuliano, F., de la Rosa-Ramírez, H., & Samper, M. D. (2026). Sol-Gel Synthesis of New Bioactive Organic-Inorganic Materials for Biomedical Use: SiO2/Ferulic Acid/PEG. *International Journal of Molecular Sciences*, *27*(6), 2698.

Effects of growth defects on corrosion performance of PVD coatings and hybrid PVD/ALD layers for implant applications

P. Terek [1*], Z. Bobić [1], L. Kovačević [1], V. Terek [1], A. Csík [2], M. Čekada [3], A. Drnovšek [3]
[1] Faculty of Technical Sciences, University of Novi Sad, Novi Sad, Serbia
[2] HUN-REN Institute for Nuclear Research, Debrecen, Hungary
[3] Institute Jožef Stefan, Ljubljana, Slovenia

Abstract:
Combining physical vapor deposition (PVD) with atomic layer deposition (ALD) represents a promising strategy for creating biocompatible surface layers with improved corrosion resistance. However, the effectiveness of this hybrid layer is largely governed by the concentration, size, and geometry of growth defects within the underlying PVD coating. In this study, the corrosion protection of TiAlSiN/TiSiN/TiAlN, CN_x/TiAlN, TiN coatings, and hybrid PVD/ALD layers with amorphous and anatase Ti-O ALD layers (100 and 200 nm thick) deposited on TiN was evaluated in Hank`s solution by electrochemical impedance spectroscopy (EIS). The TiAlSiN/TiSiN/TiAlN coating exhibited the highest density of large nodular and crater-like defects, which CN_x/TiAlN followed, while the TiN coating showed the lowest defect concentration. The results of EIS also followed this trend, yielding the lowest impedance for TiAlSiN/TiSiN/TiAlN, slightly higher values for CN_x/TiAlN, and the highest values for TiN. All examined ALD layers exhibited good adhesion to the TiN PVD coating, as evaluated by an indentation test. However, on all hybrid PVD/ALD samples, before the corrosion testing, cracks and localized delaminations were observed on larger PVD growth defects all over the surface. Depositing an ALD overlayer significantly increased impedance for all samples. The amorphous Ti–O layer provided the most pronounced improvement, whereas both anatase layers produced similar initial enhancements. After 8 hours of corrosion exposure, the amorphous layer maintained the highest impedance, the 100 nm thick anatase layer showed moderate stability, and the 200 nm thick anatase layer demonstrated the weakest long-term performance. Results of this investigation showed that large PVD defects mainly influence the initial corrosion behavior, while pinhole-like defects determine the long-term degradation of the PVD coating. In PVD/ALD systems, large PVD growth defects are the critical sites where the ALD layer tends to detach and fracture. It was found that the increase in the steepness of the protrusion growth defects of PVD coatings and a decrease in the ALD layer adhesion increase the probability of the ALD layer detachment and loss of corrosion protection.

Keywords: PVD coating, ALD layer, hybrid layer, corrosion, EIS, PVD growth defects

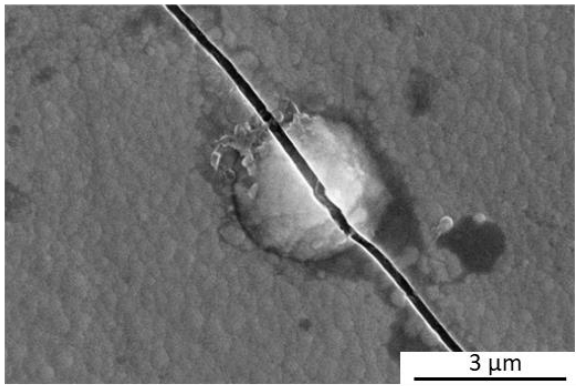

Figure 1: Surface of the hybrid PVD/ALD layer: a crack in the ALD layer propagating across the nodular PVD growth defect.

References:

1. Panjan, P.; Drnovšek, A.; Gselman, P.; Čekada, M.; Panjan, M.; Bončina, T.; Merl, D.K. Influence of Growth Defects on the Corrosion Resistance of Sputter-Deposited TiAlN Hard Coatings. Coatings 2019, 9, 1–16, doi:10.3390/coatings9080511
2. Staszuk, M.; Reimann, Ł.; Pakuła, D.; Pawlyta, M.; Musztyfaga-Staszuk, M.; Czaja, P.; Beneš, P. Investigations of TiO2/NanoTiO2 Bimodal Coatings Obtained by a Hybrid PVD/ALD Method on Al-Si-Cu Alloy Substrate. Coatings 2022, 12, 338, doi:10.3390/coatings12030338.
3. Marin, E.; Guzman, L.; Lanzutti, A.; Fedrizzi, L.; Saikkonen, M. Chemical and Electrochemical Characterization of Hybrid PVD + ALD Hard Coatings on Tool Steel. Electrochem. commun. 2009, 11, 2060–2063,doi:10.1016/j.elecom.2009.08.052.

Surface functionalization of micro-textured surfaces for antibiofouling applications of ocean sensors

Bichitra Nanda Sahoo[1*], Peter James Thomas[2], Martin Møller Greve[1]
[1]Nanophysics Group, Department of Physics and Technology, Allegaten 55, University of Bergen (UiB), 5007, Bergen, Norway
[2]Measurement of Science Group, NORCE Norwegian Research Center AS, 5008 Bergen, Norway

Abstract:
The rapid changes in oceanic phenomena are encouraging researchers to improve ocean monitoring systems. Currently, significant advancements have been made in the development of underwater environmental sensors deployed in the ocean to assess a range of seawater properties, including temperature, turbidity, CO_2 concentrations, and conductivity. However, these sensors face serious fouling issues in the constantly changing underwater environment. This fouling not only hampers data collection but also greatly shortens the sensors' operational life. The accumulation of biomass on these surfaces creates significant economic challenges for the marine industry and reduces the effectiveness of sensor technologies. Recently, there has been an increasing demand for antifouling technologies suitable for marine use. At the same time, growing concerns about environmental issues have led to stricter regulations on biocide-based coatings. Consequently, interest has grown in developing effective and environmentally friendly silicone-based fouling release coatings to mitigate the biofouling organisms on the sensor surfaces. In this abstract, we present several findings related to how microstructures created by hydrophobic polymers influence diatom settlement during prolonged immersion tests in algal solutions. Marine diatoms are a particularly problematic group to control in biofouling, and their antifouling effectiveness has been evaluated through laboratory experiments. Field Emission Electron Microscopy (FESEM) is used to examine the surface morphology of these microstructures. Additionally, a spectrophotometer was employed to assess the transparency of the films before and after biofouling tests on the specimens. Field trials were also conducted to study how microtextured surfaces affect their antifouling properties. Static and dynamic water contact angle (WCA) measurements were performed to evaluate the wettability of these surfaces. Further, fluorescence microscopy was employed to analyze the attached microorganisms on the surface. It can be concluded that the influence of microscale surface topographies and surface functionalization on the initial settlement of natural diatoms under static laboratory conditions depends on the size of micropillars, their shapes, wettability, and the surface adhesion strategies utilized by the biofouling diatom species. This research will also explore newly surface-functionalized microtextured glass surfaces, which we have highlighted for potential optical applications.

Keywords: surface functionalization, texturing, Lithography, wettability, ocean sensor, micropatterning, antibiofouling applications.

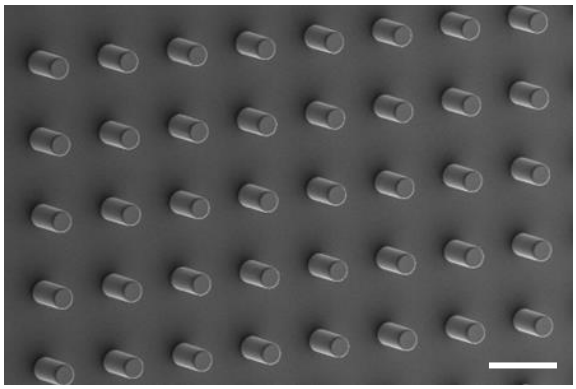

Figure 1: FESEM image of the microtextured polymer surface on the glass slide, scale bar - 100 µm.

References:

1. H. Hao, P. Liu, P. Su, T. Chen, M. Zhu, Z-B Jiang, Sea-trial research on natural product-based antifouling paint applied to different underwater sensor housing materials, *International Biodeterioration & Biodegradation* 170 (2022) 105400
2. A M. C. Maan, A H. Hofman, W. M. de Vos, and M. Kamperman, Recent Developments and Practical Feasibility of Polymer-Based Antifouling Coatings, *Adv. Funct. Mater.* **2020**, *30*, 2000936
3. J. Liang, C. Shan, H. Wang, T. Hu, Q. Yang, Haoyu Li, Xun Hou, and Feng Chen, Highly Stable and Transparent Slippery Surface on Silica Glass Fabricated by Femtosecond Laser, *Adv. Eng. Mater.* 2022, 2200708.

Microwave Cold Plasma Jets for Microbial Inactivation: From RONS Chemistry to Cell Morphology

Kristína Trebulová[1*], Veronika Loupová[1], Barbora Chobotská[1], Lukáš Kletzander[1], Pavel Kulich[2], Zdenka Kozáková[1], František Krčma[1],
[1]Brno University of Technology, Faculty of Chemistry, Purkyňova 118, 612 00 Brno, Czech Republic
[2]Veterinary Research Institute, Hudcova 296/70, 621 00 Brno, Czech Republic
*xctrebulovak@vutbr.cz

Abstract:
Cold atmospheric plasma (CAP) has emerged as a promising non-thermal technology for medical decontamination, particularly in the treatment of infected wounds and antibiotic-resistant microorganisms. In this work, the antimicrobial efficacy of microwave CAP jets[1] on both bacterial (*Staphylococcus epidermidis, Escherichia coli, Propionibacterium acnes*) and yeast (*Candida glabrata*) species was studied. Standardized protocols were applied to compare static and scanning treatment modes and to assess the influence of operational conditions on decontamination efficiency.
To better understand the underlying mechanisms, microbiological assays with visualization techniques and biochemical approaches were used. Plasma-treated liquids demonstrated that long-lived species such as hydrogen peroxide and nitrites contribute to antimicrobial action, but act on longer timescales. In contrast, the rapid microbial inactivation observed under direct plasma exposure points to a dominant role of short-lived reactive oxygen and nitrogen species. Scanning and transmission electron microscopy with the use of continual dehydration method[2] revealed progressive structural damage, including cell wall thinning, membrane rupture, and protoplast aggregation. Notably, the appearance of ghost cells and condensed intracellular aggregates provided further insight into how oxidative stress and physical plasma effects converge to inactivate microbial cells.
Together, these results highlight the broad-spectrum antimicrobial potential of microwave CAP jets and shed light on the biochemical and structural pathways of plasma–cell interactions.

Keywords: plasma medicine, oxidative stress response, RONS mapping, plasma-cell interaction, electron microscopy

References:

1. Trebulová, K., Krčma, F., Skoumalová, P., Kozáková, Z. & Machala, Z. Effects of different cold atmospheric-pressure plasma sources on the yeast Candida glabrata. Plasma Processes and Polymers 20, (2023) doi:10.1002/ppap.202300048.
2. Kulich, P. et al. Subchronic Inhalation of TiO_2Nanoparticles Leads to Deposition in the Lung and Alterations in Erythrocyte Morphology in Mice. Journal of Applied Toxicology 45, 1004-1018 (2025) doi:10.1002/jat.4759.

SICT 2026 / Plasma Tech 2026 Joint Session II. C: Plasma fundamentals / Modelling / Atomic and Molecular Processes Plasma Processing / Materials Interactions / Coatings

Comparative Study of Metal Atom, Metal Ion, and Argon Ion Fluxes in Laboratory and Industrial Sputtering Using Metallic and Alloy Targets

Petr Vasina[1,*], P. Klein[1], M. Ondryas[1], G. Lelovics[1], V. Sochora[2], M. Jilek[2], K. Mayur[3], A. Mackova[3], M. Učík[4], J. Klusoň[4], J.Hnilica[1]
[1]Department of Plasma Physics and Technology, Faculty of Science, Masaryk University, Brno, Czech Republic
[2] SHM s. r. o., Šumperk, Czech Republic
[3] Nuclear Physics Institute of the Czech Academy of Sciences, Rez, 250 68, Czech Republic
[4] PLATIT a.s., Průmyslová 3020, CZ-787 01, Šumperk, Czech Republic
*Corresponding author e-mail: vasina@pysics.muni.cz

Abstract:
Magnetron sputtering is a key technique for producing advanced functional and protective coatings in both laboratory and industrial environments. In this work, we investigate sputtering processes in both settings, focusing on quantifying the fluxes of sputtered species—neutral metal atoms, metal ions, and bombarding Ar^+ ions—arriving at the substrate.

In the laboratory, the study concentrates on high-power impulse magnetron sputtering (HiPIMS), where the strong ionization of sputtered material and dynamic plasma behavior significantly influence film growth. Industrial measurements were carried out using large-scale DC magnetron sputtering (DCMS) and moving focused-magnetic-field magnetron sputtering (F-MS), operated at high power levels with power densities comparable to HiPIMS. This combination enables direct comparison of particle fluxes across regimes with markedly different plasma characteristics.

We examine single-element targets (Ti, Al, Cr) as well as multi-component alloys, with an emphasis on AlCr and TiAl—materials widely used for high-performance hard coatings. By measuring the fluxes of neutrals, metal ions, and Ar^+ ions at the substrate, we evaluate how target composition affects ionization probability and the overall flux of film-forming species.

For example, in industrial F-MS sputtering of an AlCr cathode, we observed that the Ionized Metal Flux Fraction (IMFF) of Al was substantially lower for the alloy than for the pure Al target, while the IMFF of Cr remained essentially unchanged relative to pure Cr. The total sputtered particle flux from the alloy also exceeded the fluxes from both pure Al and pure Cr at the same applied power, and the individual Al and Cr fluxes closely followed the elemental composition of the target. These results demonstrate both composition-preserving alloy sputtering and a sputter-amplification effect.

In selected conditions, we also deposited thin films and correlated their structural and compositional properties with the measured plasma characteristics and particle fluxes, further clarifying the link between plasma behavior and film growth.

Overall, our measurements reveal distinct differences between elemental and alloy sputtering as well as between HiPIMS and industrial DCMS/F-MS modes. The findings provide deeper insight into how target material and sputtering regime jointly determine the particle fluxes that govern thin-film growth.

Keywords: magnetron sputtering, industry, ion meter, flux of metal atoms and ions, IMFF

References:

1. P. Klein et al., In-situ analysis of metal atom, metal ion and argon ion fluxes in industrial magnetron sputtering with Al, Cr and AlCr targetsSurface & Coatings Technology 526 (2026) 133364
2. P. Klein et al., Exploring ionised metal flux fraction in magnetron sputtering: Insights from laboratory and industrial applicationsSurface & Coatings Technology 500 (2025) 131866
3. P. Klein, Enhancement of ionized metal flux fraction without compromising deposition rate in industrial magnetron sputteringSurface & Coatings Technology 489 (2024)

Technological Change for future Speciality Glass Production

S. Wolf[1,*], M. Hauf[1], B. Bochtler[1], T. Golubeva[1], W. Schmidbauer[1], J. Hessenkemper[1], K. Jochem[1], S. Knoche[1], S. Knoche[1], J. Costard[1], M. Hahn[1]
[1] SCHOTT AG, Mainz, Germany

Abstract:

SCHOTT, a global leader in specialty glass manufacturing, is advancing innovative approaches for future glass production. Balancing ecological and economic aspects of production planning, we believe that future glass melting concepts must address three core areas: (1) the use of low-emission energy sources, especially electricity, (2) energy and process efficiency, and (3) flexibility to adapt to fluctuating energy prices.

The GIFFT project [1] investigates flexible-fuel plasma burners as a key technology for cost-effective future melting processes. The burner shown in Figure 1 utilizes existing oxyfuel gases combined with variable electrical boosting of flame power. This approach not only improves energy efficiency by reducing the amount of flue gas for the same power output but also provides short-term flexibility in electricity usage without compromising melting process stability. As installed renewable capacity increases, the grid will experience growing fluctuations in power output. Consequently, flexibility in electricity consumption can provide significant economic benefits by enabling dynamic adaptation to variable energy generation and market conditions. In addition, it will contribute to grid stability and and can help facilitate the clean energy transition.

The PLANET1 project [2] helps to lay the foundation for reducing CO_2 emissions for the glass-ceramics melting process through significantly enhanced electrical boosting. In a production trial, we demonstrate how an innovative electrode wiring concept reduces electrical currents—enhancing electrode lifetime—while simultaneously enabling higher boosting power. We also discuss challenges related to increased voltages and their impact on glass melt flow.

The PROSPECT projects [3] outline SCHOTT's path toward its first electric melting tank for premium pharmaceutical glass. Laboratory melts have been used to systematically investigate how electrode robustness depends on current density, temperature, and boosting frequency across various SCHOTT glass compositions. These insights guided the design of a full-electric melting tank in combination with a strongly boosted fining tank, scheduled to start operation in 2027.

Within the MiGWa project [4], we explored microwave-assisted glass melting, from fundamental tests to a lab-scale continuous melting tank. While demonstrating efficiency gains, our experiments revealed significant challenges for implementing microwave technology in industrial glass production.

Together, these projects illustrate SCHOTT's commitment to advance future glass melting technologies - combining electrification, process efficiency, and operational flexibility to create pathways for reducing carbon emissions in specialty glass production.

Keywords: process heat, flexible fuel plasma burners, electrification of energy intensive industries, future glass production, reduced carbon footprint

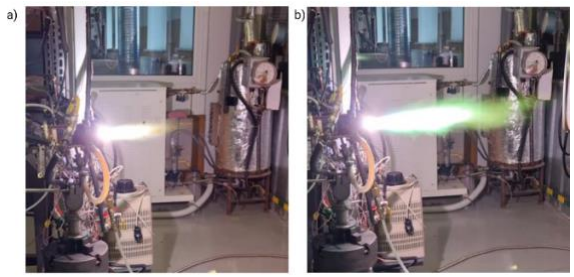

Figure 1: Flexible-fuel plasma burner operated (a) with 40kW Oxygen plasma only, and (b) with additional injection of methane, achieving a total power of ~80 kW. Image courtesy of Lithuanian Energy Institute (Kaunas, Lithuania).

References:

1. https://www.gifft-europe.eu/
2. https://www.klimaschutz-industrie.de/foerderung/dekarbonisierung-in-der-industrie/projekt/planet-1/
3. https://www.klimaschutz-industrie.de/foerderung/dekarbonisierung-in-der-industrie/projekt/prospect/
4. https://www.fona.de/de/massnahmen/foerdermassnahmen/KlimPro/migwa.php

Plasma Tailoring of Celluloses for Advanced Applications

V. Shvalya [1*], A. Oberlintner [2], N. M. Santhosh [1], U. Cvelbar [1]
1 Department of Gaseous Electronics (F6), Jožef Stefan Institute, Jamova 39, Ljubljana SI-1000, Slovenia
[2] Department of Catalysis and Chemical Reaction Engineering, National Institute of Chemistry, Hajdrihova 19, SI-1000 Ljubljana, Slovenia

Abstract:
Plasma processing is rapidly becoming the leading method for surface modification because it enables alteration of only the outer few nanometres of a material while leaving the bulk unchanged, transforming inert substrates into high-performance interfaces with minimal use of chemicals and multistep processes. Starting with bio-based cellulose, we first used mild CF4 plasmas to drive nanocellulose films into the superhydrophobic regime, demonstrating how a few seconds of fluorocarbon treatment can convert fully wettable fibres into water-repellent barriers for packaging and protective layers. [1] The same platform then served as a testbed for a more sustainable approach: by switching to nitrogen plasmas and carefully controlling the exposure, to produce fluorine-free Janus membranes with one hydrophobic and one hydrophilic face (Fig.1), enabling directional water transport and repellent coatings without persistent halogenated species. [2] Finally, a plasma-assisted soft-chemistry route couples mild and strong plasma treatments of CNFs with ultra-broadband terahertz time-domain spectroscopy (THz-TDS) up to and beyond 10 THz, resolving distinct CNF resonances and tracking how plasma etching thins the films and carbonises the surface without degrading their microcrystalline core. From the extracted optical parameters, we can define the minimum CNF thickness required for efficient THz shielding, directly linking plasma dose, surface functionality and macroscopic attenuation. [3] Together, these examples demonstrate that plasma is not just another surface treatment: it is a versatile, inline, solvent-free toolbox that can adjust wetting, cleaning and reactivity on demand, bridging from fluorinated performance standards towards precise, safe-and-sustainable-by-design surface engineering for the next generation of packaging and THz applications.

Keywords: Plasma treatment, celulose, hydrophobic cellulose, THz shielding, sustainable coatings.

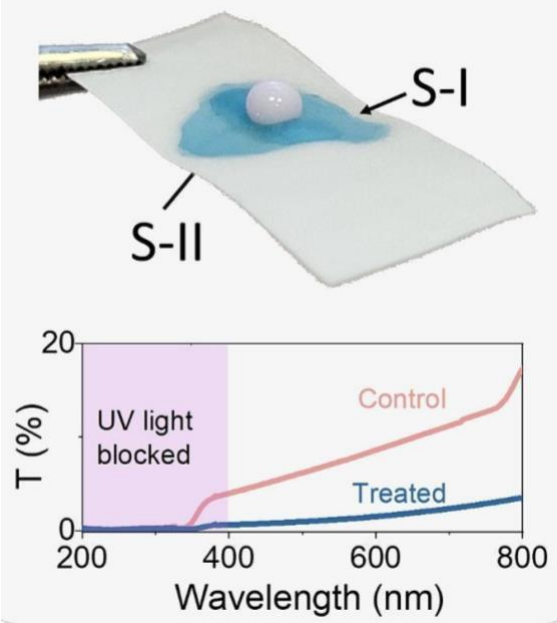

Figure 1: Example of a cellulose membrane with opposite wetting behaviour.

References:

1. Oberlintner, A., Shvalya, V., Vasudevan, A., Vengust, D., Likozar, B., Cvelbar, U., & Novak, U. (2022). Hydrophilic to hydrophobic: ultrafast conversion of cellulose nanofibrils by cold plasma fluorination. *Applied Surface Science*, *581*, 152276.
2. Oberlintner, A., Shvalya, V., Santhosh, N. M., Košiček, M., Jerman, I., Huš, M., ... & Likozar, B. (2024). Janus nanocellulose membrane by nitrogen plasma: Hydrophilicity to hydrophobicity selective switch. *Carbohydrate polymers*, *345*, 122558.
3. Santhosh, N. M., Puc, U., Jazbinšek, M., Oberlintner, A., Shvalya, V., Zavašnik, J., & Cvelbar, U. (2025). Exploring effects of plasma surface engineering on cellulose nanofilms via broadband THz spectroscopy. *Applied Surface Science*, *682*, 161698.

Complex plasma with active Janus particles in patterned confinement

V. Nosenko [1]
[1] Institut für Frontier Materials auf der Erde und im Weltraum,
Deutsches Zentrum für Luft- und Raumfahrt (DLR),
D-51170 Cologne, Germany

Abstract:
Active matter is a system of self-propelling units which convert the energy stored locally or extracted from their environment into directed motion. It has recently attracted considerable attention due to the rich new physics it displays and potential applications in various fields including materials science. Active matter found in nature is inherently complex, so model systems are of interest where its main features can be isolated and studied in laboratory experiments. An interesting instance of active matter is a suspension of active particles (e.g., the so-called Janus particles, where the two halves have different properties) in a gas discharge plasma [1].
In this presentation, we report on the experiments with active Janus particles confined within the plasma sheath over a patterned electrode and analyze how the chiral characteristics of the particle trajectories couple with chiral features in the particle confinement landscape. The Janus particles were melamine-formaldehyde microspheres with a diameter of 9.27 μm coated on one side with a 40-nm layer of gold using magnetron plasma sputtering [2].
Plasma was produced by a capacitively coupled radio-frequency (rf) discharge in argon at 13.56 MHz in a modified Gaseous Electronics Conference (GEC) rf reference cell. On top of the lower powered rf electrode, an add-on electrode with a machined asymmetric (chiral) funnel structure was placed, see Figure 1. The gas pressure was 0.66 Pa, the discharge power was 20 W.
When injected in plasma, the Janus particles formed a single-layer suspension in the plasma sheath over the lower rf electrode. The suspension conformed to the funnel-shaped confining structure in the electrode depression. The particles were levitated by the balance of the sheath electric field and gravity. Due to the Janus particles' self-propulsion, they acquired high speeds greatly exceeding the thermal speed [1]. The self-propulsion force was balanced by the neutral gas drag.
We analysed the apparently chaotic flow of Janus particles and tested whether rectification of active motion, i.e., unidirectional drift of active particles, or their sorting or separation based on the self-propulsion characteristics can be achieved in this configuration.

Keywords: complex plasma, active matter, Janus particles, patterned confinement, chiral confinement, plasma coating.

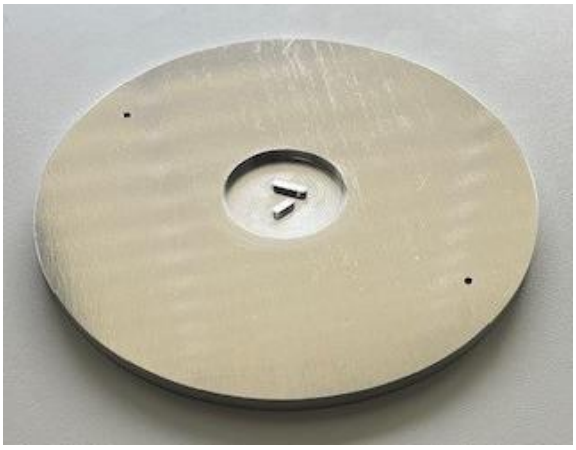

Figure 1: Add-on rf electrode with a machined structure used as a confinement for active Janus particles. The depression in the aluminium disk electrode with an elevated asymmetric funnel structure has a diameter of 30 mm.

References:

1. Nosenko, V. (2022), Two-dimensional complex (dusty) plasma with active Janus particles, *Phys. Plasmas*, 29, 123701.
2. Nosenko, V. (2025), Extended self-similarity in two-dimensional complex plasmas, *Phys. Rev. E*, 111, 045210.

Investigation of the chemical behaviour of an electrolytic discharge used to synthesize low-density mesoporous metals

C. Boudat[1,2], R. Botrel[1], F. Durut[1], C. Noël[2], T. Belmonte[2]
[1] Commissariat à l'Energie et aux Energies Alternatives (CEA), Valduc, F-21120, Is sur Tille, France
[2] Université de Lorraine, CNRS, IJL, F-54000 Nancy, France

Abstract:
As part of laser matter interactions experiments carried out, at the Laser Mégajoule (LMJ) facility, CEA needs to synthesize low-density materials with specific characteristics. In this context, cutting-edge materials in the form of low-density metallic foams are employed, with a specific focus on those produced through the technique of plasma electrolysis deposition.

This synthesis method, patented by the CEA, differs from commercial and industrial synthesis techniques for metallic foams and aerogels due to the specific properties it provides. These materials have an apparent density equivalent to approximately 1% of the bulk metal, pore sizes of about a micrometre, and a purity higher than 95%.

Because the synthesis processes for these innovative materials are complex and the underlying mechanisms have not been fully elucidated yet, studies have been undertaken to improve the understanding of the phenomena occurring during synthesis. Specifically, the different species present in solution and their influence on the reaction leading to the formation of metal foams have been examined. Additionally, the functional heterogeneity of similar solutions and cathodic and anodic processes in an aqueous medium have been the subject of specific studies. Studies were also conducted to investigate the plasma composition and the contribution of reducing species to the material formation site.

The objective of these investigations is to improve control of the structural organization and characteristics of the material, with the aim of optimizing the synthesis process and obtaining a final material that meets the required criteria.

Keywords: Low-density materials, metals, electrolytic plasma, plasma-liquid interaction

References:

1. R. Botrel. EP 2824219 B. EU patent (2015).
2. S. Rocher. Etude des mécanismes de croissance de mousses métalliques élaborées par plasma électrolytique. Doctorat de Physique-Chimie préparée au Commissariat à l'Energie Atomique et aux énergies alternatives (2019).
3. J. Pinot. Compréhension des phénomènes régissant la croissance de mousses métalliques élaborées par plasma électrolytique : application à la fabrication de cibles laser. Doctorat de Chimie préparée au Commissariat à l'Energie Atomique et aux énergies alternatives (2021).

Plasma-Catalytic Pyrolysis Via Water-Stabilized Plasma Torch for Single-Walled Carbon Nanotubes Synthesis

J. Fathi[1,2,*], A. Mašláni[1], O. Jankovský[2]
[1] Department of Plasma Chemical Technologies, Institute of Plasma Physics, Prague, Czechia
[2] Department of Inorganic Chemistry, University of Chemistry and Technology, Prague, Czechia

Abstract:
The scalable production of single-walled carbon nanotubes (SWCNTs) is often limited by the high cost of catalysts and the difficulty of maintaining stable high-temperature reaction conditions. This work presents Plasma-Catalytic Pyrolysis (PCP), a methane decomposition method powered by a hybrid water-stabilized plasma (WSP-H) torch, which enables the simultaneous synthesis of SWCNTs and hydrogen. In this process, Fe_2O_3 micro powder is introduced into a steam–argon plasma environment with core temperatures above 20,000 K, where it undergoes rapid thermal shock, melting, and in situ reduction to nanoscale Fe and Fe_xC catalytic particles. Methane fed into the 200 L entrained-flow reactor undergoes nearly complete conversion, producing hydrogen and carbon species that nucleate and grow on the freshly formed iron nanoparticles. This plasma–catalyst interaction promotes the formation of high-quality SWCNTs. Characterization using HRTEM, EFTEM, STEM–EDS, Raman spectroscopy, and XRD confirms the presence of well-structured SWCNTs embedded in iron-containing nanocomposites. The process also generates hydrogen at high concentration, demonstrating its capability as an efficient Power-to-X route. The PCP method offers an energy-efficient, scalable, and low-cost pathway for producing SWCNTs and clean hydrogen, providing new opportunities for large-scale carbon nanomaterial manufacturing.

The design and operation of the plasma–catalytic reactor system are summarized in Figure 1. The illustration depicts a hybrid water-stabilized plasma torch generating a high-temperature plasma jet that enters the reactor, where methane and Fe_2O_3 micro powder are simultaneously injected. Within the hot reaction zone, methane undergoes pyrolysis while the metal oxide precursor is rapidly reduced, enabling in situ formation of catalytic iron nanoparticles. The resulting products, SWCNTs, are shown in Figure 2.

Keywords: Plasma-Catalytic Pyrolysis, SWCNT synthesis, Water-Stabilized Plasma torch

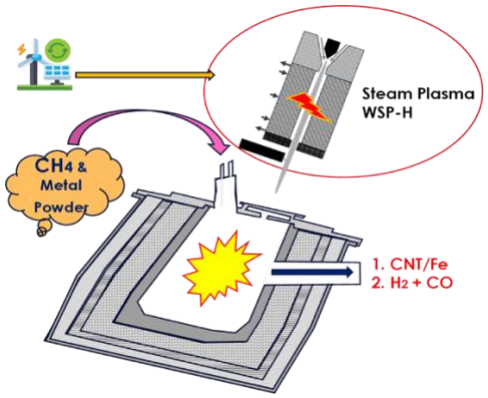

Figure 1: schematic of the plasma catalytic pyrolysis set-up.

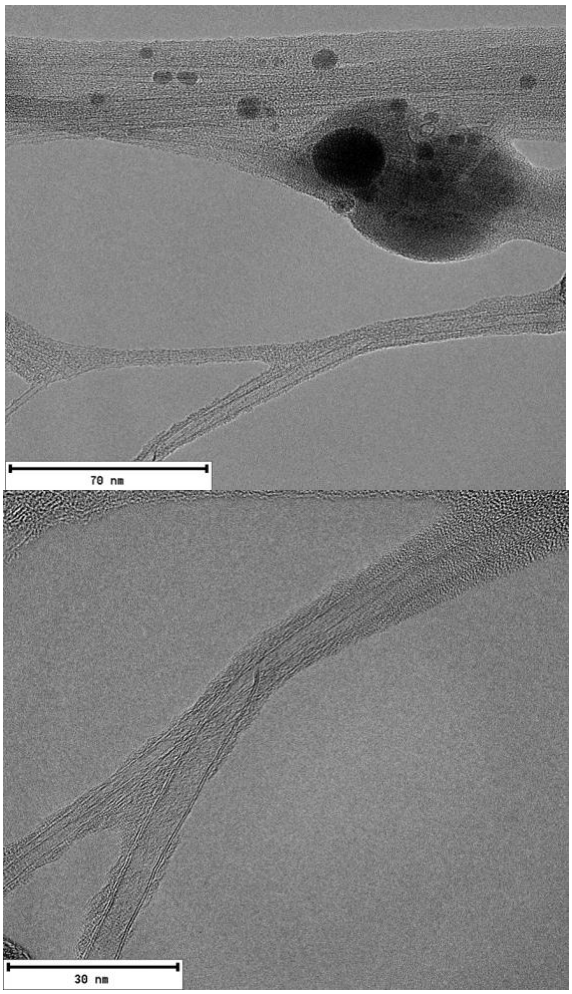

Figure 2: HRTEM images of SWCNTs

Synthesis of higher order organic compounds from hydrocarbons, alcohols and amines using a microsecond-pulsed dielectric barrier discharge

P-L. Girard-Lauriault [1*], A. Banerjee, S. Marji[1], O Armstrong[1], G. Baez-Zaldivar
[1] Plasma Chemical Processing Laboratory, Department of Chemical Engineering, McGill University, 3610 Rue University, Montreal, Canada.

Abstract:
Conventional chemical processing routes used to convert simple organic molecules into more valuable products require significant energy and resources. Plasma-based synthesis methods have been explored since the 19th century, and interest has increased in recent decades. This work summarizes recent studies on the use of non-thermal plasmas, under controlled temperature conditions, to form higher-order organic molecules at atmospheric pressure and near room temperature without added solvents.

Hexane, octane, decane, ethanol, methanol, and butylamine, either pure or in mixtures, were exposed to a microsecond-pulsed dielectric barrier discharge in argon or nitrogen in a pin-to-plane configuration. The reaction temperature was regulated by a jacketed flask and varied between −20 °C and 20 °C. Gas- and liquid-phase products were analyzed by gas and liquid chromatography coupled with mass spectrometry.

Processing of hydrocarbon and alcohol mixtures produced compounds in the C6–C20 range, which were identified and quantified. Plasma treatment of butylamine generated aliphatic and aromatic amines, nitriles, and azoles. These results support a more detailed interpretation of the reaction pathways involved. Energy efficiencies for selected products were calculated and compared with those of conventional synthesis routes, with favorable values observed. The production efficiency depended on the processing temperature, with a maximum near 0 °C. The parameter governing this temperature effect remains unresolved.

These findings indicate that plasma processing of small organic molecules may enable efficient synthesis of valuable organics and fuels. Ongoing work aims to assess the potential of this approach to reduce energy demand and solvent use in chemical synthesis.

Keywords: non-thermal plasma, dielectric barrier discharge, plasma-liquid interactions, plasma electrochemistry, plasma assisted synthesis.

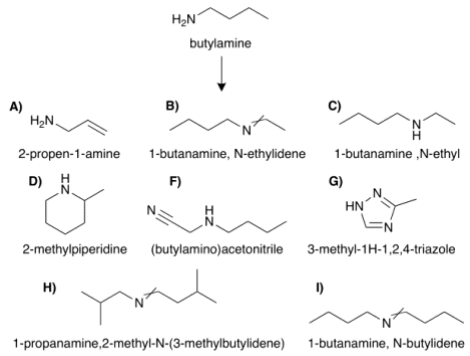

Fig. 1. Chemical structures of products obtained from plasma treatment

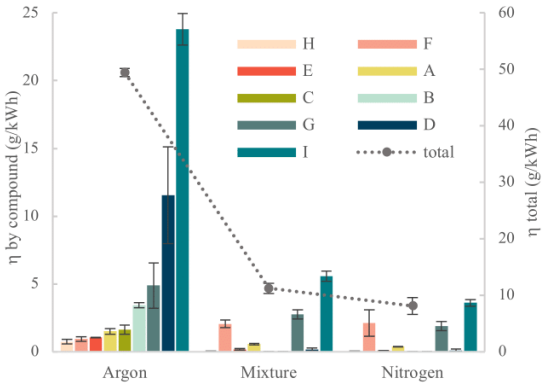

Fig. 2. Total production efficiency and production efficiency for each nitrogen-containing compound (g/kWh) with varying gas ratios after 1 hour at -20 °C

References:

1. P.J. Bruggeman et al. (2025) Advances in plasma-driven solution electrochemistry, *J. Chem. Phys. 162, 071001*
2. A. Banerjee, O. Armstrong, P.L. Girard-Lauriault. Synthesis of higher-order nitrogen-containing organic compounds from butylamine using a microsecond pulse dielectric barrier discharge, *Industrial & Engineering Chemistry Research 62 (36), 14144-14150*

Production of nitrogen oxides as fertilizers precursors via an atmospheric microwave air plasma torch

M. Troia[1,*], K. Wiegers[1], A. Schulz[1], M. Walker[1]
[1] IGVP University of Stuttgart, Stuttgart, Germany

Abstract:
About 70% of world ammonia production, which alone constitutes 20% of the energy required in the whole chemical sector, is later employed in the fertilizers industry [1] for the production of nitric acid, a precursor to their finished products, via the well-known combination of the Ostwald and the Haber-Bosch processes. The fertilizers industry needs however to undergo a strict reforming, in accordance with several EU directives and, among others, the Paris agreements. The latter in particular mandates a reduction in CO_2 emission for ammonia production of 70% by 2050.

As such, plasmochemical processes may constitute attractive alternatives to the very energy-intensive and polluting state of the art. This is due to their flexible, on-demand operating mode which allows, among other things, for an in-loco production of the fertilizers precursor NO_x at low costs, thus also reducing the costs and the degradation of fertilizers associated to long-distance transport and long-term storage, especially in developing countries. A second advantage is the almost instantaneous ignition of the plasma, which allows it to run on excess electricity on the grid.

In the current work, a commercially available microwave air-fed plasma is used to synthesize NO_x over a wide set of operating parameters [2] (Figure 1).

The resulting NO_x concentrations, comparable to the current state-of-the-art for similar plasma processes, have been further improved by optimizing the gas management in the plasma volume and in its after-glow region by means of custom-made converging-diverging nozzles with different geometries, once more over a wide set of operating parameters.

High-speed camera measurements and characterization via optical emission spectroscopy further elucidate the chemistry taking place in the plasma phase and, more importantly, at its edges and as function of decreasing temperatures.

Wit the addition of extensive “cold” gas numerical simulations carried out in both the basic configuration of the plasma reactor and the nozzle setups, together with further numerical studies benchmarked on the results here presented [3], the study finally offers several promising avenues for further improvements of the NO_x yield thus obtained and on the costs associated to such plasmochemical routes.

Keywords: atmospheric plasma torch, plasma chemistry, FEM simulations, fertilizers, agricultural applications, decarbonization.

Figure 1: Microwave, atmospheric-pressure plasma torch operating with dry air used in the current work for the synthesis of NO_x.

References:

1. International Energy Agency (2021) Ammonia Technology Roadmap, IEA, Paris.
2. Troia, M., Vagkidis, C., Schulz, A., Köhn-Seemann, A., Walker, M., Tovar, G. E. (2025), NO_x Production via an Atmospheric Microwave Air Plasma Torch, *Chemie Ingenieur Technik*, 97(5), 435-443.
3. Albrecht, M., Tsonev, I., Laitl, V., Bogaerts, A., Towards predictive multidimensional modeling for industrializing microwave air plasma-based NOx formation. Available at SSRN 5473430.

Scalable nanopulsed plasma seed disinfection using a long wire-plate DBD module

L.F.A. Wymenga [1*], J. van Turnhout[2]
[1] Electrical Components, Technologies and Materials, Delft University of Technology, Delft, The Netherlands
[2] Material Sciences & Engineering, Delft University of Technology, Delft, The Netherlands

Abstract:
Plant diseases cause major yield losses in vegetable crop production[1]. These diseases are initiated by pathogenic fungal spores and bacteria, such as *Alternaria* and *xanthomonas,* which reside on seed surfaces[2].
Chemical and/or heat treatments of seeds can inactivate these microorganisms. However, these methods are energy-intensive, leave toxic residues and often impair seedling growth.
Cold atmospheric plasma (CAP) offers an ecofriendly alternative for seed disinfection. CAP generates a rich mixture of electrons, ions, photons, and reactive oxygen and nitrogen species (RONS). It avoids heat and toxic residues, while improving the germination.
CAP is commonly created in laboratory settings using an AC-driven dielectric barrier discharge (DBD), which poses challenges for upscaling.
To address this, we present a novel scalable DBD design activated by high voltage nanopulses. Such pulses have several advantages over AC powering, such as higher RONS production and reduced energy consumption.
We successfully tested our planar long wire DBD module on cabbage and carrot seeds, infected with *xanthomonas, Alternaria* and various other microorganisms.
Treatment parameters (like duration, voltage, distance) were evaluated systematically. We also investigated the individual contributions of pulsed electric fields, electrons, positive ions, negative ions, UV photons and RONS to the overall disinfection process.
Rapid disinfection (up to 93 % in 30 min.), attributed primarily to the produced RONS, was achieved in ambient air.

Keywords: nanopulses, wire-plate DBD, scalable plasma panel, cold atmospheric plasma, seed disinfection, Alternaria, xanthomonas, upscaling.

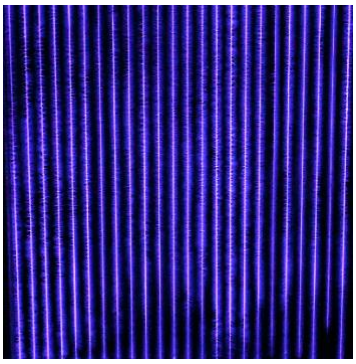

Figure 1: Plasma formation in our extensible long wire-plate DBD, showing microdischarges over a total electrode length of 7 m.

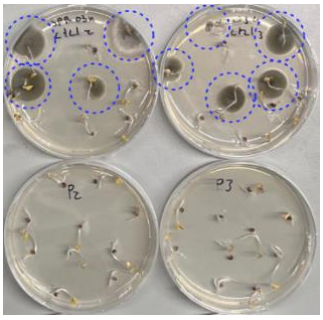

Figure 2: The top Petri dishes contain infected cabbage seeds, showing microbial colony growth six days after plating (blue circles). The bottom Petri dishes contain CAP-treated seeds, showing complete disinfection.

References:

1. Nowicki, M., Nowakowska, M., Niezgoda, A., & Kozik, E.U. (2012). Alternaria black spot of crucifers: symptoms, importance of disease, and perspectives of resistance breeding. *Journal of Fruit and Ornamental Plant Research, 76*, 5 - 19.
2. Suwannarat, S., Thammaniphit, C., & Srisonphan, S. (2021). Electrohydraulic streamer discharge plasma-enhanced Alternaria brassicicola disinfection in seed sterilization. *ACS Applied Materials & Interfaces*, *13*, 43975−43983.

Cold Plasma-Assisted Drying: A Promising Strategy for Enhancing Drying Characteristics and Quality Retention in Cannabis Processing

P.C. Das, L.G. Tabil, O.D. Baik*,
Department of Chemical and Biological Engineering, University of Saskatchewan, Canada
*Correspondence: oon-doo.baik@usask.ca

Abstract:
The cannabis industry commonly employs low-temperature hang drying of inflorescences, a slow process associated with nonuniform drying and high susceptibility to microbial contamination. High-temperature drying accelerates moisture removal but causes the loss of valuable volatile compounds. Cold plasma (CP) technology, an emerging and environmentally friendly technique, offers potential to enhance drying kinetics while preserving sensitive phytochemicals. This study investigated the effects of CP pretreatment on undried cannabis inflorescences using plasma jet powers of 300, 350, and 400 W with exposure times of 20, 30, and 40 s. Treated and untreated samples were subsequently dried under controlled conditions (25 °C and 50% relative humidity). Drying behavior, energy consumption, and chemical composition were compared to assess process performance. Untreated cannabis samples reached an equilibrium moisture content (EMC) of approximately 16% after 1260 min, whereas CP-pretreated samples achieved lower EMCs (10–14%) within 690-840 min. CP pretreatment improved moisture diffusivity and energy efficiency. Higher plasma power and longer exposure promoted partial decarboxylation of cannabinoids, increasing tetrahydrocannabinol (THC) while reducing tetrahydrocannabinolic acid (THCA), without significantly affecting total THC content. CP pretreatment demonstrated excellent terpene preservation, retaining approximately 96% of total terpenes at 400 W for 30 s and over 90% across all 300 W treatments compared with untreated controls. A life cycle assessment indicated that CP pretreatment (400 W, 30 s) could reduce environmental impact by about 50% relative to conventional drying. Overall, cold plasma-assisted drying represents a promising, energy-efficient and environment friendly approach for the cannabis industry, accelerating drying rates and maintaining superior product quality-particularly in terpene retention and cannabinoid integrity.

Keywords: Cannabis, Drying, Cold Plasma, Diffussivity, Cannabinoids, Terpenes, Sustainability.

Electrochemical Reduction of Metal Oxalates and Tartrates Using Non-Equilibrium Hydrogen/Argon Plasma

A. Guillemin[1,2], F. Rousseau[1], C. Guyon[1]
[1] 2PM, Institut de Recherche de Chimie Paris, Paris, France
[2] Centre National de la Recherche Scientifique, Paris, France

Abstract:
Metal oxalates are known to be reducible under conventional hydrogen atmospheres. Similarly, hydrogen plasmas have been employed to reduce metal oxides, although both approaches typically exhibit slow kinetics. In this study, a non-equilibrium hydrogen/argon plasma is investigated to reduce metal oxalates and tartrates. Unlike most non-equilibrium plasma processes, the reduction occurs throughout the volume of the material, and proceeds rapidly, yielding metal powders with purities exceeding 99%, suitable for direct use in powder metallurgy. The resulting powders are characterized using X-ray diffraction (XRD) and scanning electron microscopy (SEM) to confirm their quality. Plasma properties are monitored via optical emission spectroscopy (OES). Compared to existing literature, this method demonstrates notable properties. For instance, iron(III) oxalate was successfully reduced to iron metal and antimony(III) tartrate to antimony, reactions not previously reported in the litterature. These results suggest that the plasma may act as a charge carrier, enabling electrochemical reduction. This method holds promise for various recycling applications. Oxalic acid is known to precipitate many divalent metal cations, which can then be readily reduced in a plasma reactor. For example, cobalt oxalate recovered from discarded batteries can be efficiently reduced. Similarly, NiCd batteries treated with oxalic acid yield oxalates of both nickel and cadmium, which are amenable to plasma reduction. Functional results and theoretical predictions for metal production are presented in Figure 1.

Keywords: plasma, non-equilibrium, oxalates, tartrates, reduction, electrochemistry, XRD, Radio-frequency, Micro-wave, OES, SEM

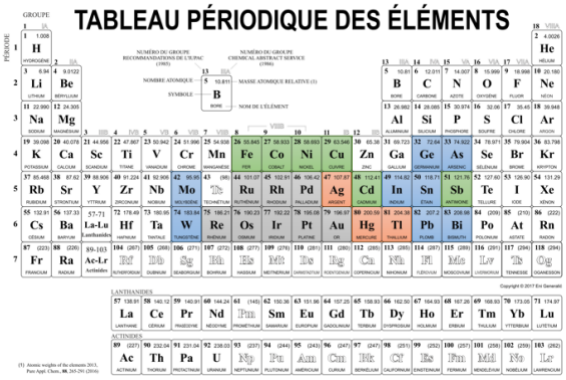

Figure 1: Reduceable metals by carboxylates under non-equilibrium H_2/Ar plasma (green : already done, Blue : doable, Grey : theoratically functional, Orange : doable but too dangerous)

References:

1. D. Dollimore et al. The thermal decomposition of oxalates. Part II Thermogravimetric Analysis of Various oxalates in air and nitrogen. 1963. Journal of the Chemical Society
2. K. C. Sabat et al. Reduction of oxide minerals by hydrogen plasma: An overview. Plasma Chem Plasma Process (2014) 34:1-23 DOI 10.1007/s11090-013-9484-2
3. S. Majumdar et al. A study on isothermal kinetics of thermal decomposition of Cobalt oxalate to cobalt. Thermochimica acta 473 (2008) 45-49

SICT 2026 / Plasma Tech 2026
Session II D:
Plasma Processing / Materials Interactions / Coatings
Plasma application in Energy and environment

Selective single-step microwave plasma conversion of hazardous aromatic hydrocarbons into few-layer graphene

O. Jašek [1*]
[1] Department of Plasma Physics and Technology, Masaryk University, Brno, Czech Republic
[*]jasek@physics.muni.cz

Abstract:
Aromatic hydrocarbons such as benzene, toluene, and xylene (BTX) are widely used industrial solvents and intermediates, but they are also hazardous air pollutants with well-documented carcinogenic, mutagenic, and ecotoxic effects [1]. BTX were converted into few-layer graphene (FLG) using reactive gas admixture, hydrogen or oxygen, in a high-temperature environment of atmospheric pressure dual-channel microwave plasma torch in Ar (Fig. 1a) [2]. Gas flow rates and delivered microwave power were investigated as main parameters of FLG synthesis. Decomposition of pure BTX vapors predominantly produced carbon nanoparticles, with up to 53 % yield. Hydrogen admixture strongly enhanced selectivity toward FLG and suppressing spherical carbon nanoparticles formation. Highest FLG yield, 23 % ≈ 360 mg/h, was achieved using benzene/H_2 (1:5) mixture at 350 W (Fig. 1b). Comparable yield was also obtained using hydrogen admixture to toluene and xylene. The use of oxygen admixture led to the FLG formation for benzene and toluene precursors, but with lower yield 4-18 %. The FLG material was analyzed by scanning electron microscopy (SEM), Raman and XPS. Plasma diagnostic was carried out by optical emission spectroscopy. In conclusion, hydrogen admixture promotes conversion to graphitic nanosheets with high sp^2 content, while oxygen moderates the process by forming carbon-oxygen compounds reducing FLG yield. These findings highlight the potential of aromatic precursors for scalable synthesis of FLG with market values significantly exceeding the cost of carbon feedstock. Continued development of scalable reactor design could enable industrial exploitation of aromatic hydrocarbon conversion as both an environmental and economic solution.
This work was supported by project LM2023039, which was funded by the Ministry of Education, Youth and Sports of the Czech Republic.

Keywords: aromatic hydrocarbons; microwave plasma, selectivity, reactive gases.

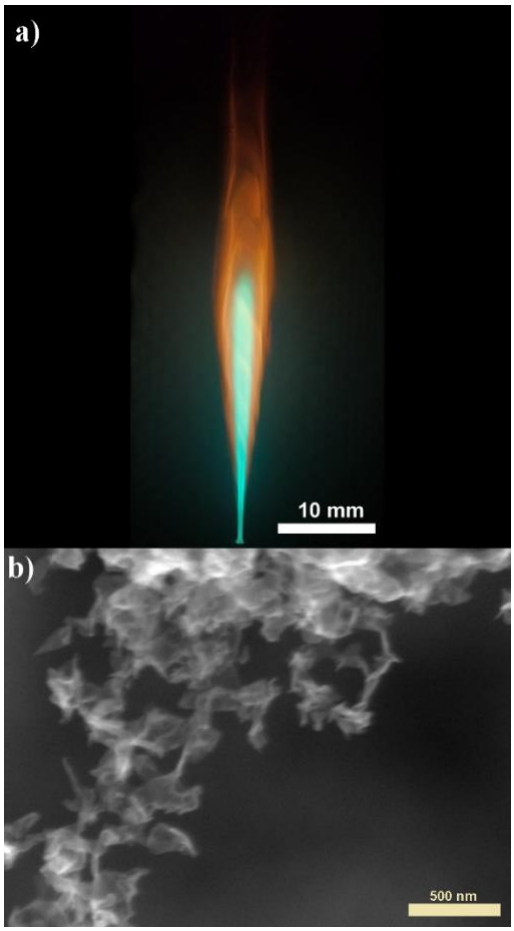

Figure 1: a) Microwave plasma discharge in Ar/Toluene and b) SEM of FLG nanosheets synthesized from mixture of benzene/H_2 at 350 W.

References:

1. Saeedi M, et al. (2024) Interaction of benzene, toluene, ethylbenzene, and xylene with human's body: Insights into characteristics, sources and health risks, *J. Hazard. Mater. Adv.*, 16, 100459.
2. Toman J et al. (2019) On the interplay between plasma discharge instability and formation of free-standing graphene nanosheets in a dual-channel microwave plasma torch at atmospheric pressure, *J. Phys. D Appl. Phys*, 52, 265205.

Conversion of plastic waste into high-quality soot by microwave-based plasma pyrolysis

D. Schüpfer [1,*], L. Beran [2], I. Kinski [1], G. Homm [1], T. Kraus [2,3]
[1] Fraunhofer Research Institution for Materials Recycling and Resource Strategies IWKS, Alzenau, Germany
[2] INM – Leibniz-Institute for New Materials gGmbH, Saarbrücken, Germany
[3] Saarland University, Colloid and Interface Chemistry, Saarbrücken, Germany

Abstract:
Plastic pollution has emerged as one of the most critical environmental challenges in today's world, with pervasive and increasing impacts on ecosystems and human health [1]. Microwave-based plasma pyrolysis utilizes a high-energy plasma with its specific plasma species to break down non-degradable polymers. Plasma pyrolysis is a promising method for the plastic transformation into valuable gases and carbon species like already shown in catalytic processes [2].
Here, the non-catalytic decomposition of plastic (high-density polyethylene, polypropylene, and polystyrene) into valuable gaseous products like hydrogen, along with carbon soot, a solid carbonaceous byproduct, is presented. The potential of microwave plasma pyrolysis as a sustainable waste-to-resource technology with the focus on carbon soot derived from virgin polymers compared to that produced from their post-consumer, single-use packaging counterparts has been explored.
A comprehensive set of characterization techniques was employed to evaluate the structure, morphology, aggregation behavior, and surface area of the soots. The different types of plastic are compared with each other, as pure materials with their waste counterparts. All soot samples show promising properties for a use in technological applications like fillers in elastomers. Despite some variation, all samples exhibited a high degree of aggregation. The results indicate that the plasma process parameters influence the decomposition rate and soot properties such as the aggregation state. They suggest that processed plastics might yield carbon materials suitable for use in composites, adsorbents, or sensing technologies, offering a pathway toward circularity in plastic waste management.

Keywords: microwave plasma, pyrolysis, plastic waste, waste decomposition, circularity, raw materials, soot, carbon black, carbon materials, microstructure analysis.

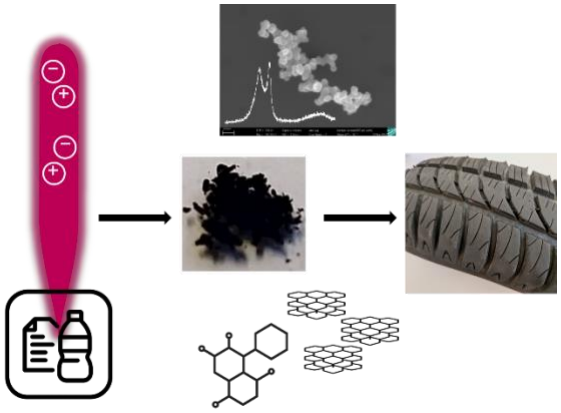

Figure 1: Plastic waste is utilized as a raw material for soot. The waste is decomposed into solid carbon structures and gases like H_2 by plasma pyrolysis. The carbon structures are applicable e. g. in elastomer products.

References:

1. MacLeod, M., Arp, H. P. H., Tekman, M. B., Jahnke, A. (2021) The global threat from plastic pollution, *Science*, 373, 61–65.
2. Chen, G., Yu, X., Rashid, A., Li, C., Widemeyer, M., Liu, L., Liu, B., Wand, Y., Homm, G., Ionescu, E., Shao, T., Weidenkaff, A. (2025) Plasma-enhanced upcycling of mixed plastic waste over $La_{0.6}Ca_{0.4}FeO_{3-\delta}$ nano spheres for co-producing hydrogen and high-value carbon. *Results in Engineering*, 25, 104039.

Experimental and simulation-based investigations into sustainable metal-catalytic plasma etching of silicon using hydrogen

L. Böhm [1,2], N. Reghunath [1], G. Umlauf [2], X. Hu [1], M. Haase [1,2], J. Schuster [1,2]
[1] Center for Micro and Nano Technologies (ZfM), Chemnitz University of Technology, Chemnitz, Germany
[2] Fraunhofer Institute for Electronic Nano Systems (ENAS), Chemnitz, Germany

Abstract:
For many years, the state of the art in deep silicon etching has been to achieve high etch rates while maintaining etch anisotropy through the use of fluorinated chemicals. SF_6 is commonly used to etch silicon. In the well-known Bosch process, C_4F_8 is also used for the necessary passivation step. Consequently, current industrial plasma-etching processes are not sustainable because they employ halogens. These per- and polyfluoroalkyl substances (PFAS), known as "forever chemicals," are environmentally persistent and degrade slowly. These halogens have harmful environmental effects, including ozone depletion and contributions to global warming. To date, there are no halogen-free and sustainable plasma-etching processes, which also poses a challenge for the growing European semiconductor industry. Hydrogen-plasma etching is inspired by the chemical transport of silicon [1]. Therefore we must identify new halogen-free methods for etching silicon with high aspect-ratio features and sufficient uniformity to meet the demands of the chip industry. To facilitate the development of these sustainable processes, atomistic insights into the fundamental elementary reaction mechanisms at the Si surface are crucial. In this work we use density functional theory (DFT) to comprehensively map the reaction energies for hydrogen-etching pathways that are assisted by a metal catalyst. Our calculations show that Ru strongly facilitates H_2 dissociation. The activation barrier on the Ru(001) surface is only 0.12 eV, compared with 0.42 eV on Si. This barrier reduction clearly reflects the strong catalytic role of Ru in facilitating H–H bond cleavage. Parallel to this, experiments are conducted in industrially scalable facilities where a metal is deliberately used as a catalyst for hydrogen-based etching.
Sun and Almquist demonstrated metal-assisted plasma etching using structured, nanometer-thick gold films to catalyze the etching of silicon in an SF_6/O_2 mixed plasma, thereby significantly increasing the etching rate in a selective manner [2]. The results of our studies on etching randomly distributed nanoparticles (diameters up to 100 nm) show anisotropic etching of silicon (see figure 1). In further investigations, defined structures will be selectively deposited onto the silicon surface using various methods. The etching results will be compared with the simulations to identify suitable process windows.

Keywords: plasma-assisted, etching, silicon, sustainable, hydrogen, density functional theory, activation energy, hydrogen-dissociation.

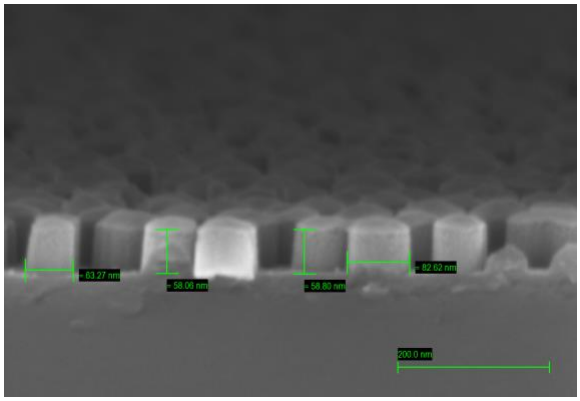

Figure 1: Anisotropic etching of silicon in a hydrogen plasma, with a metal on the surface acting as a catalyst.

References:

1. Vepřek, S., Mareček, V. (1967), The preparation of thin layers of Ge and Si by chemical hydrogen plasma transport, *Solid-State Electronics*, *11* (7), 683-684.
2. Sun, J. B. , Almquist, B. D. (2018), Interfacial Contact is Required for Metal-Assisted Plasma Etching of Silicon, *Advanced Materials Interfaces*, *5* (24), 1800836.

Degradation of Methylene Orange in Aqueous Solution Using Non-Thermal Plasma

T. NGUYEN[1], H. GERARD[1], L. SONHAFOUO MBANTIO[1], G. THOMAS[1], N. CÉDRIC[1].
[1]Institute Jean Lamour - Equipe Plasmas - Procédés - Surfaces – NANCY, France

Abstract:
Water pollution caused by organic dyes from industrial wastewater poses significant environmental challenges. Among various treatment methods, non-thermal plasma (NTP) has emerged as a promising advanced oxidation process due to its ability to generate reactive species capable of degrading organic contaminants efficiently. In this study, we investigate the degradation of Methylene Orange (MO), a model organic dye, in an aqueous solution using a pulsed DC plasma system. The primary objective is to understand the degradation mechanisms and assess the efficiency of this plasma-based treatment.

A pulsed DC plasma reactor was employed to generate reactive oxygen and nitrogen species (RONS), including hydroxyl radicals (•OH), ozone (O_3), and hydrogen peroxide (H_2O_2), which play a crucial role in the oxidation and breakdown of MO molecules [1,2]. The degradation process was analyzed by monitoring the absorbance spectra of MO at different treatment times using UV-Vis spectrophotometry. The effects of key operational parameters, including applied voltage, treatment duration, and initial dye concentration, were systematically studied to determine their influence on the degradation rate. Our results indicate that the MO concentration decreases 100% within 5 minutes of plasma treatment time. Kinetic analysis suggests that the degradation follows a pseudo-first-order reaction model, with the rate constant dependent on the applied voltage and the presence of reactive species. Additionally, the effects of solution pH and conductivity on the degradation efficiency were examined. The results show that an acidic environment enhances the degradation process, likely due to increased formation of hydroxyl radicals. The presence of electrolytes in the solution influences plasma-liquid interactions, affecting the production and diffusion of reactive species.

These findings demonstrate the potential of pulsed DC plasma as an effective method for degrading organic dyes in wastewater treatment applications. The ability of plasma to generate highly reactive species without the need for additional chemical reagents makes it an environmentally friendly alternative. Future work will focus on optimizing the process parameters, scaling up the plasma system, and exploring its application for real industrial wastewater containing a mixture of organic contaminants.

References

1. Guo, He, et al. "Plasma coupled with ultrasonic for degradation of organic pollutants in water: Revealing the generation of free radicals and the dominant degradation pathways." Process Safety and Environmental Protection 192 (2024): 793-802.
2. Tao, Xumei & Yuan, Xinjie & Huang, Liang & Shang, Shuyong & Xu, Dongyan. (2020). Fe-based metal–organic frameworks as heterogeneous catalysts for highly efficient degradation of wastewater in plasma/Fenton-like systems. RSC Advances. 10. 36363-36370. 10.1039/D0RA07402K.

Nanosecond-pulsed plasma bubbles for pollutant and pathogen elimination in water

C.A. Aggelopoulos[1,*], K. Papalexopoulou[1,2], M. Kariofillis[1,3]
[1] Foundation for Research and Technology Hellas, Institute of Chemical Engineering Sciences, (FORTH/ICE-HT), Patras 26504, Greece
[2] University of Patras, Department of Chemistry, Patras 26504, Greece
[3] University of Patras, Department of Physics, Patras 26504, Greece

Abstract:
Water contamination by persistent chemical pollutants and pathogenic microorganisms poses a critical threat to public health, ecosystems, and water security [1, 2]. Among emerging contaminants, per- and polyfluoroalkyl substances (PFAS), such as perfluorooctanoic acid (PFOA) and perfluorooctane sulfonate (PFOS), are of particular concern due to their extreme persistence, resistance to conventional treatment, and tendency to bioaccumulate [3]. In parallel, microbial contamination, represented by Escherichia coli, remains a major sanitation challenge linked to waterborne disease transmission [4]. Innovative treatment approaches capable of simultaneously addressing both chemical and biological contaminants are urgently needed.
This study investigates the use of nanosecond-pulsed plasma bubbles as a versatile and energy-efficient technology for the degradation of PFAS and the inactivation of E. coli in water. A plasma bubble reactor energized by high-voltage nanosecond pulses was developed and optimized to generate intense reactive species directly within the liquid phase. Key operational parameters including treatment time, plasma gas, initial pollutant or bacterial concentration and water matrix, were systematically examined to elucidate their impact on degradation and disinfection performance.
The plasma bubble system demonstrated rapid and effective degradation of PFOA and PFOS, achieving high degradation efficiencies across a wide concentration range and water matrices. Simultaneously, E. coli was efficiently inactivated, highlighting the dual function of the system in chemical and microbial purification. Energy consumption and treatment efficiency were evaluated to identify optimal operating conditions.
Overall, the results establish nanosecond-pulsed plasma bubbles as a promising, environmentally friendly technology for comprehensive water purification, capable of simultaneously eliminating persistent PFAS pollutants and harmful microorganisms.
Keywords: cold atmospheric plasma, plasma bubbles, PFAS, bacteria, wastewater, water sanitation.

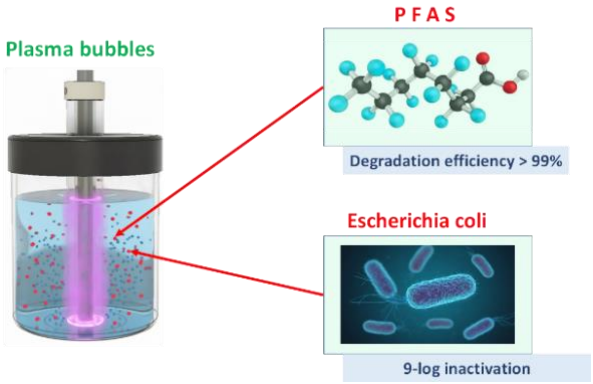

Figure 1: Schematic illustration of the plasma bubble concept for treating PFAS and E.coli contaminated water.

Acknowledgements:
This research was funded by the PRIMA Programme under Grant Agreement No. 2431 (FUSION).

References:

1. Morin-Crini, N., et al., Worldwide cases of water pollution by emerging contaminants: a review. *Environ. Chem. Lett.*, 2022. 20(4): p. 2311-2338.
2. van Elsas, J.D., et al., Survival of Escherichia coli in the environment: fundamental and public health aspects. *ISME J.*, 2010. 5(2): p. 173-183.
3. Aggelopoulos, C.A., Innovations in PFAS remediation: a review on the growing role of cold plasma technology. *Sep. Purif. Technol.*, 2026. 380: p. 135535.
4. Ali, N.M., et al., Impact of Water Pollution on Waterborne Infections: Emphasizing Microbial Contamination and Associated Health Hazards in Humans. *Discov. Water*, 2025. 5(1): p. 19.

Air atmospheric pressure plasma, a green approach for the sanitation of leafy greens vegetables

Zh. Aliyeva [1], T. Maho[1], Ph. Guillot[1], C. Muja[1]
[1] DPHE Laboratory, Toulouse University, INU J.F. Champollion, Place de Verdun, Albi, France

Abstract:
Leafy greens are a fundamental component of a healthy diet, and their global consumption has seen a notable increase in recent years, similar to a concerning rise in foodborne illness outbreaks linked to these products [1]. This significant rise in consumption has also enhanced the challenges in ensuring their microbiological safety, particularly as these minimally processed, ready-to-eat items are susceptible to contamination by human pathogens at various stages of the food production chain. Among these pathogens, *Escherichia coli* is particularly dangerous, posing significant risks, with outbreaks frequently associated with leafy greens. *E. coli* is a Gram-negative bacterium commonly linked to severe foodborne illness, can survive on lettuce surfaces even under refrigeration, and factors like leaf structure and physicochemical interactions influence its persistence on such produce. Consequently, new innovative technologies, like cold plasma, are needed to enhance the decontamination methods and decrease food-borne illnesses. Cold plasma technology, characterized by its ability to generate a diverse of reactive oxygen and nitrogen species, presents a promising non-thermal approach for ensuring food safety and extending shelf life [2]. Reactive compounds produced during plasma generation are primarily responsible for microbial inactivation through oxidative effects on microbial cell surfaces [3].

In this work, we analyze the production of ozone and nitrogen-based species produced by surface dielectric barrier discharges (SDBDs) to identify the transition from an oxygen-dominated to a nitrogen-dominated plasma regime, emphasizing the complex interaction between these reactive components. The experimental setup consisted of an SDBD plasma source coupled to a glass reaction chamber, allowing precise control of the reactive atmospheric environment. Plasma discharges were produced in ambient air using a pulsed generator operating at a fixed frequency of 20 kHz and a duty cycle of 5%, with the applied voltage ranging from 5 to 7 kV.

Glass carriers were employed as an inert reference surface, while romaine lettuce was used as a model fresh produce to assess how this transition affects microbial inactivation efficiency and product quality. This approach enabled a direct comparison between plasma treatment on a natural, complex surface and on a controlled, abiotic surface, providing insight into inactivation performance under different surface conditions. Antimicrobial efficacy testing was conducted against *Escherichia coli* O157:H7 using distinct operating modes that transition based on the operating parameters.

These results emphasize the importance of oxygen- and nitrogen-based species generation in plasma and highlight their significant implications for optimizing atmospheric-pressure plasma applications in food preservation and agriculture.

Acknowledgment:

This work was supported by the Occitanie Region, France.

Keywords: Decontamination, non-thermal process, cold plasma, leafy greens, microbial inactivation

References:

1. Machado-Moreira, B., Richards, K., Burgess, K. M., Abram, F., Brennan, F., Gaffney, M. (2021), Survival of Escherichia coli and Listeria innocua on Lettuce after Irrigation with Contaminated Water in a Temperate Climate, Foods, 10(9), 2072.
2. Ansari, A., Parmar, K., Shah, M. (2022), A comprehensive study on decontamination of food-borne microorganisms by cold plasma, Food Chemistry: Molecular Sciences, 4, 100098.
3. Sezer, B., Sakarya, F. B., Savaş, S., Kuşcu, A., Ceylan, F. D., Montoneri, Ozkan, G. (2025), Impacts of Cold Plasma Treatment on the Food Quality and Safety during Storage, ITU Journal of Food Science and Technology, 3(2), 71-90.

Cold plasma for Food Safety: Process Optimization and Quantification of Reactive Chemical Species for Effective Fungal Inactivation

T. Pushparaj Gandhi[a,*], Reetesh Kumar Gangwar[b], and Shihabudheen M. Maliyekkal[a]
[a] Department of Civil and Environmental Engineering, IIT Tirupati, Tirupati-517619, India
[b] Department of Physics & CAMOST, IIT Tirupati, Tirupati-517619, India
E-mail: Ce22d005@iittp.ac.in (*Presenting author)

Abstract:
Consuming contaminated peanuts and other food crops is a global concern that can pose a threat to humans and other living beings. Among various reported contaminants, mycotoxins such as aflatoxins are of primary concern and are considered Group 1 carcinogens, possessing high thermal stability (237 to 306ºC). Furthermore, the aflatoxin-producing fungi (*Aspergillus flavus* and *Aspergillus parasiticus*) and their spores are highly resistant and difficult to degrade. Therefore, controlling the fungi and the toxins they produce benefits human health and improves crop yield and food security.

Treatment methods, including the use of organic acids, adsorption, biological treatment, heating, and high-pressure processing, help control fungal growth. However, these technologies may compromise food quality, leave residues, produce secondary contamination, and be less effective in degrading spores. Recently, non-thermal plasma has been shown to be effective in controlling these toxins and toxin-producing fungi. The sludge-free process is sustainable and can be operated at atmospheric pressure and temperature. The plasma-generated reactive chemical species (RCS) can effectively kill fungi and fungal spores through various mechanisms, including cell wall and membrane rupture, DNA degradation, lipid peroxidation, and protein damage.

This study investigates the application of cold plasma for the rapid degradation of fungal and aflatoxin contaminants in peanut samples [1]. The cold plasma reactor was optimized via optical imaging, emission spectroscopy, and RCS quantification. Optical imaging revealed a uniform distribution of RCS (OH and N_2 second positive system) across the cold plasma plates. A non-invasive approach combining optical emission spectroscopy, collisional radiative models, and machine learning was employed to tune the RCS and determine the electron temperature and density. Additionally, gas temperature measurements confirmed the non-thermal nature of the plasma.

In addition to examining plasma operating parameters, this study investigates their effects on fungal degradation. The cold plasma reactor effectively degrades fungal spores (initial concentration = 10^5 spores/mL), achieving a 5-log reduction within 5-7 mins of plasma exposure under different experimental conditions. The results also indicate that cold plasma reactor can control fungal growth without compromising the macronutrient content or organoleptic properties of peanuts. Moreover, the study explores the mechanisms underlying fungal degradation in food. Overall, the findings demonstrate that the developed cold plasma reactor is a promising technology for eliminating fungi and fungal toxins in food, such as peanuts, while preserving food quality. The study also examines the influence of factors like electrode-to-sample distance, gas composition, and input power on fungal degradation.

Keywords: Aflatoxins degradation; Fungal removal; Non-thermal plasma; Optical imaging; OES measurement; Peanut quality

Acknowledgement: The authors acknowledge the Anusandhan National Research Foundation (Grant No.: CRG/2023/002553), India, for funding. Mr. Pushparaj Gandhi thanks the Ministry of Education, Government of India, for the Prime Minister's Research Fellowship (PMRF ID: 3201826) for supporting his PhD at IIT Tirupati.

References:

1. T. P. Gandhi, P. S. N. S. R. Srikar, S. M. Allabakshi, R. K. Gangwar, and S. M. Maliyekkal, “Removal of Aflatoxin B1 from solid and liquid matrices using cold atmospheric plasma reactors: Insights into reactor configurations and food quality testing,” *Innov. Food Sci. Emerg. Technol.*, p. 104203, Aug. 2025, doi: 10.1016/j.ifset.2025.104203.

Tribology 2026 Session II. E:
Physics or Chemistry of Tribo-Surfaces / Nanotribology
Sustainable & Green Tribology

Fracture and adhesion of viscoelastic materials

Giuseppe Carbone[1,2,3]
[1] School of Physics Nanjing University of Science and Technology, Nanjing, China
[2] Department of Mechanics Mathematics and Management, Polytechnic University of Bari, Italy
[3] CNR - Institute for Photonics and Nanotechnologies U.O.S. Bari, Italy

Abstract:
Adhesion of viscoelastic materials is a topic of utmost importance in a countless number numerous engineering applications, yet a comprehensive energy-based theoretical framework to fully describe viscoelastic adhesion remains absent from the literature. Observations of phenomena such as hysteretic losses, adhesion hysteresis, and velocity-dependent adhesive strength underline the limitations of existing models, which often rely on scale separation or assume elastic behavior. This lecture introduces a novel theoretical framework for viscoelastic adhesion, addressing these gaps and providing a robust foundation for understanding and engineering viscoelastic materials with tailored adhesive properties.
Our approach moves from the principle of virtual work to take into account the effect of the energy contribution of non-conservative internal viscoelastic stresses in determining the contact and fracture behavior of viscoelastic materials under both steady and unsteady conditions. This framework explains the physical origins of some peculiar phenomena observed in viscoelastic adhesion, including adhesion hysteresis during dynamic contacts [1,2] and delayed fracture [3,4]. The theory predicts key behaviors - such as the velocity dependent enhancement of pull-off forces [5,6,7], adhesion enhancement in unsteady contacts [8], delay time in crack propagation [9]. Notably, the theoretical framework extends beyond existing theories by elucidating the combined effects of bulk viscoelasticity and interfacial adhesion. By addressing the fundamental interplay between viscoelasticity and adhesion, we establish a theoretical foundation that enables a deeper understanding of observed phenomena and guides the engineering of advanced adhesive systems.

Keywords: viscoelasticity, adhesion, fracture, crack propagation, adhesion hysteresis, fracture energy, viscoelastic materials.

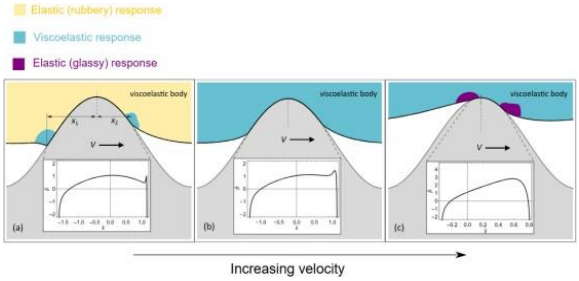

Figure 1: The sliding contact of a viscoelastic material against a moving rigid indenter in presence of adhesion.

References:

1. Li, M., et al. (2019). *Polymer Testing*, 74, 266–273.
2. Ahn, D., & Shull, K. R. (1996). *Macromolecules*, 29 (12), 4381–4390.
3. Skrzeszewska, P. J., et al. (2010). *Macromolecules*, 43(7), 3542–3548.
4. Bonn, D., et al. (1998). *Science*, 280(5361), 265–267.
5. Carbone, G., Mandriota, C., & Menga, N. (2022). *Extreme Mechanics Letters*, 56, 101877.
6. Mandriota, C., Menga, N., & Carbone, G. (2024). *International Journal of Solids and Structures*, 290, 112685.
7. Persson, B. N. J., & Brener, E. A. (2005). Physical Review E, 71(3), 036123.
8. Mandriota, C., Menga, N., & Carbone, G. (2024). *Journal of the Mechanics and Physics of Solids*, 192, 105826.
9. Carbone G., Mandriota C., Menga N., *International Journal of Solids and Fracture*, submitted (2025).

Advancing Lubricant Design with Machine Learning Molecular Dynamics

M. Clelia Righi
Department of Physics and Astronomy, University of Bologna
clelia.righi@unibo.it

Abstract:
Ab initio molecular dynamics (MD) can provide an accurate description of tribochemical reactions [1], but its high computational cost limits the accessible time and length scales. With the introduction of machine-learning potentials (MLPs) in the field of computational tribology [2] this limitation has been overcome, opening many new possibilities for the study of lubricants.
We developed the software "Strategic Configuration Sampling" (SCS) [2] for training accurate MLPs with an active learning approach particularly sutable for tribological systems. SCS automatically generate new systems and make them explore the configuration space thus creating datasets of *ab initio* energies and forces for a large amount of diverse and independent atomic configurations.
ML-MD simulation of monolayers of gallate molecules—which can reduce friction very effectively—allowed us to derive general understanding on the effects of hydrocarbon chain length on the friction coefficient [3,4].

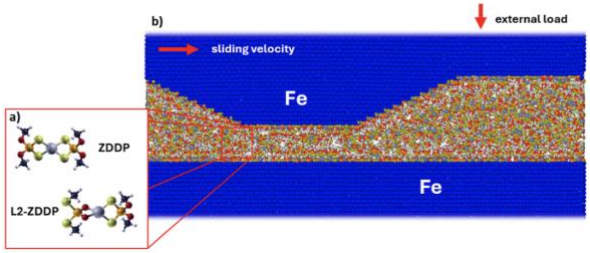

Figure 1: Setup of the ML-MD simulations of ZDDP additives a) at a sliding interface containing a nanoasperity b), adapted from [7]

Thanks to ML-MD we could simulate not only additives, but also the liquid solution where they are solubilized, and mimic in a realistic way the onset of boundary lubrication conditions at nano-asperity contacts [5,6].
ML-MD allowed us to monitor in real time the formation. of the tribofilm from the ZDDP molecules, widely used to reduce wear in severe conditions (Fig.1) [7].
Finally, thanks to combined first principles and ML-MD calculations we predicted that 2D Electrides may present ultralow friction thanks to efficient interlayer electron redistribution [8].

In conclusions, the introduction of MLPs in the field of computational tribology [2] allowed for huge progresses in the simulation of lubricants. The presented examples include the design of efficient lubricant additives and novel 2D materials.

Keywords: machine learning, molecular dynamics, lubricant additives, trobofilms**.**

References:

1. G. Zilibotti, et. al., "Load-induced confinement activates diamond lubrication by water", Phys, Rev. Lett. 111, 146101 (2013).
2. A. Pacini, et. al., "Advancing tribological simulations of carbon-based lubricants with active learning and machine learning molecular dynamics", The European Physical Journal Plus 139, 549 (2024).
3. H.T.T. Ta, et. al., "Probing additives for green lubricants with the aid of machine learning molecular dynamics: The case of gallate molecules for aqueous solutions", Applied Surface Science 695, 162836 (2025).
4. Y. Long, et al., "Reducing friction and wear with alkyl gallate additives in water-based lubricants", Materials Today Nano 30, 100629 (2025)
5. P. Restuccia et. al., "Phosphorus-based lubricant additives on iron with Machine Learning Interatomic Potentials" arXiv:2512.23583 (2025).
6. A. Pacini, et. al, "Unraveling the Complex Dynamics of Plant Derived Additives for Next-Generation Water-Based Lubricants through Machine Learning Atomistic Simulations", submitted (2026).
7. E. Pedretti, et al., "Unraveling the atomistic mechanisms underlying the anti-wear function of the ZDDP Lubricant Additive by Machine-Learning-Informed Molecular Dynamics", submitted (2026).
8. J. Qi, et al. "Interlayer Electron Redistribution Engineering for Ultralow Friction in 2D Electrides", Advanced Functional Materials https://doi.org/10.1002/adfm.202525865 (2025)

Tribological Behavior of 2D MXene-reinforced Polymer and Metal Matrix Composites

M. Marian [1,2,*]
[1] Department of Mechanical and Metallurgical Engineering, School of Engineering, Pontificia Universidad Católica de Chile, Macul, Chile
[2] Institute of Machine Design and Tribology, Leibniz University Hannover, Garbsen, Germany

Abstract:
Two-dimensional (2D) nanomaterials, particularly MXenes, have emerged as highly promising candidates for enhancing the tribological performance of engineering and biomedical systems [1-4]. This contribution presents a unified overview of recent work on $Ti_3C_2T_x$-reinforced composites across polymer and metal matrices, spanning conventional processing and additive manufacturing routes.
Starting from polymer-based systems, $Ti_3C_2T_x$-reinforced UHMWPE nanocomposites were fabricated via compression molding, demonstrating significant reductions in friction and wear—up to 19% and 44%, respectively—without compromising biocompatibility . The improvements are attributed to the formation of low-shear transfer films and favorable surface interactions under synovial lubrication. [5]
Extending this concept to metallic systems, $Ti_3C_2T_x$-reinforced CoCrMo and 316L stainless steel matrix composites were produced via laser powder bed fusion. Structural integrity of the MXene phase was retained during processing, while mechanical properties such as hardness and surface characteristics were tailored through controlled reinforcement. Bio-tribological testing revealed substantial wear reductions of up to 78% in CoCrMo-based systems and notable improvements in 316L composites, particularly at optimized MXene contents. [6, 7]
Across all material classes, the results highlight the versatility of MXenes as reinforcing phases, enabling enhanced interfacial interactions, tribofilm formation, and lubrication effects under both dry and physiological conditions. The combined findings demonstrate a consistent pathway from polymer to metal systems, underscoring the potential of MXene-reinforced composites for next-generation, high-performance, and biotribologically optimized components..

Keywords: 2D materials, MXenes, $Ti_3C_2T_x$, Bio-tribology, Additive manufacturing, Laser powder bed fusion, UHMWPE, CoCrMo, 316L, Biomedical implant

References:

1. M. Marian, D. Berman, D. Nečas, N. Emami, A. Ruggiero, A. Rosenkranz: Roadmap for 2D Materials in Biotribological/Biomedical Applications – A Review, Advances in Colloid and Interface Science, 307, 2022, 102747, DOI: 10.1016/j.cis.2022.102747
2. S. Ramteke, M. Walczak, M. De Stefano, A. Ruggiero, A. Rosenkranz, M. Marian: 2D Materials for Tribo-Corrosion and -Oxidation Protection: A Review , Advances in Colloids and Interface Science, 331, 2024, 103243, DOI: 10.1016/j.cis.2024.103243
3. S. Ramteke, S. Dwivedi, J. Ramos Grez, D. Zambrano, A. Rosenkranz, M. Marian: Laser Powder Bed Fusion of WS_2/316L Stainless Steel Nanocomposites for an Enhanced Mechanical and Tribological Performance, Langmuir, 42, 2026, 5, 4254-4268, DOI: 10.1021/acs.langmuir.5c06298
4. S. Ramteke, J. Ramos Grez, M. Marian: Enhanced mechanical and tribological performance of additively manufactured 316L steel by MoS_2-reinforcement, Materials & Design, 249, 2025, 113562, DOI: 10.1016/j.matdes.2024.113562
5. B. Rothammer, K. Feile, S. Werner, R. Frank, M. Bartz, S. Wartzack, D. Schubert, D. Drummer, R. Detsch, B. Wang, A. Rosenkranz, M. Marian: Ti3C2Tx-UHMWPE nanocomposites - Towards an enhanced wear-resistance of biomedical implants, Journal of Biomedical Materials Research Part A, 113, 2024, 1, DOI: 10.1002/jbm.a.37819
6. S. Ramteke, J. Ramos Grez, A. Rosenkranz, M. Marian: Additively manufactured 316L steel reinforced by multi-layer Ti3C2Tx for enhanced mechanical and bio-tribological performance, Surface & Coatings Technology, 511, 2025, 132321, DOI: 10.1016/j.surfcoat.2025.132321
7. S. Ramteke, D. Zambrano, J. Ramos Grez, A. Rosenkranz, M. Marian: Mechanical and Bio-tribological Behavior of Ti3C2Tx-reinforced CoCrMo Composites Fabricated by Additive Manufacturing, Tribology Letters, 73, 2025, 94, DOI: 10.1007/s11249-025-02030-y

Ice-Rubber Friction Mechanisms across Scales

A. Dalavale Kaiser Pinto [1], D. Mazuyer [1], J. Cayer-Barrioz [1,*]
[1] LTDS, CNRS UMR5513, Ecole centrale de Lyon, France

Abstract:
The interaction between rubber and ice is pivotal in defining safety, performance, and energy efficiency across various technological applications, such as automotive tires, winter sports equipment, and aerospace operations in cold environments.
This talk provides a comprehensive investigation of friction and adhesion phenomena at the rubber-ice interface, systematically elucidating the interplay between environmental temperature, sliding velocity, and rubber mechanical properties across scales. The filled rubbers selected for this work were representative of real commercial tires. Their mechanical properties covered a broad spectrum of viscoelasticity, characterized by glass transition temperatures ranging from−10◦C to−58°C and shear moduli from 1 MPa to 8 MPa. An advanced tribometer system was developed, featuring significantly enhanced temperature control, insulation, and stability, achieving environmental temperatures down to−30◦C.
Friction measurements conducted under pure sliding conditions revealed a highly non-linear relationship between interfacial shear stress and sliding velocity. For rubbers in the rubbery state, the shear stress response typically follows a bell-shaped curve. In the low-velocity regime, viscoelastic-adhesion mechanisms dominate, strongly influenced by the material proximity to its glass transition temperature. Conversely, the high-velocity regime is primarily governed by thermal effects, such as frictional heating and potential localized melting of the ice surface, which collectively reduce friction.
These findings demonstrate that friction at the rubber-ice interface emerges from the interplay of adhesion, viscoelasticity, and thermal processes, further complicated by interfacial phenomena like frost formation, ice fragmentation, and transient local melting. A comprehensive friction model was proposed to integrate these multi-scale contributions for rubbery-state elastomers under pure sliding conditions (see Fig. 1).
For materials operating near or below the glass transition temperature, more complex behaviours—such as the emergence of dual friction peaks—were observed. These phenomena reflect transitions between glassy and rubbery mechanical responses.
To more accurately replicate real-world operating conditions, experiments combining rolling and sliding motions were also performed. A significant discovery was the identification of a universal scaling relationship for dissipated power, which adheres to a power-law dependence on kinematic length, regardless of material properties or temperature, revealing fundamental similarities in dissipation mechanisms across diverse contact conditions.

Keywords: elastomer, ice, friction.

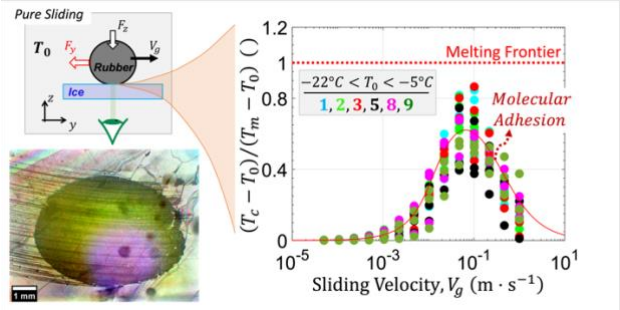

Figure 1: Friction mechanisms between ice and rubber in a sliding interface. In situ in operando real contact area visualization was performed simultaneously to measurements of contacts forces under controlled contact kinematics at low temperatures. The model shown here combines a thermal description of the interface at the macroscopic (contact) scale with a viscoelastic adhesive framework including bulk and interfacial dissipation through the dynamics of junctions resulting from molecular adhesion between elastomer chains and ice surface.

References:

1. Hemette, S., Cayer-Barrioz, J., Mazuyer, D. (2018) Friction setup and real-time insights of the contact under controlled cold environment: The KORI tribometer for rubber-ice contact application, *Review of Scientific Instruments*, 89, 123903.
2. Dalavale Kaiser Pinto, A. (2025) Friction of ice/rubber interface: Thermal, adhesive and viscoelastic contributions, *PhD thesis,* Ecole centrale de Lyon, 2025ECDL0027.
3. Dalavale Kaiser Pinto, A., Mazuyer, D., Cayer-Barrioz, J. (2026), Ice-rubber friction mechanisms across scales, *Soft Matter*., 22, 2514 – 2525.

Molecular dynamic characterization of surface active additives – sorption, solubility and diffusion

K. Falk[1*], L. Kruse[1], S. Peeters[1], G.Moras[1] and M. Moseler[1,2]
[1] MicroTribology Center µTC, Fraunhofer IWM, Freiburg, Germany
[2] Institute of Physics, University of Freiburg, Germany

Abstract:
The use of surface-active additives that form protective layers on tribological surfaces is an established approach to reduce friction and wear in the mixed and boundary lubrication regime: These layers prevent the direct contact of the substrates in asperity contact zones, where the lubricant is completely squeezed out. The effectiveness of the protective film is expected to depend on its structure and stability, which in turn depends on several factors, including the molecular structure of the additive, the additive concentration in the lubricant, as well as the pressure acting on the lubrication gap.[1] However, quantitative correlations between the tribological properties of the friction modifier films and the additive's molecular structure, which would allow a predictive modelling and targeted additive design, are missing.
In this work, the behavior of surface-active additives is examined on an atomistic level using molecular dynamics simulations. The final aim is to quantify all properties which are necessary ingredients for modelling the film building process on a continuum scale. These properties include diffusion coefficients of the additives in the oil, free energy of adsorption of additives on surfaces for different film densities, as well as ad- and desorption rates. In particular, the alchemic thermodynamic integration method [2] is used to calculate free energy differences between relevant equilibrium states (see example in Figure 1). The latter allows to quantify, for example, adsorption strength and solubility of specific additive/base-oil/surface combinations. Here, different combinations of surface-active additives (1-octanol and octylamine and tributyl phosphate), base-oils (PAO4 and DITA) and oxide surfaces (FeO and CuO) are considered and compared systematically.

Keywords: lubricant additives, friction modifyers, diffusion, physisorption, free energy calculation, adsorption and desorption rates, molecular dynamic simulations

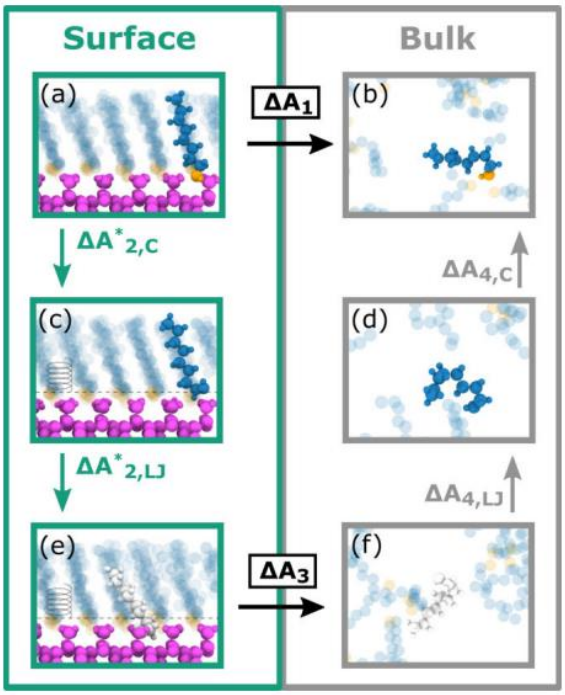

Figure 1: Alchemic thermodynamic cycle used to calculate the free energy of desorption of a 1-octanol molecule from a dense surface film into the lubricant bulk (base oil not displayed for clarity): The intermolecular interactions of the studied molecule with its environment (additive film on surface and lubricant bulk, respectively) are gradually turned off/on. For numerical reasons, the Lennard-Jones and Coulomb parts of the interaction are treated subsequently (blue: no Coulomb interactions; white: neither Coulomb nor Lennard-Jones interactions).

References:

1. H. Spikes. Friction Modifier Additives. *Tribology Letters* 60, 1 (2015)
2. C. Chipot and A. Pohorille. *Free Energy Calculations.* Volume 1. Springer Series in Chemical Physics. Springer Berlin Heidelberg, 2007, 1.

Energy Fingerprints of Wear: Decoupling Friction Instability from Thermal Dissipation in Reciprocating Tribotests

J. Qin *, S. Zhao, D. Lindell
ABB Corporate Research Center, Västerås, Sweden

Abstract:
Study of friction behavior between copper-graphite composites and metal surface over ultra-long reciprocating sliding distances is crucial in gaining in-depth understanding of progressive changes in similar type of tribological system. Accelerating/decelerating cycles close to the ends of strokes are major contributor to stick-slip events that are closely related to wear. Wear mainly occurs on the graphite composite side due to large difference in mechanical properties.

Wear models based on total dissipated energy struggle with precision because a significant portion of work injected into the tribological system is converted into heat rather than material removal.[1] MD simulation shows that in sliding contacts roughly 95% of energy is dissipated through heat.[2] Only a small fraction of frictional energy is dissipated mechanically.[3] Better understanding wear mechanism through energy approach requires accurate computation of the energy that is exclusively related to wear events. Rymuza [4] stated that estimation of mechanically dissipated energy is a rather difficult task, in his famous paper proposing the concept of coefficient of friction losses (CFL). In reciprocating sliding, the instability events captured by noisy spikes may be attributed to wear related activities, while the steady-state Coulomb friction mainly contributes to the heat generation.

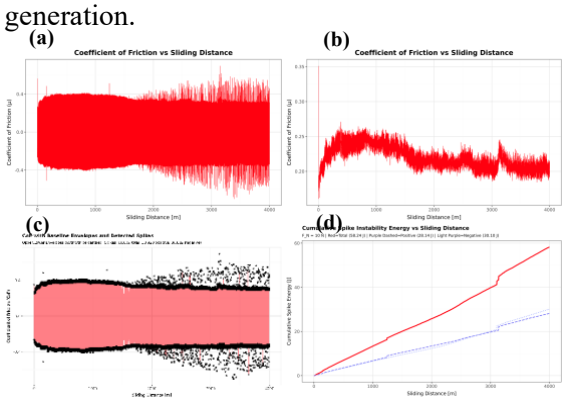

Figure 1: (a) Typical reciprocating raw data of coefficient of friction vs. distance, (b) Filtered top half curve, (c) Baseline and spikes identification, (d) Cumulative instability energy computed over the entire sliding distance.

$$E_{spike} = \int_{s_{start}}^{s_{end}} (CoF(s)_{raw} - CoF(s)_{baseline}) \cdot F_N \cdot ds \qquad (1)$$

Stochastic spikes are recorded in the unprocessed tribotest data. **(Figure 1a)** The raw data curves are often smoothened since majority of tribological studies deal with average values of coefficient of friction and the noise information are overlooked. **(Figure 1b)** In fact, small spikes have shown up in the early cycles. **(Figure 1c)** Onset of the significant spikes occurs after about 1-2 km of sliding, so this phenomenon can be missed if the cycle number is not high enough.

The instability energy is calculated by integrating the area under spikes and subsequently subtracting the area under the baseline using equation (1), where F_N is the normal force, ds is incremental distance. **(Figure 1d)** Instability energy of 60 long-distance tribotests using same test parameters but with different metal surfaces casually correlates with wear volume following a moderate monotonic trend. **(Figure 2a)** A threshold energy obtained by hockeystick fitting **(Figure 2b)** defines the transition between mild and severe wear regimes which provides a powerful indicator for wear prevention and remaining life prediction for engineers.

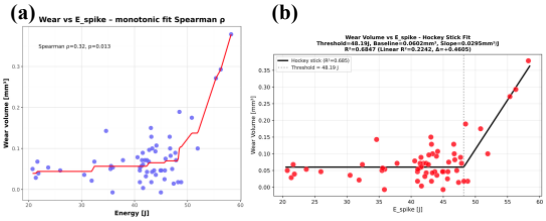

Figure 2. (a) Monotonic (b) Hockeystick correlation between wear and instability energy.

Keywords: reciprocating, tribotest, instability energy, wear prediction, graphite lubrication

References:

1. Amiri, M., Khonsari, M. M. (2010) On the thermodynamics of friction and wear-A review, *Entropy*, 12, 1021-1049.
2. Yin, Z., Wu, H., Zhang, G., Mu, C., Bai, L. (2022) Wear Estimation of DLC Films Based on Energy-Dissipation Analysis: A Molecular Dynamics Study, *Materials*, 15, 893.
3. Chen, Q, Yi, D. Y. (2005) A computational study of frictional heating and energy conversion during sliding processes, *Wear*, 259, 1382-1391.
4. Rymuza, Z. (1996) Energy concept of the coefficient of friction, *Wear*, 15, 187-196.

Tribological Performance of Contaminated Grease: Three-Body Contact and Wear–Pitting Characterization

J.H. Horng [1,2], T.N. Ta [3,*], S.J. Liao [4], C.C. Wei [4]
[1] Innovation Headquarters, Cheng Kung University, Tainan, Taiwan
[2] International Master's Program in Interdisciplinary Sustainability Studies, Cheng Kung University, Tainan, Taiwan
[3] Department of Mechanical Engineering, Chienkuo Technology University, Changhua, Taiwan
[4] Department of Power Mechanical Engineering, National Formosa University, Yunlin, Taiwan

Abstract:
Grease is widely used to lubricate transmission elements; however, in real service, these components may operate in dusty and humid environments where particle and water contamination is unavoidable and can accelerate wear and reduce service life. This study investigates the effects of two common environmental contaminants, including dust particles (silicon dioxide, SiO_2) and water content, on the tribological performance of lithium-based grease. To simulate practical industrial operating conditions, grease samples with varying concentrations of SiO_2 particles and water are prepared and evaluated under three-body contact conditions. Tribological behavior is assessed using a four-ball wear tester by measuring the friction coefficient, oil temperature, pitting area, and wear scar diameter. The results demonstrate that, regardless of water content, increasing SiO_2 concentration led to higher wear growth rates during both the running-in and steady-state stages. Similarly, the pitting growth rates increase with SiO_2 concentration under all water conditions. The average friction coefficient and its variability rise with increasing particle contamination (Figure 1), and wear scar diameter also increases with higher particle content. In contrast, a moderate water content reduces the wear scar diameter, whereas excessive water levels cause it to increase again (Figure 2). Based on these results, three-dimensional wear and pitting performance surfaces are established as functions of SiO_2 particle and water concentrations. By incorporating the combined effects of dust and moisture contamination, this work provides a practical framework for predicting the service life of grease-lubricated components under real-world environmental exposure.

Keywords: grease, wear, total acid number, water content, particles, friction, pitting

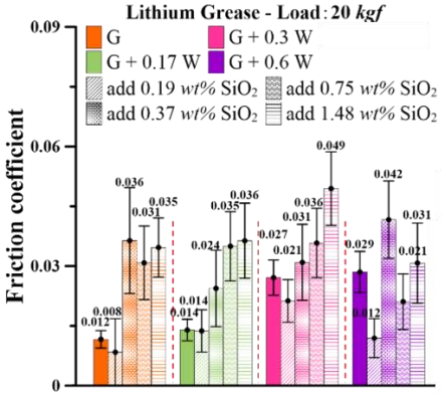

Figure 1: Figure illustrates the variation of friction coefficient with particle and water concentrations. Overall, the friction coefficient increases with SiO_2 concentration, indicating that particle contamination is the dominant factor influencing friction through three-body abrasion.

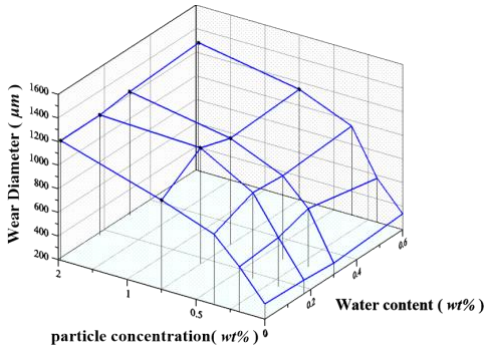

Figure 2: Variation of wear scar diameter with SiO_2 particle concentration and water content.

References:

1. Chen, Y.Y., Horng, J.H. (2024) Investigation of lubricant viscosity and third-particle contribution to contact behavior in dry andlubricated three-body contact conditions, *Front. Mech. Eng.,* 10, 1390335.
2. Horng, J.H., Ta, T.N., Kuo, C.W., Liao, S.J., Chen, Y.Y. (2025), Development of wear and pitting curves with vibration analysis for lubricating grease under contamination conditions, *Wear*, 560-561, 205625.

Enhancement of Wear Resistance and Cooling Efficiency of Additively Manufactured Nylon Gears

C. He, W. Li*, A. Daman, Z. Peng
School of Mechanical & Manufacturing Engineering, UNSW Sydney, Sydney, Australia
*corresponding author: wenhan.li@student.unsw.edu.au

Abstract:
This paper leverages the advantages of additive manufacturing (AM) technology in nylon gear design and fabrication to propose a new gear design that enhances wear performance through a passive cooling strategy. Fused deposition modelling (FDM)[1,2] was employed to fabricate both conventional nylon gears and a modified version featuring a fan structure integrated into the gear body during the design phase. During the gear testing in a spur gearbox rig, measurements of surface roughness, tooth profile, and temperature were recorded to investigate gear wear progression and temperature. These data were used to assess the wear performance and convective cooling effect provided by the gear design incorporating a fan structure. The following results have been obtained under the same operating conditions and in comparison to the FDM nylon gears without the fan structure[3]. The surface roughness of FDM nylon gears with the fan structure decreased slowly, likely due to their low wear rate. The wear depth (Figure 1) and the tooth profile deviation of the gear with the fan are smaller than those of the conventional nylon gears without the fan structure. The gear with the fan structure experienced a lower surface temperature during the test under the same operating conditions. The results demonstrate that the gear with the integrated fan structure exhibited greater wear resistance and cooling efficiency than conventional FDM-fabricated nylon gears.

Keywords: Fused deposition modelling (FDM); Nylon gear; Surface roughness; Tooth profile deviation; Wear depth.

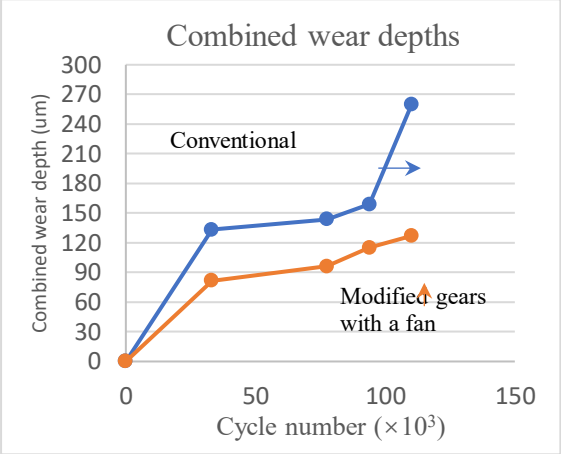

Figure 1: Combined wear depth comparison of conventional FDM-made nylon gears in blue and the gears with the fan structure in orange.

References:

1. Mohamed. O.A., Masood. S.H., Bhowmik, J.L. (2015), Optimization of fused deposition modeling process parameters: a review of current research and future prospects, *Adv. Manuf.*, 3, 42-53.
2. Zhang, Y., Purssell, C., Mao, K., Leigh, S. (2020), A physical investigation of wear and thermal characteristics of 3D printed nylon spur gears, *Tribology International*, 141, 105953.
3. Li, W., Daman, A. A. A., Smith, W., Zhu, H., Cui, S., Borghesani, P., Peng, Z. (2025), Wear performance and wear monitoring of nylon gears made using conventional and additive manufacturing techniques, *Journal of Dynamics, Monitoring and Diagnostics,* 4(2), 101–110.

Solid particle erosion behavior of cold-rolled austenitic stainless steels under Martian regolith simulant

M. Gragnanini [1*], A. Fortini [1], N. Zanini [1], A. Suman [1], M. Pierret [2]
[1] Department of Engineering (DE), University of Ferrara, Via Saragat 1, 44122 Ferrara (Italy)
[2] ISAE supméca Institut supérieur de mécanique de Paris, 3 rue Fernand Hainaut, Saint-Ouen 93407 (France)

Abstract:
Solid particle erosion (SPE) is a critical degradation mechanism for metallic components exposed to high-velocity particulate environments, resulting in progressive material removal from repeated particle impacts. In terrestrial applications, SPE affects pipeline systems, turbomachinery and power generation equipment, while extraterrestrial exploration introduces new challenges where component exposure occurs under unique environmental conditions. Understanding the interplay between microstructure, mechanical properties, and erosion resistance is essential for material selection in both conventional and space applications. This study investigates the SPE resistance of cold-rolled AISI 316L and 310 austenitic stainless steels subjected to impact by MGS-1 Martian regolith simulant. Unlike conventional erosion studies, this work evaluates the tribological behavior under extraterrestrial-relevant conditions and examines the role of strain-induced martensitic transformation in erosion mechanisms. Erosion tests were conducted according to ASTM G76 standard in a purpose-built test rig at impact velocities of 23 m/s and 36 m/s across five impingement angles (15°, 30°, 45°, 60°, 90°). The cold-rolled microstructures were characterized via optical (OM) and scanning electron (SEM) microscopy. Post-erosion analysis included mass loss quantification, surface profilometry, and X-ray diffraction (XRD) to detect phase transformations. XRD analysis revealed distinct differences in strain-induced martensitic transformation between the two alloys. The 316L steel, with lower austenite stability, exhibited significant martensite formation during erosive impact, while the 310 alloy, stabilized by higher Ni and Cr content, showed limited transformation. These microstructural responses correlated with differences in erosion resistance, surface damage morphology and material removal mechanisms. The findings demonstrate that material selection for extraterrestrial applications cannot rely solely on terrestrial erosion data, as both erodent characteristics and strain-induced phase transformations significantly influence tribological performance under simulated Martian conditions.

Keywords: solid particle erosion, austenitic stainless steels, strain-induced martensitic transformation, Martian regolith simulant.

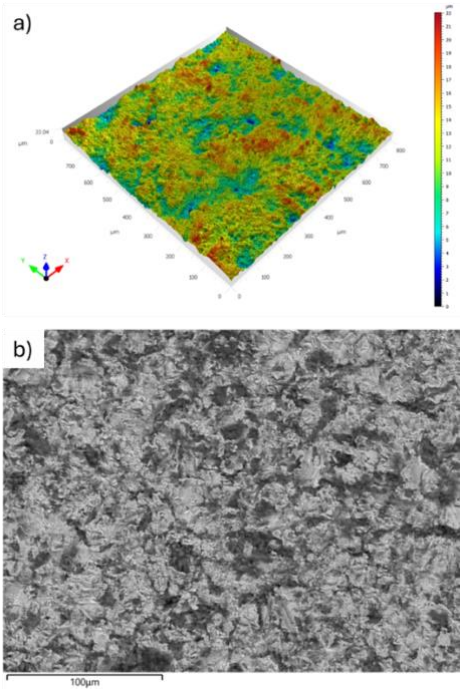

Figure 1: Erosion damage on cold-rolled austenitic stainless steel impacted by MGS-1 Martian regolith simulant: (a) optical profilometry 3D view of the erosion craterand (b) SEM image of the wear damage.

References:

1. Tarodiya R., Levy A. (2021), Surface erosion due to particle-surface interactions - A review, *Powder Technol*., 387, 527-559.
2. Fouchal Y., Ramirez R., Beloreshka M., Plis E.A. (2024), Comparative Evaluation of Spacecraft Materials Properties Under Simulated and True Space Environments, *J. Astronaut. Sci., 71*, 53.
3. Yoon-Seok L., Kazuki I., Mitsuhiro O. (2018), Influence of Strain Induced Martensite Formation of Austenitic Stainless Steel on Wear Properties, *Metals and Mat. Int.*, 25:705-712.

Study on In Situ Damage Evaluation in Rolling Friction Using Acoustic Emission Sensing

Y. Hirai [1,*], A. Hase [1,2]
[1] Graduate School of Engineering, Saitama Institute of Technology, Saitama, Japan
[2] Institute of Physical and Chemical Research (RIKEN), Saitama, Japan

Abstract:
Friction reduction mechanisms based on rolling, such as bearings and ball screws, are widely used in industrial machinery. However, damage to these components can lead to energy loss, positioning errors, and catastrophic accidents. Although diagnostic techniques using vibration and sound sensing are common, they are known to have limitations in sensitivity. Therefore, this study investigates friction reduction mechanisms using acoustic emission (AE) sensing, which can detect minute deformations, cracks, and early-stage damage [1]. Experiments were conducted using a pin-on-block-type friction and wear tester. Comparative tests involved two types of pins (stainless steel and aluminum) and four types of balls (steel, aluminum, alumina, and polyacetal) under two different load conditions. Furthermore, in situ observations were incorporated into AE sensing to monitor the real-time friction state and correlate it with the AE signals.
Figure 1 shows the results of a surface observation on a stainless steel block with a steel ball inserted between the block and a pin. Significant damage is visible on the surface of the block. Figure 2 presents the frequency analysis results of the AE signal corresponding to the experiment in Figure 1. Previous studies have investigated differences in AE signal characteristics between normal and abnormal rolling friction conditions [2]. Figure 2 shows that the characteristics match in both frequency ranges, which is consistent with the surface observation results in Figure 1.
Figure 3 shows the results of a detailed frequency analysis within the abnormal range conducted over a short period. AE extraction locations were selected from ranges showing no significant characteristics. The results in Figures 1 and 2 correspond to the leftmost bar in Figure 3. These results confirm that the steel ball combination was significantly damaged within the short time range. These experiments revealed the potential for real-time damage diagnosis using AE sensing. Furthermore, the possibility of diagnosing even minor damage by performing a detailed analysis during steady-state operation was revealed.

Keywords: friction, wear, acoustic emission, in situ measurement, frequency analysis, rolling bearing, ball screw, visualization.

Figure 1: The friction surface of the block after the experiment with a steel ball interposed between a stainless steel pin and block (normal load: 25 N).

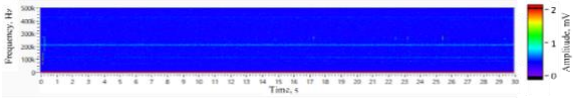

Figure 2: Frequency analysis (STFT) results show the AE signal waveform obtained by the experiment in Figure 1 for the pin side.

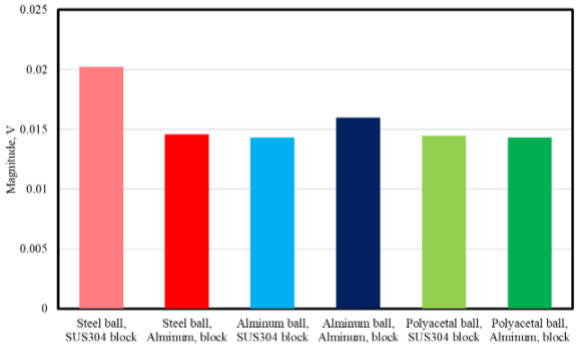

Figure 3: Comparison of the magnitude of the AE signals for different material combinations.

References:

1. Mukai, Y., Hase, A. (2025) Relationship between Acoustic Emission Signals and Surface Conditions in Rolling Contact Fatigue Tests, *The 9th Edition of the Surfaces, Interfaces and Coatings Technologies - SICT2025 International Conference Book of Abstracts*, Albufeira, p.63.
2. Hase, A. (2020), Early Detection and Identification of Fatigue Damage in Thrust Ball Bearings by an Acoustic Emission Technique, *Lubricants*, 8, 37.

Estimations of wear scar volumes based on profile measurements

P. Pawlus [1*], S. Woś [1], R. Reizer [2]
[1] Faculty of Mechanical Engineering, Rzeszow University of Technology, Rzeszow, Poland
[2] Faculty of Exact and Technical Sciences, University of Rzeszow, Rzeszow, Poland

Abstract:
The aim of wear tests is to determine the amount of material removed during a specified time period. Wear amount should be determined precisely. However, wear measurement methods are sensitive to errors [1, 2]. Gravimetric method is one of the simplest ways to measure wear. The mass loss is converted to wear volume. However, this method has some disadvantages, for example is difficult to use for for very low wear values and when both wear removal and plastic deformation occur. The profilometric method seems to be better alternative, especially recently, when areal surface topography measurement is common. This work is concerned with measuring the wear scars after the test using profilometric method. The following configurations were considered: reciprocating ball-on-flat tests, abrasive resistance tests and scratch tests. In those cases, wear of samples were studied. The measurement of the wear volume of balls employed as a counter sample in reciprocating sliding tests was also analysed. Possible errors in wear measurements were studied. Areal measurements of wear volumes were treated as reference data. However, not always they can be applied. Estimations of wear scar volumes based on profile measurements will be discussed in this article.
In the oscillating ball-on-flat configuration for strokes below 2.5 mm the measurement of three profiles perpendicular to the wear scar on flat sample in its central part and near the round side areas ensures results close to those obtained after areal surface topography measurement.
Ensuring wear resistance of products using wear resistance testing of materials by friction against loosely fixed abrasive particles is common in various disciplines including material engineering. Wear resistance of samples (Figure 1a) is typically obtained using gravimetric method. More information can be obtained from areal surface topography measurement. However, accurate results can be also obtained by measuring only few profiles.
The scratch test consists of pressing a diamond stylus onto the surface, and moving the sample at a constant speed. When a constant normal load was applied the measurements of few profiles gave the results close to those obtained using areal surface topography measurement of sample (Figure 1b).
It is possible to accurately determine wear volume of ball employed as counter sample in reciprocating sliding tests by measuring the dimensions of wear scars and performing one additional profile measurement at the central section of the wear track perpendicular to the sliding direction.

Keywords: volumetric wear, wear scar, wear measurement accuracy, profilometric method, reciprocating sliding, ball-on-flat test, abrasive resistance test, scratch test, ball wear volume.

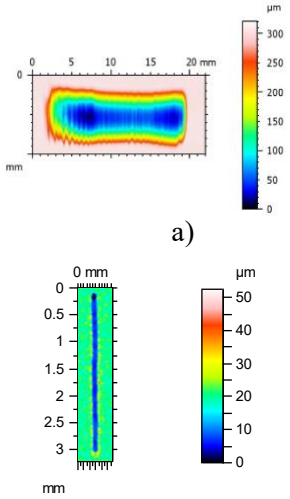

Figure 1: Contour plots of samples after abrasive resistance tests (a) and scratch tests (b)

References:

1. Blau, P.J. (2017) Lessons learned from the test-to-test variability of different types of wear data, *Wear*, 376–377, 1830-1840.
2. Maculotti, G., Goti, G., Genta, G., Mazza, L., Galetto, M. (2022) Uncertainty-based comparison of conventional and surface topography-based methods for wear volume evaluation in pin-on-disc tribological test, *Tribol. Int.*, 165,107260.

From damaging to protective oxidation: high-temperature friction and wear regimes in binder-modified cemented carbides and cermets

S. Tarancón[1]*, E. Tejado[1], J.Y. Pastor[1], B. Ferrari[2], A.J. Sanchez-Herencia[2], Tomas Polcar[3]
[1]Centro de Investigación en Materiales Estructurales (CIME)-Departamento de Ciencia de Materiales, Universidad Politécnica de Madrid, C/Profesor Aranguren s/n, 28040 Madrid, Spain
[2]Instituto de Cerámica y Vidrio, CSIC, Calle Kelsen 5, Madrid, Spain
[3]Department of Control Engineering, Faculty of Electrical Engineering, Czech Technical University in Prague, Technicka 2, 16627 Prague 6, Czech Republic.
*sandra.tarancon@upm.es

Abstract:
Predicting the operational lifespan of hard cutting-tool materials requires evaluating their tribological response under realistic thermal and mechanical conditions, where surface chemistry can change rapidly and significantly. Oxidation at high temperatures may either stabilise sliding by forming protective, shearable layers or, alternatively, speed up degradation by producing brittle, poorly adherent oxides that weaken load-bearing capacity. In this work, the role of oxide formation as a key factor in high-temperature friction and wear is systematically examined for binder-modified cemented carbides and a cermet produced by colloidal processing: WC–12Co (reference), WC–FeNi, and Ti(C,N)–FeNi.

Dry sliding ball-on-disc tests were performed against an Al_2O_3 counterbody in an oxidising atmosphere from room temperature up to 600 °C using a high-temperature tribometer. Experiments were conducted at 15 N at room temperature and 10 N at elevated temperatures, with a sliding speed of 10 cm s^{-1} and a total sliding distance of approximately 400 m. The temperature-dependent evolution of friction and wear was analysed alongside post-test surface and debris characterisation, allowing for a direct correlation between oxide chemistry and the dominant wear mechanisms.

At room temperature, all three compositions showed similar wear rates, while WC–FeNi achieved the lowest coefficient of friction, surpassing the WC–12Co reference ($\mu = 0.692$). When the temperature increased to approximately 200 °C, friction coefficients and wear rates rose for all materials, aligning with the onset of oxidation and increased surface roughness, which alters asperity-level contact conditions and encourages more severe third-body abrasion.

Above approximately 200 °C, distinct oxidation-controlled regimes were identified. In these regimes, tribological performance became less influenced by the as-processed microstructure and more by (i) the chemical nature of the oxides formed on both binder and ceramic phases, (ii) their mechanical integrity and adherence, and (iii) their retention within the contact as transient tribofilms. For the 400–600 °C range, the materials exhibited composition-dependent, non-monotonic ("anomalous") friction–wear responses closely linked to oxidation pathways involving tungsten-, iron- and titanium-based oxides. Depending on the composition, some oxides acted as transient, shearable layers that reduced interfacial shear strength and stabilized sliding (tribological "self-organisation"), while others caused surface embrittlement, cracking/spallation of oxidised zones, and increased material removal. Therefore, the competition between protective and damaging oxides determined whether friction and wear were stabilised or intensified.

SEM–EDX and Raman analyses of the wear tracks confirmed the coexistence of abrasive, adhesive, and oxidative wear mechanisms, with strongly temperature-dependent relative contributions. Raman identification of oxide species supported the mechanistic interpretation of oxidation-driven transitions, linking changes in oxide chemistry to observed shifts in friction levels and wear severity. Overall, the results demonstrate that thermally induced oxide formation becomes the primary control parameter for friction and wear at high temperatures in these cutting-tool materials. Importantly, tailoring binder chemistry (Co vs FeNi) and ceramic phase constitution (WC vs Ti(C,N)) provides a viable design pathway to bias oxidation towards more protective tribofilms and improved tribological stability, enhancing performance in high-temperature cutting-related environments.

Keywords: high-temperature tribology; cemented carbides; cermets; oxidation; tribofilm; friction coefficient; wear mechanisms; ball-on-disc.

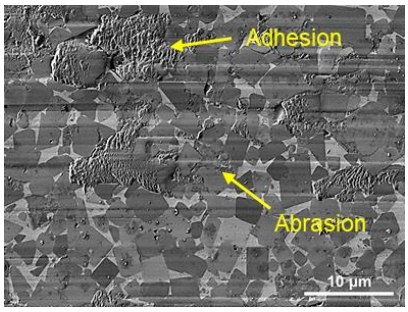

Figure 1: SEM detailed images of wear tracks/footprints with indicative wear mechanisms (abrasive/adhesive/oxidative) as a function of temperature and composition.

References:

1. R. Harouz, S. Boudebane, A. Lakehal, O. Derdy, and H. M. Montrieux, “Investigation of the tribological behaviour of WC/TiC based cermets in contact with Al2O3 alumina under high temperature,” J Mech Behav Mater, vol. 27, no. 1–2, Apr. 2018.
2. F. Cheng, J. Lin, and Y. Liang, “Friction and wear properties of a high Nb-containing TiAl alloy against WC-8Co, Si3N4, and GCr15 in an unlubricated contact,” Intermetallics (Barking), vol. 106, pp. 7–12, Mar. 2019.

A novel approach based on Greenwood-Williamson theory for the estimation of tribocorrosive wear

M. De Stefano[1*], A. Ruggiero[1]
[1]Department of Industrial Engineering, University of Salerno, Via Giovanni Paolo II, nr. 132, 84084 Fisciano, Italy
*mardestefano@unisa.it

Abstract:
Tribocorrosion is defined as the event involving the synergistic action of mechanical wear and corrosion [1]. It is particularly diffused in engineering fields such as biomedical, transportation and marine [2]. In this regard, the presence of oxygen and oxidizing species coupled with friction boosts the material loss more than the simple sum of both. In any case, that synergy can act positively or negatively, determining in the last occurrence a beneficial effect. The topic is constantly investigated from scientific community. Experimentally speaking, via sophisticated electrochemical techniques like voltammetry and impedance spectroscopy. Numerically, instead, by analytical models, most of them at macroscopic level. Indeed, the massive number of factors affecting tribocorrosion makes the theoretical dissertation complex, pushing the researchers towards empirical formula. In this regard, the work aims to propose a model based on the concept of the real contact area (RCA). More in details, the approach adopts the common theory provided by Greenwood-Williamson [3] inserted thus into tribocorrosion framework (Figure 1). Consequently, the kinetics of repassivation of oxide layer was also taken into account. Moreover, the topography was updated at each sliding cycle in agreement with the real scenario. Successively, for the validation phase, experimental trials were performed on the coupling stainless steel 316L-alumina immersed into a solution composed of 3.8 % of sodium chloride [4] for three values of sliding velocity. The tribological conditions and the kind of electrolyte were chosen respect to specific marine applications. The in-situ apparatus is equipped with linear reciprocating tribometer and potentiostat, whereas the numerical simulations were conducted by MATLAB R2024b tool. Lastly, the surface analysis was achieved through an optical laser microscope paired with an high performance post-processing software (Figure 2). The results confirmed the relevant impact of frequency on tribocorrosive variables such as potential and current. In addition, the synergy was found to be both positive and negative (antagonistic role). On the whole the modelling was coherent with the tests but future improvements are surely required, trying to yield accurate and universal laws.

Keywords: Contact Theory; Surface Topography; Synergy; Tribocorrosion; Wear Modelling

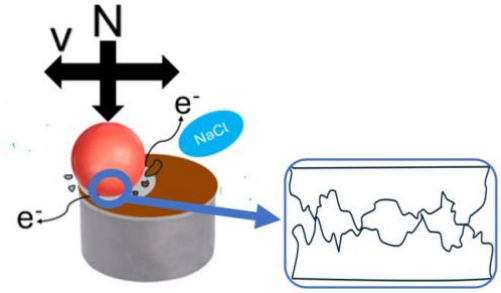

Figure 1: Schematic illustration of tribocorrosion phenomenon

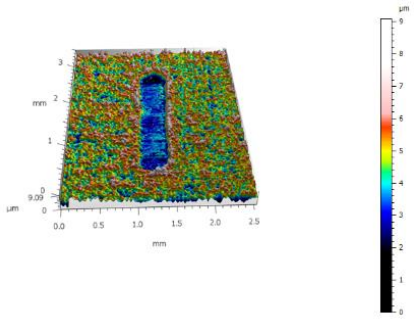

Figure 2: Example of wear track

References:

1. Ruggiero, A., De Stefano, M., (2024) The Effect of Chemical Composition of Biological Solutions on the Tribocorrosive Behavior and Synergistic Wear of Titanium Grade V Alloys for Biomedical Applications, *Journal of Bio- and Tribo-Corrosion*, 10(3), 63
2. De Stefano, M., Ruggiero, A. (2024) Tribocorrosion of couplings in seawater environment: An investigation on the positive-negative role of synergy, *Tribology International*, 200, 110143
3. Greenwood, JA, Williamson, JBP (1966) Contact of nominally flat surfaces, *Proceedings of the Royal Society of London. Series A, Mathematical and Physical Sciences*, 300-19, 295-574
4. Nahiduzzaman, MD, Ji, X., (2025) Tribocorrosion of Titanium Alloys in Seawater: Recent Advances and Strategies, *Journal of Bio- and Tribo-Corrosion*, 12(11)

Modulating the Boundary Lubrication of Orthokeratology Lenses via Polysaccharide-Protein Interfacial Interactions

H.-W. Fang [1,2,3 *], Y.-C Chang [1,2]
[1] Department of Chemical Engineering and Biotechnology, National Taipei University of Technology, Taipei, Taiwan
[2] High-value Biomaterials Research and Commercialization Center, National Taipei University of Technology, Taipei, Taiwan
[3] Institute of Biomedical Engineering and Nanomedicine, National Health Research Institutes, Miaoli, Taiwan

Abstract:
The clinical success of orthokeratology (ortho-k) lenses is often limited by the high-friction environment created by the rapid adsorption of tear film constituents, resulting in increased friction and discomfort if adsorbed components are not removed properly. This study investigates the tribological behavior of ortho-k lenses at the ocular interface, specifically examining how protein-induced friction can be mitigated through the application of alginate acid and lambda-carrageenan.Using in vitro tribological analysis , the friction coefficient of lens materials in the presence of various tear protein concentrations was investigated. The findings indicated that protein deposition significantly increases surface drag and shear resistance. To counteract this, the lubricating capacity of alginate acid and lambda-carrageenan was evaluated. Results demonstrated that these polysaccharides dramatically reduced the friction coefficient by potentially forming a hydrated, low-shear boundary layer.The underlying mechanism was explored through zeta potential and turbidity analyses, which revealed that electrostatic interactions drive the formation of polysaccharide-protein complexes. These complexes modified the interfacial energy and prevent the formation of high-friction protein films. This research provides a tribological framework for utilizing alginate and lambda-carrageenan to engineer lubricated bio-interfaces, offering a robust strategy to minimize friction-induced mechanical wear and improve wearer comfort in ortho-k applications.

Keywords: tribology, boundary lubrication, friction coefficient, orthokeratology, polysaccharides, bio-interfacial mechanics.

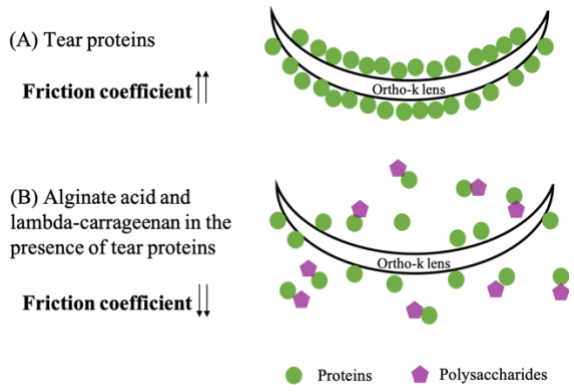

Figure 1: The potential mechanism of how polysaccharides (purple pentagons) can bring away adsorbed tear proteins (green circles) from the ortho-k lens and cause lower friction coefficient. (A) When the lens is immersed in tear protein solution, low viscosity of tear protein solution itself resulting in higher friction coefficient. (B) Electrostatic attraction and biopolymers between polysaccharides and proteins may form high viscosity of a mixed solution, resulting in lower friction coefficient of the ortho-k lens.

References:

1. Bontempo, A.R., Rapp, J. (1997) Protein-lipid interaction on the surface of a rigid gas-permeable contact lens in vitro, *Curr. Eye Res.*, 16, 1258-1262.
2. Jones, L., Brennan, N.A., Gonzalez-Meijome, J., Lally, J., Maldonado-Codina, C., Schmidt, T.A., Subbaraman, L., Young, G., Nichols, J.J. (2013) The tfos international workshop on contact lens discomfort: Report of the contact lens materials, design, and care subcommittee, *Invest. Ophthalmol. Vis. Sci*., 54, TFOS37-70.

Development of an Artificial Ageing Procedure for Polyalphaolefin (PAO) Base Oil Contaminated with Alternative Fuel

M. Kovács [1,*], D. Pintér [1]
[1] Department of Propulsion Technology and Power Electronics, Széchenyi István University, Győr, Hungary

Abstract:
In recent years, driven by increasing sustainability requirements and environmental regulations imposed on the automotive industry, alternative renewable-energy-based fuels have gained attention. A comprehensive tribological evaluation of these fuels is essential, as fuel ingress into the lubrication system can alter the lubricant's physical and chemical properties. This study presents a laboratory ageing method developed for polyalphaolefin (PAO) base oil contaminated with E20 experimental fuel. The aim of this research was to identify an optimal ageing point that allows the average wear scar diameter and coefficient of friction values of the artificially aged lubricant to fall within a minimal range. A Design of Experiments (DoE) methodology was applied to examine the effects of ageing parameters and to determine the optimal ageing settings. Tribological experiments were conducted using an oscillating tribometer (SRV®5, Optimol Instruments Prüftechnik GmbH, Germany) in a ball-on-disc configuration, while wear scars were analyzed with a digital microscope (VHX-1000, Keyence International, Mechlin, Belgium). Oil analysis was performed with a Fourier-transform infrared spectrometer (INVENIO-S, Bruker Corporation, Billerica, MA, USA). After evaluating the DoE results, the optimal ageing parameters were determined to be 140 °C and 48 hours. Using these optimal conditions, additional artificial ageing tests were performed with the addition of zinc dialkyldithiophosphate (ZDDP) anti-wear additive to investigate its effect on the lubricant and the composition of the resulting tribofilm. The tribofilms formed on wear scars were characterised using an X-ray photoelectron spectrometer (Nexsa G2, Thermo Fisher Scientific, Waltham, MA, USA).

Keywords: artificial oil ageing, design of experiment, coefficient of friction, wear scar diameter, E20 alternative fuel, FT-IR, XPS.

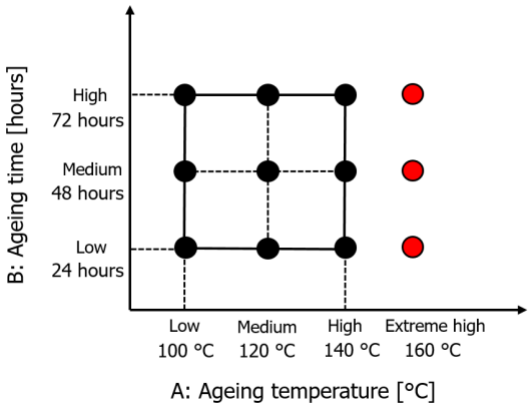

Figure 1: Two-dimensional face-centred central composite design (FCCD) showing ageing temperature (A) and ageing time (B). The black points represent the original model, which was extended by 3 additional points shown in red.

References:

1. C. Besser, A. Agocs, A. Ristic, M. Frauscher: Implementation of Nitration Processes in Artificial Ageing for Closer-to-Reality Simulation of Engine Oil Degradation, lubricants, vol. 10, no. 11, 2022. pp. 298.
2. A. L. Nagy , J. Rohde-Brandenburger, I. Zsoldos: Artificial Aging Experiments of Neat and Contaminated Engine Oil Samples, lubricants, vol. 9, no. 63, 2021.
3. S. Abdi, A. Boubakeur, A. Haddad, N. Harid: Influence of Artificial Thermal Aging on Transformer Oil Properties, Electric Power Components and Systems, vol. 39, no. 15, 2011, pp. 1701-1711.
4. H. C. Lillian, T. Cousseau, R. S. Martins: Current Knowledge on Friction, Lubrication, and Wear of Ethanol-Fuelled Engines—A Review, lubricants, vol. 11, no. 7, 2023, pp. 292.

Superlubricity with ta-C Coatings: From Model Tests to Journal Bearing Application

F. Härtwig[1], S. Makowski[1], Sachin Kattookaren[1] and Volker Weihnacht[1]
[1] Fraunhofer IWS, Dresden, Germany

Abstract:
This study demonstrates sustained superlubricity in carbon-based coating systems under industrially relevant conditions.

Pin-on-disk tribometer experiments with a-C and ta-C coatings paired with glycerol lubrication achieved remarkably stable superlubric behavior across extended operational parameters:

- temperatures ranging from room temperature to 150°C (Figure 1)
- exceptional test durations exceeding 350 hours (126 km sliding distance)
- broad load stability up to 526 MPa contact pressure

The system exhibited extremely low ball wear coefficients of 2.8×10^{-11} mm³/Nm with zero measurable coating wear, confirming the robustness of the superlubric regime.

To evaluate the practical applicability of these findings, a novel journal bearing tribometer was developed and commissioned. Initial experiments investigated sintered steel and sintered bronze bushings operating against both ta-C coated and uncoated steel shafts under glycerol lubrication. Results reveal that ta-C coatings effectively prevent shaft wear independent of the bushing material and lubricant used. Notably, the combination of sintered steel bushings, polyalkyleneglycol-based lubricant and ta-C coated shafts achieved superlubricity, demonstrating the feasibility of translating the system to realistic bearing geometries. (Figure 2)

An assessment on energy consumption and costs demonstrates that such systems could be applied with a clear overall benefit.

These findings bridge the gap between fundamental superlubricity research and engineering applications, demonstrating that ta-C/steel systems can maintain ultra-low friction and wear in practical sliding bearing configurations. The successful translation from model experiments to a journal bearing system opens new possibilities for energy-efficient, long-lasting tribological components in industrial applications, including replacement of ball bearings.

Keywords: superlubricity, ta-C, DLC, glycerol lubrication, journal bearing, PAG

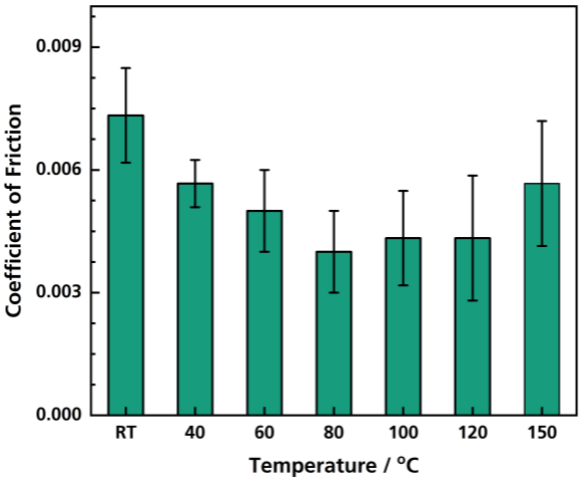

Figure 1: Temperature stability of ta-C / glycerol / steel tribology system. Superlubricity ($\mu < 0.01$) can be seen between room temperature up to 150 °C.

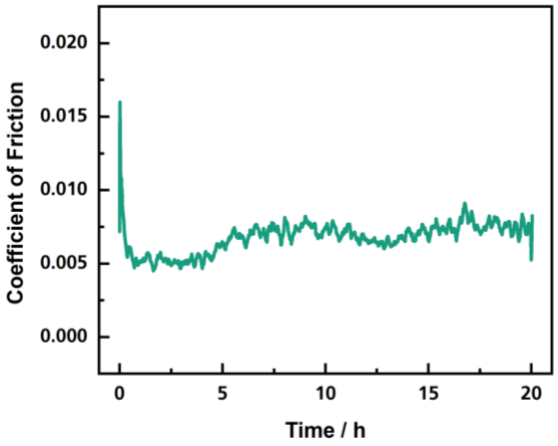

Figure 2: Friction plot of experiment with ta-C shaft / PAG-based lubricant / sintered-iron journal bearing. Experiment parameters: F_N = 800 N, T = 40 °C, v = 500 rpm (0.5 m/s).

Circular Valorization of End-of-Life Tires into High-Performance Rubber-Carbon Composites: Mechanical and Tribological Performance

Abrar Hussain [1*], Diana Bajare [1]
[1] Institute of Sustainable Building Materials and Engineering System, Riga Technical University, Paula Valdena iela 1, Riga, LV 1007, Latvia (*corresponding author email:abrar.hussain@rtu.lv)

Abstract:
Rubber–carbon composites derived from end-of-life tires (ELTs) represent a promising class of sustainable engineering materials that integrate circular economy principles with high-performance functionality. This study focuses on the development, processing, and performance evaluation of rubber–carbon composite systems produced through advanced recycling routes, particularly high-temperature high-pressure (HTHP) sintering and thermo-mechanical consolidation. ELT-derived feedstocks comprising approximately 40–50% rubber and 20–25% carbon black and mineral fillers are transformed into structurally integrated composites with enhanced functional performance. Experimental characterization demonstrates that the developed composites exhibit tensile strength in the range of 4.5-10 MPa, yield strength of 2.3-4 MPa, elastic strength of 1.5-2 MPa, and fracture strength of 1.5-2.7 MPa, reflecting the heterogeneous nature of recycled rubber systems. Dynamic mechanical analysis indicates stable viscoelastic behavior with pronounced damping characteristics, while thermal assessments confirm adequate stability for engineering applications. Tribological investigations reveal that rubber–carbon composites exhibit abrasive wear rates on the order of ~10^{-5} to 10^{-6} mm³/N·m, depending on processing conditions, filler dispersion, and interfacial bonding quality. Under controlled sliding conditions (e.g., 1 N load, 0.1 m·s^{-1} sliding speed), these materials demonstrate consistent wear resistance and frictional stability, making them suitable for contact and damping applications. Furthermore, artificial intelligence (AI) and machine learning (ML) frameworks are integrated to establish predictive process–structure–property relationships [1]. Python-based modelling and image analysis enable accurate prediction of mechanical and tribological performance, facilitating optimization of processing parameters and enabling digitalized circular manufacturing. Overall, rubber–carbon composites provide a viable pathway for valorizing ELT waste into high-value engineering materials, offering competitive mechanical resilience, energy absorption, and wear resistance. This approach supports scalable sustainable manufacturing while contributing to reduced environmental impact and enhanced resource efficiency within circular economy systems.

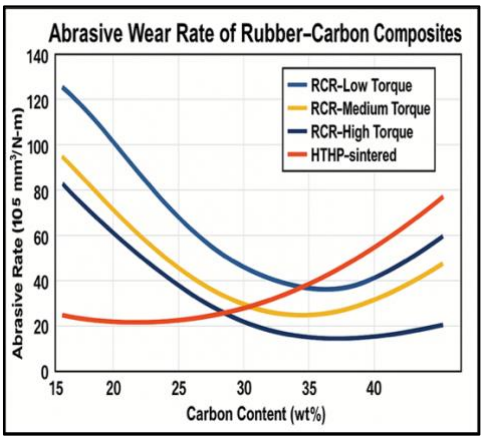

Figure 1: Abrasive testing and ML prediction.

Keywords: Circular digital manufacturing, high-performance polymer composites, end-of-life tire valorization, tribological testing, python-based machine learning studies.

Acknowledgements
This research is done under Activity 1.1.1.9 "Post-doctoral Research" of the Specific Objective 1.1.1 "Strengthening research and innovative capacities and introduction of advanced technologies in the common R&D system" of the European Union's Cohesion Policy Programme for 2021-2027 research application No 1.1.1.9/LZP/1/24/147 “Advanced Recycling and Computational Analysis of Ultra High-Performance Polyether ether ketone and Polyamide-Imide Carbon Reinforced Composites for Automotive and Aerospace Applications”

References:

1. Hussain A, Maurya HS, Goljandin D, Sinka M, Bajare D. Development of Experimental and Computational Lightweight Industrial Circularity Manufacturing Systems for Polymer Waste Recycling: Mechanical Testing and Characterization. International Journal of Lightweight Materials and Manufacture. 2025 Nov 25.

EU projects Workshop: Antimicrobial Nanocoatings: Aligning Innovation, Regulatory Compliance and Market Uptake

Controlled-release of carvacrol oil from stimuli-responsive copper doped mesoporous silica particles

M. Argaiz[1,*], L. Fiore[2], A. M Goitandia[1], F. Arduini, M. Blanco[1] B. Coto[1]
[1] Unidad de Química de Superficies y Nanotecnologías, Fundación Tekniker, Iñaki Goenaga 5, 20600, Eibar, Spain
[2]Department of Chemical Science and Technologies, University of Rome Tor Vergata, Via della ricerca scientifica, Rome, Italy

Abstract:
Microbial colonisation of surfaces forms a dangerous reservoir for pathogens, contributing to the spread of infections which can cause high costs to human life and the economy at large. There is a tangible need for innovative antimicrobial coatings that are highly effective, safe, and self-disinfecting to remove bacteria, fungi, and viruses more cost-effectively than current non-biodegradable, toxic, and fossil fuel-based coatings in use. The RELIANCE project aims to design and develop smart-response self-disinfecting antimicrobial nanocoatings based on a new range of smart antimicrobial nanoparticles. These particles consist of copper-doped mesoporous silica particles (CuMSN) modified with biobased bioactive compounds, such as carvacrol, which are essential oils (EOs) coming from non-edible plants. To achieve better control of the EOs release, the CuMSN surface is modified with stimuli-responsive polymer brushes, which are organic molecules that exhibit different polymer chain conformation in response to external stimuli, such as temperature (T) and pH [2]. Among others, (2-(dimethyl amino)ethyl methacrylate) monomer (DMAEME) is selected for the functionalization of CuMSN surface as its responses to both pH and T. These brushes are grown from CuMSN via surface-initiated atom transfer radical polymerization (SI-ATRP), which is one of the most effective methods to synthetise polymer brushes on particles surfaces [3]. The PDMAEME brushes onto CuMSN surface are characterized in terms of fourier-transform infrared spectroscopy (FTIR), thermogravimetric analysis (TGA), elemental analysis and transmission electron microscopy (TEM) to confirm the modification of CuMSN surface (CuMSNpolyDMAEMA). The variation of particle size, obtained by dynamic light scattering (DLS), also indicates the presence of polymer brushess shell, which respond to external stimuli such as pH and temperature. At ambient temperature, increasing the pH, the average diameter decreases, meaning that at protonated state (pH > $pKa_{PDMAEMA}$), the polymer brushes are probably in their open conformation, while at non-protonated state (pH < $pKa_{PDMAEMA}$), the polymer brushes seem to be in a collapse conformation. At constant pH, increasing the temperature, the average diameter decreases.
Regarding the release of the carvacrol EO, pH responsive behaviour of PDMAEMA brushes grafted on CuMSN was investigated to ensure the control leaching of this specie into the environment to fulfil the main objective of the RELIANCE project. The release was followed in real-time using an electrochemical reagent-free paper-based device, which has already been employed for a wide variety of essential oil detection [4]. Upon monitoring the electrochemical response for up to 60 minutes, the sample exhibited a clear oxidation peak, indicating that carvacrol is released from the particles during the first 60 minutes.

Keywords: smart antimicrobial particles, stimuli-responsive polymers, copper doped silica particles, essential oil.

References:

1. Reliance Project, https://reliance-he.eu/
2. Wei, M., Gao, Y., Lia, X,. and Serpe, M.J. (2017), Stimuli-responsive polymers and their applications, Polym. Chem., 8, 127-143
3. Truong, N. P., Jones, G. R., Bradford, K. G. E., Konkolewicz, D. and Anastasaki, A. (2021), A comparison of RAFT and ATRP methods for controlled radical polymerization, Nat Rev Chem., 5, 859-869.
4. Fiore, L., (2025), An ecodesigned reagent-free paper-based electrochemical sensor modified with carbon black for the detection of essential oils, Green Analytical Chemistry, 12, 100217.

Acknowledgement: RELIANCE project has received funding from the European Commision under grant agreement No. 101058570 (RELIANCE)

Antibacterial Performance of Nanoparticle-Based Coatings on Textile

Büşra Erol[1], Simen Akkermans[1], Elena Merli[2], Daniele Spinelli[2], Ilaria Canesi[2], Alexandra Karagianni[3], Adamantia Zourou[3], Ioanna Kitsou[4], Eleni Roussi[4], Athena Tsetsekou[4], Konstantinos V. Kordatos[3], Dimitra Katerinopoulou[5], Aspasia Stoumpidi[5], George Kiriakidis[5], Dmytro Kozak[1], Monika Polanska[1], Jan F.M. Van Impe[1]

[1] BioTeC+ Chemical and Biochemical Process Technology and Control, KU Leuven
Gebroeders de Smetstraat 1, 9000 Gent, Belgium
[2] Next Technology Tecnotessile Società Nazionale di Ricerca R.L., Via del Gelso 13, 59100 Prato, Italy
[3] School of Chemical Engineering, National Technical University of Athens
9 Iroon Polytechniou St., Zografou, 15780, Athens, Greece
[4] School of Mining & Metallurgical Engineering, National Technical University of Athens
9 Iroon Polytechniou St., Zografou, 15780, Athens, Greece
[5] PCN Materials, Knossou 5, VIOPA-Anopolis, 70008, Crete, Greece.

Abstract:

In recent years, concerns related healthcare-associated infections have increased and driven the need for prevention measures. When textile products become contaminated, they can act as reservoirs for pathogens that cause these infections. Therefore, they have attracted attention as candidates for antimicrobial functionalization [1].

Core-shell nanoparticles have been studied with the goal of achieving improved antimicrobial efficacy compared to the pristine nanoparticles. Previously, TiO_2 cores with carbon dots and silver, and SiO_2 cores with silver exhibited superior antibacterial performance in suspension compared to core materials and were selected for textile coatings. Cotton samples were dip-coated with anionic or non-ionic resin containing 0.5% nanomaterial. The antibacterial performance of the coated textiles was evaluated under light exposure against *Enterobacter cloacae*, using a modified ISO protocol to assess antibacterial activity under photoactivation [2]. Antibacterial efficacy was determined after 24 h light exposure.

Before and after the incubation, textile samples were transferred into sterile tubes containing 0.8% saline solution and vortexed vigorously to detach bacterial cells from the textile surface. The resulting suspensions were serially diluted in sterile saline solution and plated on tryptic soy agar for viable cell enumeration. Colony-forming units (CFU) were counted, and bacterial reduction was calculated relative to the inoculum recovered from the textile samples.

Table 1 demonstrates the antibacterial effect of coated textile samples with different nanoparticles and resins as the inactivation compared to the initial population. Among the tested systems, SiO_2 cores with silver exhibited pronounced antibacterial activity with both types of resin. However, TiO_2 core-shell material showed a different antibacterial effect depending on the resin's ionic character. In both cases, the coatings with core material did not exhibit antibacterial properties under the tested conditions. The results demonstrate that the core-shell structure is required to obtain antibacterial coatings. Overall, the results demonstrate that selection based on suspension screening successfully translated to antibacterial coated textiles. These coatings have potential for the production of functional antibacterial textiles with medical applications.

Table 1. Antibacterial performance of the nanocoated cotton.

Material	Bacterial reduction [log(CFU/cm²)]	
	Anionic resin	Non-ionic resin
No resin, no NP	No inactivation	
Resin, no NP	No inactivation	No inactivation
TiO_2	No inactivation	No inactivation
TiO_2@Ag+CD	> 3 (99.9%)	No inactivation
SiO_2	No inactivation	No inactivation
SiO_2@Ag	> 3 (99.9%)	> 3 (99.9%)

NP: Nanoparticle; No inactivation means ≤ 1 log CFU/cm² reduction compared to the initial population size.

Keywords:
Textile coating, Core-shell nanoparticles, Antibacterial textile surfaces, *Enterobacter cloacae*.

References:

1. Bakar, N. H. A., Ismail, W. N. W., Umair, M., & Kumar, A. S. K. (2025). Antibacterial Textile Coatings with Strategies for Long-Term Performance and Environmental Safety. *Advanced Nanocomposites*. 299-321.
2. ISO 27447:2019. Fine ceramics (advanced ceramics, advanced technical ceramics) — Test method for antibacterial activity of semiconducting photocatalytic materials. International Organization for Standardization, Geneva, Switzerland.

Photoactive Nanoparticles for Antimicrobial Inactivation

V. Liška [1], J. Mosinger [1]
[1] Faculty of Science, Charles University, Hlavova 2030, 128 43 Prague 2, Czech Republic

Abstract:
This work, conducted under the framework of the MIRIA project, focuses on the development of advanced antimicrobial, antiviral, and antifungal nanocoatings designed for everyday surfaces. We present a robust and scalable platform technology based on photoactive polystyrene nanoparticles.[1] These nanoparticles are prepared through a novel process involving the electrospinning of polymer membranes with encapsulated photosensitizers (e.g., tetraphenylporphyrin), followed by controlled sulfonation. This approach ensures efficient photosensitizer encapsulation while maintaining high oxygen permeability and colloidal stability in aqueous environments.

The photoactive functionality relies on the photosensitized generation of singlet oxygen ($^1O_2$), which exerts a strong localized cytotoxic effect. Our results demonstrate exceptional antibacterial activity against pathogens such as *Escherichia coli*, *Pseudomonas aeruginosa*, and *MRSA*. Furthermore, the nanoparticles exhibit significant antiviral properties against both enveloped and non-enveloped viruses, and outstanding antifungal efficacy, particularly when combined with an iodide-boost effect.[2] The integration of these photoactive nanoparticles into sol-gel systems allows for the creation of transparent, self-disinfecting coatings on glass and textile substrates, offering a promising solution for mitigating the spread of infections in public environments.

Keywords: Photoactive nanoparticles, singlet oxygen, antimicrobial nanocoatings, electrospinning, MIRIA, porphyrins, antiviral coatings, sulfonation

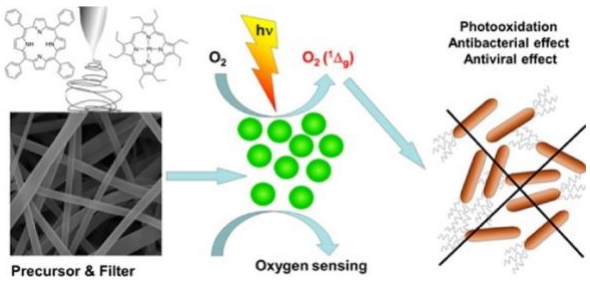

Figure 1: Schematic illustration of the photoactive nanoparticle production and application. Porphyrin-encapsulated polystyrene nanofibers are prepared via electrospinning (top left). Controlled sulfonation of these fibers yields photoactive nanoparticles (bottom left), which serve as a platform for the generation of reactive singlet oxygen ($^1O_2$) under light irradiation (center). The process concludes with the development of self-disinfecting antimicrobial coatings (e.g., via sol-gel deposition) designed for everyday surfaces within the MIRIA project framework (right).

References:

1) P. Kubát, P. Henke, V. Berzediová, M. Štěpánek, K. Lang, J. Mosinger, *ACS Applied Materials & Interfaces* **2017**, 9, 36229.
2) P. Kubát, P. Henke, J. Mosinger, *Colloids and Surfaces B: Biointerfaces* **2019**, 176, 334.

Encapsulation of Essential Oils in Silica Nanopores: A Molecular Dynamics simulation study

I. Papageorgiou,[1] K.S. Karadima,[1] L. Peristeras,[2] V.G. Mavrantzas[1,3]
[1]Department of Chemical Engineering, University of Patras, Patras, GR 26504, Greece
[2]Molecular Thermodynamics and Modeling of Material Laboratory, Institute of Nanoscience and Nanotechnology, National Center of Scientific Research "Demokritos", GR-15310 Aghia Paraskevi, Greece
[3]Macromolecular Engineering Laboratory, Department of Mechanical and Process Engineering, ETH Zürich, Zürich CH-8092, Switzerland

Abstract:
A promising direction in the design of smart-response antibacterial surfaces involves nanocoatings containing additives with strong antimicrobial activity such as mesoporous copper nanoparticles and bioactive compounds (e.g., whey proteins from milk production streams and keratin-derived peptides from chicken feathers) as well as essential oils coming from non-edible plants as effective agents against a wide range of pathogens. Typical examples of essential oils include carvacrol, eugenol, thymol, menthol, and eucalyptol which are eco-friendly, safe and easily biodegradable. The efficient incorporation of these agents in the pores of the support material (mesoporous silica) and their subsequent release depends strongly on parameters such as the size of the pores, the presence of functional groups on their walls, the use of an appropriate solvent, and the temperature or the pH in the case of triggered release, thus leaving a lot of space for optimization. Molecular modelling can greatly aid these efforts by providing fundamental understanding of the molecular mechanisms that control the encapsulation and subsequent release of these agents from the pores of the silica framework.
In this contribution, we will report results from large-scale molecular dynamics (MD) simulations concerning: a) a comparative analysis of the loading behavior of different EO within silica pores; b) assessment of pore diameter as a key control parameter influencing encapsulation and release; c) evaluation of the role of ethanol as a co-solvent during encapsulation; and d) the effect of surface silanol density on encapsulation.
Our simulations indicate how pore size, surface density, and the presence of ethanol influence EO encapsulation, mobility, and release. Pore diameters of 2 to 4 nm enable effective EO encapsulation, whereas 1 nm pores are too restrictive. Reducing the silanol density on the walls of the silica pores allows for higher EO pore occupancy, while comparative analysis across different EOs shows a strong dependence on molecular size and structure, with eucalyptol exhibiting the lower encapsulation and eugenol the higher mobility. Ethanol is also observed to have a strong effect on EO encapsulation and mobility inside the silica pores, due to its strong competition for adsorption on the silica pore walls through hydrogen bonding (Figure 1).

Keywords: MD simulations, mesoporous silica nanopores, essential oils, loading, encapsulation, release.

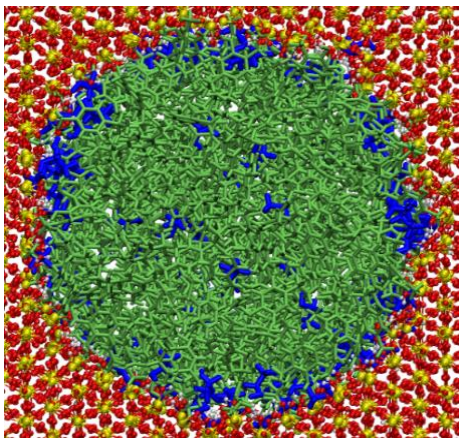

Figure 1: Representative snapshot illustrating the distribution of carvacrol (lime) and ethanol (blue) molecules within a mesoporous silica nanopore. Ethanol molecules exhibit a pronounced tendency to localize near the silica surface, highlighting their preferential interactions with surface silanol groups. The silica framework is shown with oxygen atoms in red and silicon atoms in yellow.

Particle Release from Light-Activated Antimicrobial Coatings under Simulated Dermal Contact and Cleaning

Nurshen Mutlu[a], Pascal Kock[b], Stefan Fischer[b], Simone Schulte[b], Bernd Nowack[a]
[a] Technology and Society Laboratory, Empa - Swiss Federal Laboratories for Materials Science and Technology, Lerchenfeldstrasse 5, 9014 St. Gallen, Switzerland
[b] Microbial Effects, Coating Additives, Evonik Operations GmbH, Essen 45127, Germany

Abstract:
High-touch surfaces are recognized as important vectors for pathogen transmission and are commonly encountered in public transport, schools and healthcare settings. Current mitigation strategies rely mainly on routine cleaning and disinfection using chemical agents. Although effective, these approaches provide temporary solutions, as surfaces can be rapidly re-contaminated between cleaning cycles. As a result, antimicrobial surface coatings have emerged as a promising complementary strategy to conventional hygiene practices. However, in the light of product innovation within a Safe and Sustainably by Design (SSbD) approach, assessing release of active materials to the environment or quantifying human exposure is one important step. In this study, a novel class of light activated antimicrobial coatings incorporating micron-sized upconverting particles (Li_2CaSiO_4:Pr,Na) into water-borne coating formulation was investigated [1]. These coatings convert visible light into ultraviolet radiation, which inactivates microorganisms through physical damage to DNA without relying on conventional biocidal agents. Although this approach offers promising antimicrobial performance, understanding potential particle release during real-world use is necessary to ensure user and environmental safety. Therefore, particle release was evaluated under simulated dermal contact and cleaning conditions using a crockmeter to reproduce controlled rubbing motions mimicking repeated dermal contact and disinfection. Rubbing cycles ranged from 10 to 1250 double passes. Experiments were performed using cotton wipes as a surrogate of human fingers under dry conditions, water-wetted conditions, artificial sweat, and selected disinfectants. Released material was collected on wipes, digested using an optimized acid digestion protocol, and quantified by inductively coupled plasma mass spectrometry. Release increased with increasing cycle number, with initial release attributed to loosely bound surface material followed by continued particle release during prolonged rubbing. Dry rubbing resulted in higher release compared to wet conditions, likely due to reduced friction at the coating-wipe interface in the presence of moisture. After 1250 cycles, approximately 1% and 0.2% release was observed under dry and wet conditions respectively. Overall, these findings provide insight into the stability of upconverter particles and their interaction with the coating matrix during prolonged use, supporting the evaluation of antimicrobial coatings within a Safe and Sustainable by Design (SSbD) framework.

References

1. Schröder, F., Fischer, S. & Jüstel, T. X-ray and VUV excitation studies on Pr3+ activated Li2CaSiO4. *J. Lumin.* **235**, 118046 (2021).
2. Tunali, M., Voelker, D., Burkart, C., Schwirn, K. & Nowack, B. Recommendations for making the European Commission's Safe and Sustainable by Design framework practicable for biocides. *Sustain. Chem. Pharm.* **48**, 102221 (2025).

A decorative and antibacterial coating for high-traffic objects: effectiveness and durability in a real-life-like scenario

Rocío Ortiz [1], Iñigo Ciarsolo [1], Olatz Areitioaurtena [2], Sofia Alves [1], Borja Coto [2], Eva Gutiérrez [1]
[1] Plasma coating technologies Unit, TEKNIKER, Basque Research and Technology Alliance (BRTA), C/ Iñaki Goenaga 5, 20600, Eibar, Spain.
[2] Surface Chemistry and Nanotechnologies, TEKNIKER, Basque Research and Technology Alliance (BRTA), C/ Iñaki Goenaga 5, 20600, Eibar, Spain.

Abstract:
Decorative (golden) titanium nitride (TiN) coatings were deposited by cathodic arc (CA) and modified by adding copper (Cu) nanoparticles in 3.5 and 8 percent, providing antibacterial functionality. The Cu was sputtered using magnetron sputtering (less energetic than CA) to allow for fine control of the Cu content. These coatings were deposited on polished stainless-steel sheets and silicon wafers for coating characterization, and on chromium-plated brass taps as prototypes (Figure 1). All the coatings had a thickness of about 500 nm.
The antibacterial activity of the coated stainless-steel samples was evaluated using a methodology based on the standard ISO 22196:2011 with *S. aureus* (ATCC® 6538 TM) and *E. Coli* (ATCC® 8739 TM). TiN-coated samples (without Cu nanoparticles) were used as controls. The antibacterial activity (R) of TiN coatings with 3.5% and 8% Cu content was calculated from the average number of viable bacteria recovered per cm^2, yielding R = 2.43 (99.6%) and 4.72 (100%) for S. Aureus, respectively, and R = 3.62 (99.9%) and 4.27 (100%) for E. Coli.
A wet abrasion washability test (Figure 2) was used to evaluate the coating resistance and the synergistic effects of wear produced by cleaning procedures and the chemical attack of the cleaning fluids. These tests were carried out following the standard UNE EN ISO 11998:2006 and using non-ecotoxic (Proteo Flow) and an ecotoxic cleaning fluid (sodium dodecylbenzene sulfonate). A minimum of 3650 cycles represented 2 years of regular cleaning and 1 year of special cleaning. With these considerations, TiNCu samples with 3.5% and 8% Cu content were tested for 3650, 18250, and 36650 cycles with no signs of wear or degradation. Ecotoxicity assays were performed using the fluids collected from the washability tests to measure Cu-ion release by Inductively Coupled Plasma (ICP). The results showed that the coatings' Cu content did not harm the viability of luminescent bacteria "Vibrio fischeri" (NRRL B-11177).
Finally, the antibacterial activity was evaluated on samples exposed to a high-traffic real environment (toilet facilities) for 20 weeks.
Non-ecotoxic TiNCu coatings showed high resistance to ageing under mechanical wear, simulating more than 20 years of cleaning procedures. The TiNCu-coated samples displayed antibacterial activity (>99%) both after washability tests simulating 10 years of special ageing, and after exposure to a real environment (toilet facilities).

Keywords: thin film coating; cathodic arc; magnetron sputtering; decorative coatings; antibacterial coatings; high-traffic objects.

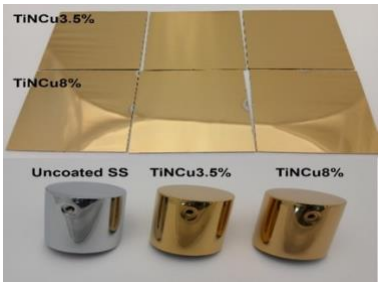

Figure 1: Stainless-steel sheets and chromium-plated brass taps coated with TiNCu coatings by cathodic arc and magnetron sputtering.

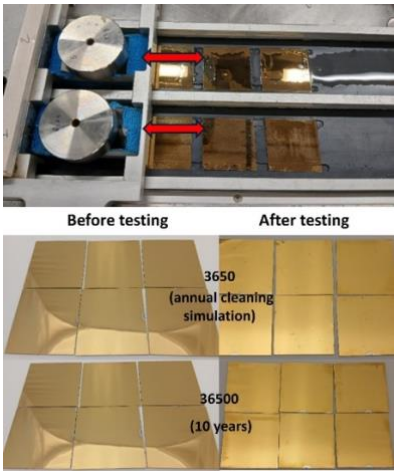

Figure 2: Wet abrasion washability test applied to TiNCu-coated stainless-steel sheets.

References:

1. ISO 22196:2011 - Measurement of antibacterial activity on plastics and other non-porous surfaces.

2. UNE-EN ISO 11998:2007 – Paints and varnishes – Determination of wet-scrub resistance and cleanability of coatings.
3. EN ISO 11348-2:2008 Water Quality- Determination of the inhibitory effect of water samples on the light emission of Vibrio fischeri (luminescent bacteria test)- Part 2: Method using liquid dried bacteria.
4. ISO 11885:2009 -Water quality. Determination of selected elements by inductively coupled plasma optical emission spectrometry (ICP-OES).
5. OECD Nº 23 (2018) – Guidance Document on Aqueous-Phase Aquatic Toxicity Testing of Difficult Test Chemicals (OECD Series on Testing and Assessment No. 23, Second Edition).
6. OECD Nº 201 (2011) – Guidelines for the testing of chemicals: Freshwater Alga and Cyanobacteria, Growth Inhibition Test
7. OECD Nº 202 (2004) – Guidelines for the testing of chemicals: Daphnia sp., Acute Immobilisation Test.
8. OECD Nº 203 (2025) – Guidelines for the testing of chemicals: Fish, Acute Toxicity Testing.

NanoBloc: From Laboratory Development to Industrial Upscaling of Sputtered Antimicrobial Coatings

A. Luceri[1,*], O. Benzine[2], M. Donalisio[3], D. Lembo[3], C. Balagna[1]
[1] Department of Applied Science and Technology, Politecnico di Torino, Turin, Italy
[2] INTERPANE Entwicklungs- und Beratungsgesellschaft mbH. Sohnreystraße 21 37697 Lauenförde Germany
[3] Department of Clinical and Biological Sciences, Università di Torino, S. Luigi Gonzaga Hospital, Turin, Italy

Abstract:
The increasing demand for effective strategies to prevent pathogen transmission has highlighted the importance of functionalized surfaces with antimicrobial and antiviral properties [1].

In this context, the transition from laboratory-scale coatings to industrially viable solutions represents a critical challenge.

The NanoBloc project addresses this issue by developing multifunctional nanocoatings and enabling their upscaling through industrially compatible processes. In this work, the focus on the transfer of a lab-scale coating, based on silver nanoclusters embedded in oxide matrices, to large-scale production using co-sputtering (PVD) technologies.

Upscaling was achieved using industrial roll-to-roll and batch coating systems, allowing the deposition of composite coatings on large-area and flexible substrates.

The process was implemented and optimized by AGC-Interpane, by adapting co-sputtering parameters to ensure uniformity, adhesion, and functional performance over extended surfaces.

The optimized coating was fully characterized by FESEM, EDS, UV–Vis spectroscopy, and XRD analysis, confirming the homogeneous distribution of silver nanoclusters within the matrix.

It demonstrated the best balance between antimicrobial effectiveness and resistance to washing. Antibacterial performance was evaluated through standardized tests against *Staphylococcus epidermidis* and *Escherichia coli*, while washability tests were conducted to assess the stability of the antibacterial effect after water exposure.

Antiviral tests against SARS-CoV-2 further validated the functional performance of the upscaled coatings.

These results demonstrate the successful transition from lab-scale development to industrial-scale production, highlighting the potential of PVD-based multifunctional coatings for real-world applications in air filtration, textiles, and high-contact surfaces.

Keywords: Upscaling, PVD, antimicrobial coatings, composite materials, silver nanoclusters, industrial processes, multifunctional materials.

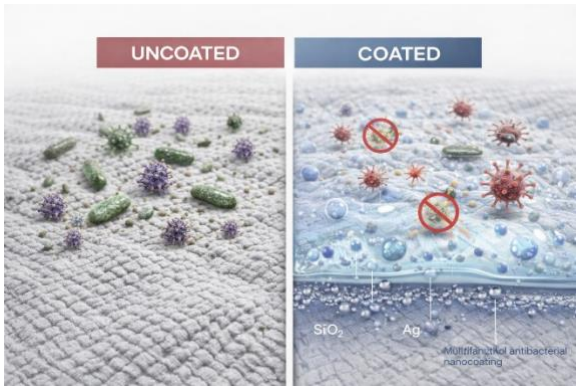

Figure 1: Schematic representation of antibacterial coating performance: comparison between uncoated and coated surfaces. The uncoated substrate shows significant bacterial proliferation, while the coated surface inhibits bacterial growth and promotes inactivation due to the presence of the functional nanocoating.

References:

1. Yong, L. X.; Calautit, J. K. *A Comprehensive Review on the Integration of Antimicrobial Technologies onto Various Surfaces of the Built Environment*. Sustainability, 2023, 15, 3394.

A novel 3D-printed stamping device to assess antibacterial performance of coatings under simulated realistic touch transfer

Alexander J Cunliffe [1*], Peter Askew[2], Gillian Iredale[2], Abby Marchant[2], Alisha Awan[2], James Redfern [1]
[1] Department of Natural Sciences, Manchester Metropolitan University, Manchester, UK
[2] Industrial Microbiological Solutions Ltd, Reading, UK

Abstract: Antibacterial materials can act as a first line of biofilm control in the built environment by preventing initial colonisation. However, current methods of validating candidate materials (e.g. ISO 22196 [1]) specify environmental conditions that the material will likely not experience when in use (e.g. relative humidity above 90%), allowing materials that require moisture (e.g. silver nanoparticles) to present artificially prolonged efficacy. Additionally, the method of surface inoculation is often considered unrealistic, using high volumes of liquid. The aim of this study is to develop a reproducible method for surface transfer of bacteria using a 3D-printed device to simulate gloved-hand transfer of *Staphylococcus aureus* in the built environment [2]. A custom-designed 3D-printable stamping device was developed to accurately simulate gloved-hand contact under realistic environmental conditions. The stamping device was designed and printed to be UV sterilisable and for glove sections to be efficiently attached, followed by stamping an inoculated agar surface to acquire a uniform bacterial load (*Staphylococcus aureus*). The device was then stamped (1 kg weight to simulate human touch pressure) on to recipient surfaces (stainless steel and copper) and the survival over time in varying relative humidity conditions measured via total viable count assays. Consistent initial bacterial transfer occurred on each material type with slight but statistically significant differences between materials (lower recovery from copper than stainless steel) in some cases. No significant reduction in bacterial viability was observed on stainless steel coupons, but varying antibacterial efficacy of copper surfaces was observed (lower efficacy at lower relative humidity environments). The variation in bacterial viability highlights not only the importance of moisture to the antibacterial efficacy of some materials, but also the requirement for standardised testing methods (e.g. ISO standards) to incorporate conditions more analogous to those the material would experience when in use. Furthermore, this novel technique could be applied to biofilm growth after touch colonisation and contact transfer of pre-formed biofilm.

Keywords: Antimicrobial coating, Photocatalytic, Method development, Copper, Standards, ISO 22196, Touch transfer, Relative humidity, 3D printing

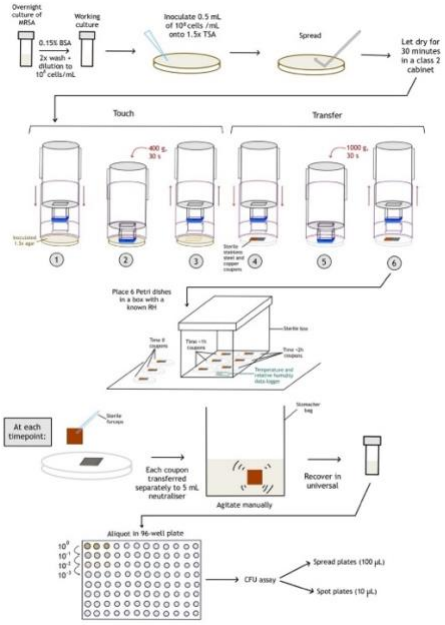

Figure 1: Protocol to assess antibacterial efficacy of copper using dry touch transfer. Prior to apparatus use, a TSA plate (1.5× concentration) was inoculated with a 10^8 cells/mL culture of MRSA in 0.15% BSA, spread evenly, and allowed to dry for 30. The apparatus was used accordingly; Step 1: The inner shell is pushed through the outer shell; Step 2: The stamp device "touches" the donor surface and weight is applied; Step 3: The inner shell is removed from the outer shell; Steps 4–6: The same process as steps 1–3 is repeated on the recipient surface but with 1,000 g weight applied. Coupons were then transferred to a chamber with controlled environmental conditions (~20°C, <30/40–60/>70% relative humidity) and recovered at specific timepoints (0 h, 1 h, 2 h) into neutralizer separately, followed by quantification by dilution plate count.

References:

1. ISO, ISO22196: Measurement of antibacterial activity on plastics and other non-porous surfaces. 2011.
2. Chareyre, E., et al., A novel and validated 3D-printed method for the consistent and reproducible dry transfer of microorganisms for the determination of antimicrobial surface efficacy. Applied and Environmental Microbiology, 2025: p. e00802-25.

Atmospheric Plasma-assisted Deposition of Antimicrobial Coatings on Complex 3D Automotive Interior Surfaces

M. Nilkar [1, *], M. Milani [1]
[1] Molecular plasma Group, Grand Duchy of Luxembourg

Abstract:
Molecular Plasma Group (MPG) develops cold atmospheric plasma technology for deposition of permanent functional nanocoatings on a wide range of substrates, including temperature-sensitive polymers and complex three-dimensional parts. MolecularGRIP™ is a single-step, solvent-free, and dry process operated at room temperature and atmospheric pressure. By injecting the precursor in the plasma afterglow, functional moieties can be better preserved, enabling application-specific surface chemistry while maintaining compatibility with sensitive materials and industrial processing constraints.

In the RELIANCE project, MPG's PlasmaSpot® technology is applied to the deposition of antimicrobial coatings on chrome-plated automotive interior parts, with particular focus on the transfer from flat laboratory substrates to complex 3D console geometries (Figure 1). This represents an important industrial challenge, as successful implementation requires not only antimicrobial functionality, but also coating homogeneity, process robustness, and compatibility with part appearance and geometry.

Using MPG's PlasmaSpot® technology, several antimicrobial precursor systems were deposited on chromed substrates representative of automotive interior applications. A key aspect of the work was the optimization of plasma operating conditions to preserve functional groups and maximize coating performance. The results showed that appropriate plasma tuning can significantly improve the antimicrobial efficacy of deposited thin coatings. In parallel, the plasma head configuration was adapted to the part geometry. Different nozzle designs were evaluated to optimize coating coverage on curved, recessed, and edge-containing regions. The results further showed that nozzle geometry strongly affects deposition distribution and coating homogeneity, underlining the importance of part-specific plasma head design for complex 3D surfaces. In addition, UV-tracer molecules were used as a simple quality-control tool to directly visualize coating homogeneity on real parts.

Overall, this work demonstrates the potential of MPG's atmospheric plasma technology to bridge laboratory-scale development and industrial implementation for biofunctional coatings on complex automotive interior components, while highlighting key aspects required for scale-up, process control, and industrialization.

Keywords: MPG cold atmospheric plasma technology, antimicrobial coatings, automotive interior surfaces, nozzle design, industrialization

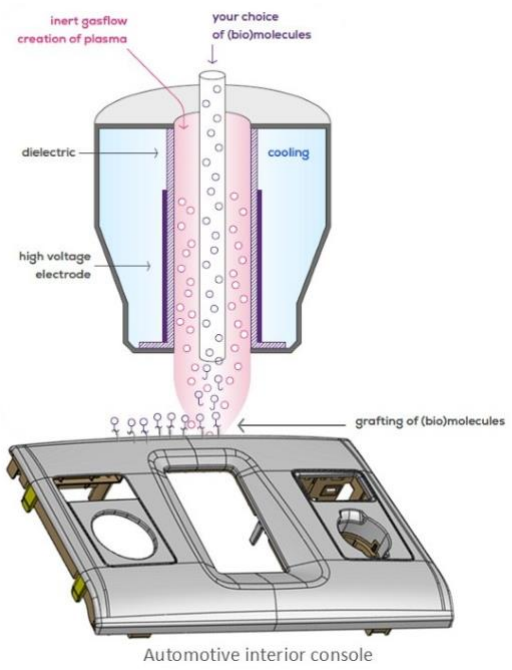

Figure 1: Schematic illustration of MPG's PlasmaSpot® process for atmospheric plasma-assisted grafting of biomolecules onto a 3D automotive interior console.

SICT 2026 / Plasma Tech 2026 Session III. A: Coatings for Energy and Environmental Applications

Metal oxide cathode coating of NASICON cathode materials to enhance cathode performance in Na-ion batteries

S. Lavela, C. Pérez Vicente, P. Lavela, J. L. Tirado*
Departamento de Química Inorgánica e Ingeniería Química
Instituto Universitario de Energía y Medio Ambiente,
Universidad de Córdoba, Campus de Rabanales, 14071, Córdoba, Spain

Abstract:

Coating cathode materials with metal oxides forms a durable protective layer that isolates the active material from the electrolyte, reducing side reactions that cause degradation, capacity loss, and poor cycling stability. Certain metal oxides further enhance electrochemical performance by improving charge-transfer kinetics and facilitating ion and electron transport at the electrode–electrolyte interface [1,2].

Amorphous alumina (a-Al_2O_3)- and zinc oxide (ZnO)-coated NASICON-type phosphate cathodes were developed to enhance the electrochemical performance and durability of $Na_3VAl(PO_4)_3$ and $Na_3VFe(PO_4)_3$/C systems, respectively. The a-Al_2O_3-coated $Na_3VAl(PO_4)_3$ samples were synthesized through a low-cost, scalable, and environmentally friendly sol-gel process, while the ZnO-coated $Na_3VFe(PO_4)_3$/C samples were prepared using a scalable two-step method. Structural analyses confirmed that the coatings did not alter the crystal structure of the host materials, as evidenced by X-ray diffraction. Raman, NMR, and electron microscopy revealed the coexistence of amorphous carbon and oxide coatings uniformly deposited on the substrate surfaces. Ex-situ XRD and XPS analyses demonstrated the reversibility of sodium insertion and the redox participation of $V^{5+}/V^{4+}/V^{3+}$ in $Na_3VAl(PO_4)_3$ and V/Fe species in $Na_3VFe(PO_4)_3$/C, with aluminum oxyfluoride formation indicating effective HF removal and improved electrode stability (Figure 1).

Electrochemical evaluations confirmed that oxide coatings significantly enhanced sodium-ion transport kinetics and rate capabilities. For a-Al_2O_3-coated $Na_3VAl(PO_4)_3$, 1-3% coatings improved high-rate capacity, lowered cell resistance, and increased capacitive contributions and diffusion coefficients, with the 2% coating showing optimal performance and excellent capacity retention at both room and low temperatures. Similarly, ZnO-coated $Na_3VFe(PO_4)_3$/C samples with 1-3% coatings exhibited superior high-rate performance due to reduced impedance and enhanced Na^+ exchange at the electrode-electrolyte interface. The 3% ZnO coating delivered the best long-term cycling stability and maintained high diffusion coefficients after extended cycling.

Overall, these findings demonstrate that controlled surface engineering with thin oxide coatings such as a-Al_2O_3 and ZnO effectively enhances sodium-ion transport, suppresses interfacial degradation, and extends the lifespan of NASICON-type phosphate cathodes for high-performance sodium-ion batteries.

Keywords: Sodium-ion batteries, Aluminum oxide, zinc oxide, coating, NASICON, sodium vanadium phosphate.

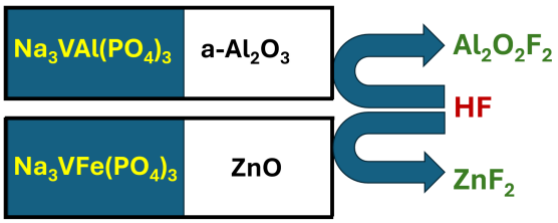

Figure 1: Mechanism of protection against fluoride anions by Al_2O_3 ad ZnO coatings.

References:

1. Lavela, S., Pérez Vicente, C., Lavela, P., Tirado, J. L. (2025) Boosting the cycling stability of $Na_3VFe(PO_4)_3$ cathodes for sodium-ion batteries by zinc oxide coating. *J. Energy Storage* 118, 116295.
2. Lavela, S., Pérez Vicente, C., Lavela, P., Tirado, J. L. (2025) Dual surface-bulk aluminium modification in a-Al_2O_3@ $Na_3VAl(PO_4)_3$ sodium-ion batteries cathode to boost high voltage utilization and electrolyte protection. *J. Power Sources* 625, 235703.

Optimizing Slot-Die Coating of High-Viscous Slurries for Energy and Green Technology Applications

Kristoffer V. Graae, Jeppe Hansen and Vladimir Popok *
FOM Technologies, Copenhagen, Denmark

Abstract:
Slot-die coating has established itself as a key deposition technique for thin and uniform functional coatings, particularly for low-viscosity inks where micrometer-scale wet film thickness and nanometer-scale dry coating can be achieved with high uniformity [1, 2]. However, the transition to high-viscous slurries, such as those used in battery electrode manufacturing and in technologies of carbon dioxide capture, presents significant challenges in flow distribution and coating homogeneity especially if the film width is high.

In this work, we present recent developments on the optimization of slot-die head (SD) for high-viscous slurries carried out at FOM Technologies. By employing computational fluid dynamics (CFD) simulations, we systematically iterated through manifold designs to minimize internal flow resistance and improve homogeneity while maintaining a compact SD geometry. A key objective was to achieve a wide coating width while minimizing the distance from the inlet manifold to the lip, thereby preserving low internal volume and usability in a lab environment, while ensuring a stable, uniform coating process. In Figure 1, one can see how the change of SD configuration allowed to approach homogeneous delivery of the ink across the SD with width of 30 cm. It was found that variation of the ink speed can be significantly reduced if the SD has three inlets instead of one. However, such configuration would complicate manufacturing and following operation of SD with the pump during the coating. Therefore, we kept one inlet but rather changed volume and shape of manifold inside the SD that allowed to reduce the ink speed relative deviation across the width to 1.5%.

Experimental validation of the newly optimized SD in application to typical carbon-containing slurries used in coating of battery electrodes (viscousity of up to 20 Pa.s) showed an order of magnitude improvement in homogeneity of the films compared to a standard head. In the presentation, we will show both CFD simulation results and experimental coating data highlighting the critical role of application-specific slot-die head design in achieving high-performance coatings. These findings underscore the necessity of tailored manifold geometries for different material systems, paving the way for enhanced precision in functional coatings for energy storage and green technology applications.

Keywords: slot-die coating, high-viscous slurry, computational fluid dynamics, battery electrodes, carbon capture.

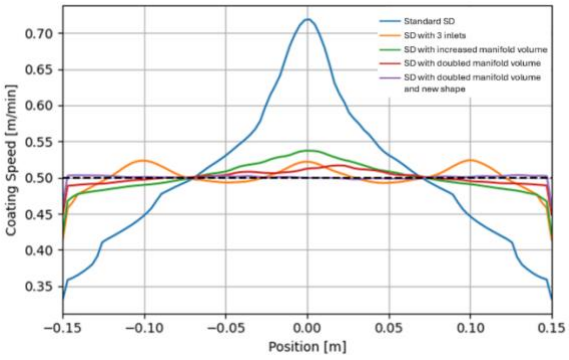

Figure 1: Dependence of coating speed on position at 30 cm wide slot ("0" corresponds to middle of SDH, while "-0.15" and "0.15" indicate edges) for different designs of manifold.

References:

1. Ding, X., Liu, J., Harris, T.A.L.(2016) A review of the operating limits in slot die coating processes, *Amer. Inst. Chem. Eng, J.*, 62, 2508.
2. Sarka, F., Tobis, Z. (2022) Design Issues for Slot-Die Coating Heads - Case Study, *IOP Conf. Ser.: Mater. Sci. Eng.*, 1237, 012014.

Sequential Surface Treatment and Insulation Testing of Additively Manufactured Litz Conductors

Andrzej P Sankowski[1], Dominic North[1], Nick Simpson[1]
[1]Department of Electrical and Electronics Engineering, University of Bristol, Bristol, UK

Abstract:
As electric mobility and power electronics continue to develop, the demand for more compact and efficient high-performance components is driving innovation in conductor design and manufacturing. Additive manufacturing (AM) offers new geometric and integration possibilities for high-voltage winding such as Litz hairpins but also introduces surface roughness and microstructural inconsistencies that may compromise insulation reliability. Surface topology, interfacial cleanliness, and coating integrity are all critical to ensuring long-term electric performance. In this work, we will investigate the evolution of surface morphology and insulation quality in AM Litz hairpins through a sequential process of treatment and characterisation. Initially as-printed copper hairpins will be evaluated using X-ray computer tomography (CT) and surface roughness measurements to quantify defects and surface features. Electropolishing will then be applied to reduce the surface roughness, followed by repeat CT and profilometry to assess morphological changes. A polymer dielectric coating is then subsequently deposited via electrostatic powder coating and final CT scan will evaluate coating uniformity and filling. To assess the dielectric performance of the full process chain, breakdown voltage measurements will be conducted of full treated and coated samples. The results are expected to reveal correlations between surface conditioning and electrical performance, offering insights into the role of post-processing in enabling reliable insulation of AM components for high-performance applications.

Keywords: additive manufacturing, copper, Litz bar conductors, electropolishing, surface roughness, PEEK coating, electrical insulation, breakdown voltage

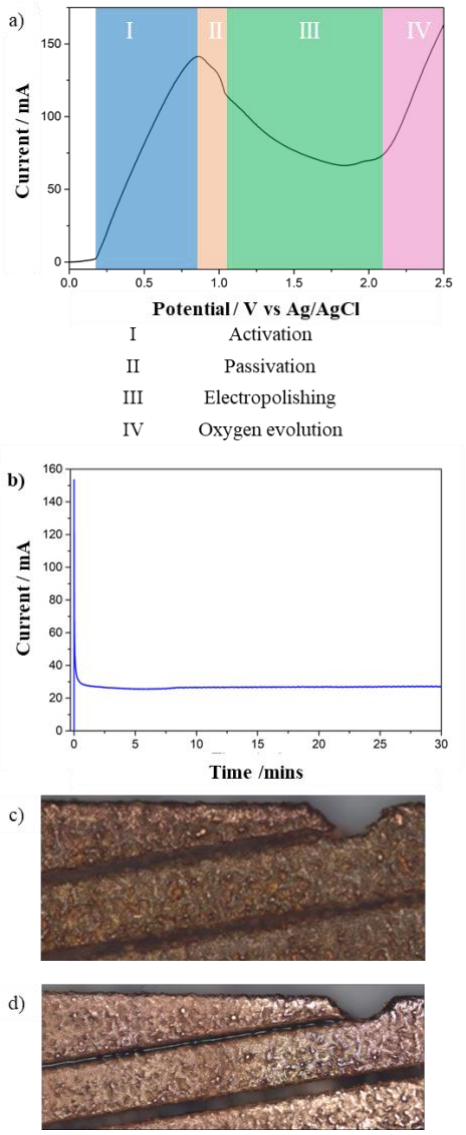

Figure 1 (a) Linear sweep voltammogram of copper showing the different regions between 0 and 2.5 V vs Ag/AgCl, (b) chronoamperometric response of the electropolishing process at a fixed potential of 1.5 V vs Ag/AgCl. (c) and (d) light microscopy images of AM copper before and after the process carried out in (b). Electrochemical measurements were done in 85 % H3PO4 electrolyte with AM copper as the working electrode, Cu wire as the counter electrode and a Ag/AgCl reference electrode.

Surface Engineering of 3D-Printed PVA Structures for the Integration of Functionalized UCNPs into Stable Hydrogel Systems.

Abril Peñaloza Guachalla*, Mirko Maturi, Alberto Sanz de León, Miriam Herrera
Dpto. Ciencia de los Materiales, I. M. y Q. I., IMEYMAT, Facultad de Ciencias, Universidad de Cádiz, Campus Río San Pedro, s/n, 11510 Puerto Real (Cádiz), Spain.

Abstract:
The integration of functional nanoparticles into additively manufactured nanocomposite systems remains a significant challenge due to interfacial incompatibility between nanoparticle surfaces and polymer matrices [1]. Overcoming this limitation is essential to fabricate structurally robust hybrid materials with advanced functionalities.
In this work, poly (vinyl alcohol) (PVA) porous structures were first fabricated via fused deposition modeling (FDM) and subsequently transformed into hydrogels through controlled swelling and crosslinking processes. Critical parameters, including crosslinker concentration and reaction time, were systematically optimized according to geometry and mass to preserve structural integrity during hydrogel formation.
To enable efficient nanoparticle incorporation, PVA was chemically modified via Steglich esterification [2] to introduce a chromophore and improve interfacial compatibility. The upconversion nanoparticles (UCNPs), lanthanide-doped nanomaterials capable of converting near-infrared excitation into visible emission, are promising for optical sensing applications. The modified polymer was then used in a ligand exchange process to render the UCNPs surface compatible with the PVA structures prior to hydrogel formation. This sequential strategy ensured interfacial compatibility, homogeneous nanoparticle distribution, and structural stability throughout the transformation from printed polymer to hydrogel.
As proof of concept, the resulting hybrid hydrogels exhibited a selective visible optical response upon exposure to Cu^{2+} ions, demonstrating successful functional integration of the nanostructures. A schematic representation of the sequential process, from printing, nanoparticles functionalization and incorporating to hydrogel formation and sensing is presented in Figure 1.
These results establish a scalable approach for integrating functional nanoparticles into 3D-printed polymer structures and highlight the critical role of interfacial control in the development of robust hydrogel-based functional materials.

Keywords: 3D printing, PVA, hydrogels, upconversion nanoparticles, surface engineering, additive manufacturing, sensors.

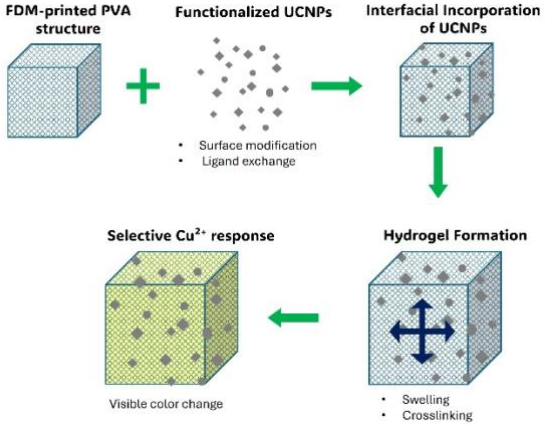

Figure 1: Schematic overview of UCNP integration into 3D-printed PVA hydrogels for selective Cu^{2+} sensing.

References:

1. Arai, M. S., & de Camargo, A. S. S. (2021). Exploring the use of upconversion nanoparticles in chemical and biological sensors: From surface modifications to point-of-care devices. In *Nanoscale Advances* (Vol. 3, Issue 18, pp. 5135–5165). Royal Society of Chemistry.
2. Lutjen, A. B., Quirk, M. A., & Kolonko, E. M. (2018). Synthesis of Esters Via a Greener Steglich Esterification in Acetonitrile. *Journal of Visualized Experiments: JoVE*, *140*.

Characterization and Optimization of a Plasma Source for the Biological Decontamination of Wastewater in Volume

M. Saba*, C. Muja, Ph. Guillot, Th. Maho
Univ Toulouse, INUC, DPHE, Albi, France
Contact: maria.saba@univ-jfc.fr

Abstract:
Antibiotic residues in hospital wastewater promote the development and spread of antibiotic resistance, making it a major environmental source of antibiotic-resistant bacteria (ARB) and antibiotic-resistance genes (ARGs). The limited efficiency of conventional wastewater treatment systems in removing ARB and ARGs [1] highlights the need for sustainable and advanced treatment solutions.
Cold plasma constitutes an alternative to conventional wastewater treatment methods due to its ability to generate reactive species with biocidal effects. This project aims to characterize and optimize a modular wastewater decontamination system based on the generation of immersed atmospheric-pressure plasma, which is expected to reduce bacterial and viral loads within a reasonable treatment time.
The plasma reactor consists of a 50 ml glass container with a tube for gas injection (figure 1). The gas is introduced into the tube and released from its submerged end, forming bubbles in the water. A high-voltage electrode is inserted into the tube and connected to a pulsed power supply that generates voltage pulses with duration shorter than 3 µs. The applied voltage amplitude ranges from 1 to 20 kV, with a fixed repetition frequency of 20 kHz. A grounded counter-electrode is wrapped around the outer surface of the water container. The standard tube can be easily replaced with tubes featuring different nozzle designs, allowing different bubbles generation in the water.
An equivalent electrical circuit was used to estimate the energy deposited into the plasma discharge during a single pulse. The total current was measured with a current monitor (PEARSON™ 6585), while the applied voltage was recorded with a voltage probe (Tektronix P6015A). Both waveforms were captured by a digital oscilloscope (ROHDE & SCHWARZ RTE1204). Optical emission spectroscopy (PI-HRS-750 coupled with a PI-MAX4) was conducted to identify the reactive species generated by the plasma for various gas mixtures. Additionally, an ICCD camera (PI-MAX1) was used to follow the plasma propagation in the water during a single pulse.
Plasma–liquid interactions were investigated by measuring the concentrations of various reactive oxygen and nitrogen species (RONS) under different gas mixtures, including H_2O_2, O_3, NO_3^-, NO_2^-, and OH. These measurements enabled the selection of the optimal gas mixture and reactor configuration for water decontamination. Finally, clean water and wastewater models were inoculated with *Escherichia coli* to assess the system's decontamination efficiency.

Keywords: Plasma, decontamination, equivalent circuit, optical emission spectroscopy, ICCD camera, RONS.

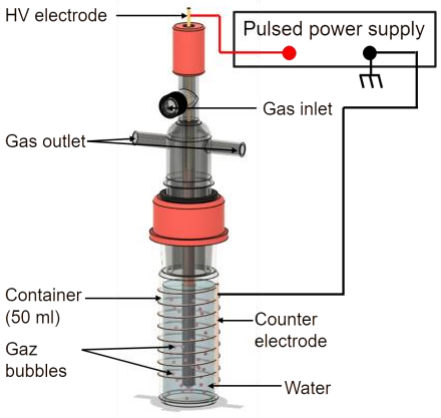

Figure1: Schematic of the experimental setup

References:

1. Evoung Chandja, W. B., Onanga, R., Mbehang Nguema, P. P., Lendamba, R. W., Mouanga-Ndzime, Y., Mavoungou, J. F., & Godreuil, S. (2024). Emergence of antibiotic residues and antibiotic-resistant bacteria in hospital wastewater: A potential route of spread to african streams and rivers, a review. *Water*, 16(22), 3179.

How Silicone–Acrylic Coatings Deliver Durable Ice Repellency for Wind Turbine Blades under Harsh Environmental Conditions

F. Eslampanah*[1], G. Momen[1,2], R. Jafari[1]
[1] Department of Applied Sciences, Université du Québec à Chicoutimi (UQAC), Chicoutimi, Canada
[2] Department of Aerospace engineering, École de technologies supérieures, Montréal, Canada

Abstract:
In response to the growing global demand for reliable operation in harsh climates, both wind-energy and aerospace sectors increasingly deploy critical structures in cold and high-altitude environments. In such conditions, atmospheric icing and environmental weathering can severely compromise surface functionality: ice accretion increases drag and mass, reduces aerodynamic efficiency, and accelerates mechanical fatigue, while UV and moisture-driven degradation progressively deteriorate polymeric and composite surfaces. Conventional anti-icing strategies are typically evaluated using a single coating formulation under simplified laboratory conditions, which limits their ability to predict coating performance in realistic service environments [1-3]. In this study, durable silicone–acrylic hybrid coatings are developed as a protective layer that balance long-term mechanical and environmental stability with ice-phobic performance. Although the preparation methods and different performance of silicone-based coatings have been widely investigated, reports on the weathering durability behavior of modified silicone–polyacrylate systems remain limited. At the molecular level, silicone side chains migrate toward the surface and lower the surface energy, which reduces ice adhesion, while the acrylate segments improve bonding to the substrate and maintain mechanical strength. The longer alkyl side chains increase chain flexibility, which promotes surface enrichment of the low-polarity silicone moieties and results in more effective and durable ice-phobic behavior (Figure 1). Two commercial silicone–acrylic resins with distinct chemical architectures were formulated using different curing agents and crosslinking densities. Structure–property relationships were systematically established through FTIR spectroscopy, surface profilometry, pendulum hardness, and adhesion testing, and correlated with anti-icing metrics including water contact angle, contact angle hysteresis, freezing-delay time, static push-off ice-adhesion strength, centrifugal adhesion testing, and cyclic icing/de-icing durability. The optimized formulation exhibits low ice-adhesion strength (≈ 12 kPa), prolonged freezing delay, and stable over 50 cycles with no delamination or cohesive failure, and ~3× lower ice adhesion than aluminum in CAT (Centrifugal Adhesion Test). Accelerated UV aging (3000 h) showed that the silicone–acrylic coatings retained their surface and anti-icing performance better than conventional silicone elastomers. These results demonstrate that silicone–acrylic hybrid coatings offer a scalable and durable solution for wind-turbine anti-icing applications, with potential extension to other outdoor energy infrastructures exposed to severe icing environments.

Keywords: silicone–acrylic hybrids; wind-turbine blades; durability; surface chemistry, ice-phobic coatings.

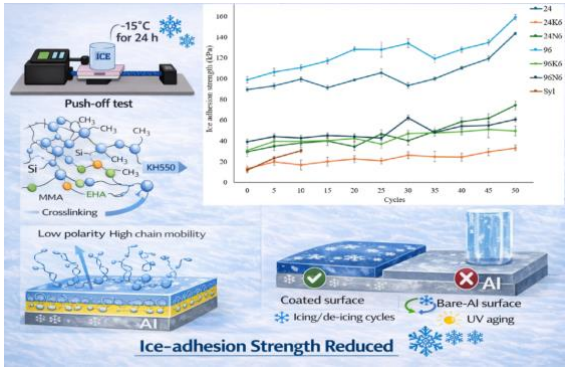

Figure 1: Schematic illustration of the chemistry–surface–performance relationship in silicone–acrylic hybrid coatings.

References:

1. Zheng, Z., et al., Preparation of protective coatings for the leading edge of wind turbine blades and investigation of their water droplet erosion behavior. Wear, 2024. **558-559**: p. 205568.
2. Minoofar, G., et al. Progress in Icephobic Coatings for Wind Turbine Protection: Merging Chemical Innovation with Practical Implementation. Crystals, 2025. **15**, 139
3. Zhu, T., et al., A polydimethylsiloxane coating with excellent large-scale deicing property and durability. Journal of Industrial and Engineering Chemistry, 2024. **139**: p. 492-501.

Enhancing the Photocatalytic Activity of BiOBr Supported by Graphene Oxide for Antibiotic Degradation in Wastewater

S. Promrit [1,*], C. Sronsri[1,2], S. Kaowphong [1,3],
[1] Department of Chemistry, Faculty of Science, Chiang Mai University, Chiang Mai 50200, Thailand
[2] Office of Research Administration, Chiang Mai University, Chiang Mai 50200, Thailand
[3] Materials Science Research Center, and Center of Excellence in Materials Science and Technology, Faculty of Science, Chiang Mai University, Chiang Mai 50200, Thailand

Abstract:
The development of bismuth-based photocatalysts offers a promising approach for wastewater treatment. In this work, bismuth oxybromide (BiOBr) was synthesized using a hydrothermal method and modified with graphene oxide (GO) at various loadings (0.5, 0.75, 1, 1.5, 2, and 3 wt%) to improve its photocatalytic performance. The photocatalytic activity of the BiOBr/GO composites was evaluated through the degradation of three antibiotics: ciprofloxacin (CIP), tetracycline (TC), and amoxicillin (AMX) under visible-light irradiation from a 100 W LED lamp. The residual concentrations of the antibiotics after reaction were quantified using UV-Vis spectrophotometry. X-ray diffraction (XRD) confirmed that BiOBr and all BiOBr/GO composite catalysts was a tetragonal phase. Scanning electron microscopy (SEM) and transmission electron microscopy (TEM) revealed that GO sheets were uniformly distributed on the square-like BiOBr microplates. UV-Vis DRS analysis showed that all synthesized material absorbed in the visible-light region, indicating their ability to utilize visible irradiation. Moreover, the GO/BiOBr composites demonstrated stronger visible-light absorption with increasing GO content. Among all compositions, the 2%wt-GO/BiOBr photocatalyst exhibited the highest activity, achieved degradation efficiencies of 60% for CIP, 68% for TC, and nearly complete removal of AMX within 210 minutes. Reactive species trapping experiments were carried out to identify the dominant species involved in the reaction. Electrochemical analysis indicated that the incorporation of GO facilitated charge carrier separation and suppress electron-hole recombination. This work demonstrates that incorporating an appropriate amount of GO into BiOBr improves its photocatalytic performance toward antibiotic degradation, demonstrating the potential of BiOBr/GO composites for wastewater treatment.

Keywords: bismuth-based photocatalyst, photocatalytic activity, graphene oxide, antibiotic degradation, wastewater treatment

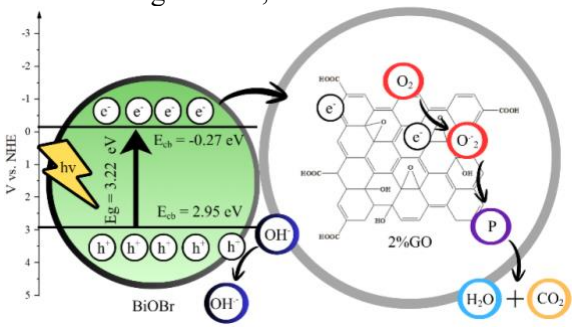

Figure 1: Proposed photocatalytic mechanism of the 2 wt% GO/BiOBr catalyst, showing GO acting as an electron acceptor to support charge separation and promote the degradation of antibiotic pollutants under visible-light irradiation.

References:

1. Li, C., Wang B., Zhang, F., Song, N., Liu, G., Wang C., Zhong S. (2020), Performance of Ag/BiOBr/GO composite photocatalyst for visible-light-driven dye pollutants degradation, *J. Mater. Res. Technol*., 9, 1, 610–621.
2. Wang, Y., Ding, K., Xu, R., Yu, D., Wang, W., Gao, P., Liu, B. (2020), Fabrication of $BiVO_4$/$BiPO_4$/GO composite photocatalytic material for the visible light-driven degradation., *J. Clean. Prod*., 247, 119108.
3. da Silva, P.H.D.A., de Souza, D.A., Filho, R.L.D.F., et al. (2024), GO@β-Ag_2MoO_4 composite: one-Step synthesis, characterization, and photocatalytic performance against RhB dye. *ACS. Physical Chemistry Au*, 4, 6, 632-646.

Atmospheric-Pressure Plasma for the Degradation of Bisphenols as Emerging Contaminants in Aqueous Systems

C. Ruzafa Silvestre[1]*, V.M. Serrano Martínez[1], L. Peinado Medrano[1], M.I. Maestre López[1], H. Pérez Aguilar[1], M.D. Romero Sánchez[1]

[1]Footwear Technology Center (INESCOP), Pol.Ind. Campo Alto, 03600, Elda, Alicante, Spain

Abstract:

Bisphenols (e.g., BPA and BPF), widely used endocrine-disrupting compounds, are increasingly recognized as emerging contaminants and represent a challenge for conventional water-treatment systems due to their persistence and incomplete removal by standard processes. These compounds are commonly employed in the manufacture of polycarbonate plastics and epoxy resins, which are widely used in food packaging, coatings, thermal papers, and leather finishing applications, leading to their continuous release into aquatic environments. As a result, their presence has been frequently detected in industrial effluents and surface waters. Plasma-Activated Water (PAW) [1], generated by non-thermal atmospheric-pressure plasma, has been proposed as a chemical-free oxidative medium capable of promoting the transformation of such contaminants.

The interaction between plasma and the liquid phase generates a complex mixture of short- and long-lived reactive oxygen and nitrogen species (RONS), which can trigger advanced oxidation pathways capable of degrading or transforming a wide range of recalcitrant contaminants [2]. In this work, we evaluate the ability of PAW to induce chemical transformations in selected bisphenols used as representative model pollutants. Specifically, several model compounds were examined, including bisphenol A (BPA), bisphenol F (BPF), and related analogues, in order to assess how plasma parameters, discharge configuration, and gas composition affect RONS generation, the evolution of liquid-phase chemistry, and ultimately the transformation efficiency of these compounds.

Complementary analytical techniques, including High-Performance Liquid Chromatography coupled with Tandem Mass Spectrometry (HPLC-MS/MS), together with the measurement of key physicochemical parameters and reactive species in solution, provide detailed insight into the degradation mechanisms of the selected bisphenols. The results demonstrate that PAW promotes the chemical degradation of these compounds, enabling the identification of specific oxidative pathways and structural modifications induced by plasma-generated reactive species.

This study contributes to a better understanding of plasma–liquid interactions by examining the effect of Plasma-Activated Water on selected bisphenol model compounds. Rather than making broad technological claims, this work focuses on elucidating the specific chemical transformations induced by PAW and the oxidative processes involved. These findings represent a first step toward assessing the potential of PAW-based approaches for contaminant removal, while highlighting the need for further systematic studies before drawing conclusions regarding scalability or large-scale implementation.

Keywords: Plasma-Activated Water, plasma–liquid interactions, emerging contaminants, oxidative water treatment, bisphenol degradation, reactive species chemistry, environmental plasma technologies.

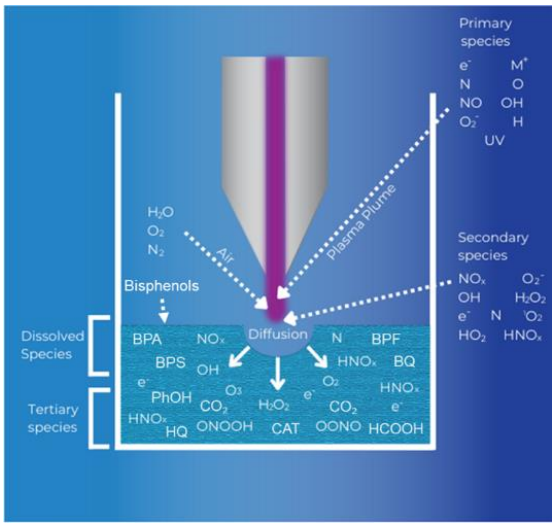

Figure 1: Schematic of the reactive species and bisphenols degradation products in PAW using an atmospheric plasma jet.

References:

1. Al-Sharify ZT, Al-Sharify TA, al-Obaidy baker W, et al. Investigative Study on the Interaction and Applications of Plasma Activated Water (PAW). IOP Conf Ser Mater Sci Eng 2020; 870: 012042.
2. Zhou R, Zhou R, Wang P, et al. Plasma-activated water: generation, origin of reactive species and biological applications. J Phys D Appl Phys 2020; 53: 303001

Tribology 2026 Session III. B: Health, Safety & Industrial Impact / Biotribology

Recent Insights and Perspectives in In-Silico Modeling of Synovial Lubricated Total Hip Replcaements

Alessandro Ruggiero
Department of Industrial Engineering, University of Salerno, Fisciano (SA), Italy

Abstract:
The aim of this keynote was to describe the latest research results achieved at the Department of Industrial Engineering of the University of Salerno by the research group headed by the Author, in the framework of the computational (bio) tribological and biomechanical modelling of lubricated total hip replacements (THR), accounting for the possibility to consider the topography of the contact surfaces during the unsteady conditions.

Main aim of the research was, in fact, to accurately predict the in-silico wear of artificial implants, modelling the complex tribological phenomena acting in the joints due to the synovial lubrication, considering unsteady loading of the joint and the real contact surfaces morphology observed during detailed optical analysis executed on retrieved systems.

In this speech were underlined recent computational approaches obtained by merging multibody models, solving the inverse dynamics of musculoskeletal systems, and synovial mixed elasto-hydrodynamic lubrication models, also in presence of rough surfaces.

The effectiveness of the proposed analysis consists in the possibility of examining many physical activities, characterized by cyclic kinematic and loading joint conditions like running, swimming and sport in general, in order to predict the implant duration overcoming excessive time and money consumption due to the experimental set-up and investigation, moreover taking into account the complexity of a mixed lubrication model adaptable to several synovial fluid lubrication properties and that considers the surfaces' contact.

Keywords: Computational Biotribology, Biomechanics, Total Hip Replacements, Synovial Lubrication, Wear.

Tribological Investigation of Gear Ratio Effect on Wear Behaviour in Standard Spur Gears

Y. Li[1*], H. K Nguyen[1], Z. Peng[1]
[1] School of Mechanical and Manufacturing Engineering, University of New South Wales, Australia

Abstract:
The influence of gear ratio on wear behaviour in standard spur gears is critical for understanding gear performance and lifespan in mechanical systems. Despite considerable advances in tribology and gear mechanics, and numerous studies examining gear wear under different loads and lubrication conditions, the effect of gear ratio – an important design factor – on gear wear behaviour remains largely understudied. As a result, detailed experimental data quantifying the influence of gear ratio on wear characteristics, surface degradation, and wear particle generation are scarce.
The present study investigates three pairs of standard spur gears with varying gear ratios (19/52, 27/44, and 35/36) subjected to wear testing under dry-running conditions using a single-stage spur gearbox rig. To facilitate the examination of the gear teeth during the wear process, a moulding method was employed to obtain gear tooth mould samples. Tooth surface roughness was performed on the moulds using laser scanning microscopy and quantitative characterisation, while the wear depth measurements were conducted using optical microscopy. Results showed that higher gear ratios lead to greater overall wear, higher average wear depth, and increased particle concentration. The findings offer deeper insight into how gear ratios influence wear evolution. The experimental data provides a foundation for developing effective, real-time gear wear monitoring techniques.

Keywords: gear ratio, spur gears, wear depth, surface roughness, wear particles, laser scanning microscopy, optical microscopy.

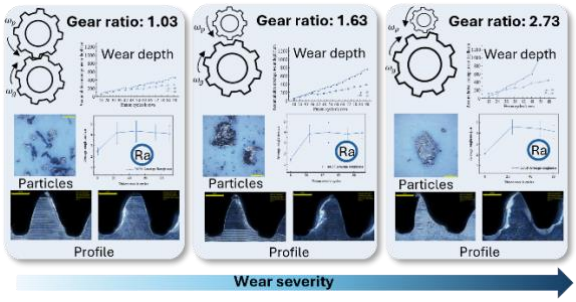

Figure 1: This figure summarises the central experimental problem we aim to solve: How does gear ratio influence wear progression under identical operating conditions? What is the influence of gear ratio on the wear behaviour of spur gears under identical operating conditions, and how do particle morphology, surface roughness, wear depth, and tooth-profile evolution collectively reflect the underlying wear mechanisms?

References:

1. Saboohi, Y., & Farzaneh, H. (2008). Model for optimizing energy efficiency through controlling speed and gear ratio. *Energy Efficiency*, *1*(1), 65-76.
2. Gao, B., Liang, Q., Xiang, Y., Guo, L., & Chen, H. (2015). Gear ratio optimization and shift control of 2-speed I-AMT in electric vehicle. *Mechanical Systems and Signal Processing*, *50*, 615-631.
3. Ravivarman, R., Palaniradja, K., & Sekar, R. P. (2018). Influence of gear ratio on wear depth of nonstandard HCR spur gear drive with balanced fillet stress. *Materials Today: Proceedings*, *5*(9), 17350-17359.

Tribological Evaluation of Oral Lubrication and Soft Tissue Interactions

Y.C. Chang [1,2], H.-W. Fang [1,2,3] *
[1] Department of Chemical Engineering and Biotechnology, National Taipei University of Technology, Taipei, Taiwan
[2] High-value Biomaterials Research and Commercialization Center, National Taipei University of Technology, Taipei, Taiwan
[3] Institute of Biomedical Engineering and Nanomedicine, National Health Research Institutes, Miaoli, Taiwan

Abstract:
Xerostomia, or chronic dry mouth, significantly impairs quality of life by reducing the lubricating efficacy of saliva, which leads to painful mechanical irritation during chewing and speech. This study aims to establish a tribological framework to guide the development of longer-lasting artificial saliva substitutes that mimic natural oral functions. The in vitro and ex vivo friction testing systems using a micro-tribometer to simulate the oral environment were developed here. Polydimethylsiloxane (PDMS) and porcine tongue tissues were utilized to model soft-tissue-to-soft-tissue interactions under varying physiological loads and speeds. The findings reveal that under lubricated conditions, increased normal loads elevate the friction coefficient, suggesting that current lubricants may fail under the high pressures of mastication. Furthermore, tongue surface roughness was found to be a critical clinical variable; while roughness aids in reducing friction in dry states, it may inadvertently increase resistance in the presence of certain lubricants due to component adsorption or specific rheological properties. These results demonstrate that artificial saliva must be engineered not just for moisture, but for specific interfacial behaviors and rheological stability. By understanding the relationship between surface asperity deformation and lubricant interaction, clinicians and researchers can develop targeted therapies that reduce mechanical wear on oral tissues, ultimately improving nutritional intake and social comfort for patients with reduced salivary function.

Keywords: Xerostomia, artificial saliva, soft tissue irritation, oral lubrication, surface roughness.

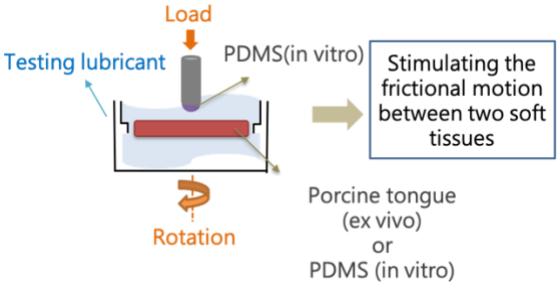

Figure 1: The in vitro and ex vivo friction testing systems established in this study can be applied to screen lubricants for artificial saliva applications.

References:

1. Kumar, B., Kashyap, N., Avinash, A., Chevvuri, R., Sagar, M.K., Shrikant, K. (2017) The composition, function and role of saliva in maintaining oral health: A review. *Int. J. Contemp. Dent. Med. Rev.,* Article ID 011217:1-6.
2. Stokes, J.R., Boehm, M.W., Baier, S.K. (2013) Oral processing, texture and mouthfeel: From rheology to tribology and beyond. *Curr. Opin. Colloid Interface Sci.*, 18, 349-359.

Simulating Tire Wear in the Laboratory: Linking Wear Behaviour of NR/BR Rubber Compounds with Fracture Energy

D. Rebenda [1,2,*], R. Stocek [1]
[1] Centre of Polymer Systems, Tomas Bata University in Zlin, Zlin, Czechia
[2] Faculty of Mechanical Engineering, Brno University of Technology, Brno, Czechia

Abstract:
Tire friction and wear are among the most critical parameters that determine the service life, fuel efficiency, and safety of road-going vehicles. In addition to performance and economic considerations, tire wear has also recently attracted growing attention due to its environmental implications. The progressive removal of rubber material during tire–road interaction leads to the formation of tire and road wear particles (TRWP), which are released into various components of the environment [1]. These particles constitute a major source of non-exhaust traffic emissions and are now widely recognized as a significant contributor to microplastic pollution.
This study aims to investigate the friction and wear behaviour of natural rubber (NR) and butadiene rubber (BR) compounds under tire-simulating conditions. Study combines tribological testing under rolling and sliding configurations with fracture energy measurements to assess how intrinsic fracture properties govern wear processes under different tire operating conditions.
Friction and wear behavior of the NR/BR rubber compounds simulating truck and bus radial (TBR) tire treads was evaluated using laboratory test methods simulating different tire contact conditions. Rolling friction and abrasion were measured on a Coesfeld Friction & Wear Tester (CFWT) under a controlled load, speed and side angle, while wear was quantified by measuring the volume loss of the specimens. Sliding tests were performed using a Coesfeld Linear Friction Tester to provide steady-state coefficients of friction (COF) values under linear contact conditions. The fracture mechanical properties of the compounds were determined using an Intrinsic Strength Analyser, from which the crack initiation energy (T_0), so called intrinsic strength, and ultimate strength (T_C) were obtained.
The measured wear rates correspond well with the results of field measurements [2], indicating that the applied methodology provides field-relevant results. The results showed a decrease in COF and wear rate with increasing BR content, which is consistent with the well-known practical observations from tires in service. An increase in intrinsic strength corresponded to a reduction in wear rate (Fig. 1), indicating that crack nucleation governs the wear behaviour of the investigated NR/BR compounds under the applied testing conditions. In addition, a positive correlation between maximum surface temperature and wear rate was found. Increased surface temperature promotes wear by reducing the effective resistance to crack initiation and enhancing viscoelastic dissipation.
In summary, the applied methodology can provide field-relevant data on rubber wear and enables its mechanistic interpretation based on the fracture behaviour of rubber. The results highlight how BR content and fracture properties govern the wear behaviour of NR/BR compounds. The obtained data therefore provide a basis for predicting tire lifespan, optimizing compound formulations, and assessing environmental emissions from tire wear particles.

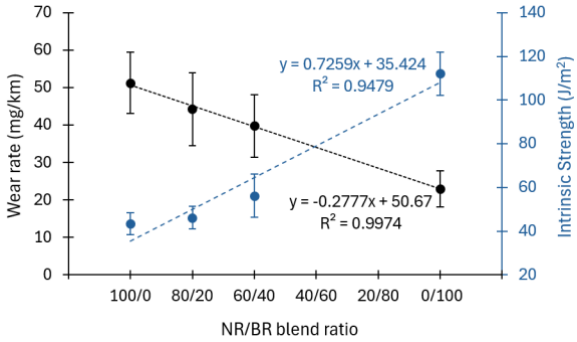

Fig. 1 Wear rate and Intrinsic strength for tested NR/BR blends

Keywords: NR/BR blend, tire wear, rubber abrasion

References:

1. Wang, Y., Li, W., Yang, W., Pu, Q., He, W., Li, X. (2024) A review of tire wear particles: Occurrence, adverse effects, and control strategies, *Ecotoxicol. Environ. Saf.*, 283, 116782.
2. Liu,Y., Chen H., Wu S., Gao J., Li Y., An Z., Mao B., Tu R., Li T. (2022) Impact of vehicle type, tyre feature and driving behaviour on tyre wear under real-world driving conditions, *Sci. Total Environ.*, 842, 156950.

Development of Process Optimization for FNC Brake Disc using DOE method

SM. Lee [1,*]
[1] Chassis Metal Materials Development Team, Hyundai Motor Company, Hwasung, Korea

Abstract:
This study examines the development and performance evaluation of an FNC disc produced by Ferritic Nitrocarburizing (FNC) for application in automotive chassis and power transmission systems. The objective is to enhance surface-related properties, including wear resistance and fatigue durability, through the application of optimized nitriding-based surface treatment processes while preserving adequate core toughness to ensure structural reliability under service conditions.
The limitations of conventional heat treatment methods for disk-type components subjected to repeated contact and cyclic loading are first addressed. In response, gas-based ferritic nitrocarburizing processes are investigated as an alternative surface engineering approach. The influence of key process parameters—such as treatment temperature, duration, and nitrogen potential—on nitrogen diffusion behavior, compound layer formation, and microstructural evolution in the diffusion zone is systematically analyzed.
Experimental results reveal that the optimized process leads to a significant increase in surface hardness and a marked improvement in wear performance compared to untreated and conventionally heat-treated counterparts. Microhardness profiling confirms the formation of a stable diffusion layer characterized by a gradual hardness gradient, which is beneficial for reducing stress concentration and improving fatigue resistance. Metallographic observations indicate that precise control of compound layer thickness is essential to prevent excessive brittleness and surface cracking.
Mechanical performance evaluations demonstrate that the FNC disc exhibits superior durability under simulated operating conditions, highlighting its suitability for demanding automotive applications. Overall, the findings confirm that ferritic nitrocarburizing is an effective surface modification technique for disk-type components, providing an optimal balance between surface strength and core integrity. This study offers practical insights for process optimization and supports the expanded application of FNC disc technology in advanced automotive material development.

Keywords: FNC, Brake disc, DOE

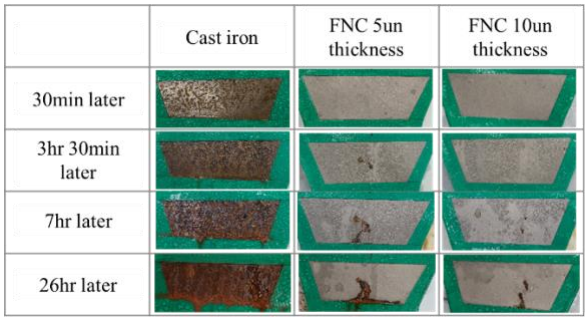

Figure 1: Figure illustrates the corrosion test results of three different disc specimens subjected to salt spray conditions. The basic cast iron specimen exhibited visible rust formation on the surface within 30 minutes. In contrast, the thicker FNC-coated disc demonstrated significantly higher corrosion resistance, with no observable rust until 26 hours of exposure. Based on these experimental results, the target FNC coating thickness for the brake disc was determined and applied in this study.

References:

1. 1. X.Hua et al. Recent progress in battery electric vehicle noise, vibration, and harshness, Science Progress, Vol. 104, 2021.
2. 2. M.Motta et al. Corrosion Stiction in Automotive Braking Systems, Vol. 16, 2023.
3. 3. S.Nousir, K.Winter, Enhancing Brake Performance: FNC-Smart-ONC® Technology to Address Corrosion Challenges and Extend the Durability of GCI Rotors, SAE Brake colloquium & Exhibition, 2024.

Adhesive Performance of Mushroom-Shaped Microstructure in Wet Condition: the Role of Deformation

L. Nasca[1*], M. Santeramo[1], C. Putignano[1], E. Pierro[1], G. Carbone[1,2]
[1] DMMM, Polytechnic University of Bari, Via Orabona 4 - 70125 Bari - Italy
[2] School of Physics, Nanjing University of Science and Technology, Nanjing - China

Abstract:
This study investigates the adhesion performance of bioinspired mushroom-shaped microstructures in wet environments, focusing on the detachment process mediated by a water droplet. Drawing from natural adhesive systems like insect pads [1], the research highlights how these structures outperform flat surfaces by leveraging deformability, capillary forces, and viscous effects.

The mathematical framework integrates fluid-structure interaction FSI [2] using a substructure approach. The solid deformation is modeled via finite element method FEM with a reduced stiffness matrix for computational efficiency, while the fluid flow follows the Reynolds equation solved by finite differences. Capillary pressure is captured through the Laplace equation, decomposing forces into bridge pressure and interfacial tension components. The model assumes axisymmetric geometry, incompressible fluid, and linear elasticity.

Numerical simulations reveal two phases: capillary attachment, with no imposed velocity to reach equilibrium, and forced detachment (Figure 1), with constant separation speed. Results show that mushroom deformability enhances adhesion by reducing meniscus curvature, amplifying negative Laplace pressure and suction. Pull-off force depends on dimensionless initial separation α, detachment velocity $\tilde{w}$, and droplet volume V. Lower α and higher V increase adhesion via stronger capillary suction and viscous un-squeeze, with forces up to 20 times higher than cylindrical structures. From the contour plots on pull-off force we will illustrate how viscous contributions dominate at high speeds, while capillary effects prevail at low speeds.

Validated against literature[3], the model provides a predictive tool for optimizing bioinspired adhesives in robotics, biomedicine, and microfluidics, emphasizing the need for precise control of droplet volume and velocity to maximize performance and minimize losses.

Keywords: wet adhesion, fluid-structure interaction, deformable interfaces, liquid bridge mechanics, bio-inspired contacts.

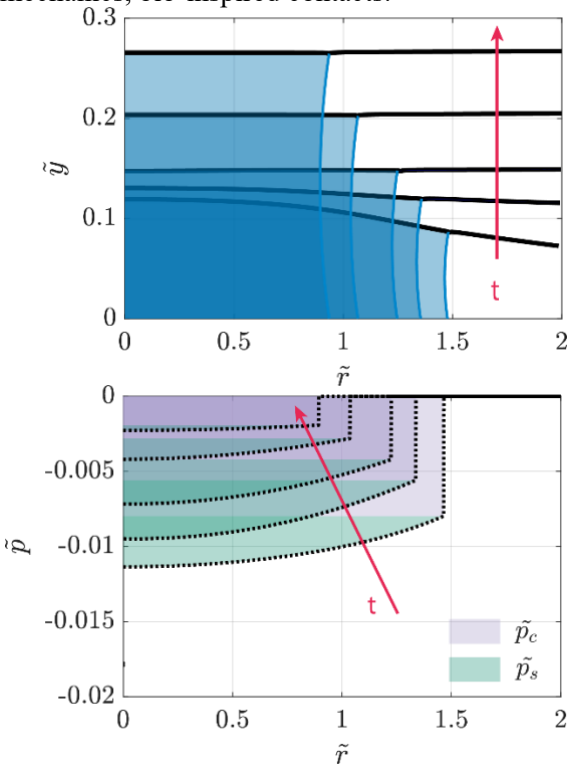

Figure 1: *Top*: Shape of the dimensionless deformed mushroom surface $\tilde{y}$ (black solid line) and the capillary bridge profile (blue solid line) of the drop (blue area); *Bottom*: Normalised pressure profile $\tilde{p}$ (black dotted line) as time t increases.

References:

1. Carbone, G. et al. (2011) Origin of the superior adhesive performance of mushroom-shaped micro structured surfaces, *Soft Matter*, 7, 5542.
2. Putignano, C. et al. (2022) Squeeze lubrication between soft solids: a numerical study, *Tribol. Int.,* 176, 107824.
3. Alexander, E. K. et al. (2012) Wet versus dry adhesion of biomimetic mushroom-shaped microstructures, *Soft Matter*, 8, 7560.

Posters Sessions

Influence of Diffusion-Modified Sublayers on the Performance of PVD Coatings on Austenitic Stainless Steel

K. Korsós [1*], D. Kovács [1]
[1] Department of Materials Science and Engineering, Faculty of Mechanical Engineering, Budapest University of Technology and Economics, Műegyetem rkp. 3., H-1111 Budapest, Hungary

Abstract:
Low-temperature thermochemical surface treatments are widely applied to austenitic stainless steels to improve their load-bearing capacity while preserving corrosion resistance. In parallel, hard ceramic coatings can be employed to enhance wear performance, although their effectiveness is often limited by insufficient substrate support.
In this work, the influence of different diffusion-modified sublayers on the mechanical support and tribological performance of a arc-based physical vapor deposition coating was systematically investigated. Austenitic stainless steel samples were prepared in eight conditions: untreated, untreated and coated, low-temperature plasma nitrided, low-temperature plasma nitrided and coated, low-temperature carburized, low-temperature carburized and coated, low-temperature carburized and low-temperature plasma nitrided and lastly low-temperature carburized and low-temperature plasma nitrided and coated. The resulting expanded austenite layers, alone and in combination, were characterized in terms of microstructure, surface hardness, layer thickness, and phase composition, while the tribological performance were assessed, using a ball-on-disc wear setup.
The tribological and mechanical testing revealed that diffusion-treated substrates significantly improve the load-bearing capacity and durability of the deposited coating compared to the untreated reference. The results highlight the critical role of sublayer design in optimizing PVD coating performance on austenitic stainless steels.

Keywords: low-temperature plasma nitriding, low-temperature carburizing, PVD, stainless steel, wear, tribology

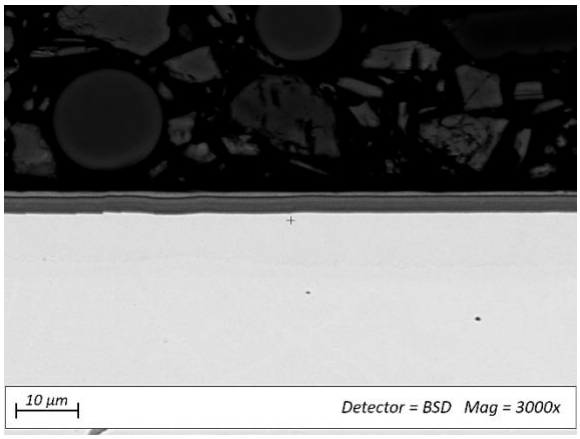

Figure 1: Illustrates the cross-section of the low-temperature plasma nitrided and AlTiN+TiCN physical vapor deposition coated sample

References:

1. Bello, K. A., Abubakar, I. I., Dodo, R. M., Bala, M. N., Bello, L. O., & Musa, Z. (2025). Effect of Low-Temperature Carburization on the Tribological and Corrosion Behavior of AlSl316 Austenitic Stainless Steel . FUOYE Journal of Engineering and Technology, 10(1), 125–133.
2. Zhou, Z., Sun, D., Li, H., Hao, J., Jiang, Y., Yong, J., Zhou, Z., Li, L., & Fei, Q. (2025). Wear performance of plasma nitrided and DLC coated AISI 316L stainless steel. *Surface and Coatings Technology*, *515*, 132672.

Patterned Nafion–Enabled Selective-Area Doping and Stable Low-Resistance Contacts in 2D WSe_2

Sewoong Oh, Seongil Im*
Physics, Yonsei University, Seoul, Republic of Korea

Abstract:
Selective-area doping and the reduction of contact resistance (R_C) remain critical challenges for two-dimensional (2D) semiconductor electronics. Unlike conventional three-dimensional semiconductors, ion implantation is not applicable to atomically thin materials, making spatially controlled doping in 2D systems particularly challenging. In addition, achieving low and stable R_C in 2D semiconductors has proven difficult. Here, we report a practical strategy for selective-area doping in 2D materials based on electron-beam patterning of a sulfonated tetrafluoroethylene-based fluoropolymer–copolymer (Nafion) underlayer with a high work function (Figure 1). The patterned Nafion underlayer selectively increases the hole density in p-type WSe_2, reducing the sheet resistance to levels compatible with integrated circuit applications. Top-gated WSe_2 field-effect transistors with Nafion-patterned channels exhibit a sevenfold enhancement in field-effect mobility compared to devices without Nafion. When selectively patterned at the contact regions, Nafion directly lowers R_C to ~6 kΩ·μm, which remains stable for over two months under ambient conditions and is preserved after N_2 annealing at 200 °C. This work demonstrates a versatile and robust approach to selective-area doping and stable contact engineering in 2D semiconductors, offering a technologically relevant pathway toward scalable 2D electronic devices.

Keywords: Selective-area doping, Contact resistance(R_C), Two-dimensional (2D) semiconductors, Nafion, Electron-beam patterning

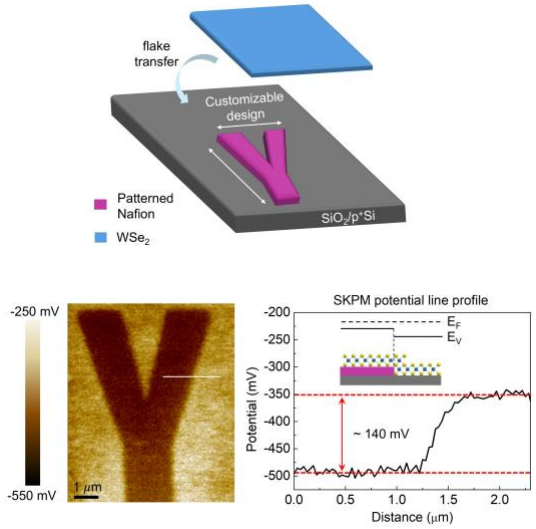

Figure 1: Electron-beam patterned underlayer Nafion excessively increases the hole density of p-type WSe_2. SKPM image and potential line profile of p-WSe_2 on 'Y' patterned Nafion, resulting from the electron charge transfer or hole doping which causes E_F-lowering or work function increase.

References:

1. Manzeli, S., Ovchinnikov, D., Pasquier, D., Yazyev, O. V. & Kis, A. (2017) 2D transition metal dichalcogenides. *Nat. Rev. Mater.* 2, 17033.
2. Allain, A., Kang, J., Banerjee, K. & Kis, A. (2015) Electrical contacts to two-dimensional semiconductors. *Nat. Mater.* 14, 1195–1205.

Functionalization of silica by nitrogen-containing silanes

K. Simanová [1,2,*], I. Melnyk [1]
[1] Institute of Geotechnics of SAS, Watsonova 45, 040 01 Košice, Slovak Republic
[2] Technical University of Košice, Letná 9, 040 01 Košice, Slovak Republic

Abstract:
Surface functionalization of silica with nitrogen-containing silanes is a widely used strategy to tailor the interfacial properties of silica-based materials by introducing organic groups that alter surface polarity, wettability, and charge, while simultaneously providing coordination sites for metal ions. In most cases, functionalization proceeds via hydrolysis of trialkoxysilanes followed by condensation with surface silanol groups (Si–OH**),** forming stable Si–O–Si linkages and an anchored organic layer. The extent of grafting**,** the spatial density of functional groups**,** and the choice of solvent strongly influence the resulting surface chemistry and accessibility of nitrogen donor atoms [1]. Alternative post-grafting approaches, including the use of pre-functionalized organosilanes, are also well established and can offer improved control over functional group placement and minimize unwanted side reactions during surface modification [2].
Incorporation of nitrogen functionalities (e.g., aliphatic amines, aniline-type groups, or pyridine moieties) creates Lewis-basic sites that can protonate in aqueous media and coordinate transition-metal cations through **N**-donor interactions. This enables the formation of specific surface complexes and makes N-functionalized silicas attractive as selective sorbents for water treatment, as well as supports for catalysis, chromatography, sensing, and hybrid bioactive systems [1].
In the present work, silica prepared from talc was functionalized using three nitrogen-containing trialkoxysilanes bearing N-phenylaminomethyl, 2-(4-pyridylethyl), and N-ethylaminoisobutyl substituents (Fig.1). The adsorption performance of the resulting materials was evaluated in multicomponent aqueous solutions containing Co^{2+}, Cu^{2+}, Ni^{2+}, and Cd^{2+} at comparable initial concentrations (~20 $mg \cdot L^{-1}$ each). Sorption capacities were determined from the differences between initial and equilibrium metal concentrations. Across all sorbents, a pronounced preference for Cu^{2+} was observed, with substantially lower uptake of Co^{2+}, Ni^{2+}, and Cd^{2+}. Such behavior is consistent with the strong tendency of Cu(II) to form stable complexes with nitrogen donor sites on amino-functionalized silica, particularly under competitive conditions. Among the prepared materials, silica modified with N-ethylaminoisobutyltrimethoxysilane exhibited the highest Cu^{2+} adsorption capacity, suggesting that the flexible aliphatic amine functionality provides more accessible and favorable coordination environments for copper binding than the more rigid aromatic or heteroaromatic nitrogen groups.

Keywords: silica-based materials, surface functionalization, metal ions adsorption.

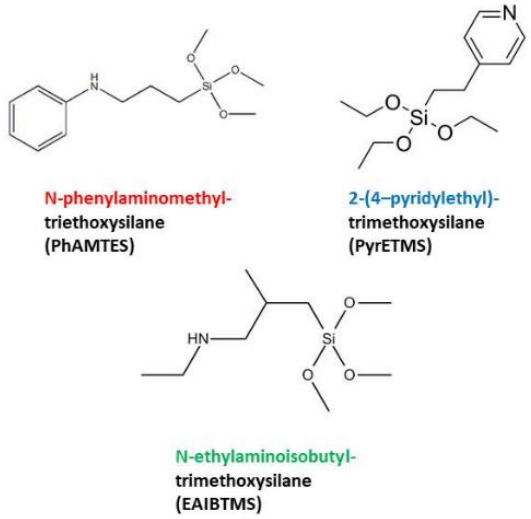

Figure 1: Chemical structures of the silane modifiers used for silica functionalization: PhAMTES, PyrETMS and EAIBTMS.

Funding: VEGA 2/0138/24 and the Recovery and Resilience Plan for Slovakia 09I03-03-V02-00029.

References:

1. Marzullo, P., Campisciano, V., Liotta, L.F., D'Anna, F., Giacalone, F., Gruttadauria, M. (2024) Trialkoxysilane grafting in alcohols: a simple approach towards modified silica-based materials, *Molecules*, 29(19), 4730.
2. Park, J.-W., Park, Y.J., Jun, C.-H. (2011) Post-grafting of silica surfaces with pre-functionalized organosilanes: new synthetic equivalents of conventional trialkoxysilanes, *Chem. Commun.*, 47, 4860–4871.

Voltex-Assisted Scale-Up of Intense Pulsed Light Surface Treatment of Low-Grade Carbon Fibers for Epoxy Composite Applications

Y.-J. Park[1], T.-Y. Kim[2], K.-S. Kim[1,*]
[1] Carbon & Light Materials Group, Korea Institute of Industrial Technology, Jeonju 54853, Korea
[2] Corporate Research Center, Onyx Co. Ltd., Jeonju 54870, Korea

Abstract:
This study investigates the scale-up of intense pulsed light (IPL) surface treatment of low-grade carbon fibers for epoxy composite applications using a 42 L vortex-forming chamber (Figure 1). To increase treatment capacity while maintaining processing uniformity, vortex flow conditions were examined to achieve homogeneous dispersion, stable suspension, and random rotation of chopped carbon fibers during IPL irradiation. Low-grade carbon fibers were chopped to 6 mm, desized in acetone for 2 h, dried at 110 °C for 2 h, and treated at 800–1400 V under fixed conditions of 4 ms pulse width, 1 Hz frequency, and 20 pulses. The vortex-assisted process achieved a treatment capacity of 0.64 kg/h. Surface energy increased at all applied voltages and reached a maximum of 39.2 mN/m at 1200 V, indicating that the optimal treatment voltage identified in a previous lab-scale study was preserved after scale-up. Repeated measurements at the same condition showed a surface-energy uniformity of 95.57%, indicating stable large-capacity processing. Interfacial shear strength (IFSS) with epoxy, evaluated by a microdroplet test, increased from 18.6 MPa for pristine fibers to 42.1 MPa at 1200 V. The matching voltage dependence of surface energy and IFSS suggests that the scale-up process maintained the essential surface-activation effect of IPL treatment. These results demonstrate that vortex-assisted IPL treatment is an effective scale-up strategy for surface activation of low-grade carbon fibers, providing improved fiber/resin interfacial performance for composite manufacturing.

Keywords: Intense pulsed light (IPL), low-grade carbon fiber, vortex-forming chamber, interfacial shear strength (IFSS), epoxy composites.

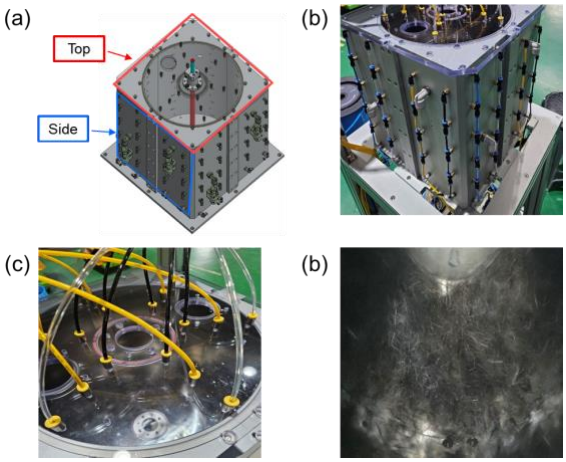

Figure 1 : (a) Schematic diagram of the air injection directions in the vortex chamber, (b) side hose fittings, (c) top hose fittings, and (d) photograph of carbon fibers inside the chamber after surface treatment.

References:

1. Kim, M., Goh, B., Kim, J., Kim, K.-S., Choi, J. (2022). Regeneration of interfacial bonding force of waste carbon fibers by light: Process demonstration and atomic level analysis, *iScience*, 25, 105367.
2. Rich, M.J., Drown, E.K., Askeland, P., Drzal, L.T. (2013). Surface treatment of carbon fibers by ultraviolet light + ozone: its effect on fiber surface area and topography, *In Proceedings of the ICCM Conference*, pp. 1196-1204.

Bouncing characteristics of multi-component droplets with viscosity contrast for a control of the hydrodynamics

S. Yun
Department of Mechanical Engineering, Korea National University of Transportation, 27469, Republic of Korea

Abstract:
Multi-component droplets consist of two or more immiscible liquid phases separated by a stable internal interface. Recent advances have demonstrated that coupling such droplets with engineered surface geometries can promote asymmetric rebound or directional propulsion [1–3]. In this study, combined experimental measurements and numerical simulations are performed to investigate how substrate curvature governs the rebound dynamics and separation characteristics of Janus droplets. The impact behavior is systematically examined over a broad range of Weber numbers and viscosity ratios to capture the dominant physical mechanisms.

Upon impact, the Janus droplet—with distinct viscosities in each compartment—preserves its biphasic structure while undergoing pronounced deformation and retraction. The results reveal critical Weber numbers that determine separation onset, which depend on droplet size, viscosity contrast, and surface curvature. A regime map is developed to classify the separation modes in terms of Weber number and viscosity ratio. The findings show that curved substrates intensify asymmetries in mass redistribution and momentum evolution during spreading and retraction. This curvature-induced asymmetry, coupled with anisotropic geometric confinement, markedly reduces the residence time of the droplet. The present study provides new insights into curvature-mediated control of multi-component droplet dynamics and offers design guidelines for applications requiring rapid separation and rebound manipulation.

Keywords: superhydrophobic surface, self-cleaning, interfacial dynamics

Acknowledgments:
This was supported by the National Research Foundation of Korea (NRF) grant funded by the Korea government (MSIT) (No. RS-2025-23523856).

References:

1. Clarke, A. (2002). Coating on a rough surface. AIChE Journal, 48(10), 2149-2156.
2. Bhushan, B., & Jung, Y. C. (2011). Natural and biomimetic artificial surfaces for superhydrophobicity, self-cleaning, low adhesion, and drag reduction. Progress in Materials Science, 56(1), 1-108.
3. Clanet, C., Béguin, C., Richard, D., & Quéré, D. (2004). Maximal deformation of an impacting drop. Journal of Fluid Mechanics, 517, 199-208.

Effect of Post-Heat Treatment on the Structural and Mechanical Properties of CrAlN/Al_2O_3 Functionally Graded Coatings for Tool Applications

W. R. kim, B. M. Lee, I. W. Park and S. B. Heo *
Dongnam regional division, Korea Institute of Industrial Technology, Busan, Republic of Korea

Abstract:
Nitrides and oxide coatings have emerged as key surface engineering technologies for withstanding various environmental stresses in advancedelectronics, aerospace amd cutting tool industries. These coatings are widely applied in demanding applications due to their excellent mechanical properties, such as outstanding wear resistance amd high temperature stability, which ensure enhanced furability and reliability. In particular, in the cutting tool industry, extensive research has been cinducted to overcome extreme conditions such as high heat and pressure generated during cutting and grinding processes. Functional graded CrAlN-Al_2O_3 coatings were deposited onto WC-Co substrate by a unbalanced magnetron sputtering system using CrAl and Al_2O_3 composite targets under N_2/Ar atmosphere. XRD analyses revealed that the synthesized CrAlN-Al_2O_3 films were consisting of nanosized (Cr,Al)N crystallites.
The composition of the coating film was analyzed by EPMA (electron probe X-ray microanalyzer). As the power applied to the CrAl and Al_2O_3 target increased, to 300 W ~ 600 W. Subsequently, post-heat treatment was performed at temperatures ranging from 300°C to 800°C, and the resulting microstructure and mechanical properties were investigated. The hardness of the CrAlN-Al_2O_3 films exhibited the maximum hardness values of 35 GPa. The tribometer was used to analyze the friction characteristics of the coating film. As a result of the friction test after heating up to 700 ℃, the coefficient of friction decreased and the lowest value was 0.35. It was confirmed that the mechanical properties were enhanced through recrystallization and grain growth induced by the post-heat treatment. These excellent mechanical properties of CrAlN-Al_2O_3 films could be help to improve the performance of machining tools and cutting tools with application of the film

Keywords: CrAlN, Al_2O_3, Functional graded, Coatings, Cutting tools, heat treatment

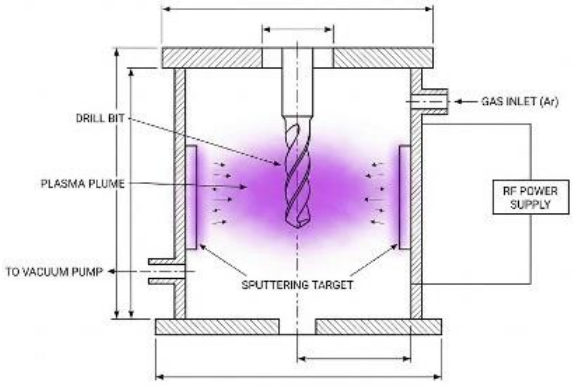

Figure 1: Schematic representation of the RF and pulsed DC sputtering system designed for the plasma hard coating(CrAlN-Al_2O_3) of drill bit substrates. The diagram illustrates the side-mounted target configuration and the plasma plume distribution within the vacuum chamber.

Functional exterior and interior coatings involving surface treated nano-dispersions

Secil Yilmaz Turan [1*], Wei Zhao [1], Pinar Kasaplar[2]
[1] RISE Research Institutes of Sweden, Bioeconomy, Stockholm, Sweden
[2] Kansai Altan Boya Sanayi ve Ticaret Anonim Sirketi, Izmir, Turkey

Abstract:
Titanium dioxide (TiO_2) is among the most widely used white pigments, with various applications from pharmaceuticals to plastics and paints. Achieving and maintaining a homogeneous suspension of TiO_2 is critical for ensuring high-quality end products. The presence of any aggregates adversely affects key performance parameters of the products, such as gloss, storage stability, opacity and viscosity. Therefore, the development of robust and stable TiO_2 nano-dispersions remains a challenge for both researchers and the industry. Within the Exploit4InnoMat project, funded by the Horizon Europe research and innovation programme of the European Union, we investigate various surface treatment strategies to engineer stable TiO_2 dispersions. Our approach combines surfactant systems under controlled pH conditions, and polymeric stabilizers combined with high shear homogenization techniques. This methodology aims to tailor particle interactions and prevent aggregation at nano-levels. To elucidate the structural properties of TiO_2 nanoparticles and formulations involving these, we employ advanced characterization techniques such as small-angle X-ray scattering (SAXS). Nano-dispersion development is scaled-up to pilot level, bridging fundamental research with pre-industrial validation. The stabilized TiO_2 dispersions are subsequently incorporated into coating formulations that are designed to demonstrate further performance characteristics including antibacterial properties and solar reflectance. These coatings are applied and evaluated under real life conditions, with systematic monitoring of their impact on energy efficiency and hygiene performance.

Keywords: surface treatment, bead mill, nanoparticles, dispersions, particle size.

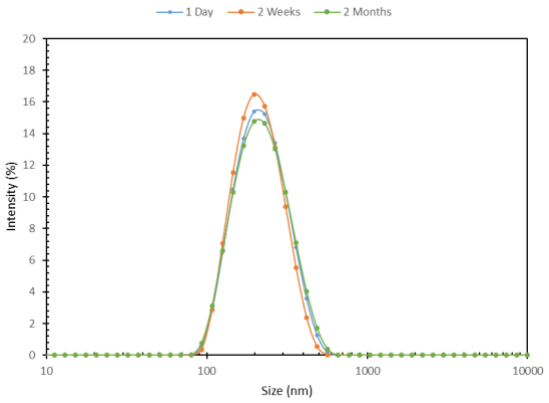

Figure 1: Particle size distribution of surface-treated TiO_2 dispersion after certain storage time.

References:

1. Ikyo, M., Tahara, T., Iwaki, T., Iskandar, F., Hogan Jr., C. J., Okuyama, K. (2006) Experimental investigation of nanoparticle dispersion by beads milling with centrifugal bead separation, *J. Colloid. Interface Sci.,* 304, 2, 535-540.
2. Othman, S. H., Abdul Rashid, S., Ghazi, M., Abdullah, N., Fan, W. (2012), Dispersion and stabilization of photocatalytic TiO_2 nanoparticles in aqueous suspension for coatings applications, *J. Nanomater.*, 1, 718214.

Preparation and characterisation of YIG thin films deposited via DC Magnetron Sputtering for magnonic research applications

V. Faldu [1,*], T. Reimann[1,2], O. Surzhenko[1], T. Friedrich [1,3], A. Gopakumar[1], O. Beier[1], A. Pfuch[1]
[1] INNOVENT e.V. Technology Development, Pruessingstrasse 27B, D-07745 Jena, Germany
[2] matesy GmbH, Loebstedter Str. 101-103, 07749 Jena, Germany
[3] University of Applied Sciences Jena, Department SciTec, Carl-Zeiss-Promenade 2, D-07745 Jena, Germany

Abstract:
The persistent quest for greater efficiency and higher integration density in microelectronics is approaching fundamental physical limits, driving the search for alternative methods of information processing. Magnonics, which utilises spin waves (magnons) for data transfer, offers a promising route—especially through the use of Yttrium Iron Garnet (YIG), which is a ferrimagnetic insulator with the smallest known magnetic relaxation parameter[1]. Current high-quality YIG film fabrication techniques, such as Liquid Phase Epitaxy (LPE) and Pulsed Laser Deposition (PLD), are limited by substrate choices (typically GGG) and scalability issues for large-area production. This work addresses these challenges by presenting a scalable, cost-effective method for producing YIG thin films via reactive direct current (DC) co-sputtering from metallic yttrium (Y) and iron (Fe) targets, followed by thermal annealing. For this, sub-100 nm-thick YIG films were deposited on both (111) Gadolinium Gallium Garnet (GGG) and (100) Silicon (Si) substrates by investigating the influence of deposition parameters, including sputter cathode power, reactive gas concentration, and target-substrate distance, on the film properties. The stoichiometry of the deposited films was characterized by XRF and spectral ellipsometry measurements. The morphology and the crystalline performance of the YIG films were characterized by AFM and SEM as well as by XRD and EBSD measurements. The study highlights precise process control through electrical discharge monitoring and stoichiometry analysis, alongside comprehensive structural, morphological, and magnetic characterisation of the films. Optimisation of thickness and stoichiometric homogeneity over large-area deposited films was achieved. A ferromagnetic resonance (FMR) linewidth (ΔH_{FWHM}) of 10.28 Oe at 6.502 GHz was measured for a 75 nm thick sputtered film (Figure 1), demonstrating film quality comparable with the best RF sputtered-grown films[2]. The FMR linewidth was determined by a Lorentz fit of a magnetic field scale, which was converted from a frequency spectrum[3]. The demonstrated process allows for accurate stoichiometric control and the production of highly crystalline, single-orientation films on GGG, representing a significant step towards industrial-scale magnonic devices.

Keywords: magnonics, spin waves, YIG, thin films, DC magnetron sputtering, post-annealing, thin film characterisation

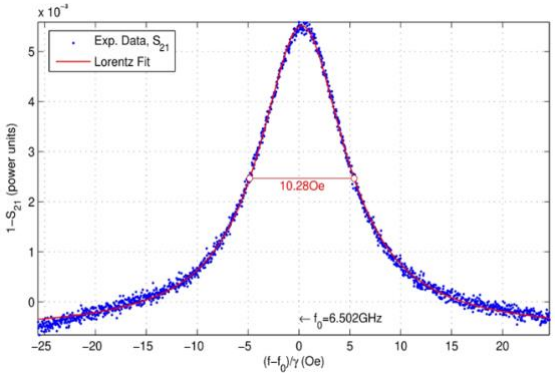

Figure 1: FMR measurement curve of a DC-sputtered YIG film on a 3x4 mm^2 GGG substrate and post-annealed at 700°C for 1 hour at 2 k/min.

References:

1. LeCraw, R. C., Spencer, E. G., & Porter, C. S. (1958). Ferromagnetic resonance line width in yttrium iron garnet single crystals. *Physical Review*, *110*(6), 1311–1313. https://doi.org/10.1103/PhysRev.110.1311
2. Askarzadeh, N., & Shokrollahi, H. (2025). Advances in YIG thin films: Deposition strategies and substrate effects. *Results in Chemistry*, *16*, Article 102390. https://doi.org/10.1016/j.rechem.2025.102390
3. Dubs, C., Surzhenko, O., Linke, R., Danilewsky, A., Brückner, U., & Dellith, J. (2017). Sub-micrometer yttrium iron garnet LPE films with low ferromagnetic resonance losses. *Journal of Physics D: Applied Physics*, *50*(20), Article 204005. https://doi.org/10.1088/1361-6463/aa6b1c

Influence of Gas Admixtures and Target Materials on Plasma Gun Emission Characteristics

Marek Moravčík[1*], Kristína Trebulová[1], Eric Robert[2], Augusto Stancampiano[2], František Krčma[1],
[1]Brno University of Technology, Faculty of Chemistry, Purkyňova 118, 612 00 Brno, Czech Republic
[2]GREMI, UMR7344 CNRS/University of Orleans, 14 Rue d'Issoudun, 45067 Orléans, France
*marek.moravcik@vut.cz

Abstract:
Optical emission spectroscopy (OES) is a key diagnostic tool for understanding the reactive species composition of atmospheric-pressure plasma jets and for optimizing their performance in biomedical applications. In this study, OES was employed to systematically investigate the influence of plasma gas composition and target material on the emission characteristics of a helium-based plasma jet[1] intended for medical decontamination.

Plasma operation with controlled admixtures of oxygen and nitrogen was examined, including mixed gas conditions. Distinct changes in plasma plume intensity, spectral composition, and relative emission of reactive species were observed as a function of gas composition. Oxygen admixture enhanced atomic oxygen emission lines, particularly at 777 nm and 844 nm, while higher oxygen concentrations led to a reduction in these emissions, suggesting a shift toward the formation of secondary reactive species. Nitrogen addition resulted in the appearance of characteristic molecular nitrogen bands, reflecting modified excitation and ionization pathways driven by helium–nitrogen interactions.

In addition to gas composition, the presence and nature of the target material significantly influenced the recorded emission spectra. Measurements performed with plastic, agar, and porcine skin revealed notable differences in emission intensity and relative species contributions, indicating strong plasma–surface interactions and material-dependent energy dissipation. These effects highlight the importance of considering realistic biological targets when interpreting plasma diagnostics.

Overall, the OES results demonstrate that both plasma gas composition and target material play a critical role in shaping the reactive species environment of atmospheric plasma jets. These findings provide essential guidance for tailoring plasma operating conditions to achieve optimized decontamination efficacy in medical applications.

Keywords: reactive species, optical emission spectroscopy, cold atmospheric plasma, plasma medicine,

References:

1. Robert, E., Darny, T., Dozias, S., Iseni, S. & Pouvesle, J. M. New insights on the propagation of pulsed atmospheric plasma streams: From single jet to multi jet arrays. *Physics of Plasmas* **22**, (2015) doi:10.1063/1.4934655.

Challenges in determining the surface loss coefficient of hydrogen atoms on stainless steel in low-temperature plasmas

A. Remigy [1], M. Kassayová [1], S.-J. Klose [2], A. Vahl [1], F. Hempel [1], N. Lang [1], J. H. van Helden[3]
[1] Leibniz Institute for Plasma Science and Technology (INP), Felix-Hausdorff-Str. 2, 17489 Greifswald, Germany
[2] Research Department Plasmas with Complex Interaction, Ruhr University Bochum, Universitätstr. 150, 44801 Bochum, Germany
[3]Experimental Physics V – Spectroscopy of Atoms and Molecules by Laser Methods, Faculty of Physics and Astronomy, Ruhr University Bochum, 44801, Bochum, Germany

Abstract:
Hydrogen plasmas are omnipresent in surface engineering and plasma applications. Reliable modelling of such plasmas requires the knowledge of the surface loss coefficient for the hydrogen atoms interacting with surfaces in presence. Determination of these coefficients is cumbersome due to the difficulty and sometimes impossibility to control all parameters that may influence it.
In this work, we study the interaction of H atoms with stainless steel (SST) V4A surfaces in an electron cyclotron resonance (ECR) plasma in a pure hydrogen atmosphere at low pressure [1]. The surface loss coefficients are derived from the density distribution of H atoms in the vicinity to the investigated surfaces. Two-photon absorption laser-induced fluorescence (TALIF) spectroscopy was employed to determine the spatial distributions of the H atoms near the surface. In parallel, the surface element composition was monitored using x-ray photo-electron spectroscopy (XPS). The nature of chemical bonds of iron (Fe) and chromium (Cr) atoms on the surface is determined by carefully analyzing the Fe 2p3/2 and Cr 2p3/2 peaks. Using these techniques, we monitor the time evolution of the surface loss coefficient of hydrogen atoms on their surface, as well as surface composition and nature of chemical bonds of iron and chromium atoms.
Three samples are studied: Sample 1 was treated in a chamber contaminated with Si [2], while Sample 2 and 3 were treated in a clean chamber. Despite the sample having the same specifications, a contamination with Na was detected with XPS on Sample 3, testifying the difficulty to obtain reproducible conditions. We study the impact of the surface contaminants nature of chemical bonds of Fe and Cr atoms. Figure 1 presents the percentage of metallic Fe bonds on the surface (the rest are oxide/hydroxide) as a function on plasma treatment time for the three samples. While on the clean sample, the pure hydrogen plasma only partially reduces Fe oxide after 5000 min of plasma treatment, the presence of reductant contaminants on the surface enables the reduction. The reductant identified on the surface are sodium (Na) and silicon (Si), and an enhanced reduction rate of Fe is observed for contaminants with the lower reduction potential: i.e reduction is faster in the presence of Na is faster than with Si. A similar effect is observed on Cr atoms.
The impact of these contaminants on the surface loss coefficient is less obvious, but may be deciphered in the future using bigger data sets and statistical tools.

Keywords: surface loss coefficient, low pressure hydrogen plasma, stainless steel, x-ray photo-electron spectroscopy

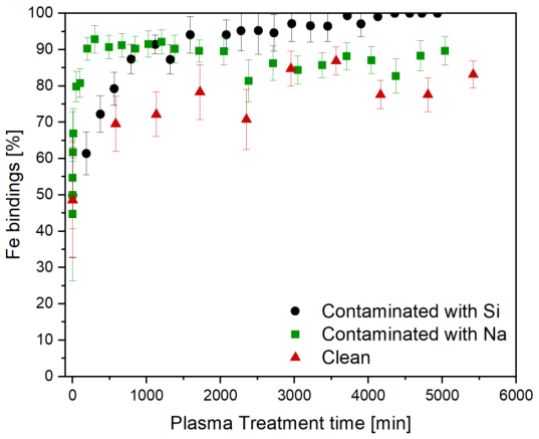

Figure 1: Percentage of metallic Fe as a function of plasma treatment time for samples contaminated with Si, contaminated with Na and a non-contaminated sample.

References:

1. F. Sigeneger *et al.* Plasma Sources Sci. Technol. 31, 105011 (13pp) (2022).
2. A. Remigy *et al.* J. Appl. Phys. 137, 173301 (2025)

Cold Plasma–Liquid Synthesis and Optical Tuning of Surfactant-Free Au and Ag Nanoparticles for SERS Trace Explosives Detection

J. Olenik[1], J. Štrbac[1,2], U. Cvelbar[1,2], J. L. Walsh[1], V.Shvalya[1,2]
[1]Department of Gaseous Electronics, Jožef Stefan Institute, Ljubljana, Slovenia
[2]Jožef Stefan International Postgraduate School, Ljubljana, Slovenia

Abstract:
Cold atmospheric-pressure plasmas (CAP) interfaced with liquids create redox environments for metal-ion reduction and nanoparticle formation, enabling reagent-free synthesis routes that avoid chemical reducing agents and surface-bound stabilisers. This is particularly relevant for plasmonic substrates used in surface-enhanced Raman spectroscopy (SERS), where surfactant layers can inhibit analyte adsorption and reduce enhancement. In this work, we present an extended study of plasma–liquid synthesis and tuning of surfactant-free gold nanoparticles (AuNPs) and expand the approach to silver nanoparticles (AgNPs) synthesized directly from $AgNO_3$ using a CAP jet. We systematically explore how controllable plasma exposure and precursor formulation influence nanoparticle optical response and morphology-relevant signatures, with the objective of identifying reproducible operating windows that yield stable colloids and strong plasmonic performance.
To translate the synthesis outcomes into functional materials while maintaining the primary focus on plasma–liquid chemistry, colloidal AuNPs and AgNPs are deposited onto silicon (Si) and gold-plated substrates, then dried to form simple SERS-active surfaces. The resulting NP-coated chips are evaluated by SERS using representative small-molecule targets relevant to security and environmental monitoring, including explosive analytes, to benchmark enhancement behaviour, spectral reproducibility, and practical substrate preparation. Au- and Ag-based substrates are assessed separately to highlight material-dependent performance trends and to support application-driven selection rules for plasmonic sensing. Overall, the study links CAP operation with plasma–liquid chemistry and functional nanomaterials.

Keywords: atmospheric-pressure plasma jet, plasma–liquid interactions, surfactant-free nanoparticles, Au nanoparticles, Ag nanoparticles, reduction, plasmonics, SERS, explosives detection.

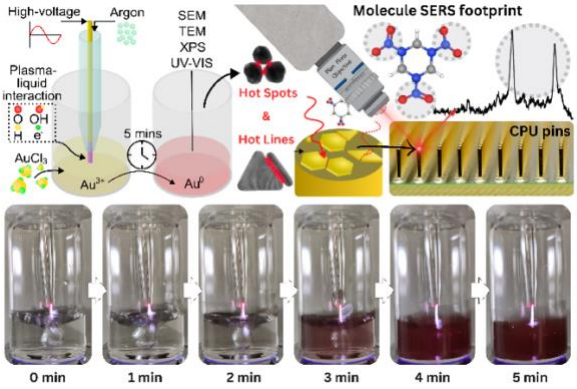

Figure 1: Figure 1. Schematic overview of the atmospheric-pressure argon microplasma–liquid route for surfactant-free nanoparticle synthesis and its translation into SERS substrates. A high-voltage microplasma jet interacts with an aqueous Au precursor (illustrated as $AuCl_3$), generating reactive plasma–liquid species (e.g., electrons and radicals) that drive the reduction of Au and nanoparticle formation within minutes (example shown: 5 min).

References:

1. Shvalya, V., Vasudevan, A., Modic, M., Abutoama, M., Skubic, C., Nadizar, N., ... & Cvelbar, U. (2022). Bacterial DNA recognition by SERS active plasma-coupled nanogold. *Nano letters*, 22(23), 9757-9765.
2. Olenik, J., Shvalya, V., Modic, M., Vengust, D., Cvelbar, U., & Walsh, J. L. (2024). Microplasma Controlled Nanogold Sensor for SERS of Aliphatic and Aromatic Explosives with PCA-KNN Recognition. *ACS sensors*, 10(1), 387-397.

Laser irradiation for removal of a metallized coating on polymeric substrate

S. Monteiro[1], G. Marques[1], P. Santos[1], R. Santos[1], L. Rodriges[2], F.M. Costa[1], A. Lopes da Silva[2], A. Barros[3], N.M. Ferreira[1,*]

[1] i3N & Physics Department, University of Aveiro, Aveiro, Portugal

[2] Maxiplas, Pombal, Portugal

[3] CICECO & Chemistry Department, University of Aveiro, Aveiro, Portugal

Abstract:

In industrial applications the removal of metallization from polymeric materials is a crucial step. Especially, when the metallized area has a complex shape with high definition, case of electronic circuits, company logos or QR-codes. Laser-based paint stripping has emerged as a precise, efficient, and environmentally sustainable technique for removing paints/coatings from polymer composites. In this study, was explored the use of laser technology as an innovative approach, to selectively remove metallic layers from polycarbonate pieces. Laser technology offers significant advantages compared to traditional methods, allowing for precise and controlled removal of metallization while minimizing damage to the underlying polymer substrate. Several laser parameters, such as scanning speed, power, frequency, nanosecond pulse width, and pitch, were evaluated to promote laser selectivity in metallization removal. The results obtained demonstrate the feasibility of this approach and its potential for the electric circuits, images or logos. Moreover, the surface of the substrate (polycarbonate) after laser processed is possible to keeps its surface characteristics (roughness and wettability) or even improves them, according with laser parameters. Moreover, controlling laser parameters is possible to control oxidation degree resulting in colour change, been interesting images and logos graving.

Keywords: Laser technology, removal, metallization, polycarbonate

Figure 1: Foto of shape removal of Al coating by laser irradiation, without the PC substrate degradation.

References:

1. Shiyao Zhu et. al, A critical review on laser-assisted paint removal from carbon fibre-reinforced polymer: Insights into process parameters, material integrity, and numerical modelling, Composites Part C: Open Access, 18 (2025) 100654, doi: 10.1016/j.jcomc.2025.100654.
2. L. Allen, (2017) Essentials of Lasers, Elsevier.
3. X. Li et al, The influence of nanosecond laser pulse energy density for paint removal, Optik 156 (2018) 841-846, doi: 10.1016/j.ijleo.2017.11.010
4. J. Jeong et. al, Effect of laser surface texturing pattern on mechanical properties in metal-polymer direct joining, Optics & Laser Technology 181 (2025) 112049, doi: 10.1016/j.optlastec.2024.112049

Optimization of laser parameters for the injection moulds residues cleaning

P. Silva[1], F. Batista[1], R. Santos[1], T. Ferreira[2], M.Ferro[3], J. Figueiredo[4], F. Oliveira[3], L. Pereira[4], F.M. Costa[1], N. M. Ferreira[1,*]

[1] i3N & Physics Department, University of Aveiro, Aveiro, Portugal

[2] IPN - Instituto Pedro Nunes, Figueira da Foz, Portugal

3 CICECO, , University of Aveiro, Aveiro, Portugal

[4] MicroPlasticos, Gala, Figueira da Foz, Portugal

*- nmferreira@ua.pt

Abstract:

In the polymers injection, the moulds must be regularly cleaned to avoid the residues accumulation on their surface, otherwise, the dimensions of the pieces produced are compromised.

Several examples of using lasers to clean moulds could be found. Such as using a CO2 laser to clean the moulds in the glass industry or the laser fibre in the elastomers industry. The major difficulties to implement such technology is when the mould surface and the residues interact in the same manner with the laser beam used. A study of the implementation of the laser technology to clean the metallic mould according with the type of polymer injection and coating were addressed (Fig. 1). The residues are from different types of polymeric and can be removed by ablation, using a fibre laser. However, this radiation is also highly absorbed by the mould surface and its coating, been a challenge. The optimization of the laser parameters such as power, frequency, scan speed, etc, is required for efficient residues removal according with the types of polymers,without the degradation of the mould surface and coatings. The present study report the optimization of laser parameters according with the polymers specification and the existence or not of coatings at the mould surface. The results obtained show the efficiency of laser technology in cleaning these moulds on each polymer and surface (coated or not). Moreover, also show the need of laser parameters specifications according with the polymers types and surface used.

Keywords: Fiber Laser; clean moulds; injection moulds; polymers type

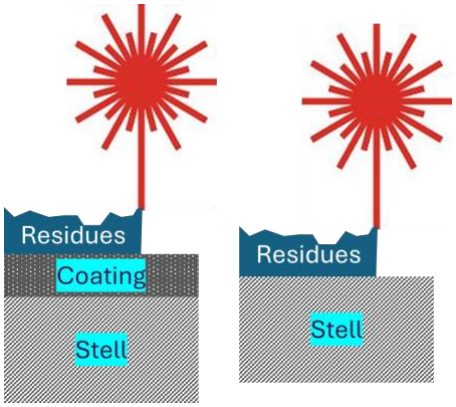

Figure 1: Figure illustration of the methodology to clean the mould using laser technology.

Acknowledgment:

Project funded by FEDER funds – European Regional Development Fund, through the Innovation and Digital Transition program of the project "CleanMouldPlus - Coating with low laser interaction for predictive cleaning monitoring: Clean 4.0, CENTRO2030-FEDER-00545400

References:

1. https://www.ua.pt/en/news/9/92148
2. Yao Lu et. Al, An advanced ultraviolet nanosecond pulsed laser cleaning oceanic micro-biofouling from steel surface, Optics & Laser Technology, 185 (2025) 112618, doi; 10.1016/j.optlastec.2025.112618.
3. Hyoungwon Park et. al, Wear and corrosion behaviors of high-power laser surface-cleaned 304L stainless steel, Optics & Laser Technology, 168 (2024) 109640, doi: 10.1016/j.optlastec.2023.109640
4. Mincheoul Seong et. al, Characterization of laser cleaning for removing welding by-products from SPFH590 steel, Journal of Manufacturing Processes, 157 (2026) 687-697, doi: 10.1016/j.jmapro.2025.12.027

New hybrid technology for deposition of transparent conductive oxide films for solar cell applications

A. Lacoste[1], Z. En-naji[1], A. Bès[1], P. Carroy[2] , S. Béchu[1]
[1]Univ. Grenoble Alpes, Grenoble INP*, CNRS, LPSC-IN2P3, 38000 Grenoble, France
* Institute of Engineering Univ. Grenoble Alpes
[2]CEA Liten INES, Grenoble, France

Abstract:
A new technique for thin film deposition using a very low pressure microwave plasma-assisted evaporation is presented. This hybrid technique (HPD) allows film deposition on sensitive substrates, such as those used in silicon heterojunction (SHJ) or perovskite solar cells, without ionic and thermal damage to growing films and/or substrates . It is well known that in traditional techniques, such as magnetron cathode sputtering, negative ions produced in the presence of a reactive oxygen-based plasma or on the surface of an oxide target (such as transparent conductive oxides, TCO) can reach and bombard the deposition surface with energies of few hundred eV[1]. This disadvantage is overcome in the HPD technique[2], which does not lead to the formation of high-energy either negative ions or neutrals. This technique (Figure 1) is based on a thermal evaporator containing a solid-state TCO that is integrated into a microwave applicator (915 MHz) producing electron cyclotron resonance (ECR) plasma, which helps to enhance and improve the performance of a conventional evaporator.
The electrical properties of the plasma, as determined by a Langmuir probe and a retarding field energy analyser, will be presented. These confirm that the ion energy on the grounded substrate does not exceed 30 eV, and that films with a uniformity greater than 96% can be obtained on M2 cells (156 x 156 mm²).

TCO films (IWO, ITO) obtained using the HPD technique are of high quality. Structural analysis shows uniformly distributed crystallized grains and optical transmission greater than 80% across the entire visible spectrum. Electrical measurements indicate low resistivity (*e.g.*, 4.16 × 10^{-4} Ω·cm for IWO films) and carrier mobility (42 $cm^2 \cdot V^{-1} \cdot s^{-1}$ for IWO) with a corresponding carrier concentration of 3.57 × 10^3 cm^{-3}. A SHJ cell, although taken out of the production line for the deposition of an IWO electrode on the rear side, achieved a high efficiency of 23.89%, demonstrating the great potential of the new HPD technique.

Keywords: Hybrid Plasma Deposition, Low-damage deposition, Transparent conductive oxides, Solar cells.

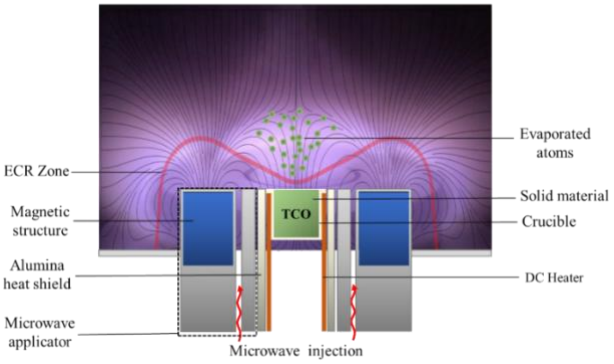

Figure 1: Illustration of the working principle of the HPD technique. The system operates through two integrated components, a coaxial microwave applicator with a magnetic structure and a DC thermal evaporation device containing the TCO material.

References:

1. Welzel, T., Ellmer, K. (2013) Negative ions in reactive magnetron sputtering. Detecting the cause of damages in sensitive TCO films with energy resolved mass spectrometry, *52 ViP,* **25**, 2.
2. En-Naji, Z., Bes, A., Carroy, P., Haake, M., Lacoste, A. (2025) High performance IWO thin films deposited with a new hybrid technology for solar cell application, *Vacuum* 239, 114395.

Atomistic Insight into Sustainable Etching: Unraveling Halogen-Free Hydrogen and Fluorine Reaction Kinetics on the Si Surface

B. Bamdad [1,2,*], X. Hu [1,2], J. Schuster [1,2]
[1] Center for Micro and Nano Technologies (ZfM), Chemnitz University of Technology, Chemnitz, Germany
[2] Fraunhofer Institute for Electronic Nano Systems (ENAS), Technologie-Campus 3, Chemnitz, Germany

Abstract:
The urgent shift towards environmentally conscious semiconductor manufacturing necessitates the development of new, halogen-free plasma etching chemistries for materials like silicon and silicon dioxide [1]. To facilitate the design of these sustainable processes, atomistic insight into the fundamental elementary reaction mechanisms occurring at the Si surface is crucial. In this work, we employ Density Functional Theory (DFT) to comprehensively map the reaction energetics for both hydrogen- and fluorine-based etching pathways. Thereby we compare established fluorine etch-chemistries to more sustainable ones like hydrogen. Transition-state barriers were rigorously determined using the Nudged Elastic Band (NEB) method. Subsequently, rate constants were calculated via Transition State Theory (TST) [2]. Our investigation evaluated two distinct mechanistic routes: a gas-phase pathway (Figure 1) and a diffusion pathway (Figure 2). Our findings reveal significant mechanistic differences between the two etch-species and pathways: The diffusion pathway exhibited high activation barriers of approximately 2 eV for the elementary steps involving both hydrogen and fluorine (Figure 3). In contrast, along the gas-phase pathway, fluorine reactions proceed rapidly without an activation barrier, while hydrogen encounters a barrier of approximately 0.2 eV (Figure 3). Based on these rigorously computed energetics and rate constants, we derived parameters by fitting the data to a modified Arrhenius expression. These automictically-derived constants provide a crucial, validated chemistry model suitable for subsequent plasma microkinetic simulations, accelerating the development and optimization of next-generation, sustainable semiconductor processes.

Keywords: plasma etching, silicon, density functional theory (DFT) calculations, chemistry model, reaction kinetics.

Figure 1: Schematic representation of the gas pathway.

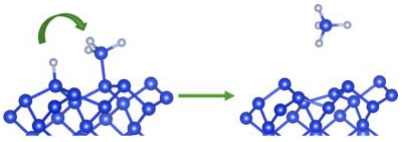

Figure 2: Schematic representation of the diffusion pathway.

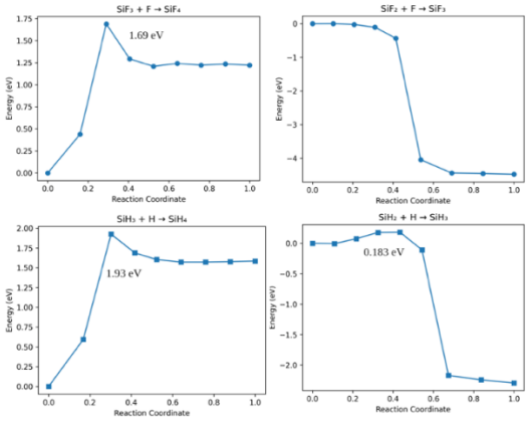

Figure 3: Energy profiles for F (top) and H (bottom) reactions on a silicon surface for diffusion pathway (left) and for gas pathway (right).

Acknowledgments: Funded by the European Union. Views and opinions expressed are however those of the author(s) only and do not necessarily reflect those of European Innovation Council and SMEs Executive Agency (EISMEA). Neither the European Union nor the granting authority can be held responsible for them. HALOFREEETCH has received funding from the European Union under grant agreement n° 101161153.

References:

1. M. Weber (2023), *ACS Mater. Au* 3, 274.
2. Sukkaew (2017), *J. Phys. Chem. C*, 121(2), 1249–1256.

Influence of the plasma discharge regime on the structure of metallic foams synthesized by plasma electrolytic

R. Botrel[1], C. Boudat[1,2], F. Durut[1], A. Zentz[1], C. Noël[2], T. Belmonte[2]
[1] Commissariat à l'Energie et aux Energies Alternatives (CEA), Valduc, F-21120, Is sur Tille, France
[2] Université de Lorraine, CNRS, IJL, F-54000 Nancy, France

Abstract:
As part of laser matter interactions experiments carried out at the Laser Mégajoule (LMJ) facility, CEA needs to synthesize low-density materials with specific characteristics. In this context, cutting-edge materials in the form of low-density metallic foams are employed, with a specific focus on those produced through the technique of plasma electrolysis deposition.
This synthesis method, patented by the CEA, differs from commercial and industrial synthesis techniques for metallic foams and aerogels due to the specific properties it provides. These materials have an apparent density equivalent to approximately 1% of the bulk metal, pore sizes of about one micrometer, and a purity higher than 95%.
In order to control the structure of the synthesized materials, studies have been conducted to better understand the interaction mechanisms that occur between electric arcs and the ionic liquid. For this purpose, electrochemical measurements have been carried out during the synthesis to characterize the evolution of the ionic flux in the electrolyte and its influence on the morphology of the structures obtained.
The results highlight a strong correlation between the ionic flux measured during the discharge and the structure of the formed material. At low applied voltage, a high ionic flux is observed, leading to the formation of very thin and highly branched metal filaments. These structures exhibit similar morphologies of those associated with streamer-type phenomena in plasma discharges in liquid media. As the applied voltage increases, the morphology gradually evolves towards thicker and less branched structures, accompanied by more pronounced crystallization. These results suggest the existence of distinct synthesis regimes controlled by the applied voltage. At low voltage, the growth of the material seems to be dominated by charge transfer process involving the transport of cations and localized micro-discharges at the electrode-electrolyte interface. At higher voltage, the process appears to be more governed by a thermal plasma regime, promoting the growth of more massive structures and increased crystallization.
All of these observations underscore the central role of the plasma discharge regime in controlling the morphology and structuring of mesoporous metallic materials synthesized by electrolytic plasma.

Keywords: Low-density materials, metals, electrolytic plasma, plasma-liquid interaction

Plasma-Induced Polymerization of an Allyl Ether-Substituted Six-Membered Cyclic Carbonate with High Functional Group Retention

E. M. Niemczyk[1,2], A. Gomez-Lopez[3], J. R. N. Haler[1], G. Frache[1], H. Sardon[3] and R.Quintana[1,*]
[1] Luxembourg Institute of Science and Technology (LIST), Belvaux, Luxembourg
[2] University of Luxembourg, Esch-sur-Alzette, Luxebourg
[3] University of the Basque Country UPV/EHU, Donostia-San Sebastián, Spain

Abstract:
Atmospheric-pressure plasma-induced free-radical polymerization is an attractive route for solvent-free fabrication of functional polymer coatings, though monomer fragmentation can limit functional group retention. In this work, we demonstrate the plasma-induced polymerization of an allyl ether-substituted six-membered cyclic carbonate (A6CC) using an argon dielectric barrier discharge (DBD) operated at room temperature. Thin liquid layers of A6CC were exposed to plasma, achieving ~90% allyl conversion in less than 5 min.
FTIR and ^{1}H/2D NMR spectroscopy confirmed rapid consumption of the allyl groups alongside excellent preservation of the pendent cyclic carbonate, evidenced by persistent carbonate C=O bands and diastereotopic ring protons, even at extended exposure times. Gel permeation chromatography revealed the formation of low-molecular-weight oligomers (200–1000 $g \cdot mol^{-1}$), consistent with the limited polymerization tendency of allyl monomers.
Coupled GPC-HRMS enabled assignment of oligomer structures up to seven repeating units, with dominant hydrogen-terminated chains, indicating hydrogen abstraction as the main initiation and termination mechanism. Minor hydroxyl-terminated oligomers and allyl-derived end groups were also detected, together with a low-molecular-weight byproduct tentatively attributed to plasma-induced deallylation.
These results establish that atmospheric-pressure plasmas can efficiently polymerize allyl-functional cyclic carbonates while retaining the cyclic functionality, opening pathways for plasma-deposited coatings bearing reactive carbonate groups for post-functionalization, adhesion, and sensing applications.

Keywords: plasma polymerization; cyclic carbonate; atmospheric-pressure DBD.

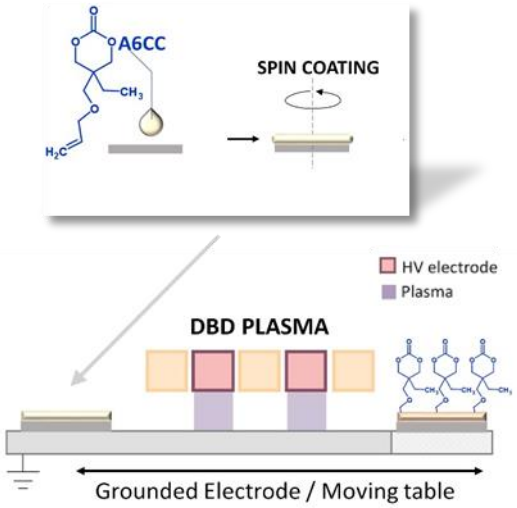

Figure 1: Schematic representation of the process for the atmospheric-pressure plasma-induced polymerization of liquid layers of the allyl ether-substituted cyclic carbonate (A6CC) at room temperature.

References:

1. Hopfe, V.; Sheel, D.W. Atmospheric-Pressure Plasmas for Wide-Area Thin-Film Deposition and Etching. *Plasma Process. Polym.* **2007**, *4*, 253–265.
2. Niemczyk, E.M.; Gomez-Lopez, A.; Haler, J.R.N.; Frache, G.; Sardon, H.; Quintana, R. Insights on the Atmospheric-Pressure Plasma-Induced Free-Radical Polymerization of Allyl Ether Cyclic Carbonate Liquid Layers. *Polymers* **2021**, *13*, 2856.

Quantitative measurement of hydrogen peroxide from plasma jet on soft materials

Wanqi Zhang and Daren Caruana*
Department of Chemistry, Christopher Ingold Laboratories, UCL, 20 Gordon St., London, WC1H 0AJ UK

Abstract:
Atmospheric pressure plasma jet (APPJ) presents a non-equilibrium chemically rich media which is finding new uses in applications ranging from automobile manufacture to treatment of skin cancers[1,2]. The common aspect of all plasmas is the generation of highly reactive radicals, ions and free electrons, which drive chemical reactions very rapidly on a surfaces[3]. One such surface is hydrated soft materials, which are considered as model system for biological system. Quantifying the precise chemical changes within soft materials is not trivial, but is essential to understand the safe deployment especially for medical applications. In this work, agar gels mimic biological environments relevant to plasma medicine; therefore, a systematic investigation of reactive species generation, stability, and diffusion within gels is essential for bridging plasma liquid chemistry with plasma–biological interactions. We employ electrochemical methods to quantitatively probe H_2O_2 generated in agar-based gels exposed to the kINPen. Cyclic voltammetry and chronoamperometric at a purpose built electrochemical cell, Fig.1, to reveal only the redox signature of H_2O_2 at platinum electrode, ensuring that the measured concentrations are not influenced by other reactive species, as determined by changing electrode material. Depth-resolved analysis revealed a pronounced decrease in H_2O_2 levels with increasing gel thickness, indicating that plasma-derived reactive species predominantly penetrate the gel to a distance of 4 mm. We also explore the H_2O_2 concentration as a function of plasma nozzle gel surface separation distance. By comparing buffered and unbuffered gels and measuring depth-dependent chemical penetration, we elucidate how acidity and transport constraints regulate the plasma-induced production of long-lived reactive species. This study provides mechanistic insight into plasma–gel chemistry and establishes an electrochemical framework for characterizing H_2O_2 in soft condensed systems. The results provide insights for optimising plasma applications in biomedical and material science contexts where controlled reactive species delivery is critical.

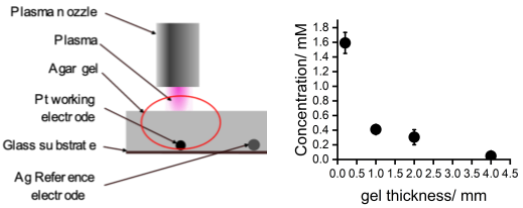

Figure 1: Schematic cross section of the electrochemical cell, showing the position of the working and reference electrode in relation to the plasma impinging on the gel.

Keywords: Cold atmospheric plasma, hydrogen peroxide, agar gel, reactive species, electrochemical quantification

References:

1. Lin, A., et al., Uniform nanosecond pulsed dielectric barrier discharge plasma enhances anti-tumor effects by induction of immunogenic cell death in tumors and stimulation of macrophages. Plasma processes and polymers, 2015. 12.
2. Schlegel, J., J. Köritzer, and V. Boxhammer, Plasma in cancer treatment. Clinical plasma medicine, 2013. 1.
3. De Geyter, N. and R. Morent, 7 - Cold plasma surface modification of biodegradable polymer biomaterials, in Biomaterials for Bone Regeneration, P. Dubruel and S. Van Vlierberghe, Editors. 2014, Woodhead Publishing, 202-224.

Comparison of DECR and ASPN Plasma Contamination Inspection Using the Temporal Evolution of NO-γ and OH UV Emission Bands

L. Bortoletto [1,2], C. Noël [1], R. Hugon [1], T. Czerwiec [1], A. Vidal [1,2], G. Marcos [1]
[1] Institut Jean Lamour (IJL), Département CP2S, Université de Lorraine, Nancy, France
[2] Laboratório de Materiais (LabMat), Department of Mechanical Engineering, Universidade Federal de Santa Catarina, Santa Catarina, Brazil

Abstract:
Plasma assisted nitriding treatments can be done utilizing different configurations of plasma sources. A common characteristic shared between these setups is the utilization of a low pressure reactor chamber. When the chamber is opened to introduce a new sample, oxygen-containing species from ambient air adsorb onto the reactor walls and internal components. Understanding the behavior and removal of these species is essential to avoid process inconsistencies, such as the formation of undesirable coating characteristics. It is well established that, in pure nitrogen atmospheres, NO-γ bands emission can serve as a contamination indicator in Active Screen Plasma Nitriding (ASPN) systems, where the temporal decay after chamber venting is used as the reference baseline. However, Dipolar Electron Cyclotron Resonance (DECR) plasma sources operate at significantly lower pressures, and their cleaning dynamics remain less explored. Also, in N_2/H_2 plasmas, which are the typical gas mixture used for nitriding treatments, the NO emission is completely suppressed, preventing its use as a contamination indicator [2]. For this reason, an alternative species inspection is required. This study compares the cleaning performance of the different plasma sources by analyzing the single-exponential decay time at different temperatures and using the OH band as an alternative indicator in N_2/H_2 atmospheres. Experiments were conducted, and NO-γ emissions in the 210 - 290 nm and OH in the 306 - 309 nm range were monitored using time-resolved optical emission spectroscopy to extract the decay constants. The plasma diagnostic suggests the existence of different kinetics in each configuration of plasma source and temperature values on inner walls and sample-holder. It was observed that the DECR source in comparison with ASPN exhibited a time constant reduced by a factor of about three (11,68 versus 27,8 min), indicating a more efficient cleaning process.

Keywords: surface engineering, plasma diagnostics, nitriding, contamination, optical emission spectrometry, desorption, DECR, ASPN.

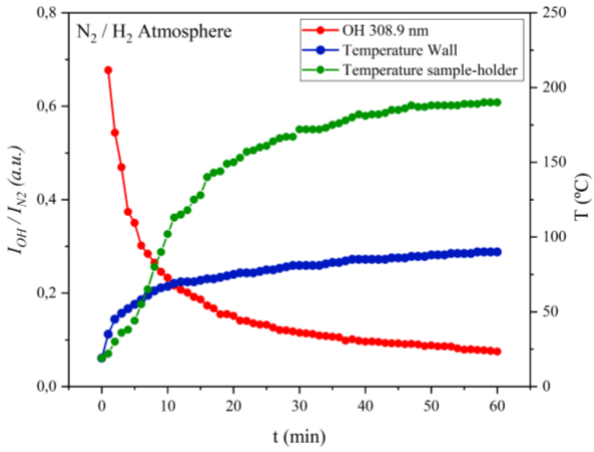

Figure 1: Temporal evolution of OH 308.9 nm and temperature of sample-holder and inner walls in DECR plasma configuration (N_2/H_2 at 3,6 Pa).

References:

1. Carrivain, O., Hugon, R., Marcos, G., Noël, C., Skiba, O., Czerwiec, T. (2021) Inspection of contamination in nitrogen plasmas by monitoring the temporal evolution of the UV bands of NO-γ and of the fourth positive system of N_2, *J. Appl. Phys.*, 130, 173304.
2. Czerwiec, T., Carrivain, O., Masieiro, M., Hugon, R., Cardinaud, C., Belmonte, T., Noël, C., Cardoso, R.P., Marcos, G. (2025) Production of NO in nitrogen-based active screen plasma nitriding devices, a disadvantage or an opportunity?, *Surf. Coat. Technol.*, 500, 131896.

Improvement of the surface tribological properties of 42CrMo4 steel through the slide burnishing process

A. Dzierwa [1,]
[1] Faculty of Mechanical Engineering and Aeronautics, Department of Manufacturing Processes and Production Engineering, Rzeszow University of Technology, Rzeszow, Poland

Abstract:
Burnishing is a surface treatment technique that helps to slow down wear processes [1]. During burnishing, a hard and smooth tool is applied to the machined surface with sufficient pressure, generating sliding friction in the contact area. This process results in surface smoothing and improves the properties of the surface layer. Burnishing enhances surface hardness, achieves excellent smoothness, introduces compressive stress in the top layer, and removes abrasive contaminants from the surface. These improvements positively influence various functional characteristics, such as wear resistance, fatigue strength, and corrosion resistance.

Most studies on the impact of burnishing on the tribological properties of friction pairs predominantly utilize diamond or diamond composite tools as the burnishing elements. While effective, this approach is relatively expensive. There is limited discussion regarding the use of more affordable burnishing tools, particularly in the context of CNC machine tools, to enhance these properties. Expanding the use of ceramic materials [2] for this purpose could significantly lower the costs associated with the burnishing process, especially when achieving surface quality comparable to that of diamond tooling. Additionally, it could reduce or even eliminate the need for labor-intensive finishing operations such as honing, grinding, polishing, or superfinishing.

In our research burnishing process was performed using a vertical Hass VF-1 machining center. The discs were made of 42CrMo4 steel. Three different pressure forces of the tool were applied. A single tool pass was used at a constant feed rate of 0.05 mm. The finishing treatment of the discs was completed with various types of ceramic balls. In addition, discs in which grinding and polishing processes were the finishing treatment were tested.

Tribological tests in rotational movement were conducted using a tribological tester T-11 (Fig. 1). Dry sliding tests were carried out at room temperature (20–22 °C). Before and after tribological tests disc surfaces were measured by a white light interferometer Talysurf CCI Lite (Fig. 2) in order to determine the amount of wear. Friction coefficient of frictional couples was also calculated. Experimental investigations proved the possibility of improving selected tribological properties of friction pairs thanks to the use of slide burnishing process.

Keywords: slide burnishing, surface topography, wear, friction.

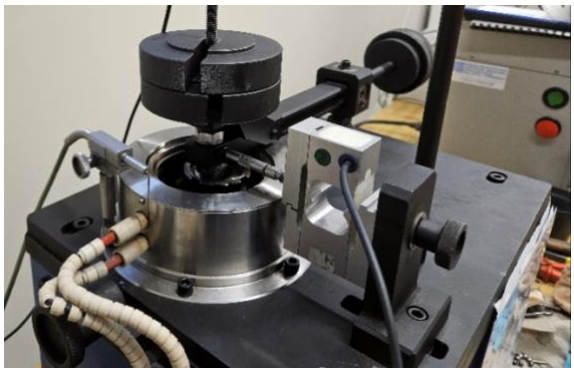

Figure 1: Tribological tester T-11.

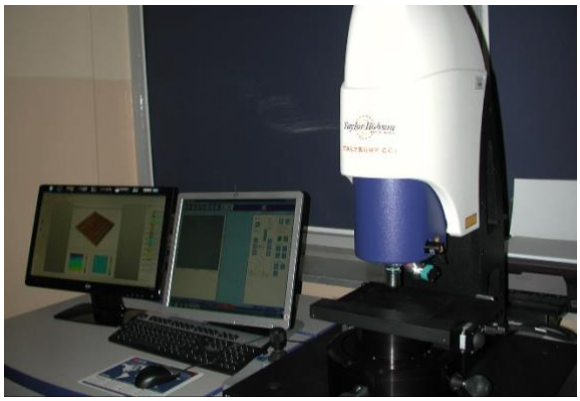

Figure 2: A white light interferometer Talysurf CCI Lite.

References:

1. Priyadarsini, Ch., Venkata Ramana, V.S.N., Aruna Prabha, K., Swethaa, S. (2019), A review on ball, roller, low plasticity burnishing process, *Materials Today: Proceedings.* 18(7), 5087-5099.
2. Revankar, G.D., Shetty, R., Rao, S.S., Gaitonde, V.N. (2017), Wear resistance enhancement of titanium alloy (Ti-6Al-4V) by ball burnishing process, *J. Mater. Res. Technol*. 6, 13-32.

Testing of friction connections of the spherical cap type

M. Wozniak[1,*], A. Ryslki[2]., S. Zakrzewski[1], D. Batory[1], K. Siczek[1]
[1] Department of Vehicles and Fundamentals of Machine Design, Lodz University of Technology, Lodz, Poland
[2] Instititute of Materials Science and Engineering, Lodz University of Technology, Lodz, Poland

Abstract:
Following paper describes the numerical and experimental study of ball joints in selected automotive vehicles. Finite element method (FEM) simulations were conducted using Ansys software to determine the maximum and average stress and strain values occurring at the interface of the steel pin and plastic raceway friction pair. The forces and boundary conditions for the studied pair were defined in Ansys. The geometry of the components was modelled based on actual parts using Inventor software. Experimental tests were carried out on a specially designed tribological tester (Figure 1) for ball joints. The prepared ball joint samples from the studied vehicles were tested under various rotational speeds, angular positions of the joint and with constant axial and side forces. Friction torques and temperatures were recorded during the test. After the tests, the mass of the raceway was measured and compared with the mass of new raceways to assess the material loss—indicative of wear.

Keywords: ball joint; suspension; vehicle; grease; tribology; roughness; friction; fem.

Figure 1: The tribotester equipped with a force sensor and torque meter.

References:

1. Patil, P.B.; Kharade, M.V. Finite Element Analysis and Experimental Validation of Lower Control Arm. International journal of Engineering Development and Research 2016, 4(2), 1914-1922.
2. Yao, J.; Wang, M.; Li, Z.; Jia, Y. Research on Model Predictive Control for Automobile Active Tilt Based on Active Suspension. Energies 2021, 14(3), 671.
3. Chung, S.S.; Lee, Y.Z.; Park, S.O. Practical Evaluation of Ball Stud Plating Effects on the Increase of Free Gap of Ball Joints in the Vehicle. Int.J Automot. Technol. 2020, 21, 1107–1111

Anodic Aluminum Oxide Coating as a Dielectric Platform for Electrically Tunable Lubrication

M. García-Pérez [1*], S. D. Fernández-Silva [1], C. Roman [1], L. Lazar [2], J. D. Mozo [3], M. A. Delgado [1], M. García-Morales [1]
[1] Pro2TecS Research Center, University of Huelva, Huelva, Spain
[2] Department of Chemical Engineering, Technical University of Iasi, Iasi, Romania
[3] CCTH - Centro Científico Tecnológico de Huelva, University of Huelva, Huelva, Spain

Abstract:
Electrically tunable lubrication is emerging as a route to dynamically control friction in mechanical systems [1,2]. However, the implementation of electro-responsive lubricants is hindered by the risk of short circuiting when metal tribopairs serve as opposing electrodes [1]. In parallel, aluminum alloys are increasingly used for their low density, although their poor wear resistance makes surface treatments necessary for tribological applications. Anodizing yields anodic aluminum oxide (AAO) coatings, commonly adopted to improve hardness and wear resistance of aluminum components [3]. In this experimental work, we leverage an additional feature of AAO, namely its dielectric insulation, to allow electric field application across a lubricated contact while restricting the electrical conduction between counterparts.
Anodizing was performed on EN AW-6082 alloy coupons in a sulfuric acid electrolyte at low temperature, in order to promote compact, hard, wear-resistant AAO coatings. The effect of anodizing time and hydrothermal sealing were studied. AAO coatings were characterized in terms of thickness, dielectric strength, hardness and wear resistance. The electro-tribological response was evaluated through lubricated sliding tests at different electric potentials, using an electro-responsive fluid based on castor oil containing the commercial organo-modified nanoclay Closite 15A. Such tribological tests were conducted in a Physica MCR 302e rheometer using a ball-on-three-plate configuration, with the anodized coupons as the plates and a stainless-steel bearing ball (1.4401, grade 100).
The results indicated that a minimum coating thickness was required to sustain an effective electric field across the lubricated contact without electrical conduction. When this condition was met, the application of the electric field produced marked changes in friction and wear, particularly in the wear of the steel ball. These findings support AAO coatings as a promising platform for electrically controlled lubrication, expanding AAO's functional roles beyond conventional wear protection.

Keywords: anodic aluminum oxide, electrically tunable lubrication, electro-responsive lubrication, potential-controlled friction.

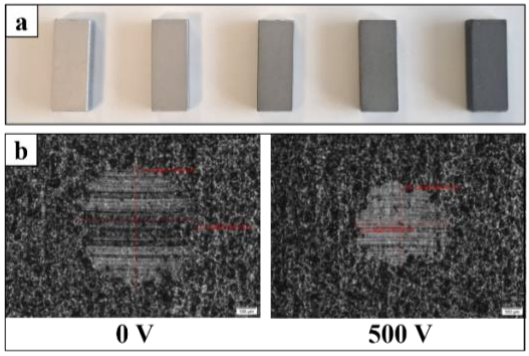

Figure 1: a) Anodized plates, using different anodizing times (from left to right: 30, 45, 60, 90 and 120 min). b) Wear scars on the coated plate after lubricated sliding test at 0 V and 500 V.

References:

1. Spikes, H. A. (2020) Triboelectrochemistry: Influence of Applied Electrical Potentials on Friction and Wear of Lubricated Contacts, *Tribol. Lett.*, 68:90.
2. Wang, Z., Chen, C., Ye, R., Singh, S.S.K., Wu, S., Zhao, X. (2024) Review of triboelectricity-controlled fluid technologies for enhancing the lubrication performance on the coupled surface, *Tribol. Int.*, 195, 109584.
3. Campbell, W. (1951) Anodised Aluminium Surfaces for Wear-Resistance, *Trans. IMF*., 28:1, 273-291.

Acknowledgements:

María García-Pérez acknowledges the support of a predoctoral grant (PREP2023-001594) funded by MCIU/AEI/10.13039/501100011033 and by FSE+.
Research Project PID2023-151761NB-I00, funded by MICIU/AEI/10.13039/501100011033 and FEDER, UE.

Modelling of the wear process in a two-surface system separated by a granular medium using DEM and reconstruction of the contact fields

K. Ligier [1*], M. Lemecha [1], O. Vrublevskyj [1]
[1] Departament of Technical Sciences, University of Warmia and Mazury in Olsztyn, Poland

Abstract:
Wear in systems where two surfaces are separated by a fine-grained medium with controlled flow is process-based: the local interaction conditions change over time and result from the collective dynamics of the grains. Under such conditions, simple Archard-type approaches [1] (wear as a function of load and hardness) or single-particle parameter-based approaches (e.g. Oka-type erosion relations [2]) do not explicitly describe the key mechanism: the evolution of the grain layer as a metastable dissipative structure. This layer forms metastable states that determine the energy dissipation channels, and transitions between them can abruptly increase the proportion of energy leading to surface destruction, generating an important part of the total loss.
This work presents a simulation model based on the discrete element method (DEM), reproducing the actual geometry and kinematics of the laboratory bench and the organised movement of the granular medium in the contact area. The granular material was described as a mixture of fractions with varying characteristics, thus capturing the variability of interactions typical of natural materials. The use of virtual sensors in the DEM environment enabled the reconstruction of the contact fields: distributions of the number of contacts [3], particle velocities, normal and tangential energies and the total contact energy assigned to a selected area of the surface. The data obtained provide the basis for a quantitative description of the energy balance of the wear process and an estimate of how much of the dissipative energy is associated with material loss.

Keywords: abrasive wear, DEM, granular medium, interlayer, contact fields.

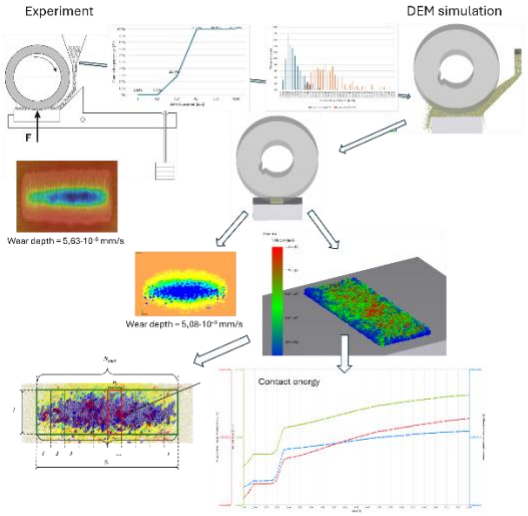

Figure 1: Modelling the wear process in a system of two surfaces separated by a granular medium using a DEM and reconstructing the contact fields to quantitatively describe the energy balance of the process and estimate the dissipated energy associated with material loss.

References:

1. Archard, J.F. (1953). Contact and Rubbing of Flat Surfaces. Journal of Applied Physics, 24(8), 981–988.
2. Oka Y.I., Okamura K., Yoshida T., (2005) Practical estimation of erosion damage caused by solid particle impact. Part 1: Effects of impact parameters on a predictive equation. *Wear* 259 95–101.
3. Vrublevskyi O., Ligier K., & Lemecha M. (2025). The use of entropy to estimate the course of abrasive wear. *Wear*, 206444.

Geometric modeling of granular bed particles in DEM simulations using image analysis methods

M. Lemecha [1*], K. Ligier [1], O. Vrublevskyi [1]
[1] Faculty of Technical Sciences, University of Warmia and Mazury in Olsztyn, Olsztyn, Poland

Abstract:
The Discrete Element Method (DEM) is a fundamental numerical tool for simulating the behavior of granular materials, in which the abrasive medium is treated as a collection of discrete particles interacting via Newton's laws of motion and contact models [1]. The predictive accuracy regarding flow processes, segregation, and abrasive wear depends significantly on the precise representation of particle geometry and contact parameters [2]. In practice, simplified particle representations in the form of spheres or their clumps (Fig. 1) remain dominant. However, such approximations fail to faithfully reproduce the irregular morphology of natural grains, leading to discrepancies between simulations and experimental results [3, 4].

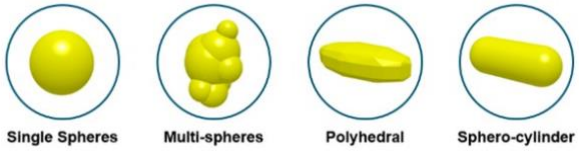

Figure 1. Types of particle shapes used in numerical simulations [5]

The developed approach integrates quantitative 2D and 3D image analysis, automated segmentation, clustering, and multi-parametric morphological description into a cohesive processing chain for generating particle models for DEM simulations. The application of 23 shape factors, including non-linear parameters, enables the characterization of complex geometric features and surface topography that are not captured by classical sphericity and roundness indices derived from visual methods [6]. The elimination of redundant coefficients based on correlation analysis allows for a synthetic and unambiguous representation of morphology, which can be directly implemented within the EDEM environment.

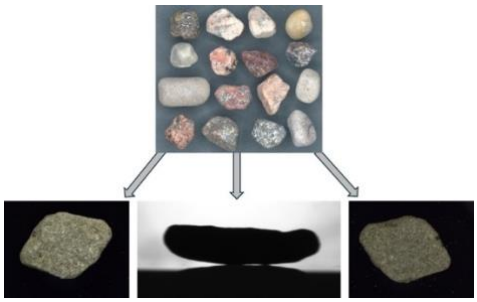

Figure 2. Schematic of the integrated 2D/3D image analysis and particle morphology parameterization process for DEM model generation

A crucial element of the research is the generation of realistic particle geometries directly from measurement data and their systematic calibration using the angle of repose experiment. This allows for the linking of geometry with the mechanics of contact interactions and reduces the arbitrariness in selecting model parameters [2, 7]. Such an approach establishes a foundation for building a digital twin of granular materials that is scalable and adaptable to various material types and operating conditions.
The obtained results indicate a significant correlation between simulations and experimental data compared to models based on simplified shapes. The presented approach enables the modeling of abrasive wear processes, transport, and particle interactions at a level consistent with current trends in computational engineering and abrasive technology.

Keywords: Abrasive wear, Granular materials, Discrete Element Method (DEM), Particle morphology, Shape factors, Digital twin, Image analysis

References:

1. Cundall, P. A., Strack, O. D. (1979). A discrete numerical model for granular assemblies. geotechnique, 29(1), 47-65.
2. Coetzee, C. J. (2016). Calibration of the discrete element method and the effect of particle shape. Powder Technology, 297, 50-70.
3. Zhu, H. P., Zhou, Z. Y., Yang, R. Y., Yu, A. B. (2008). Discrete particle simulation of particulate systems: a review of major applications and findings. Chemical Engineering Science, 63(23), 5728-5770.
4. Lu, G., Third, J. R., Müller, C. R. (2015). Discrete element models for non-spherical particle systems: From theoretical developments to applications. Chemical Engineering Science, 127, 425-465.
5. https://community.altair.com/
6. Krumbein, W. C. (1941). Measurement and geological significance of shape and roundness of sedimentary particles. Journal of Sedimentary Research, 11(2), 64-72.
7. Roessler, T., Katterfeld, A. (2019). DEM parameter calibration of cohesive bulk materials using a simple angle of repose test. Particuology, 45, 105-115.

Tribo-induced microstructural evolutions and wear mechanisms of CoCrFeMnNi high-entropy alloy composite enhanced by Al/Ti doping and hBN/TiC dual ceramic reinforcement at elevated temperatures

Wenbo Ma [1*], Oleksandr Tisov [1]
[1] School of Aerospace Engineering, Xi'an Jiaotong University, Xi'an 710049, China

Abstract:
Aerospace tribological systems demand metallic materials with superior wear resistance across wide temperature ranges, a critical challenge for conventional alloys. High-entropy alloys (HEAs) show great potential for extreme conditions due to their excellent thermal stability and strength-ductility synergy, yet single modification strategies limit their tribological performance.In this study, a CoCrFeMnNi high-entropy alloy composite (HEAC) modified by 2 wt% Al/2 wt% Ti doping and 0.5 wt% hBN/15 wt% TiC dual ceramic reinforcement was fabricated via mechanical alloying and spark plasma sintering. Its tribological behavior from room temperature to 900 °C was systematically investigated, and the wear-induced microstructural evolution mechanisms were elucidated via multi-scale characterization. Results show HEAC achieves exceptional high-temperature wear resistance with wear rates at the order of 10^{-6} $mm^3/N·m$ at 600 °C and 900 °C.At 600 °C, a wear-induced gradient structure (amorphous-nanocrystalline oxides/fine-grain layer/TiC particles) and interfacial structural transitions at metal-ceramic boundaries enhance micro-strength and plastic deformation resistance. At 900 °C, a dense crystalline glaze layer (outer Mn_2O_3/inner fine-grained Cr_2O_3) effectively suppresses oxidative and adhesive wear. This work validates the synergistic enhancement of elemental doping, hard ceramic reinforcement and solid lubrication, providing an innovative design strategy for high-temperature wear-resistant metallic materials for aerospace tribological systems.

Keywords: CoCrFeMnNi high-entropy alloy; high-temperature wear; Al/Ti doping; hBN/TiC reinforcement; wear mechanism.

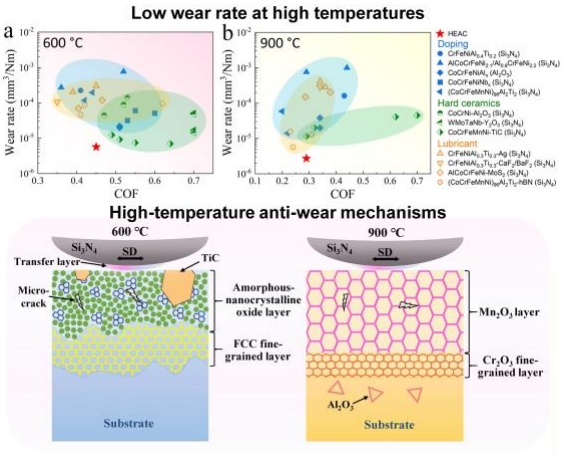

Figure 1: Wear rate vs. COF for HEAC and other various kinds of multi-principal alloys at 600 °C and 900 °C. Wear mechanism diagram of HEAC at 600 °C and 900 °C

References:

1. Ma W, Zhao Y, Łępicka M, Tisov O. Enhanced microstructure, mechanical, and tribological properties of Al, Ti, and nano-hBN-modified CoCrFeMnNi high-entropy alloy composites at elevated temperatures. *Wear*. 2025;572-573.
2. Ma W, Tisov O, Łępicka M. From abrasive to glaze: evolution of wear mechanisms in TiC-modified CoCrFeMnNi high-entropy alloys from room temperature to 900 °C. *Wear*. 2026;584-585.

Investigation of contact-separation induced phenomena at the Silica-Gold interface

Nisha Ranjan*, Tolga Acartürk, Ulrich Starke
Interface Analysis, Max-Planck Institute For Solid State Research, 70569 Stuttgart, Germany

Abstract:
Contact electrification, or Contact-separation (CS) electrification at solid interfaces, constitutes a fundamental concept, yet an uncertain and irreproducible phenomenon [1, 2]. The silica-gold contact-pair represents an ideal case of a dielectric-metal system with overlapping elastic modulus but still shows large deviations in charging properties, like polarity reversal amongst the CS surfaces [3]. Here, we aim to provide deeper insight into the phenomenon by investigating interfacial interactions and chemical composition using direct, microscale measurements under ultra-high vacuum conditions at the silica-gold interface. Atomic Force Microscopy – Force Spectroscopy (AFM-FS) was used to quantify interfacial properties, such as electrostatic and van der Waals interaction, contact area, contact pressure, and deformation. Repeated approach–retraction cycles enabled correlation of mechanical response with charge accumulation and compositional change. ToF-SIMS was employed for surface composition mapping to assess mechanochemistry. AFM-FS measurements revealed reproducible interactions, with adhesion force increasing systematically during 20-40 CS cycles; after ≈23 cycles, an abrupt decrease was observed shown in the Figure 1 (b). This indicates that the magnitude of the force is strongly influenced by the charge accumulation. Concurrently, a change in surface composition was observed. The measurement was reproducible only when the surface was free from organic contaminants. These observations provide direct evidence about the interplay of electrical and mechanochemical properties of the surface during CS processes.
Our findings demonstrate that AFM-FS in combination with ToF-SIMS offers a powerful method to probe contact electrification and mechanochemistry at the microscale under controlled condition.

Keywords: triboelectrification, mechanochemistry, ToF-SIMS, AFM-force spectroscopy, DMT model

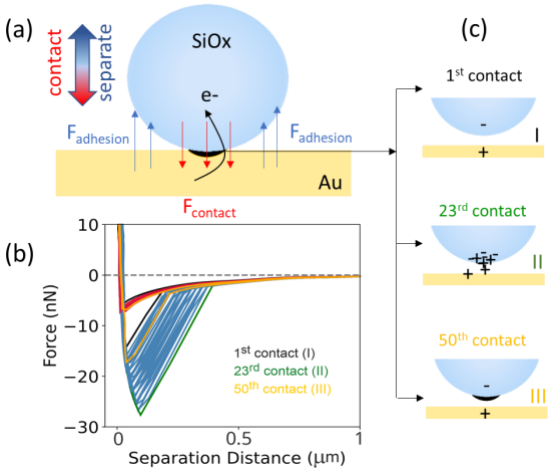

Figure 1: (a) Sketch of AFM contact-separation interaction amongst silica microsphere - flat gold surface geometry, based on Derjaguin, Muller, Toporov model (DMT model) [4], (b) Force vs. separation distance curves, and (c) I, II, and III represent the proposed mechanism of charge generation, accumulation, and change in the chemical composition at the contact point.

References:

1. Ignaas Jimidar et al. (2025) The enduring puzzle of static electricity, Physics Today 78 8, 54–55.
2. Daniel J. Lacks (2012) The Unpredictability of Electrostatic Charging, *Angew. Chem. Int. Ed.,* 51, 6822 – 6823
3. Giulio Fatti et al. (2023) Uncertainty and Irreproducibility of Triboelectricity Based on Interface Mechanochemistry, *Phy. Rev. Lett*, 131, 166201
4. B. V. Derjaguin, V. M. Muller, YU. P. Toporov (1975) Effect of Contact Deformations on the Adhesion of Particles, *Journal of Colloid and Interface Science*, 53, 2, 314-326

Rapid Detection of Indoor Microbial Toxins on Various Surfaces with Direct Analysis in Real Time - Mass Spectrometry

Mikkola, Raimo[1], Salonen Heidi[1,2]
[1] Department of Civil Engineering, Aalto University, Espoo, Finland[2]
[2]Queensland University of Technology, Brisbane, Australia

Abstract:
The presence of toxin-producing microbes in moldy buildings has been considered a health risk [1]. The routine surveillance of indoor toxin contamination presently relies on labor intensive protocols: dust is collected, extracted with organic solvents and analysed by high performance liquid chromatography or gas chromatography mass spectrometry. In this work we introduce a rapid direct analysis of microbial toxins on contaminated surfaces using Direct Analysis in Real Time (DART) coupled to a Quadrupole Time of Flight mass spectrometer (QTOF-MS, Agilent). As a model analyte we selected valinomycin, a heat stable cyclic dodecadepsipeptide potassium ionophore (Fig. 1) produced by *Streptomyces griseus* strains that have been isolated from moisture damaged buildings [2]. Valinomycin (Merck) was prepared at 1 ng μL^{-1} in methanol, and 10 µL of this solution was deposited onto stainless steel wire mesh. The mesh was introduced directly into the DART source; within $\leq$ 60 s a full scan spectrum was acquired, displaying the characteristic ions of valinomycin (Fig. 2). The detected concentration was in the low nanogram range, demonstrating that DART-QTOF-MS can identify trace amounts of a toxin directly from a solid surface. Cereulide, another heat stable cyclic dodecadepsipeptide potassium ionophore (M = 1153.40 g mol^{-1}) shares a near identical structure with valinomycin. Cereulide is a well-known emetic toxin (3) produced also by *Bacillus cereus* strains found from water damaged construction materials. The same DART MS workflow is therefore expected to enable its rapid detection, providing a valuable tool for monitoring a broad spectrum of indoor microbial hazards. These results establish DART-QTOF-MS as a fast method for direct surface screening of microbial toxins. Ongoing work expands the analysis of target toxins, evaluates performance on heterogeneous substrates (gypsum board, carpet fibers, food matrices), and develops quantitative calibration strategies, facilitating timely risk assessment and remedial actions in the event of hazardous microbial contamination of buildings.

Keywords: Microbial toxin, surface, indoor air, DART, Mass spectrometry, valinomycin, building materials, moldy buildings

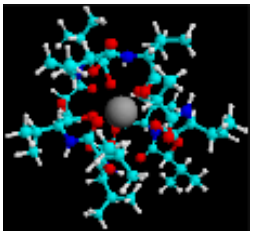

Fig. 1 Valinomycin (1110.3 g mol^{-1}) is a cyclic dodecadepsipeptide, mitochondrial toxin, capable of binding K^+ to the molecular cavity.
Colors indicate atoms, white; H, turquoise; C, red; O, blue; N and grey; K^+

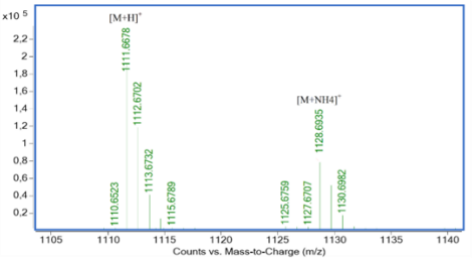

Fig. 2 Analysis of valinomycin (10 ng) by DART - QTOF-MS. Valinomycin mass spectra showed protonated mass ions *m/z* at 1111.6678, $[M+H]^+$ and *m/z* at 1128.6935, $[M+NH4]^+$ as ammonium adduct.

References:

1. Saghir S.A., Bancroft J., Ansari R.A. (2025), Molds and mycotoxins indoors I: Current issues and way forward. *Arch Clin Toxicol*., 7, 1-7.
2. Andersson M.A., Mikkola R., Kroppenstedt R.M., Rainey F.A., Peltola J., Helin J., Sivonen K., Salkinoja-Salonen M.S. (1998), The mitochondrial toxin produced by *Streptomyces griseus* strains isolated from an indoor environment is valinomycin. *Appl Environ Microbiol*., 64, 4767-73.
3. Eskes, C., Cortiñas-Abrahantes, J., Bottex, B., Dorne, J.L.C.M., Dujardin, B., de Sousa, R.F., Horvath, Z., Kouloura, E., Bordajandi, L.R., Rizzi, V., Steinkellner, H., Gilsenan, M. (2026) Rapid risk assessment on acute reference dose (ARfD) of cereulide in infants and information on acute consumption of infant formulae. *EFSA Journal*, 24(1), e9941.

In Situ Gold Functionalization of Gallium Nitride Nanoparticles Mediated by Polyethyleneimine for Enhanced Electrochemical Sensing of Erythromycin

Oana-Elena Carp[1]*, Denisse-Iulia Bostiog[1], Elena Laura Ursu[1], Rares Mocanu, Narcisa-Laura Marangoci[1], Ion Tighineanu[1,2,3], Alexandru Rotaru[1]

[1] Centre of Advanced Research in Bionanoconjugates and Biopolymers, "Petru Poni" Institute of Macromolecular Chemistry of the Romanian Academy, Grigore Ghica Voda 41A Alley, 700487 Iasi, Romania.

[2] National Center for Materials Study and Testing, Technical University of Moldova, Chisinau, Republic of Moldova.

[3] Academy of Sciences of Moldova, Chisinau, Republic of Moldova.

Abstract:

Hybrid nanomaterials that integrate surface functionality, colloidal stability, and efficient electron-transfer properties are highly attractive for electrochemical sensing applications. In this work, gallium nitride nanoparticles functionalized with polyethyleneimine and decorated with gold nanoparticles (GaN-PEI-Au) were synthesized and evaluated as an electrode modification layer for enhanced differential pulse voltammetric (DPV) detection of erythromycin. Branched polyethyleneimine (PEI, 25 kDa) served as a multifunctional interfacial agent, providing nanoparticle stabilization, amine-rich surface chemistry, and enabling the in situ formation of Au nanoparticles on the GaN surface under thermal conditions.

Systematic tuning of the Au precursor content revealed a strong influence on the physicochemical properties of the nanocomposites, including hydrodynamic size, surface charge, and optical behavior, as confirmed by dynamic light scattering, ζ-potential analysis, and UV–Vis spectroscopy. The optimized GaN-PEI-Au formulation exhibited high colloidal stability, a distinct localized surface plasmon resonance band in the 520–525 nm range, and well-distributed Au nanodomains anchored to the GaN framework, as further confirmed by electron microscopy.

When applied as a coating on gold electrodes, the GaN-PEI-Au nanocomposite significantly enhanced the electrochemical oxidation response of erythromycin compared to bare Au and GaN-PEI-modified interfaces. This improvement is attributed to synergistic effects arising from increased electroactive surface area and improved interfacial charge-transfer kinetics. Under optimized DPV conditions, the modified electrodes enabled sensitive and reliable erythromycin quantification over a concentration range of 5 nM to 2 µM, with a detection limit of 52.5 nM, highlighting the potential of GaN-PEI-Au nanocomposites as a robust and adaptable platform for pharmaceutical electrochemical sensing.

Keywords: Gallium nitride nanoparticles; Polyethyleneimine; Gold nanoparticles; Differential pulse voltammetry; Erythromycin; Electrochemical sensing; Nanocomposites

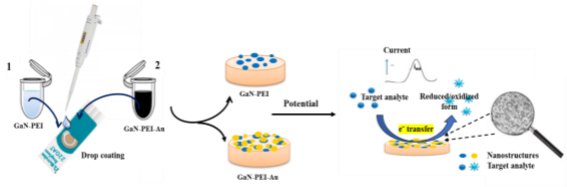

Figure 1: Schematic illustration of the drop-casting protocol for the deposition of GaN-PEI (1) and GaN-PEI-Au (2) films onto conventional gold electrodes.

References:

1. Chen, X., Li, X., Zhang, Y. et al. Gold nanoparticles modified porous GaN electrode for electrochemical determination of catechol. J Nanopart Res 27, 104 (2025). Hu, D., Liang, H., Wang, X., Luo, F., Qiu, B., Lin, Z., & Wang, J. (2020) https://doi.org/10.1007/s11051-025-06310-5.
2. Highly sensitive and selective photoelectrochemical aptasensor for cancer biomarker CA125 based on AuNPs/GaN Schottky junction. Analytical Chemistry, 92(14), 10114-10120. https://doi.org/10.1021/acs.analchem.0c02117

Functionalized Carbon Dots as Multifunctional Biointerface Nanomaterials for MRI and Fluorescence Imaging

Adina Coroaba [1,*], Bogdan-Florin Craciun [1], Adrian Fifere [1], Narcisa-Laura Marangoci [1]
[1] Center of Advanced Research in Bionanoconjugates and Biopolymers (IntelCentru), "Petru Poni" Institute of Macromolecular Chemistry, Iasi, Romania

Abstract:
Carbon dots (CDs) have become increasingly attractive for biomedical imaging because they combine good biocompatibility with adjustable fluorescence and flexible surface chemistry[1,2,3]. Their very small size, usually below 10 nm, together with the possibility of tuning their surface properties, makes them especially interesting for applications involving biological interfaces, where interactions between the material and the surrounding biological environment are critical for imaging performance. In this context, both surface functionalization and compositional tuning are important approaches for designing CDs with multimodal imaging capabilities.
In the present study, three categories of carbon dots were examined and compared: manganese-doped carbon dots (Mn-CDs)[3], polyethyleneimine-functionalized carbon dots (PEI-CDs)[2], and undoped CDs[1]. The Mn-CDs displayed both strong fluorescence and paramagnetic behavior, which supports their use in combined MRI and fluorescence imaging. The PEI-CDs showed intense fluorescence and surface features that could promote cellular uptake and improve imaging contrast. The undoped CDs also performed well as fluorescent agents and, in addition, exhibited marked antioxidant activity, particularly under conditions associated with oxidative stress.
Overall, the results indicate that both doping and surface modification have a strong effect on the behavior of carbon dots, influencing not only their optical properties but also their interactions at the biological interface. These findings suggest that carbon-dot-based nanostructures are promising candidates for multifunctional imaging systems and may be valuable in the development of advanced biointerface materials and diagnostic technologies for nanomedicine.

Keywords: carbon-based nanomaterials, carbon dots, surface functionalization, multimodal imaging, fluorescence imaging, biointerfaces, magnetic resonance imaging (mri).

Acknowledgments: This work was financially supported by a grant from the National Research Authority, project no. PNRR-III-C9-2022-I8-291, IntelDots, contract no. 760081/23.05.2023, within the National Recovery and Resilience Plan.

References:

1. Coroaba, A.; Ignat, M., Carp, O.-E., Stan, C. S., Filipiuc, S. I., Uritu, C. M., Simionescu, N., Marangoci, N.-L., Pinteala, M., Ania, C. O. (2025) Antioxidant activity and in vitro fluorescenc imaging application of N-, O-functionalized carbon dots, *Sci. Rep.*, 15, 25834.
2. Craciun, B.-F., Bostiog, D.-I., Coroaba, A., Simionescu, N., Sandu, A.-I., Dascalu, I.-A., Marangoci, N.-L., Pinteala, M., Ania, C. O. (2026) Green-emitting carbon dots from Protocatechuic acid and branched PEI: A multifunctional platform for bioimaging and gene delivery, *J Colloid Interface Sci.*, 703, 139147.
3. Turin-Moleavin, I.-A., Coroaba, A., Fifere, A., Marangoci, N. L., Pinteala, M., Uritu, C. M., Filipiuc S. I., Dobromir, M., Tigoianu, I. R., Pinteala, T. (2025) α-Ketoglutaric acid-derived carbon nanodots doped with manganese as fluorescent and MRI contrast agents, *Nanoscale*, 17, 20107-20122.

Practical Applications of Electron Microscopy for the Structural and Functional Characterization of Organic Nanoparticles

F. Doroftei [1,*], R. Ghiarasim [1] , N. Marangoci [1], M. Pinteala [1]
[1] Centre of Advanced Research in Bionanoconjugates and Biopolymers (IntelCentru), "Petru Poni" Institute of Macromolecular Chemistry, Iasi, Romania

Abstract:
Advanced organic nanocarriers require reliable characterization methods to provide comprehensive structural and functional insights at the nanoscale. *Scanning Transmission Electron Microscopy* (STEM) serves as a versatile and practical tool for evaluating a wide variety of nanoparticle formulations. In this study, two distinct nanoparticle series were investigated. The first series comprised polymeric micelles, including empty and drug-loaded micelles, some of which were surface-functionalized with bioactive proteins. The second series included liposomes, specifically *Small Unilamellar Vesicles* (SUVs) and *Large Unilamellar Vesicles* (LUVs), examined both unloaded and drug-loaded. STEM enabled precise determination of particle morphology, size distribution, and structural integrity. For polymeric micelles, contrast variations provided information on drug encapsulation and surface functionalization, while for liposomes, STEM revealed vesicular architecture and size differences between SUVs and LUVs. Comparative imaging across the two series highlighted the sensitivity of STEM in detecting subtle structural and functional variations, making it an essential tool for the evaluation of nanocarrier performance. Overall, this work demonstrates the practical utility of STEM in the structural and functional characte-rization of organic nanoparticles, providing critical insights to guide the design and optimization of advanced drug delivery systems.

Keywords: scanning transmission electron microscopy, micelles, liposomes, drug, protein, size, drug delivery systems.

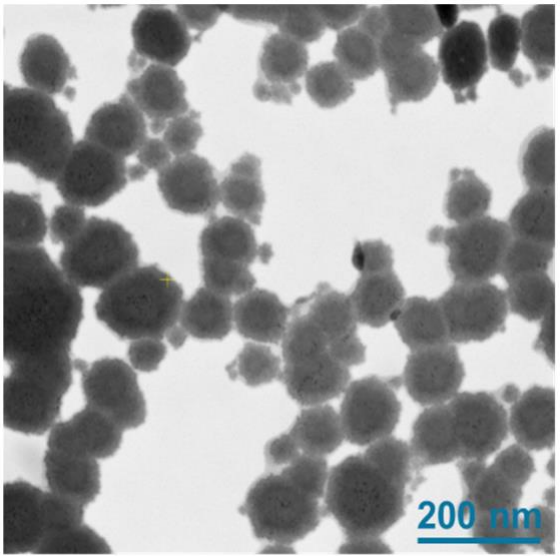

Figure 1: Scanning Transmission Electron Microscopy (STEM) image of copolymer micelles functionalized with proteins on their surface, illustrating their morphology, size distribution, and surface decoration.

References:

1. Ghiarasim, R., Tiron, C. E., Tiron, A., Dimofte, M. G., Pinteala, M., Rotaru, A. (2022), Solid-Phase Synthesized Copolymers for the Assembly of pH-Sensitive Micelles Suitable for Drug Delivery Applications, Nanomaterials, 12(11), 1798.
2. Tiron, C. E., Luta, G., Ghiarasim, R., Tiron, A., Nastasa, V., Anita, D. C., … Dimofte, M. G. (2025), Trastuzumab-Conjugated pH-Sensitive Micelles Exhibit Antitumor Activity and Induce Mesenchymal-to-Epithelial Transition in Triple-Negative Breast Cancer Cell Lines, Pharmaceutics, 17(12), 1554.

Acknowledgements
This work was financially supported by the Romanian National Authority for Research, project no. PNRR-III-C9-2023-I8-161, contract no. 760285/27.03.2024, within the National Recovery and Resilience Plan.

Antibacterial Textile Surfaces Enabled by the Fungal Pigment Xylindein Produced by *Chlorociboria aeruginascens*

T. Onggar[1], E. Sommer[1], M. Zschätzsch[2], A. Werner[2], L. Kliem[3], A. Pfriem[3], Th. Walther[2] und Ch. Cherif[1]

[1]Institute of Textile Machinery and High Performance Material Technology, Technische Universität Dresden, Dresden, Germany

[2]Institute of Natural Product Technology, Bioprocess Engineering, Technische Universität Dresden, Dresden, Germany

[3]Institute of Natural Product Technology, Wood Technology and Wood-Based Bioeconomy, Technische Universität Dresden, Dresden, Germany

Abstract:

Natural fungal pigments represent a promising class of sustainable functional colorants for advanced material applications. Xylindein, a highly intense blue-green secondary metabolite produced by fungi of the genus *Chlorociboria aeruginascens*, has attracted increasing attention due to its remarkable color stability [1], antimicrobial activity, and photoactive properties [2]. These characteristics make Xylindein a suitable candidate for the development of multifunctional textile dye [1] with additional antibacterial functionalities.

In this contribution, we report the cultivation of the producer strain *Chlorociboria aeruginascens* (Fig. 1a) and the extraction of Xylindein, carried out at the Institute of Natural Product Technology. The application of the pigment onto textile substrates (Fig. 1b), including both natural and synthetic fibers, is performed at the Institute of Textile Machinery and High Performance Textile Technology. Various components of the fungal culture are investigated regarding their suitability for textile functionalization, including purified Xylindein extracts, fungal biomass, and culture supernatants. Due to its water-insoluble nature, Xylindein exhibits excellent wash and light fastness, supporting its potential as a durable textile dye.

Furthermore, we evaluate the antimicrobial performance of Xylindein both in extract form and in the textile-applied state against Gram-negative (*Escherichia coli*) and Gram-positive (*Bacillus subtilis*) bacteria. The influence of active compound concentration as well as storage time of the extracted pigment on antimicrobial efficacy is discussed.

Potential fields of application particularly include medical textiles (Fig. 1c) requiring antimicrobial protection. In addition, the intrinsic photoactivity of Xylindein opens new perspectives for its use as an organic semiconductor material in optoelectronic devices. This study highlights the potential of fungal-derived pigments as sustainable multifunctional agents for next-generation textile.

Keywords: Xylindein, *Chlorociboria aeruginascens*, antimicrobial textiles, natural product-based functional materials, medical textiles, photoactive dye, optoelectronic applications.

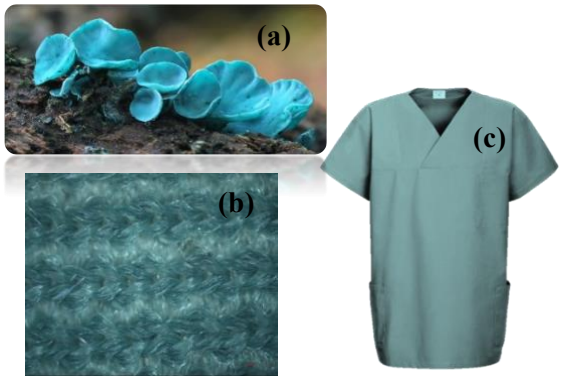

Figure 1: Overview of (a) the fungal pigment Xylindein from *Chlorociboria aeruginascens*, (b) its application to textile substrates, and (c) potential application areas, especially medical textiles.

References:

1. Hinsch E.M. and Robinson S.C. (2018), Comparing Colorfastness to Light of Wood-Staining Fungal Pigments and Commercial Dyes: An Alternative Light Test Method for Color Fastness, *MDPI Coating*, 8, 189
2. Krueger, T.D., Giesbers, G., Van Court, R.C., Zhu, L., Kim, R., Beaudry, C.M., Robinson, S.C., Ostroverkhova, O., Fang, Ch. (2021), Ultrafast Dynamics and Photoresponse of a Fungi-Derived Pigment Xylindein from Solution to Thin Films, *Photochemistry*, 27, 5627 – 5631

Characterization of a plasma discharge for the treatment of chronic wounds

Sessi Narcisse DEGUENON, Cristina MUJA, Florent SAINCT, Thomas MAHO, Philippe GUILLOT
Univ Toulouse, INUC, DPHE, Albi, France

Abstract:
Chronic wounds generally affect immunocompromised patients, particularly diabetics. They are characterized by prolonged healing times and bacterial proliferation, often from biofilms. Although conventional treatments reduce the bacterial load, they are highly time-consuming [1].
Cold plasmas emerged as a promising alternative treatment, due especially to reactive oxygen and nitrogen species (RONS) production, interacting with biological tissues. These interactions result in an effective decontamination while promoting biological mechanisms involved in tissue healing [2]. The objective of this project is to develop a Dielectric Barrier Discharge (DBD) with biocidal capabilities for a future treatment of cutaneous wounds on a few cm².
In this work, the first step of the project concerning the plasma source characterization is presented. The cylindrical DBD consists of an upper chamber and a lower chamber separated by a divider. The high-voltage electrode is a metallic rod placed inside the source. A first grounded electrode is located outside the upper chamber and a second optional one can be connected to the target. Two gases are used at a flow rate of 2 $l.min^{-1}$: He (reference) and He-0.2% O_2.
The discharge is powered by a pulsed high-voltage generator delivering a power between 1 W and 100 W. The range of pulse repetition frequency is 20-100 kHz. In this work, the experiments were carried out at a frequency of 20 kHz and a duty cycle of 8%. Diagnostics include electrical and optical measurements. The applied voltage is monitored using a high-voltage probe (Tektronix P6015A). The total current is measured with a current transformer (PEARSON™ 6585). Optical emission spectroscopy is used to characterize plasma emissions in both discharge chambers (upper and lower) and to analyze the spatial distribution on the target surface (exemple on figure 1). An ICCD camera is used to investigate the discharge homogeneity and its spatio-temporal evolution. As a function of the gas conditions, the electrical and optical results will be presented end discussed.

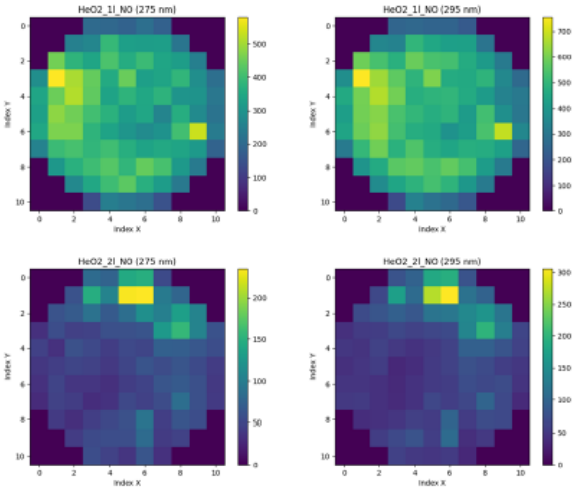

Figure 1 : Spatial distribution of two NO emission lines from an He-0.2% O_2 plasma on a glass target surface (6 cm diameter).

Keywords: Dielectric Barrier Discharge, RONS, electrical measurements, optical emission spectroscopy, ICCD camera.

Acknowledgements

This work has been supported by the Occitanie region, the European Regional Development Fund (ERDF), and the French government, through the France 2030 project managed by the National Research Agency (ANR) with the reference number “ANR-22-EXES-0015”.

References:

1. Cavallo, I.; Sivori, F.; Mastrofrancesco, A.; Abril, E.; Pontone, M.; Di Domenico, E.G.; Pimpinelli, F. (2024) Bacterial Biofilm in Chronic Wounds and Possible Therapeutic Approaches. *Biology*, 13, 109
2. Moszczynska, J.; Roszek, K.; Wisniewski, M. (2023) Non-Thermal Plasma Application in Medicine – Focus on Reactive Species Involvement. *Int. J. Mol. Sci*., 24, 12667

Non-Thermal Plasma for Sustainable Seed Technologies

P. Ličková[1,*], D. Kostoláni[2], S. Mošovská[3], M. Khalaf[1], R. Švubová[2], V. Medvecká[1], D. Kováčik[1], A. Zahoranová[1]

[1] Department of Experimental Physics, Faculty of Mathematics, Physics and Informatics, Comenius University Bratislava, Mlynska Dolina F1, 842 48 Bratislava, Slovakia

[2] Department of Plant Physiology, Faculty of Natural Sciences, Comenius University Bratislava, Ilkovičova 6, Mlynská dolina, 842 15 Bratislava, Slovakia

[3] Department of Nutrition and Food Quality Assessment, Faculty of Chemical and Food Technology, Slovak University of Technology, Radlinského 9, 812 37 Bratislava, Slovakia

Abstract:

Traditional pre-sowing technologies rely heavily on synthetic chemicals (powder fillers, pesticides, fertilizers, etc.) to enhance seed handling, crop protection, and nutrient delivery [1]. Growing concerns about the ongoing environmental pollution caused by these agrochemicals, as well as the reduced quality of the resulting crops, are driving the development of innovative, green, sustainable processes and technologies and their integration into practice. Non-thermal plasma (NTP) offers a sustainable alternative by utilizing a complex mixture of UV radiation, electrons, and reactive oxygen and nitrogen species (RONS) to modify seed properties and initiate many important biochemical pathways [2]. Beyond acting as a rapid, chemical-free decontaminant against various pathogens, NTP significantly enhances seed vigor and resilience against abiotic stressors such as drought and salinity [3]. Physically, plasma-induced surface etching and the deposition of polar functional groups increase seed coat wettability, effectively overcoming natural hydrophobicity. This surface modification ensures the uniform adhesion and retention of low-dose dressings, allowing for a 50–90% reduction in fungicide application without compromising plant physiology [4]. Consequently, NTP technology represents a high-efficiency tool for sustainable agricultural growth, bridging the gap between high yields and environmental protection.

This contribution presents key findings from our recent experimental work on the multiple benefits of NTP in agriculture. Our results show that NTP-induced improvements in germination remain stable for up to six months post-treatment, confirming that plasma-activated seeds are suitable for long-term storage and conventional supply chains [5]. To address industrial feasibility, we evaluated the energy efficiency of a dielectric barrier discharge reactor by comparing a laboratory-scale setup with an up-scale prototype designed for high-throughput processing of seeds [6]. Additionally, the antimicrobial efficacy of these and other plasma sources was successfully validated by inactivating pathogens on different seed types, highlighting NTP's potential as a robust, chemical-free decontamination tool [7].

The successful transition from laboratory experiments to energy-efficient prototypes confirms NTP as a commercially viable solution for reducing the environmental footprint of modern crop production. Furthermore, industrial integration of plasma technologies could support the global shift toward chemical-free, sustainable farming.

This work was supported by the Slovak Research and Development Agency under the Contract no. APVV-21-0147. Funded by the EU NextGenerationEU through the Recovery and Resilience Plan for Slovakia under the project No. 09I03-03-V04-00143.

Keywords: non-thermal plasma, sustainable agriculture, up-scaling, seed treatment, germination, decontamination.

References:

1. Pedrini, S., Merrit, J. et al. (2017) Seed Coating: Science or Marketing Spin?, *Trends Plant Sci.*, 2, 106-116.
2. Bilea, F. et al. (2024), *Crit. Rev. Plant Sci.,* 6, 428–486.
3. Holubová, Ľ., Kyzek S. et al. (2020), *Int. J. Mol. Sci.*, 21, 9466.
4. Hoppanová, L., Medvecká, V. et al. (2020), *Acta Chim. Slovaca*, 1, 26–33.
5. Šrámková, P., Kostoláni, D. et al. (2025), *Sci. Rep.,* 15, 35001.
6. Šrámková, P., Švubová, R. et al. (2026), *Innov. Food Sci. Emerg. Technol.*, 107, 104385.
7. Mošovská, S., Khalaf, M., Šrámková, P. et al. (2026), *Food Bioprocess Technol.*, 19, 1 (1-15).

Non-Thermal Atmospheric Plasma-Induced Transformation of Agro-Industrial By-Products into Soil Improvers

V. Crespo-Torbado [1], A. Álvarez-Ordóñez[1], R. Bodelón [1], Y. Chourak [2], PF. Rizzo [2], E. Garcia-Muchart [2], M. González-Raurich [1], M. Prieto [1], M. López [1], M. Oliveira [1]
[1]Department of Food Hygiene and Technology, University of León, León, Spain.
[2]BETA Technological Centre (UVic-UCC), Vic, Spain.

Abstract:
Food waste management represents a major global challenge, with around 20% of food produced in the European Union being lost or wasted. A significant portion arises from food processing industries that generate nutrient-rich by-products suitable for valorisation within a circular economy. In this framework, non-thermal atmospheric plasma (NTAP) emerges as a promising, sustainable technology for nitrogen fixation and the production of soil improvers.
This study assessed the potential of NTAP to convert liquid waste streams from vegetable processing—particularly potato—into high-value soil improvers. Plasma treatment using a catalyst reactor (Fig. 1) was performed at 180 V, 54 µs, 1500 Hz, for 30 minutes, with an air flow rate of 0.8 L/min, which led to a three-fold increase in nitrite and a forty-fold increase in nitrate concentrations, confirming the technology's efficiency in enhancing nitrogen availability.
A controlled greenhouse experiment was carried out to evaluate extracts derived from NTAP-treated potato liquid waste stream on wheat (*Triticum aestivum*) growth under normal and water stress conditions. Four treatments were established: control (T1), mineral fertilizer (T2), NTAP-treated potato liquid waste stream (T3), and the same extract under water stress (T4). Plants were grown in 3 L pots with 50% peat, 25% vermiculite, and 25% perlite substrate under controlled temperature, humidity, and a 12 h photoperiod. Water stress conditions were maintained at 35% of the water-holding capacity (WHC), while non-stress treatments were kept at 70% WHC.
Results showed that NTAP-treated extracts improved plant growth compared to the control, promoting higher tiller production and fresh biomass even under stress. Moreover, T3 helped maintain a more stable soil pH, indicating a buffering effect that could enhance nutrient availability and soil stability, and T4 showed higher total phosphorus content, highlighting its potential to improve soil fertility.
Overall, NTAP-treated potato waste streams represent an eco-efficient alternative to conventional fertilizers, supporting resilient and circular agricultural systems.

Keywords: non-thermal atmospheric plasma, nitrogen fixation, food waste, valorisation, soil improvers, circular economy, soil fertility, sustainable agriculture.

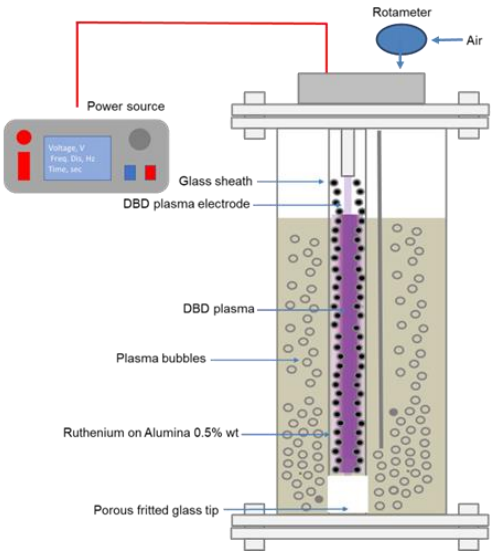

Figure 1: Scheme of NTAP treatment using catalyst reactor to convert vegetable waste into soil improvers.

Influence of Plasma and Plasma Treated Water on Plant Vitality in Short and Long-Term Applications

Z. Kozáková [1*], L. Krejsová [1], K. Šindelková [1], E. Neroda [1], K. Šťastná [1]
[1] Faculty of Chemistry, Brno University of Technology, Brno, Czech Republic

Abstract:
Due to the significantly increasing world population, drought or global warming, the nowadays agricultural production is exposed to many challenges. Therefore, new methods are being investigated in order to ensure the required crop production. Methods based on interactions of non-thermal plasma with biological object (seeds, plants, etc.), joined under the global research direction as Plasma agriculture, seem to be promising to enhance seed germination, plant growth and vitality.

Interactions of non-thermal plasma with liquids induce both physical and chemical changes leading to the formation of various reactive species containing oxygen and nitrogen with high redox potential (RONS) [1]. After the plasma application, such affected water or water solution is called plasma treated water (PTW) [2]. Due to the presence of RONS, plasma treated water gains antimicrobial properties as it induces oxidative and nitrosative stress in cells. Therefore, such stressing conditions can either inactivate microorganisms or stimulate the cell production and growth, depending on the cell kind and PTW exposition. Moreover, higher content of nitrogen species contributes to the plant growth and nutrition. Applied on seeds, PTW enhances their wettability and stimulates germination. Therefore, plasma treated water solutions offer an alternative form of a modern fertilizer with antifungal properties which can be prepared from water by minimal electric energy supply without any environmentally harmful additives and without any waste.

Our work deals with both quantitative and qualitative study of plasma and plasma treated water effects on seeds and plants in short (7 day) and long (3 month) term experiments. Several non-thermal plasma sources based on DBD were applied on seeds prior to their germination. Plasma treated water solutions were prepared by the modified pin-hole system generating plasma inside water volume with additional gas bubbling which produce high amount of nitrites, nitrates, and hydrogen peroxide. Stability of the prepared PTW was evaluated over the studied period, too. Both short-term hydroponic experiments with garden cress (*Lepidium sativum*, Figure 1) and long-term pot experiments with chives (*Allium schoenoprasum*) and lettuce (*Lactuca sativa*) followed up our previous study with growth and vitality of radish (*Raphanus sativus* L.) [3] extending it by more qualitative plant parameters such as content of polyphenols, chlorofylls, etc.

Keywords: plasma activated water, plasma agriculture, seed treatment, plant vitality, polyphenols, chlorophyll.

Figure 1: Garden cress after the 7-days hydroponic treatment by tap watering (left) and PTW watering (right).

References:

1. P.J. Bruggemann et al. (2016), Plasma–liquid interactions: a review and roadmap, *Plasma Sources Sci. Technol.* 25, 053002.
2. N. Puač, M. Gherardi, M. Shiratani (2018), Plasma agriculture: A rapidly emerging field, *Plasma Processes and Polymers* 15, 1700174.
3. T. Vozár, K. Trebulová, Z. Kozáková, F. Krčma, V. Enev, L. Čechová (2025), Influence of plasma activated water on the growth and vitality of radish (*Raphanus sativus* L.), *J. Phys. D: Appl. Phys.* 58, 185206.

Growth, Hydrogen Permeation, and Crystal field induced Stark shifts of Er_2O_3 thin film on SS316L and Si (001)

Halim Choi [1], Yongmin Kim [2,*],
[1] Department of Electronics Technology, Budapest University of Technology and Economics, Budapest, Hungary
[2] Department of Physics, Dankook University, Cheonan, Korea

Abstract:
The permeation of hydrogen and its isotopes in fusion materials is one of the key issues for nuclear fusion operation in relation with safety, fueling, reliability, and economy. A quantitative hydrogen-isotope detection system, which requires high vacuum (~ 10^{-8} Torr) and high temperature (~ 1000°C) for nuclear fusion applications, was designed and constructed in order to study the permeation behaviors in the solid materials consisting of fusion materials.
We fabricated an Er_2O_3 thin film on a type-316L stainless-steel substrate by using a metal-organic chemical vapor deposition technique for use as a hydrogen-isotope permeation barrier. Electron-microscopy-based imaging and energy-dispersive X-ray spectroscopy measurements, together with X-ray diffraction experiments, indicate a sound film quality. We also measured deuterium permeation in the film at high temperatures ranging from 600°C to 800°C. The permeation reduction was most apparent at 650°C. Above 800°C, we confirmed that the film was damaged and did not work as a permeation barrier.
Optical transitions of an Er_2O_3 film on a Si substrate were investigated. Numerous sharp transitions corresponding to the Er^{3+} ionic levels were observed, which show Stark shifts induced by the crystal field. With decreasing temperature from 300 K to 5 K, all transition peaks exhibit spectral red-shift. We believe that such red-shift behavior is due to the change of the crystal field together with the change of strain field induced by the film and the substrate in varying temperature. An interesting result is the total amount of red-shifts between 300 K and 5 K. We obtain that the higher transition energy peaks show bigger red-shifts. This is very consistent to all transition peaks. This is because the dipole moments between the transition levels are different that lead to different amounts of Stark shifts.

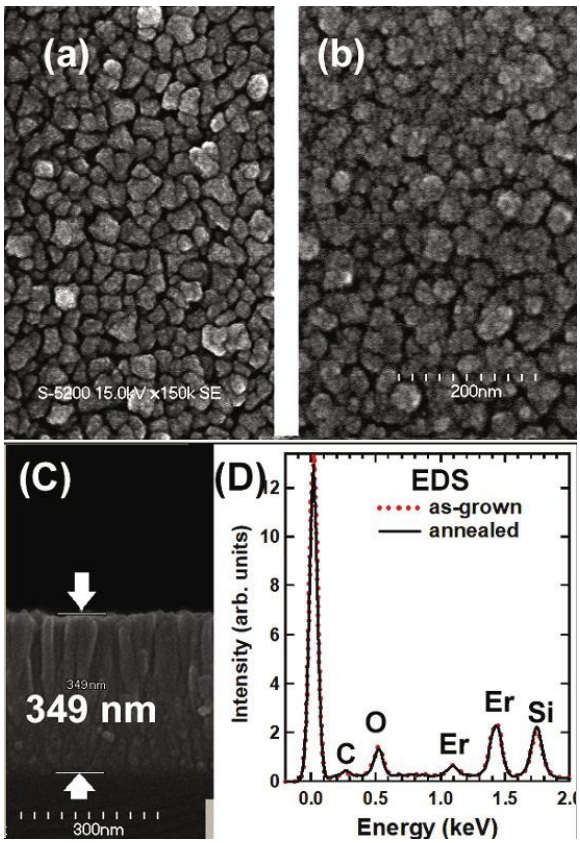

Figure 1: (a) and (b) Scanning electron microscopy images of the as-grown and the heat-treated samples, respectively. Both samples show granular-shape polycrystals with an average grain size of ~30 nm. (c) The thickness of the Er_2O_3 film is 349 nm. (d) EDS spectra of the as-grown (dashed red line) and the heat-treated (solid black line) samples. Both samples exhibit identical amounts of each element.

Keywords: chemical vapor deposition, hydrogen permeation, nuclear fusion applications, Stark shifts, crystal field, strain field, spectral red-shift.

Development of Pd and Pd-Ag Thin Films by Magnetron Sputtering for High-Performance Hydrogen Separation Membranes

A. D'Angelo [1*], S. Esposito [1], G. Rossi [1], C. Diletto [1], R. Volpe [1], M. Lanchi [2]
[1] Energy Technologies and Renewable Sources Department, Italian National Agency for New Technologies, Energy and Sustainable Economic Development - ENEA, Portici (NA), Italy
[2] Energy Technologies and Renewable Sources Department, Italian National Agency for New Technologies, Energy and Sustainable Economic Development - ENEA, Rome, Italy

Abstract:
Steam reforming of fossil and renewable fuels, is a key process for hydrogen production but requires temperatures higher than 800 °C in conventional reactors. The integration of selective membrane can significantly lower operating temperatures, thereby enabling the reactor coupling with renewable energy sources (such as concentrated solar thermal) and mitigating thermal and mechanical stresses on the component itself.
Pd and Pd-Ag alloys are among the most effective materials for membrane fabrication thanks to their high hydrogen permeance, selectivity, and stability. For high temperature applications, they are typically deposited on ceramic supports; however this membrane typology suffer from thermal stress and issues related to thermal cycling. This work investigates the deposition of Pd and Pd-Ag thin films on metallic supports via magnetron sputtering using an ENEA prototype deposition system. Substrate pre-treatments and process parameters such as power, working pressure, substrate translation and rotation speed, were optimized to achieve dense and defect-free films.
AFM (Atomic Force Microscopy) quantified surface roughness, while XRD (X-Ray Diffraction) provided insights into lattice strain and alloy composition, confirming an Ag content of 23 wt%. The optimized films exhibit thicknesses in the range of 200–300 nm and controlled microstructural properties, indicating significant potential for integration into membrane-assisted steam reforming reactors. These results are consistent with recent advancements in Pd-based membrane technologies and identify optimal conditions for Pd and Pd-Ag thin film, providing useful guidelines for the fabrication of high-performance membranes for steam reforming reactors.
In conclusion, this study demonstrates a scalable approach for the fabrication of high-performance membranes, paving the way toward more efficient and sustainable hydrogen production technologies.

Keywords: Thin film, H_2 separation, Pd membranes, Pd-Ag membranes, Steam reforming reactors, Magnetron Sputtering, H_2 production technologies-

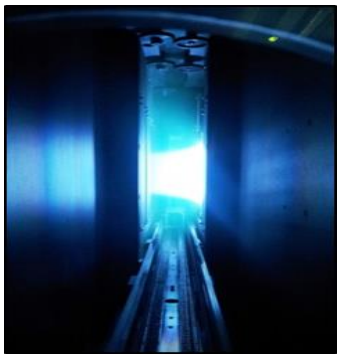

Figure 1: View of the plasma discharge within the ENEA sputtering system.

Acknowledgments:

This work was carried out within the Operational Research Plan (POR) on green Hydrogen developed by ENEA and financed by the Ministry of the Environment and Energy Security - project code: I83C22001170006 -National Recovery and Resilience Plan (Mission 2. Investment 3.5) financed by the European Union as part of the Next Generation EU program.

References:

1. Petersa, T.A., Rørvika, P.M., Sundea, T.O., Stangea, M., Ronessb, F., Reinertsenb, T.R., Rædera, J.H., Larringa, Y., Bredesena, R. (2017), Palladium (Pd) membranes as key enabling technology for precombustion CO_2 capture and hydrogen production, *Energy Procedia*, 114 37 – 45.
2. Cerone, N., Zito, G.D., Florio, C., Fabbiano, L., Zimbardi, F. (2024), Recent Advancements in Pd-Based Membranes for Hydrogen Separation, *Energies*, 17 (16), 4095.

Surface Modification Approaches on Porous Hastelloy for Long-Lasting Hydrogen Separation Membranes

`G. Rossi [1,*], A. D'Angelo [1], C. Diletto [1], S. Esposito [1], A. Guglielmo [1], G. Rametta [1]
[1] Energy Technologies and Renewable Sources Department, Italian National Agency for New Technologies, Energy and Sustainable Economic Development - ENEA, Portici (NA), Italy

Abstract:
Hydrogen production and separation are pivotal for achieving a sustainable energy transition. Integrating palladium (Pd)-based membranes into steam reforming reactors represents an efficient route, enabling an equilibrium shift toward products and high conversion under milder conditions, while reducing capital costs.
However, fabricating ultra-thin, defect-free Pd layers on porous metallic supports remains challenging due to surface roughness, large pore sizes, and potential metal interdiffusion.
This work addresses the aforementioned limitations by exploring chemical-physical treatments applied to commercial Hastelloy X substrates, along with the development of ceramic interlayers fabricated via sol-gel techniques (spin/dip coating), sputtering, and selective oxidation of thin metallic films. Surface morphology evolution in terms of roughness, porosity, and pore size distribution was studied using SEM (Scanning Electron Microscopy), AFM (Atomic Force Microscopy), and profilometry, while structural properties were analyzed by XRD (X-Ray Diffraction).
In-depth process optimization enabled predictive control of ceramic layer thickness, morphology and stoichiometry as a function of process parameters and material formulation.
Provisional results show that the optimized interlayer effectively mitigates the main limitations of metallic supports, with an average surface roughness reduction of about 70% and a decrease in large pore sizes of approximately 40%. Preliminary stability tests under representative membrane-assisted steam reforming conditions indicate encouraging stability and effective barrier properties of the intermediate layers against metal diffusion from the metallic support.
Overall, the proposed approach supports the design of optimized intermediate layers for the deposition of dense, ultra-thin Pd-based films, paving the way toward scalable membrane reactor technologies for industrial hydrogen production.

Keywords: H_2 separation, Dip coating, Sputtering, Intermediate ceramic layer, Pd-based membranes, Thin film, Steam reforming.

Acknowledgments

This work was carried out within the Operational Research Plan (POR) on green Hydrogen developed by ENEA and financed by the Ministry of the Environment and Energy Security - project code: I83C22001170006 -National Recovery and Resilience Plan (Mission 2. Investment 3.5) fi-nanced by the European Union as part of the Next Generation EU program.

References:

1. Cerone, N, Zito, G. D., Florio, C., Fabbiano L. and Zimbardi F. (2024), Recent Advancements in Pd-Based Membranes for Hydrogen Separation, *Energies,* 17(16), 4095; https://doi.org/10.3390/en17164095
2. Alique D., Martinez-Diaz D., Sanz R. and Jose A. Calles J. A. (2018), Review of Supported Pd-Based Membranes Preparation by Electroless Plating for Ultra-Pure Hydrogen Production, *Membranes* 8, 5; doi:10.3390/membranes8010005.
3. Anand, A., Singh, S.V. and Upadhyay R.K (2025), Effect of CeO_2-YSZ intermediate layers for enhanced hydrogen permeance of palladium membrane supported on porous α-Al_2O_3 tube. *Res Chem Intermed*, https://doi.org/10.1007/s11164-025-05797-w.

Radiative cooling coating solution: principle and applications

H. Lee [1,2,*], H. K. Im[1], J. I. Park [1,2]
[1] Department of Materials Science and Engineering, Korea University, Seoul, Korea
[2] Zerc Co. Ltd, Seoul, Korea

Abstract:
Radiative cooling is a breakthrough technology that can lower the temperature of an object without consuming energy. Radiative cooling reflects the sunlight of the company as much as possible, and the heat of the material is radiated as much as possible in the form of infrared rays to be cooled. In general, a metal thin film such as silver is used as a reflective layer for incident sunlight, and on it, it is transparent to visible light but has high absorption to long-wavelength infrared rays, so radiative cooling is possible by coating inorganic ceramic or polymer materials that can be emitted well.
In this presentation, ceramic particles were dispersed in a transparent polymer binder to scatter and reflect incident sunlight and emit long-wavelength infrared rays. That is, a radiative cooling material in the form of coating solution was developed. If applied this radiative cooling coating solution on wood, glass, metal, and plastic plates to form a coating film, the surface temperature will be lower than the ambient temperature even during the daytime when the sun shines.
In this presentation, we report radiative cooling results that are lower in temperature than ambient air temperature in various systems coated with radiative cooling coating solution, The result of radiative cooling coating solution on refrigerated warehouse was also reported. Reduction of more than 25% of the electricity usage to maintain -20 ℃ of inner temperature was observed for the warehouse coated with radiative cooling coating solution.

ZERC Co., Ltd. is a spin-op start-up in Korea University's laboratory and commercializes radiative cooling coating solution.

Keywords: radiative cooling, total solar reflection, sky window, IR emission, coating solution.

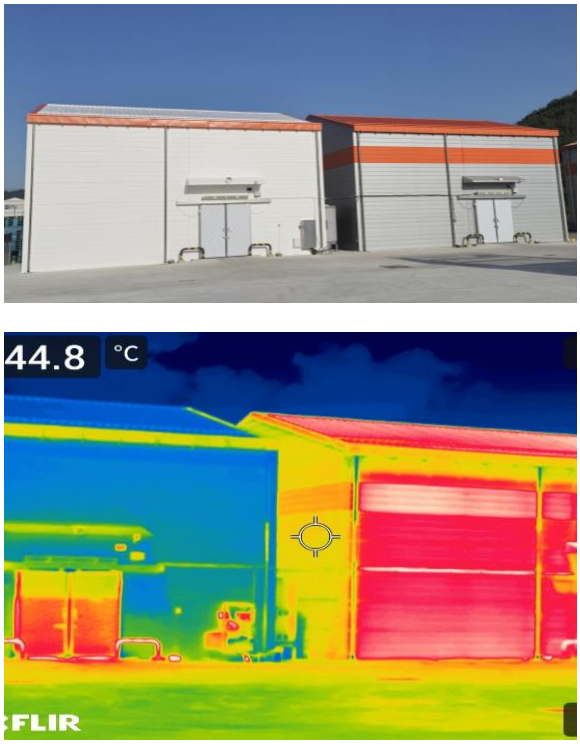

Figure 1: Figure illustrating the electrical power-reduction experiment for cooling. Only left warehouse was coated with rasiative cooling coating solution and the internal warehouse of both warehouses were set to −20 °C, and electricity consumption required to maintain this temperature was measured.

References:

1. Yun, J., Chae, D., So, S., Lim, H., Noh, J., Park, J., Kim, N., Park, C., Lee, H. & Rho, J., (2024) Optimally Designed Multimaterial Microparticle-Polymer Composite Paints for Passive Daytime Radiative Cooling, ACS Photonics. 10, 8, p. 2608-2617

Bismuth-Rich Oxyiodides as Highly Efficient Photocatalysts for the Visible-Light Photooxidation of As(III)

S. Kittiwachana [1,2,*], S. Kaowphong[1,2], T. Charoensuk[1], C. Sronsri[1,3]
[1] Department of Chemistry, Faculty of Science, Chiang Mai University, Chiang Mai 50200, Thailand
[2] Materials Science Research Center, and Center of Excellence in Materials Science and Technology, Faculty of Science, Chiang Mai University, Chiang Mai 50200, Thailand
[3] Office of Research Administration, Chiang Mai University, Chiang Mai 50200, Thailand

Abstract:
Semiconductor-mediated photocatalysis is a promising approach for addressing water contamination caused by hazardous pollutants. Bismuth oxyiodide (BiOI) is a well-known photocatalyst due to its layered crystal structure and visible-light responsiveness, giving it useful physicochemical and photocatalytic properties. However, its performance is limited by the fast recombination of photogenerated electrons and holes, largely due to its narrow band gap (1.77 eV), which lowers the efficiency of visible-light utilization. In addition, the relatively weak reduction potential of electrons in the conduction band (CB) and the weak oxidation ability of holes in the valence band (VB) further restrict its broader photocatalytic use. Bismuth-rich oxyiodides ($Bi_xO_yI_z$) provide tunable elemental ratios and adjustable electronic band levels. Increasing the Bi content results in a more negative CB and a more positive VB, offering more suitable redox potentials. In this study, $Bi_xO_yI_z$ materials (BiOI, $Bi_7O_9I_3$, and Bi_5O_7I) were successfully synthesized using a cyclic microwave irradiation method. The influence of NaOH content on material formation was investigated. The results revealed that NaOH content controlled the x, y, and z ratios in $Bi_xO_yI_z$. BiOI formed when 0, 2, or 4 mmol NaOH were added, whereas $Bi_7O_9I_3$ and Bi_5O_7I were produced when 6 and 8 mmol NaOH were used, respectively. Among the synthesized photocatalysts, Bi_5O_7I exhibited the highest photooxidation activity toward arsenite (As(III)), converting it into the less harmful arsenate (As(V)). $Bi_7O_9I_3$ exhibited a moderate level of activity, whereas BiOI showed the lowest. The superior performance of Bi_5O_7I relative to $Bi_7O_9I_3$ and BiOI is attributed to its more efficient charge separation and migration, along with more suitable band positions that strengthen the redox ability of the charge carriers and facilitate the generation of reactive species.

Keywords: bismuth-rich oxyiodides, visible-light photocatalysis, As(III) photooxidation, wastewater treatment

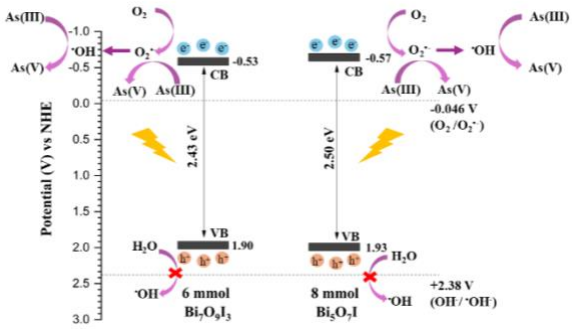

Figure 1: Proposed photocatalytic mechanism of $Bi_7O_9I_3$ and Bi_5O_7I, illustrating the generation of reactive species under visible-light irradiation.

References:

1. Luangwanta, T., Chachvalvutikul, A., Watwiangkham, A., Jungsuttiwong, S., Kaowphong, S. (2024), Ethylene glycol-assisted microwave synthesis of bismuth-rich oxychlorides photocatalysts with oxygen vacancies for efficient degradation of bisphenol A and oxidation of arsenite, *J. Environ. Chem. Eng.*, 12, 114100.
2. Chachvalvutikul, A., Jakmunee, J., Thongtem, S., Kittiwachana, S., Kaowphong, S. (2019), Novel $FeVO_4/Bi_7O_9I_3$ nanocomposite with enhanced photocatalytic dye degradation and photoelectrochemical properties, *Appl. Surf. Sci.*, 475, 175-184.

Hydrothermal synthesis of BiOBr/$Bi_{24}O_{31}Br_{10}$ Heterojunction Under pH-Controlled Conditions for Enhanced Dye Degradation, Antibiotic Removal, and Arsenite Oxidation

S. Kaowphong [1,2,*], P. Wisedkoon[1], C. Sronsri[1,3]
[1] Department of Chemistry, Faculty of Science, Chiang Mai University, Chiang Mai 50200, Thailand
[2] Materials Science Research Center, and Center of Excellence in Materials Science and Technology, Faculty of Science, Chiang Mai University, Chiang Mai 50200, Thailand
[3] Office of Research Administration, Chiang Mai University, Chiang Mai 50200, Thailand

Abstract:
Bismuth oxybromide (BiOBr) is a promising photocatalyst for clean energy use and environmental purification. However, its photocatalytic activity is limited because photogenerated charge carriers recombine quickly, which suppresses the formation of reactive species. Improving its photocatalytic performance therefore remains a challenge. One practical strategy is to develop BiOBr-based heterojunction systems. Bismuth-rich oxybromides ($Bi_xO_yBr_z$) have also received attention due to their simple synthesis, tunable morphology with controllable stoichiometry, and improved light absorption. In this study, BiOBr, $Bi_{24}O_{31}Br_{10}$, and BiOBr/$Bi_{24}O_{31}Br_{10}$ were hydrothermally synthesized using $Bi(NO_3)_3 \cdot 5H_2O$ and KBr as precursors, with NH_4OH used to adjust the suspension pH. The results showed that pristine BiOBr formed at the initial pH solution. When the pH was increased to 9, pure $Bi_{24}O_{31}Br_{10}$ was obtained, while adjusting the pH to 7 produced the BiOBr/$Bi_{24}O_{31}Br_{10}$ heterojunction. The photocatalytic activity of the materials was evaluated through the degradation of organic pollutants, including rhodamine B and ciprofloxacin, under visible-light irradiation. The BiOBr/$Bi_{24}O_{31}Br_{10}$ heterojunction delivered the highest activity for both pollutants, removing 99.06% of rhodamine B, compared to 52.07% for BiOBr and 81.96% for $Bi_{24}O_{31}Br_{10}$. For ciprofloxacin, the heterojunction achieved 88.67% removal, whereas BiOBr and $Bi_{24}O_{31}Br_{10}$ showed 63.68% and 68.35%, respectively. The material was further examined for photooxidation of arsenite (As(III)) at different pH values, and higher oxidation levels were observed in basic solutions. The enhanced photocatalytic activity of the heterojunction is attributed to its ability to use visible light more effectively and its improved charge separation and migration. This performance is further supported by the close interfacial contact between BiOBr and $Bi_{24}O_{31}Br_{10}$, which leads to the formation of a Type-II heterojunction. Evidence from electrochemical analysis, scavenging experiments, and X-ray photoelectron spectroscopy confirms the charge transfer pathway and the role of the interface in driving the photocatalytic process.

Keywords: bismuth-based photocatalyst, heterojunction, visible-light photocatalysis, organic photodegradation, As(III) photooxidation, wastewater treatment

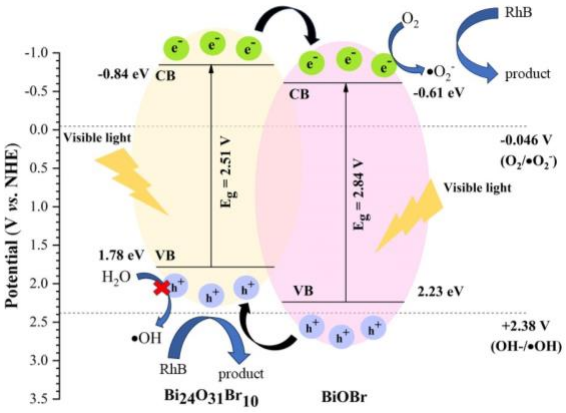

Figure 1: Proposed charge transfer pathway and photocatalytic mechanism of RhB photodegradation catalyzed by the BiOBr/$Bi_{24}O_{31}Br_{10}$ heterojunction.

References:

1. Luangwanta, T., Thiraphatchotiphum, C., Kaowphong, S. (2025), Microwave-synthesized BiOCl-$Bi_4O_5Br_2$ solid-solution photocatalysts with tunable band structures for efficient visible-light-driven removal of Cr(VI), As(III), and bisphenol A, *J. Water Process Eng.*, 80, 109171.
2. Chachvalvutikul, A., Luangwanta, T., Kaowphong, S. (2021), Double Z-scheme $FeVO_4$/$Bi_4O_5Br_2$/BiOBr ternary heterojunction photocatalyst for simultaneous photocatalytic removal of hexavalent chromium and rhodamine B, *J. Colloid Interface Sci.*, 603, 738-757.

Titanium Nitride Protective Coatings for High-Performance Proton Exchange Membrane Water Electrolysis

Bhavesh Chavan [a,c], Ruud Kortlever [b,c], J. Ruud van Ommen [a,c*]
[a] Product and Process Engineering, Department of Chemical Engineering, Faculty of Applied Sciences, TU Delft
[b] Large-Scale Energy Storage, Process and Energy, Faculty of Mechanical Engineering, TU Delft
[c] e-Refinery Institute, TU Delft
[*]corresponding author: j.r.vanommen@tudelft.nl

Abstract
Proton-exchange membrane (PEM) water electrolysis is a leading technology for green hydrogen production, offering high efficiency and compact design. However, its widespread adoption is hindered by the reliance on costly platinum group metals and titanium-based components required to endure the acidic, oxidizing environment during operation [1].
Titanium-based components, such as the porous transport layer (PTL) and bipolar plates, play critical roles in facilitating mass transport, ensuring uniform current and heat distribution, and providing mechanical stability to the system. Yet, under operational conditions, these components form semiconducting oxide layers, which reduce electrical conductivity and compromise system efficiency. Additionally, they require high hydrophilicity to improve gas-liquid contact and mass transfer. To address these challenges, these components are often coated with thick layers (~200nm) of precious metals such as platinum or gold, increasing costs significantly [2].
In this work, titanium nitride (TiN) coatings are investigated as a cost-effective alternative to conventional Pt or Au coatings on PTLs, aiming to provide high corrosion resistance, conductivity, and hydrophilicity [3,4]. Three gas-phase coating techniques to make TiN are explored in this work: atomic layer deposition (ALD), reactive sputtering (physical vapor deposition), and direct plasma nitridation. ALD offers excellent coating conformality and high penetration depth but involves a more complex and time-intensive process. In contrast, reactive sputtering is a simpler and more cost-effective method, though it can compromise coating conformality. The conformality achievable with direct plasma nitridation remains uncertain and requires further evaluation.
Initial studies involved TiN film deposition on silicon wafers to evaluate coating quality, followed by application on 3D PTL structures. Electrochemical testing was first conducted in a three-electrode setup, after which the coated PTLs were evaluated under PEM water electrolysis conditions. The results of our work demonstrate the potential of titanium nitride coatings as a scalable protective layer for PEM water electrolysis components, offering a pathway toward cost-effective and efficient green hydrogen production.

References

1. U. Babic, M. Suermann, F.N. Büchi, L. Gubler and T.J. Schmidt*, J. Electrochem. Soc.*, 164(4), F387, **2017**.
2. T. Srour, K. Kumar, V. Martin, L. Dubau, F. Maillard, B. Gilles, J. Dillet, S. Didierjean, B. Armoury, T. Dung Le and G. Maranzana, *Int. J. Hydrogen Energy,* 58, 351-361, **2024**.
3. G. Liu, D. Shan, B. Fang and X. Wang*, Int. J. Hydrogen Energy*, 48(50), 18996-19007, **2023**.
4. N. Rojas, M. Sanchez-Molina, G. Sevilla, E. Amores, E. Almandoz, J. Esparza, M.R. Cruz Vivas and C. Colominas*, Int. J. Hydrogen Energy*, 46(51), 25929-25943, **2021**.

Acknowledgments

This project receives a Dutch National Growth Fund contribution from the NXTGEN programme HIGH-TECH.

Equivalent-circuit based electrical characterization of an immersed DBD plasma source for liquid decontamination

M. Saba, C. Muja, Ph. Guillot, T. Maho
Univ Toulouse, INUC, DPHE, Albi, France
Contact : maria.saba@univ-jfc.fr

Abstract:
Dielectric barrier discharge (DBD) plasma sources operating in direct contact with liquids are promising tools for advanced water treatment and biological decontamination. Indeed, they enable efficient generation and transfer of reactive oxygen and nitrogen species (RONS) at the plasma-liquid interface. In these systems, electrical diagnostics are essential for understanding energy deposition mechanisms and plasma-liquid coupling, because they govern both discharge regimes and treatment performance [1]. This work reports a detailed electrical characterization of an immersed DBD plasma source developed for biological decontamination of liquids.
The reactor consists of a coaxial glass configuration. A pulsed high voltage is applied to a metallic rod inserted into a gas injection tube, while a grounded electrode is wrapped around the outer wall of the liquid container. It is filled with sterile water. Helium or helium-based mixtures injected through the tube at a total flow rate of 2 $l.min^{-1}$ generates a continuous stream of bubbles in which discharges ignite and interact directly with the surrounding liquid. The discharge is powered by a pulsed high-voltage supply delivering 4 µs pulses reaching several kilovolts at a repetition rate of 20 kHz (8% duty cycle). Electrical diagnostics are based on a combined analysis of voltage-current waveforms and charge-voltage characteristics using the equivalent electrical circuit method (Figure 1) [2]. The applied voltage is measured using a high-voltage probe (Tektronix P6015A) and the total current via a current transformer (PEARSON™ 6585). A Q-V (Lissajous) method was implemented using a known measurement capacitor and a second sinusoidal generator operating at 20 kHz to determine the intrinsic capacitances of the reactor. A key aspect of this work is the temporal monitoring of sterile water conductivity during plasma treatment for different gas compositions (He, He-Air, He-O_2, He-N_2). The time-dependent evolution of water conductivity is then incorporated into the power deposition calculations. In the equivalent electrical circuit of the system, the resistive behavior of water is accounted for as a time-varying parameter that evolves according to the measured conductivity. It allows a more accurate determination of the actual power transferred to the plasma throughout the treatment process.
This electrical analysis provides characterization of the operating regimes of the immersed DBD reactor. By accounting for the time-evolving liquid conductivity in the equivalent-circuit model, the method can be extended from initially sterile water to more complex aqueous matrices, including biologically or chemically contaminated solutions. These results represent a key step toward establishing quantitative correlations between electrical energy deposition, reactive species generation, and biocidal efficiency of plasma-treated liquids.

Keywords: immersed DBD plasma source, electrical diagnostics, equivalent-circuit modeling

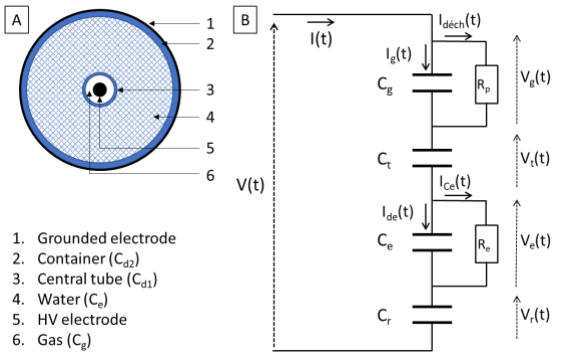

Figure 1: A) Cross section and B) Equivalent-circuit of the DBD plasma source.

References:

1. Zeghioud, H., Nguyen-Tri, P., Khezami, L., Amrane, A., Amen Assai, A., (2020) Review on discharge Plasma for water treatment: mechanism, reactor geometries, active species and combined processes, J. Water Process Engineering, 38, 101664
2. Pipa, A. V., Koskulics, J., Brandenburg, R., Hoder, T., (2012) The simplest equivalent circuit of a pulsed dielectric barrier discharge and the determination of the gas gap charge transfer, *Rev. Sci. Instrum.* 83, 115112

Sustainable removal of carbamazepine from aqueous solutions using dielectric barrier discharge plasma: Efficiency, toxicity assessment, and environmental impact

Qayam U. Din [1,*], G. Iervolino [1], V. Vaiano[1]
[1] Department of Industrial Engineering
University of Salerno, Salerno, Italy

Abstract:
Non-thermal plasma has emerged as a promising advanced oxidation technology for the removal of contaminants of emerging concern (CECs) from water. However, the relationship between plasma discharge characteristics and pollutant degradation performance remains insufficiently understood. In this study, a dielectric barrier discharge (DBD) figure 1 (a) reactor was systematically optimized for the degradation of carbamazepine (CBZ), a model recalcitrant pharmaceutical compound. To interpret plasma liquid interaction mechanisms, non-intrusive optical emission spectroscopy (OES) was employed to characterize key plasma parameters, including electron density, rotational temperature, and vibrational temperature[1]. The influence of applied voltage (10–14 kV), frequency (9–11 kHz), gas flow rate (0.2–0.4 NL), liquid flow (100–200 rpm), and feeding gas composition (air and O_2) on discharge stability and reactive species formation was investigated. Oxygen discharges exhibited enhanced emission intensity and improved plasma stability, indicating higher production of reactive oxygen species (ROS), which directly correlated with degradation performance. Complete (100%) CBZ degradation was achieved at 12 kV (0.2 NL O_2, 10 kHz) within 8 minutes. The degradation process followed pseudo first-order kinetics, with higher rate constants corresponding to increased electron density and optimized discharge conditions. Energy yield analysis further demonstrated improved process efficiency under stable plasma regimes. Total organic carbon (TOC) measurements demonstrated substantial mineralization, indicating progressive oxidation beyond transformation of the parent compound. LC–MS analysis confirmed the formation of intermediate products during treatment and verified the absence of detectable CBZ after 8 minutes[2]. These results highlight the critical role of plasma parameter optimization in controlling reactive species generation and advancing the mechanistic understanding of plasma assisted degradation processes in aqueous systems.

Keywords: Nonthermal plasma; DBD plasma reactor; CEC's degradation; Plasma Characterization; Plasma species RONS; advance oxidation processes

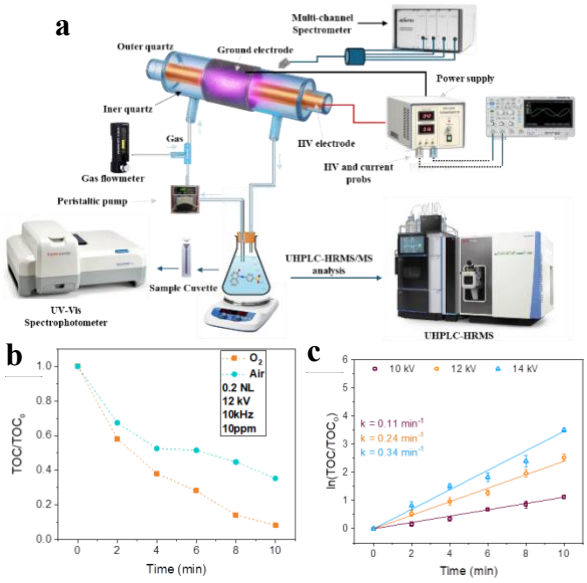

Figure 1: Plasma reactor and its degradation efficiency, (a) shows the experimental setup (b) shows the TOC efficiency of rector and different feeding gas, (c) first order kinatics for the TOC degradation on different input voltages.

Acknowledgments:

This work has been carried out within the framework of the European MSCA project NANAQUA.

References:

1. Iqbal, Z., et al., *Efficient Degradation and Cytotoxicity Assessment of Carbamazepine Using Non-Thermal Atmospheric Pressure Plasma Jets.* 2025: p. 117644.
2. Liu, Y., et al., *Investigation of Dielectric Barrier Discharge Plasma for the Degradation of Erythromycin Solution.* 2025. **30**(3): p. 625.

Revealing the role of temperature in Non-Thermal Atmospheric Plasma-based water disinfection

Á. Francés, M. Oliveira, R. Cordero-García, M. González-Raurich, A. Alvarez-Ordóñez, M. López
Department of Food Hygiene and Technology, University of León, León, Spain

Abstract:
Microbial contamination of water remains a persistent challenge for food safety and public health, urging the development of rapid and sustainable disinfection strategies that avoid the formation of harmful chemical residues and excessive energy consumption. Among emerging technologies, Non-Thermal Atmospheric Plasma (NTAP) has attracted increasing attention due to its ability to inactivate a wide range of microorganisms through the action of reactive oxygen and nitrogen species. These species, formed when a gas is exposed to an electrical discharge at ambient pressure, can damage cell envelopes, nucleic acids, and other vital biomolecules, leading to microbial death. Despite its promising advantages, including short treatment times and operation at room temperature and atmospheric pressure, little is known about how water temperature influences NTAP effectiveness. Thus, this study aimed to elucidate the role of water temperature on the bacterial inactivation capacity of NTAP.
Tap water was adjusted to temperatures ranging from 5 to 60 °C and inoculated with a three-strain cocktail of *Listeria monocytogenes* (~7 log CFU/mL). Treatments were performed for 30 s in a bubble spark discharge reactor (175 V, 1600 Hz), using air (0.8 L/min) as the working gas.

NTAP exhibited its highest bactericidal activity at 5 °C, achieving a 4-log reduction, whereas its efficacy progressively declined with increasing temperature and become negligible above 30 °C. For example, log reductions of 3.2, 3.0, 1.8 and 1.0 were obtained at 10, 15, 20 and 25 °C, respectively (Figure 1). To further discern whether this temperature-dependent effect was associated to plasma generation or to the application temperature itself, plasma-activated water (PAW) was generated at 5 or 50 °C (175 V, 1600 Hz, 240 s) and subsequently equilibrated to different temperatures (5, 10, 20, 30, 40 and 50 ºC) prior to inoculation. PAW generated at 5 °C maintained strong antimicrobial activity (5.7–7.0 log reduction) regardless of its final temperature, while PAW produced at 50 °C exhibited no bactericidal effect under any condition.

Overall, these results demonstrate that refrigeration conditions markedly enhance the antimicrobial potential of NTAP against *L. monocytogenes* in water, underscoring the crucial role of temperature in optimizing plasma-based disinfection processes.

Keywords: non-thermal atmospheric plasma, plasma-activated water, water disinfection, temperature, *Listeria monocytogenes*.

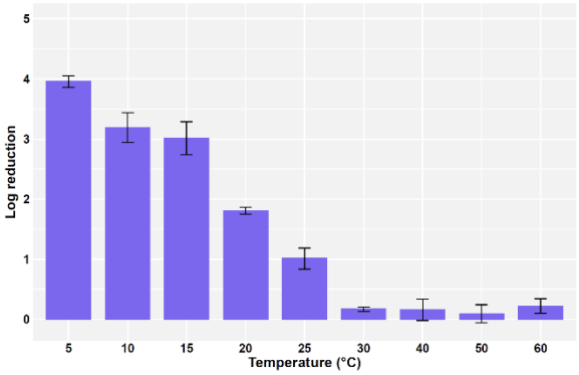

Figure 1: Inactivation rates of *L. monocytogenes* in tap water, at different temperatures, after NTAP treatments.

Acknowledgements:

This work forms part of projects TED2021-131427B-C21 and TED2021-131427B-C22 funded by Ministerio de Ciencia e Innovación (MCIN/AEI/10.13039/501100011033) and by European Union NextGenerationEU/PRTR. Ángel Francés is a beneficiary of a pre-doctoral contract grant (BOCYL-D-17102024-8) funded by Junta de Castilla y León and co-funded by European Social Fund Plus (ESF+).

SETCOR
Conferences & Exhibitions